Michaela Hissa

Ignition and combustion studies of alternative engine fuels

ACTA WASAENSIA 558

University of Vaasa
VAASAN YLIOPISTO

ISBN 978-952-395-203-4 (print)
978-952-395-204-1 (online)

ISSN 0355-2667 (Acta Wasaensia 558, print)
2323-9123 (Acta Wasaensia 558, online)

URN https://urn.fi/URN:ISBN:978-952-395-204-1

PunaMusta Oy, Joensuu, 2025.

ACADEMIC DISSERTATION

To be presented, with the permission of the Board of the School of Technology and Innovations of the University of Vaasa, for public examination on the 20th of August, 2025, at noon.

Article based dissertation, School of Technology and Innovations, Energy Technology

Author	Michaela Hissa https://orcid.org/0000-0002-3068-2386
Supervisor(s)	Professor Seppo Niemi University of Vaasa. School of Technology and Innovations, Energy Technology.
	Dr Jukka Kiijärvi University of Vaasa. School of Technology and Innovations, Energy Technology.
Custos	Professor Seppo Niemi University of Vaasa. School of Technology and Innovations, Energy Technology.
Reviewers	Associate Professor Risto Ilves Estonian University of Life Sciences. Institute of Forestry and Engineering, Engineering.
	Dr Teemu Sarjovaara Neste Corporation.
	Professor Teemu Turunen-Saaresti LUT University. School of Energy Systems, Energy.
Opponent	Docent, Dr Mika Huuhtanen University of Oulu. Faculty of Technology, Environmental and Chemical Engineering.

Tiivistelmä

Tieliikenteessä sähköistyminen ja hybridisaatio lisääntyvät. Työkoneissa ja laivoissa polttomoottoreita tarvitaan kuitenkin vielä kauan, koska niiden vaatimaa suurta käyttöenergiamäärää on vaikea korvata sähkövarastoilla. Moottorien päästöjä on kuitenkin jatkuvasti vähennettävä ilmastonmuutoksen hillitsemiseksi. Jätteistä ja tähteistä tuotetut uusiutuvat polttoaineet ovat hyvä ja suositeltava vaihtoehto fossiilisille polttoaineille, sillä uusiutuvien polttoaineiden kasvihuonekaasupäästöt ovat pienet.

Tämän tutkimuksen päätavoitteena oli selvittää vaihtoehtoisten polttoaineiden vaikutus puristussytytteisten moottorien syttymisviiveeseen ja sylinterin sisäiseen palamiseen sekä tarkastella polttoaineen soveltuvuutta moottorikäyttöön. Pääkohteiksi valitut polttoaineet olivat uusiutuva, raa'asta mäntyöljystä valmistettu nafta sekä kierrätystalouteen perustuva käytetyistä voiteluaineista valmistettu meridiesel.

Ensin tutkimuksessa havainnoitiin polttoaineiden syttymisherkkyyttä erillisessä polttokammiossa ja kahdella setaanilukuanalysaattorilla. Seuraavaksi polttoaineiden syttymistä ja palamista tutkittiin laboratoriossa käyttämällä niitä nopeakäyntisessä työkonedieselmoottorissa ja keskinopeassa laivamoottorissa.

Uusiutuvan naftan pitkä syttymisviive rajoitti moottorin kuormitusta. Syttymisherkkyyden parantamiseksi naftaan sekoitettiin fossiilista dieseliä. Seos syttyi helposti, palaminen oli tehokasta, ja savutus väheni dieseliin verrattuna. Hiilivety- ja hiilimonoksidipäästöt kuitenkin kasvoivat, kun seosta käytettiin työkonemoottorissa. Meridiesel sen sijaan vähensi hiilivety-, hiilimonoksidi- ja savutuspäästöjä tässä moottorissa. Laivamoottorissa sekä meridiesel että naftaseos vähensivät pakokaasujen kokonaishiukkaslukumäärää huomattavasti. Naftan alhainen leimahduspiste on huomioitava turvallisuuskäytännöissä. Meridieselin huono voitelevuus saattaa rajoittaa sen käyttöä polttomoottorissa.

Sekä käytetyistä voiteluaineista valmistettu meridiesel että uusiutuva nafta osoittautuivat teknisesti käyttövalmiiksi polttomoottoripolttoaineiksi joko sellaisenaan tai seosten osana. Huolenaiheena on, miten molempien polttoaineiden raaka-aineiden riittävyys vaikuttaa polttoaineiden saatavuuteen ja hintaan.

Asiasanat: dieselmoottori, syttymisviive, palamisen tehokkuus, laivan kierrätyspolttoaine, meridiesel, uusiutuva nafta

Abstract

Electric and hybrid propulsion systems are expanding rapidly in road transport. Nevertheless, internal combustion engines will continue to dominate marine and non-road applications for the foreseeable future, due to the high energy density of their fuels. Urgent emission reductions are needed to mitigate climate change. Fuels derived from waste or residues are favoured because their greenhouse gas emissions are low, and they help in offsetting diminishing crude oil reserves amid increasing global energy demand.

After studying a range of alternative fuels, two novel candidates were selected for detailed investigation in this dissertation. One is renewable naphtha, derived from crude tall oil; the other is circular economy-based marine gas oil (MGO), produced from waste lubricating oils. The main objective was to study how the selected fuels affect ignition delay and in-cylinder combustion, and to consider their suitability for engine applications.

Five experimental studies were performed. First, the ignition quality of the alternative fuels was observed in a constant-volume combustion chamber and two ignition quality analysers. Then, the fuels' ignition and combustion were studied under laboratory conditions in two compression-ignition engines: one a high-speed, non-road engine; the other a medium-speed, marine engine.

Renewable naphtha has a long ignition delay limiting engine loading, and its ignition quality needs to be improved by blending or using other fuel for engine start-up and shutdown. In addition, naphtha's low flash point requires additional safety procedures. The ignition quality was improved by blending naphtha with low-sulphur light fuel oil (LFO). The blend ignited easily and combustion was efficient, showing reduced smoke emissions compared to LFO. However, hydrocarbon and carbon monoxide emissions varied between the engines. MGO derived from waste lubricating oils reduced hydrocarbon, carbon monoxide and smoke emissions in the high-speed engine. Both MGO and the naphtha-LFO blend showed a significant reduction in the total particulate number compared to LFO in the medium-speed engine. The lower lubricity of MGO can be a limiting factor for its use.

Both circular economy-based MGO and renewable naphtha can be considered technologically viable as drop-in or blend fuel for compression ignition engines. However, the primary concern is the limited availability of their respective feedstocks and the resulting uncertainty of fuel pricing.

Keywords: compression-ignition engine, ignition delay, combustion performance, recycled marine gas oil, renewable naphtha

ACKNOWLEDGEMENT

The research work for this doctoral thesis has been inspired by the Master thesis, "High-speed engine results with various renewable fuels", that I started in 2012 in Professor Seppo Niemi's "Renewable Energy" -research group in the former Faculty of Technology in the University of Vaasa. The Master thesis was part of the Future Combustion Engine Power Plants (FCEP) -research program.

The spark towards the research work of alternative fuels stayed in my mind during my career in industry and kicked me back to University of Vaasa in the beginning of 2016. I received the position of project researcher and doctoral student in the EU Hercules-2 -project, WP1: Fuel flexible engine. This doctoral thesis is mainly based on the research results of Hercules-2, where the target of the project was a fuel flexible large marine engine, optimally adaptive to its operating environment.

During my doctoral studies I have also been able to show my interest in teaching, complete a degree in Professional Teacher Education and be part of teaching activities in the School of Technology and Innovations, Energy Technology -programme.

I owe my deepest gratitude to Professor Seppo Niemi, my supervisor, for his unquestioning faith and support during my studies and research path. His talented teaching was the main reason why I chose Energy Technology as my major in the first place during my master's studies. Ever since, I have been privileged to work under his encouraging and appreciative guidance.

I am sincerely grateful for my other supervisor, Dr Jukka Kiijärvi for his support during this dissertation work. His valuable advice during the finalisation of this dissertation ensured the thesis's highest possible overall quality.

I thank my preliminary examiners, Professor Teemu Turunen-Saaresti, Dr Teemu Sarjovaara and Associate Professor Risto Ilves, for their constructive feedback. Warm thanks also to Docent, Dr Mika Huuhtanen for agreeing to be my opponent.

I wish to thank my colleagues during this research journey. Especially, Dr Katriina Sirviö for her open collaboration and support in every turn. It has been a joy to share all the research and teaching ideas with her and work together towards the goals. Thank you for your support, Professor Maciej Mikulski, Dr Teemu Ovaska, Mrs Sonja Heikkilä, Mr Olav Nilsson, Dr Kirsi Spoof-Tuomi, Dr Anne Mäkiranta, Ms Saana Hautala among others. My special thanks to Mrs Maikki Niemi for her kind hospitality during my studies in Turku.

I wish to thank University of Vaasa for giving me the necessary working time for the research work. Moreover, I thank AGCO Power, Wärtsilä, Neste, UPM, Herzog by PAC and the Novia University of Applied Sciences for sharing their knowledge and providing the equipment and facilities necessary for the experiments. Furthermore, I want to thank all co-authors who have contributed to the publications.

The experimental research and dissertation work have been funded by European Union, Business Finland and University of Vaasa. I am grateful for their financial support. I would also like to thank the Henry Ford Foundation for awarding twice a personal scholarship to support my postgraduate studies.

I want to thank my friends for their comprehensive support on my never-ending journey of learning. You have been my inspiration.

Unfortunately, my father Jaakko passed away just before I started my doctoral studies. I know he would stand proudly beside me today. I wish to thank my mother Paula, who has always encouraged me to pursue my dreams – especially related to studies. Many thanks for my siblings, Diana, Marjut and Teemu and their families, for sharing everyday life. My hearty thanks also to Leena and Pasi, and Kari for their help and childcare assistance whenever it is needed.

Finally, I want to thank my children Arthur, Bea and Fia for keeping my feet on the ground and heart full of joy and happiness. I wish the most loving thanks to Mikko for his love and support.

Laihia, June 2025

Michaela Hissa

Contents

Figures

Tables

Symbols and abbreviations

λ	relative air-fuel ratio
r	repeatability
U	expanded standard uncertainty
ABP	after burning period
ASTM	American Society for Testing and Materials
BTDC	before top dead center
BTE	brake thermal efficiency
CD	combustion delay
CH_4	methane
CI	cetane index
CID510	Cetane ignition 510-analyser
CIMAC	International Council on Combustion Engines
CN	cetane number
CO	carbon monoxide
CRU	Combustion Research Unit
CTO	crude tall oil
CVCC	constant-volume combustion chamber
DCN	derived cetane number
EC	end of combustion
EU	European Union
FTIR	Fourier-transform infrared spectroscopy
HC	hydrocarbon
HRR	heat release rate
HVO	hydrotreated vegetable oil
ICE	internal combustion engine
ID	ignition delay
IQT	ignition quality tester
ISO	International Organization for Standardization
LFO	light fuel oil
LHV	lower heating value
MCP	main combustion period

MFB	mass fraction burned
MGO	marine gas oil
MRD	main reaction delay
NO	nitric oxide
N_2O	nitrous oxide
NO_2	nitrogen dioxide
NOx	nitrogen oxides
PCP	pre-combustion period
PM	particulate matter
PN	particle number
RME	rapeseed methyl ester
ROHR	rate of heat release
RSD	relative standard deviation
TPN	total particle number

Publications

This doctoral dissertation consists of the following five publications:

[1] Hissa, M., Niemi, S. & Sirviö, K. (2018). Combustion Property Analyses with Variable Liquid Marine Fuels in Combustion Research Unit. *Agronomy Research 16(S1), 1032–1045*. https://doi.org/10.15159/ar.18.089

[2] Hissa, M., Niemi, S. & Sirviö, K. (2019). Ignition Studies of Liquid Marine Fuels with Different Ignition Analyzers. *Paper 121. 29th CIMAC World Congress 2019, Vancouver, Canada*.

[3] Hissa, M., Niemi, S., Sirviö, K., Niemi, A. & Ovaska, T. (2019). Combustion Studies of a Non-Road Diesel Engine with Several Alternative Liquid Fuels. *Energies 12(12), 2447*. https://doi.org/10.3390/en12122447

[4] Hissa, M., Niemi, S. & Niemi, A. (2020). Combustion and emission studies of a common-rail direct injection diesel engine with various injector nozzles. *Agronomy Research 18(3), 2033–2048*. https://doi.org/10.15159/AR.20.165

[5] Niemi, S., Hissa, M., Ovaska, T., Sirviö, K., Heikkilä, S., Nilsson, O., Hautala, S., Spoof-Tuomi, K., Suomela, J., Niemi, A., Kiikeri, A., Portin, K. & Asplund, T. (2020). Performance and Emissions of a Medium-Speed Engine Driven with Sustainable Options of Liquid Fuels. *SAE Technical Paper 2020-01-2126*. https://doi.org/10.4271/2020-01-2126

Author's contribution

Paper 1: Hissa is the main author. Hissa and Sirviö designed the experiments. The ignition and combustion experiments were performed by the research partner. Sirviö performed the fuel parameter analyses. Hissa analysed and visualised the data. Hissa and Niemi wrote the paper.

Paper 2: Hissa is the main author. Hissa and Sirviö designed and performed the ignition experiments. Sirviö performed the fuel parameter analyses. Hissa analysed and visualised the data. Hissa and Niemi wrote the paper.

Paper 3: Hissa is the main author. Hissa, S. Niemi, Sirviö and Ovaska designed the measurements. The engine experiments were carried out by Hissa and Ovaska. Sirviö performed the fuel parameter analyses. Hissa and A. Niemi analysed the data. Hissa and Ovaska visualised the data. Hissa and S. Niemi wrote the paper.

Paper 4: Hissa is the main author. Hissa and S. Niemi designed the experiments. The engine experiments were performed by Hissa. Hissa and A. Niemi analysed the data. Hissa visualised the data. Hissa and S. Niemi wrote the paper.

Paper 5: Hissa is the co-author. Hissa and S. Niemi designed the experiments. The engine experiments were performed by Ovaska, Heikkilä, Nilsson, Hautala, Spoof-Tuomi, Suomela and Kiikeri. Sirviö performed the fuel parameter analyses. Hissa and A. Niemi analysed the data. Hissa, S. Niemi and Ovaska visualised the data. S. Niemi, Portin, Asplund, Hissa and Sirviö wrote the paper.

1 INTRODUCTION

Internal combustion engines are at a turning point. Electric and hybrid propulsion is expanding rapidly in road transport, particularly in urban areas. (Zacharof et al., 2024; Feng & Khan, 2024). Nevertheless, internal combustion engines will dominate marine, hybrid power plant and non-road applications for a long time (Pu et al., 2024; Bakhchin et al., 2023). Many attributes support this: high energy-density, strength, durability, the ability to burn various fuels, rapid response to load changes and affordability. Development work to improve internal combustion engine is ongoing, targeting better combustion, more efficient exhaust aftertreatment and superior control systems. (Gabiña et al., 2019; Gilkes, 2019; Reitz et al., 2019;Kalghatgi, 2018; Llamas & Eriksson, 2018).

Urgent emission reductions are required to slow down climate change and negative impacts on human health and the environment. The Paris agreement (United Nations, 2015) set a goal to limit global warming to 2 °C. The entire transport sector must accelerate the transformation towards zero emissions to achieve this goal (Hellström, 2023). Maritime transport produces approximately 3 % of global greenhouse gas emissions; agricultural machinery approximately 1 % (European Agricultural Machinery Association 2022). Furthermore, the European Union (EU) has created an ambitious “Fit for 55” legislation package (European Council, 2024), whereby overall emissions are reduced by at least 55 % by 2030. It assumes climate-neutrality by 2050 (European Council, 2024). Fit for 55 includes maritime transport, where the target is to move towards carbon-neutral fuels and reduce ships’ carbon footprint by 80 % by 2050, compared to the average in 2020 (European Council, 2024). Similar emission reduction regulations can also be expected for non-road applications by 2030 (Hellström, 2023).

The emission reduction targets, together with increasing global energy demand, gradual reduction of crude oil reserves, volatility of conventional fuel prices and fuel availability issues, will affect fuel markets significantly during the next decade (Unglert et al., 2020). In fact, these issues already have triggered strong interest in and growth of alternative energy sources (Hunicz et al., 2020). Sustainable fuels are seen to provide the biggest reduction potential in the longer run (Hellström, 2023). Carbon-neutral fuels, including low-carbon and carbon-negative fuels from biogenic or non-biogenic origin (biomass, waste, renewable hydrogen) could resemble current marine fuels (diesel-type, methane and methanol) (Aakko-Saksa et al., 2023). Fossil marine fuels already can be switched to non-fossil versions that are chemically similar but produced differently (Aakko-Saksa et al., 2023). These so-called drop-in fuels do not require major engine modifications. They most often mimic diesel, liquefied

natural gas (mainly composed of methane) or methanol (Aakko-Saksa et al., 2023). However, according to Aakko-Saksa et al. (2023) these drop-in alternatives currently are not much used in marine applications: less than 1 % of marine fuel today is biofuel and even less meets the stringent criteria such as the Renewable Energy Directive update (European Parliament, 2023).

The fuel feedstock palette is enormous, and fuels from waste or residue are preferred since their greenhouse gas emissions are low (Su et al., 2018; Pietikäinen et al., 2015; Niemi et al., 2002). However, biofuel production for the transport sector is limited, creating challenges for large-scale replacement of fossil marine fuels with their carbon-neutral or low-carbon counterparts (Aakko-Saksa et al., 2023). The International Maritime Organization limited sulphur content to 0.5 % in 2020 (International Maritime Organization, 2020). The consequent demand impacted on the availability and price of low-sulphur marine fuels (Aakko-Saksa et al., 2023). Other alternative fuel choices are oils and fats, as raw in large marine diesel engines, as transesterified fatty acid methyl esters for vehicles and non-road applications, as hydrogenated paraffinic fuel (hydrotreated vegetable oil, HVO), or as pyrolysis oil. Of these, only HVO fuels can be used in diesel engines as a drop-in fuel. Others require at least blending with other fuel to improve fuel properties, or further refining. Blending, however, is not so straightforward and compatibility testing is a common procedure for marine fuel blends (Aakko-Saksa et al., 2023). New fuels and fuel blends may require modifications in fuel handling, engine adjustments, retrofitting injectors and engine optimisations. Some fuel compatibility problems can be tackled during fuel processing and upgrading (Aakko-Saksa et al., 2023).

One of the alternative fuel choices is crude tall oil (CTO) derived renewable naphtha. CTO can be seen as a cost-effective and favourable feedstock for fuel production as it is a side product and it is produced simultaneously during the pulping process (Churchill et al., 2024; Peters & Stojcheva, 2017). The main drivers to increase CTO-derived renewable fuel production are good experimental engine results (renewable diesel), improved production cost-effectiveness and non-edible feedstock. Legislation is already including tall oil fuels in the EU (Churchill et al., 2024;Aro & Fatehi, 2017; Peters & Stojcheva, 2017). The European Commission (2021) has stated that renewable and low-carbon fuels should represent between 6 % and 9 % of the international maritime transport fuel mix in 2030, and between 86 % and 88 % by 2050, to contribute to the EU economy-wide greenhouse gas emission reduction targets.

The second interesting alternative fuel is circular economy based marine gas oil (MGO) made from waste lubricating oils. Waste lubricating oil has been designated as hazardous waste (European Comission, 2024), giving strong motivation to find reuse and regeneration opportunities to convert waste lubricating oil into valuable and

cleaner products (Moses et al., 2023). Waste lubricating oil is generated globally (Moses et al., 2023), which is one of the main factors favouring its use. It is an effective option for generating energy fuel and is a source of valuable chemicals. Legislation is already pushing the collection and reusability of waste lubricating oil as high as possible. The European Commission suggests a target to increase the share of collected waste oil for conversion into base or fuel oils to at least 80 % or even to 95 %, depending on the country, by 2030 (European Commission, 2024).

Combustion systems need to be able to operate with the variety of carbon-neutral fuels in order to reach carbon dioxide reduction targets and sustainability goals. It is more and more obvious that the range of different fuel types is growing, and available fuel choices variate globally. This requires fuel-flexible engine operation, with optimised combustion methods and effective aftertreatment systems (Hunicz et al., 2020; Unglert et al., 2020). Fuel quality also plays an important role. The quality affects the choice of engine materials and dictates limits for engine calibration and optimisation, in turn affecting emissions, power output, drivability and safety (Röj, 2014; CIMAC, 2011).

The fuel-air mixture in diesel combustion ignites spontaneously under high in-cylinder pressure and temperature. Fuel composition and properties affect, inter alia, fuel injection timing and duration, fuel-air mixture formation, ignition, combustion phase durations, in-cylinder temperature, pressure, engine performance and parameters, exhaust emissions and safe fuel handling.

Factors that determine the ignition characteristics of a diesel fuel or alternative diesel-type fuel include cetane number (CN), kinematic viscosity and density. Several other fuel properties may also limit the use of a certain fuel or require additional safety actions. Examples of these are sulphur content, lubricity, oxidation stability, combustibility and acid value. Each of the properties can affect equipment performance and reliability, personnel safety or the safe operation of the engine (International Association of Classification Societes, 2018). Therefore, fuel suppliers must specify the fuel properties and confirm compliance with industry standards.

A variety of alternative fuels was studied in the research papers supporting this dissertation. Of these, the dissertation now focuses on two novel fuel choices: naphtha derived from renewable crude tall oil; and marine gas oil (MGO) produced from waste lubricating oil in the circular economy. The main objective was to study how these selected alternative fuels affect ignition delay and in-cylinder combustion. The suitability of the fuels for engine use was also discussed.

The research provides measured data for various users, from fuel producers and engine manufacturers to policy- and decision-makers. It aims to enhance knowledge

and understanding of alternative fuel solutions and their benefits and constraints. Three key research questions were set to verify the above research objective for the thesis.

Q1: How do various fuels impact on the combustion process, especially on the ignition delay and in-cylinder combustion? Focus on constant-volume combustion chamber (CVCC) and ignition analysers.

Q2: How do various fuels affect combustion in engines, especially ignition delay and in-cylinder combustion? Focus on non-road and marine applications.

Q3: How does the hole number of the injection nozzle affect combustion and emission formation in a high-speed, non-road research engine?

The thesis consists of five research papers (Figure 1) in which the results were originally presented.

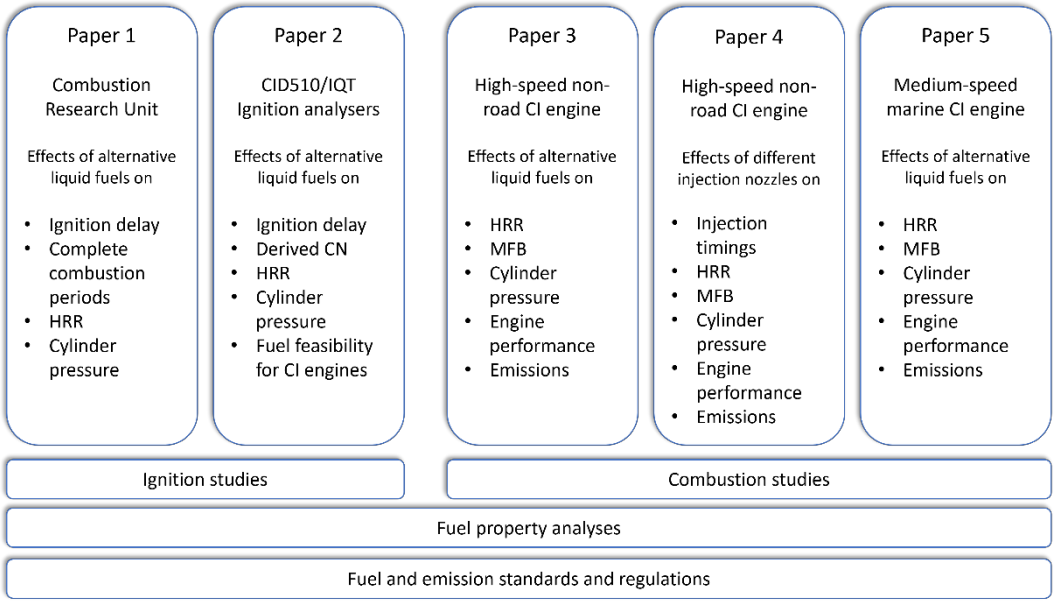

Figure 1. The content of the dissertation, based on five research papers

It is important to analyse fuel properties to find out the fuel's feasibility for the planned application, before any engine measurements.

In the ignition studies of Papers 1 *"Combustion property analyses with variable liquid marine fuels in combustion research unit"* and 2 "*Ignition Studies of Liquid Marine Fuels with Different Ignition Analyzers*", the research focus was on how various properties of the fuels impact the combustion process, especially ignition delay and in-cylinder combustion. Additionally, Paper 2 compared two different measurement methods of

fuel cetane number. The ignition quality of nine marine and power-plant fuels was analysed in the two papers.

The above-mentioned analyses of fuels' ignition and combustion properties were used as a basis to select alternative fuels for further combustion studies. The first of these were engine measurements performed with a high-speed, non-road diesel engine. The results are presented in Paper 3, "*Combustion Studies of a Non-Road Diesel Engine with Several Alternative Liquid Fuels*". The studied fuels were low-sulphur LFO (baseline); circular economy-based MGO; rapeseed methyl ester; renewable diesel (HVO); fossil kerosene; renewable wood-based naphtha and its blend with LFO. This study focused on in-cylinder combustion to understand different alternative fuels' combustion properties. It also provides information about what engine hardware modifications may be needed.

The fuel injection system is one of the most critical elements when an engine is modified to suit new fuels or a different combustion method. However, optimal injector parameters depend on the engine type and require modern simulations that needs to be still verified with engine testing to ensure optimal nozzle performance. Additionally, injector suitability for each fuel must be studied individually. This is the topic investigated in Paper 4, *"Combustion and emission studies of a common-rail direct injection diesel engine with various injector nozzles."* It evaluated three different injector nozzles in the high-speed, non-road diesel engine. The study investigated and compared injection and combustion characteristics, together with gaseous emissions.

The results from Papers 1–3 determined the selection of sustainable fuel options for assessment in a medium-speed engine. Paper 5, "*Performance and Emissions of a Medium-Speed Engine Driven with Sustainable Options of Liquid Fuels*" evaluated how three liquid fuel alternatives perform in a medium-speed engine. The fuels were low-sulphur LFO (baseline), circular economy-based MGO and a blend of renewable naphtha and LFO.

2 COMBUSTION IN A COMPRESSION-IGNITION ENGINE

All the engines used in this dissertation were direct-injection compression-ignition engines with multi-spray injection systems. This chapter deals with the fundamentals of the combustion process of these kinds of engines. The examination begins from the start of injection and extends to the end of combustion. Essential factors for assessing the combustion process are the ignition delay (ID) period and burned fuel's mass fractions of, e.g., 5, 50 and 95 % (Merker & Teichmann, 2019). In its latter part, this chapter also contains some basics of pollutant formation, especially those linked to the effects of the ID period and combustion duration.

2.1 Ignition delay

The period between the starts of fuel injection and ignition is called as the ignition delay (ID). A number of processes take place during this period: fuel brakes up to droplets, evaporates and mixes with air, becoming then ready for ignition. First radicals are formed, working as carriers in chain reactions. After there is a certain quantity of these radicals, enough heat releases to increase the temperature for ignition. (Merker & Teichmann, 2019) Heywood (2018) writes that the chemical processes resulting in the autoignition of the fuel's combustible species are the pre-major-heat-releasing combustion reactions of the fuel, air and residual gas mixture. Many factors affect both above physical and chemical processes: engine design and operating variables, and fuel properties (Heywood, 2018).

The injection system of the engine has a key role when looking at the physical factors affecting the ID. Heywood (2018) lists here the injection timing, injection quantity or engine load, fuel drop size, injection velocity and rate. Additional physical factors are the temperature and pressure of the intake air, engine speed, wall effects of and swirl rate in the combustion chamber, and oxygen concentration in the charge (Heywood, 2018). Merker & Teichmann (2019) mention that the temperature and pressure in the combustion chamber control the ID but these depend on the pressure and temperature of the intake air, engine's compression ratio, start of injection and wall temperatures of the combustion chamber. Additionally, injection pressure, the geometry of the fuel nozzle's orifices and the mixture flow in the combustion chamber essentially affect the ID and determine the ignition region (Merker & Teichmann, 2019). Guibet (1999) states that an increase in the engine speed from 1000 rpm to 4000 rpm makes the ID longer in crank angle degrees but shortens it in seconds.

The physical properties of diesel fuel do not, however, considerably affect the ID in fully or partly warmed-up engines while instead the fuel's chemical characteristics

are much the more important (Heywood, 2018). Merker & Teichmann (2019) also say that the fuel's ignition tendency essentially affects the ID. This tendency or sensitivity is described by means of cetane number (CN) (Merker & Teichmann, 2019). According to Heywood (2018), paraffinic compounds with straight chains have the best ignition quality (a high CN), they auto-ignite more quickly. The trend improves when the chain length increases. Aromatic compounds, instead, have poor ignition quality (a lower CN). Guibet (1999) also states that the ID of a paraffinic compression-ignition fuel is shorter than that of a fuel which contains a lot of naphthene and aromatic compounds. The measured IDs have seemed to correlate well as a function of the CN under constant operating conditions and at a constant compression ratio of the engine. (Heywood, 2018)

The CN of a conventional diesel fuel is affected by the source of crude oil, the refining process and by the additives or ignition improvers. Generally, the ID achieved with the cetane improved blends are found to be equivalent to those, obtained with natural diesel fuels of the same CN. The CN numbers of commercial diesel fuels vary from 40 to 55. (Heywood, 2018) In Finland, the CN of those fuels is usually slightly higher, 50 to 57, approximately (Neste Ltd, 2024; Niemi, 2024).

Heywood (2018) writes that ID tests with fuels of different front-end volatility throughout the CN range of 38 to 53 showed no discernible differences in the ID. The same was detected with fuels of substantially different front-end ignition quality for the same average CN. Variations of fuel viscosity over a factor of 2.5 also showed no considerable effect on the ID. The conclusion was that, in a warmed-up engine, variations in fuel atomization, spray penetration and evaporation rate over reasonable ranges do not seem to affect the length of ID significantly. In other words, the physical properties of diesel fuel do not appear to considerably affect the ID in fully or partly warmed-up engines. (Heywood, 2018) Guibet (1999) writes that diffusion phenomena and surrounding flow characteristics affect the ID more than the fuel's evaporation temperature.

The region where ignition occurs depends heavily on the mixture strength in the combustion chamber (Merker & Teichmann, 2019). According to Higgins et al. (2000), is fuel is said to ignite in the regions where the relative air-fuel ratio (λ) varies from 0.25 to 0.65. The results are based on the measurements in a heavy-duty combustion chamber. Pischinger (2009), in turn, is said to give a local λ range of 0.6 to 0.8.

2.2 Combustion phases

The combustion process can be divided into three phases. The first is called premixed combustion. Merker & Teichmann (2019) calls the second as main combustion

and the third as post-combustion, whereas Heywood (2018) uses the expressions mixing-controlled combustion and late combustion, respectively. The key issue for the thermodynamic quality of the whole combustion process is the released thermal energy. It determines the heating up of the fuel-air mixture and the increase of temperature and pressure. (Merker & Teichmann, 2019)

2.2.1 Pre-mixed combustion

The fuel injected during the ID has formed an almost homogeneous mixture and it burns very fast in the first combustion phase. The rate of the chemical reactions and the quantity of fuel-air mixture determines the heat release rate (HRR). The pressure in the combustion chamber increases rapidly, also causing combustion noise, typical of compression-ignition engines. Noise can be suppressed by a proper injection timing, but the use of one or more pre-injections are effective ways to curb the HRR, speed of the pressure rise, and noise. Pre-injections shorten the ID of the main injection, diminish the pre-mixed phase and reduce noise. (Merker & Teichmann, 2019)

2.2.2 Mixing-controlled or main combustion

In the second or main combustion phase, the turbulent fuel-air mixing processes control the HRR, why the phase is also called mixing-controlled combustion. Injection, spray formation, evaporation and combustion continue and pollutants are formed. According to the conceptual model of Dec (1997) and Flynn et al. (1999), liquid fuel penetrates the combustion chamber, mixes with air and evaporates. The relative air-fuel ratio (λ) increases both with increasing distance from the injector tip and from the spray axle. A rich zone forms downward of the liquid region. Here, fuel is partly oxidized, and the temperature reaches 1600 K. Flynn et al. (1999) say that the λ is within the range of 0.25 to 0.5 and some 15 % of the total heat is released. There are also forerunner species that lead to particle formation farther in the middle of the spray (Merker & Teichmann, 2019).

A diffusion flame forms around the spray on the region where the mixture is stoichiometric. The partially oxidized products of the rich zone and particles move further and end up into the diffusion flame, where they are fully oxidized. The temperature rises even up to 2700 K. Due to the high temperature, in the presence of oxygen, oxides of nitrogen (NO_X) are formed on the leaner side of the diffusion flame. Nearby the injector tip, the evaporation process and chemical reactions determine the distance where the diffusion flame is established. The axial distance between the tip and flame is called light-off length. It is an important feature of a diesel flame related to smoke formation. (Merker & Teichmann, 2019)

The above model describes the quasi-stationary phase of the main combustion. Strictly speaking, it is only valid during quiescent surroundings in the combustion chamber (Merker & Teichmann, 2019). Heywood (2018) adds two important practical areas to be incorporated into the above conceptual model. They are air swirl and multiple fuel injections. The swirling air motion, perpendicular to each fuel spray, forces additional air to the spray. This increases the spray's λ and leads to less-rich mixture within the spray. The first premixed phase of the autoignition process occurs sooner. (Heywood, 2018)

2.2.3 Late or post-combustion

After the end of injection, there are zones of partly oxidized products from rich regions of preceding combustion phases in the combustion chamber. Diffusion flames surround these zones. The temperature decreases during the engine's expansion phase and so do the reaction rates; combustion is again controlled by chemistry. This combustion phase has great importance regarding smoke formation and oxidation. At low temperatures, the oxidation becomes slow. (Merker & Teichmann, 2019)

2.3 Emissions formation

In practice, all today's applications of compression-ignition engines must be equipped with exhaust aftertreatment systems, because the emissions legislation with increasing demands limits the permitted amounts of exhaust pollutants. Nevertheless, the optimization of the in-cylinder processes or engine cycles and combustion methods has crucial importance when aiming at the reduction of pollutant emissions and optimization of fuel consumption, noise and total costs (Merker & Teichmann, 2019). In a compression-ignition engine, the fuel distribution is nonuniform throughout most of the essential parts of the combustion. The pollutant formation strongly depends on the fuel distribution and how mixing with hot air changes it with time. (Heywood, 2018)

This section deals with some basics of formation of relevant pollutants and opens fundamental connections of ID and compression-ignition combustion with the engine's exhaust emissions. The main emphasis is on the emissions of nitrogen oxides (NO_X) and particulate matter (PM), because the control of these emissions is of special importance in compression-ignition engines. Mostly, there is also a trade-off between the NO_X and PM emissions; when one of them decreases, the other increases (Merker & Teichmann, 2019). Some attention is also paid to the origin of unburned organic or hydrocarbon (HC) emissions, because they form a portion of the PM.

2.3.1 Oxides of nitrogen

Of the oxides of nitrogen, nitric oxide (NO) forms in the high-temperature regions of burned gas. The distribution of temperature and air-fuel ratios within the burned gases are nonuniform. The formation rates of NO are highest in the close-to-stoichiometric reaction zone of the diffusion flame. (Heywood, 2018)

In addition to the flame front, NO also forms in the post-flame gases. The engines' combustion pressure is high, and the flame reaction zone is very thin and residence time within this zone is short. The cylinder pressure also rises during most of the combustion process, meaning that early burned gases are compressed to a higher temperature than they reached immediately after combustion. Therefore, NO formation in the post-flame gases almost always dominates any flame-front-originated NO. (Heywood, 2018)

The dependence of the NO formation rate on temperature in the exponential term is evident. Already a small temperature rise increases the formation considerably. High temperatures and oxygen contents lead to high NO formation rates. The initial NO formation rate seems to peak 10 % lean of the stoichiometric composition, approximately, and decreases rapidly when the mixture then becomes richer or leaner. (Merker & Teichmann, 2019; Heywood, 2018) NO is the primary oxide of nitrogen, formed during the combustion in a compression-ignition engine. However, engine-out emissions also contain nitrogen dioxide NO_2. Therefore, we speak about the oxides of nitrogen or NO_x when we examine the exhaust pollutant emissions, the expression including the sum of NO and NO_2. In compression-ignition engines, the share of NO_2 can, however, be 10 to 30 % of the total NO_x in engine-out emissions. The highest ratios are recorded at low loads, the engine speed also affecting the ratio. (Heywood, 2018)

Results from cylinder-dumping experiments have shown that almost all the NO forms within the 20 crank angle degrees following the start of combustion. NO levels increase at high load with higher peak pressures and temperatures and with a larger area and longer-lasting regions of close-to-stoichiometric diffusion-flame-generated burned gas. At decreasing loads, the injected fuel quantity decreases, but almost all the fuel still burns close to stoichiometric. NO emissions should, therefore, be roughly proportional to the mass of fuel injected, provided burned gas temperatures and pressures in the diffusion flame do not change largely. (Heywood, 2018)

2.3.2 Carbon monoxide and unburned hydrocarbons

The mixture strength primarily controls the carbon monoxide (CO) emissions from internal combustion engines. If the mixture is rich, CO concentrations in the exhaust increase steadily with decreasing relative air-fuel ratio or λ. For lean mixtures, CO concentrations are low. Because compression-ignition engines always operate well on the lean side, their CO emissions are low enough to be insignificant. Major reductions can also be achieved with exhaust catalysts, if especially required. (Heywood, 2018)

Engine-out organic or hydrocarbon (HC) emissions from compression-ignition engines are also low throughout much of the engine's operating range, generally less than 1 % of the fuel. The emissions are the consequence of incomplete combustion of the hydrocarbon fuel. The HC levels are usually specified in terms of total hydrocarbon content given in parts per million carbon atoms (C_1). (Heywood, 2018)

Fuel composition can considerably affect the composition and magnitude of organic or HC emissions. Fuels with high proportions of aromatics and olefins generate relatively higher concentrations of reactive hydrocarbons. Many of the organic compounds recorded in the exhaust are, however, not present in the fuel indicating that significant pyrolysis and synthesis occur during the combustion process. (Heywood, 2018)

The ID and combustion progress also have their role in HC formation. The compression-ignition engine combustion has a complex heterogeneous nature with several processes that can contribute to HC emissions. Hydrocarbons originate in regions where excessive dilution with air prevents the combustion process from starting or going to completion (over-leaning) or where the flame quenches on the walls (flame quenching). A further source of hydrocarbons is fuel vaporizing from the sac volume of the injector tip during the later stages of the combustion. Another source is linked to the opening and closing of the injector needle. Every time the needle is opened or closed, droplets of poor quality are formed into the combustion chamber. Fuel absorption into and desorption from oil layers on the cylinder liner can also have relevance. Over-fueling can cause undermixing with a high HC, but only under heavy acceleration conditions, if at all. (Kiijärvi, 2022; Heywood, 2018)

The magnitude of over-leaning HC depends on the fuel amount injected during the ID, the mixing rate during it, and the extent to which cylinder conditions are conducive to auto-ignition. When the ID increases, the HC emissions increase at a growing rate. (Heywood, 2018)

The level of HC emissions from compression-ignition engines varies widely with operating conditions. Engine idling and low-load operation produce substantially higher HC emissions than full-load operation. Over-leaning is an important HC source, particularly under low-load operation. If the engine is over-fuelled to reach an excessive torque, HC emissions quite obviously increase significantly. (Heywood, 2018)

2.3.3 Soot and particulate matter

Particulate emissions make an issue in compression-ignition engines. Soot is formed within the developing fuel sprays. Although much of the soot burns up inside the cylinder, a part of it does not and is exhausted. The gases then cool, nuclei condense and form small particles that absorb condensing higher-molecular-weight hydrocarbons. The size distribution of particles builds up. Particles within the diameter range of 50 to 500 nm are categorized as the accumulation mode while the particulates below 50 nm in diameter, approximately, constitute the nucleation mode. (Heywood, 2018) Sometimes, particles of below 100 nm in diameter are also called ultrafines.

Soot forms in the core of the fuel spray that contains a rich mixture of unburned fuel and hot entrained air. The soot formation process can be summarized by dividing it into two stages. The first condensed-phase material forms from the fuel molecules through their partial oxidation and as pyrolysis products. The diffusion region's flame oxidizes soot when it contacts oxygen. Particulates from compression-ignition engines consist, primarily, of combustion-generated carbonaceous material or soot which has absorbed organic compounds of the exhaust gases. Most particulate material originates from incomplete combustion of fuel hydrocarbons but some results from the lubricant. At high temperatures of above 500 °C, the individual particles are mainly clusters of many small spheres or spherules of carbon. (Heywood, 2018)

When temperatures decrease below 500 °C, the particles become coated with condensed and adsorbed heavy organic compounds. This is the second phase, where particles grow, including surface growth, coagulation and aggregation. These particles include unburned hydrocarbons, oxygenated hydrocarbons and polynuclear aromatic hydrocarbons. Depending on the sulphur content in the fuel, the condensed material also includes species like sulphur dioxide and sulphuric acid (or sulphates). Adsorption into the surface of soot particles and condensation to form new particles of hydrocarbon species in the exhaust gases occur in the exhaust system. There is, however, an overlap and the processes may occur simultaneously in a certain region of elemental mixture within the engine's combustion chamber. Due to the heterogeneous mixture and the overlap of fuel injection and combustion, different processes are in progress at any given time in various regions or packets of fluid. (Heywood, 2018)

The magnitude of PM and particle number (PN) emissions can be assessed based on the above formation and oxidation theories. There are, however, some quite universal observations about the factors affecting the magnitude of the particulate emissions. Of the fuel hydrocarbons, paraffins, olefins and aromatics have proved to contribute to particle emissions but as a group, aromatics appeared to be the greatest contributors. The fuel sulphur content is another obvious player, as is the fuel ash content. (Heywood, 2018)

Additional factors are, e.g., the temperature after the end of injection. If it is high, the exhaust particle emissions are usually lower. Thorough mixing of fuel and air or improved homogenization during a lengthened ID also reduces particle emissions. The flow intensity and interaction of the spray and the walls of the combustion chamber naturally affect the quality of the mixing process. In addition to ID and combustion noise, pre-injection affects both NO_X and particulate emissions (e.g., Musculus, 2004). Post-injection close to the end of the main injection can be used for the reduction of the particle emissions (Payri et al., 2002). The reduction of the peak HRR has shown to reduce PM (and CO) at a given NO_X without any penalty in the efficiency. (Merker & Teichmann, 2019)

3 MATERIALS AND METHODS

The experimental measurements were performed by the University of Vaasa at the internal combustion engine laboratory of Technobothnia Research Centre and at the University of Vaasa's Energy Laboratory in Vaasa, Finland. Ignition studies with the combustion research unit (CRU) were performed at the fuel laboratory of Wärtsilä Finland Ltd in Vaasa, Finland.

3.1 Fuels

The studied fuels were selected with the aim of increasing the choice of fuel alternatives with various fuel properties suitable for compression-ignition engines. Table 1 lists the properties of the investigated fuels. Most of the properties were analysed by the Energy Laboratory of the University of Vaasa but some of the fuel analyses were performed by other laboratories. These analyses were cetane number/cetane index, distillation, lubricity, sulphur content and lower heating value (LHV) for the fuels.

The reference fuel, used in Papers 1–3 and 5, was a commercial low-sulphur light fuel oil (LFO). It complies with SFS-EN 590 (2022) fuel standard. The same LFO was part of the fuel blends in Papers 2, 3 and 5. The fuel used in Paper 4 was low-sulphur diesel fuel oil.

In Paper 1, a range of renewable and "net-zero-carbon" fuels were studied in the CRU. The focus was on how various properties of the fuels impact the combustion process. Ignition characteristics of four marine and power-plant fuels were studied: LFO (baseline), circular economy-based marine gas oil (MGO), kerosene (Jet A-1 -type) and neat wood-based renewable naphtha. MGO represents recycled fuels because it is produced from used lubricant oils. LFO and kerosene may be described as heavier fuels, and naphtha represents lighter fractions. The used naphtha was renewable wood-based naphtha, which was a side-product of wood-based renewable diesel production.

Paper 2 focused on ignition quality of nine marine and power-plant fuels. The fuels were categorised into four different groups: Group 1 – low-sulphur light fuel oils (baseline); Group 2 – commercial alternative fuels; Group 3 – renewable alternative fuels; and Group 4 - fuel blend with renewable share. Table 1 lists the properties of the studied fuels, divided into these four groups.

Table 1. Properties of the studied fuels in Papers 1–5

Paper		Fuel	Kinematic viscosity, mm^2/s (40°C) EN ISO 3104/ ASTM D7042	Density, kg/m^3 (15 °C) EN ISO 12185/ ASTM D7042	Cetane number [a] cetane index EN 15195/ ASTM D6890	LHV, MJ/kg [b] Literature value ASTM D240	Sulphur content, mg/kg [c] wt.-% EN 20846	Lubricity, µm/60 °C [d]value incl. additive EN ISO 12156-1	Flash point, °C ASTM D93-A or C
1		LFO	3.0	836	54[a]	43	<0.01 [c]	345	64
		MGO	8.0	843	68	43	Max. 0.1[c]	491	110
		Kerosene	0.94	787	41	43	0.1[c]	-	Min. 38
		Naphtha	0.5	722	34	44	-	-	20
2	Group 1	Fuel 1	3.1	836	-	43	6	350	-
		Fuel 2	2.9	833	-	43	-	-	-
	Group 2	Fuel 3	7.7	843	-	43	<100	491	-
		Fuel 4	3.7	838	-	43	30	484	-
		Fuel 5	3.9	886	-	42	-	-	-
		Fuel 6	1.0	787	-	44	900	447[d]	-
	Group 3	Fuel 7	4.5	883	-	38	<5	196	-
		Fuel 8	3.5	813	-	44	<5	-	-
	Group 4	Fuel 9	1.8	810	-	43	<5	335	-
3		LFO	1.8	827	52	43	8.3	345	63
		MGO	7.7	843	68	43	<100	491	110
		Kerosene	0.94	787	41	43	1000	447[d]	38
		RME	4.5	883	53	37-38[b]	<5	-	179
		HVO	3.5	813	65	-	<1 [b]	228[b]	78[b]
		Naphtha	0.5	722	34	44	-	-	20
		Naphtha-LFO	1.37	805	51	-	6.8	391	-
4		DFO	-	835	54	43	3.3	-	-
5		LFO	3.1	836	58	43	6	350	-
		MGO	3.7	838	54	43	30	484	-
		Naphtha-LFO	1.8	809	52	44	4.5	335	-

Paper 3 covers the engine experiments conducted with a high-speed, non-road diesel engine. LFO and six alternative liquid fuels were investigated to understand their combustion properties. The fuels were LFO (baseline); circular economy-based MGO; kerosene; rapeseed methyl ester; renewable diesel (HVO); neat renewable wood-based naphtha; and a renewable naphtha-LFO blend.

Paper 5 explores the performance and emissions of a medium-speed engine driven with sustainable options of liquid fuel. The fuels were circular economy-based MGO and a blend of renewable naphtha and low-sulphur LFO. Neat LFO served as the base-line fuel.

The most important fuel properties are cetane number (CN) or cetane index (CI), fuel viscosity, density, heating value and sulphur content. However, water content, lubric-ity, flash point or acid value may limit the use of a certain fuel or require additional safety actions.

A total of 24 fuel samples were analysed in the dissertation. This chapter considers the most relevant fuel properties affecting fuel-air mixing, fuel vaporisation and com-bustion.

The measured fuel analysis results at the University of Vaasa are the arithmetic means of two replicate measurements. The analysis methods had been previously validated in the laboratory (Sirviö, 2018). The relative standard deviations (RSD) of the analysis methods (Jaarinen & Niiranen, 2005), were calculated using validation samples with Equations

$$s(x) = \sqrt{\sum_{i=1}^{n} \frac{(x_i - \bar{x})^2}{n-1}} \tag{1}$$

and

$$\mathrm{RSD} = \frac{s(x)}{\bar{x}} \tag{2}$$

where s is standard deviation, n is number of measurements, x_i is measured value, $\bar{x}$ is arithmetic mean value of all measurements, and RSD is relative standard deviation.

The relative standard deviations were for kinematic viscosity <1 %, density <1 % and for flash point 3.0 % (Sirviö, 2018). Relative standard deviations of the analysis meth-ods of other laboratories were not known. The analyses were cetane number/cetane index, distillation, lubricity, sulphur content and LHV for the fuels.

3.1.1 Cetane number or cetane index

Cetane number has a critical role in fuel ignition and directly affects combustion and its duration. Fuel standards define a minimum CN value. SFS-EN 590 (2022) for automotive and non-road applications sets a CN minimum of 51. The most common marine gas oil (MGO) standard is ISO 8217/ISO-F-DMB (2017) with a minimum cetane index (CI) of 35. Higher CN is known to lower hydrocarbon (HC), carbon monoxide (CO) and particle matter (PM) emissions, but increase nitrogen oxides (NO_X) emissions; (Ahmad et al., 2021; Xue et al., 2011).

LFO, MGO, kerosene and renewable naphtha were studied in the CRU in Paper 1. Neat kerosene, neat naphtha and a blend of naphtha and LFO were used in the high-speed engine measurements (Paper 3). In the medium-speed engine measurements, naphtha was used as a blend with LFO (Paper 5).

Chapter 4.1.2 discusses the ignition quality results of Paper 2. Table 1 shows the CN or CI of the fuels used in the other four papers.

3.1.2 Viscosity

Kinematic viscosity has an important role in fuel injection and droplet formation. High viscosity leads to poor atomisation and decreases the injector's flow performance, resulting in longer total injection duration and leading to incomplete combustion (Bae & Kim, 2017; Nabi et al., 2012). Conversely, low viscosity may cause mechanical problems, manifesting as a leakage through the injector or fuel pump system, as well as problems with ignition and engine starting. Low viscosity together with low CN may cause increased NO_X, smoke and noise emissions due to prolonged ignition delay and retarded start of combustion (Kuszewski, 2019; Subramanian et al., 2018). However, lower viscosity could improve fuel atomisation, evaporation and fuel-air mixing (Subramanian et al., 2018).

SFS-EN 590's (2022) limits for kinematic viscosity (at 40 °C) are a minimum of 2.0 and a maximum of 4.5 mm^2/s. ISO 8217/ISO-F-DMB (2017) sets a maximum value of 11.0 mm^2/s but there is no minimum value.

Kinematic viscosity of all the fuel samples varied from 0.5 mm^2/s for neat renewable naphtha to 8.0 mm^2/s for circular economy-based MGO in Papers 1–3. However, the second patch of circular economy-based MGO, in Paper 5, had a viscosity of 3.7 mm^2/s which was in SFS-EN 590's (2022) limits.

3.1.3 Density

SFS-EN 590 (2022) sets a minimum density value (at 15 °C) of 820 kg/m^3, and a maximum of 845 kg/m^3. ISO 8217/ISO-F-DMB's (2017) maximum limit for density is 900 kg/m^3.

Density of all the fuel samples ranged from 722 kg/m^3 for renewable naphtha to 886 kg/m^3 for Fuel 5: marine gas oil. Thus, renewable naphtha is below SFS-EN 590's (2022) minimum limit. This can directly affect the progress of fuel pressure in the injection system, consequently influencing the dynamic start of fuel injection. Lower density may limit maximum engine power and affect volumetric fuel consumption (Heywood, 2018). On the other hand, a higher viscosity combined with higher density may lead to poor fuel atomisation, resulting in incomplete combustion (Nabi et al., 2012).

3.1.4 Lower heating value

Lower heating value (LHV) defines a fuel's effectiveness as an energy carrier. It must meet the level of conventional fuels to avoid fuel consumption problems (Bae & Kim, 2017). A high, mass-basis, LHV indicates a good heat release rate as the fuel burns, improving engine performance.

LHV of the studied fuels varied from 38 MJ/kg for Fuel 7 (biodiesel) to 44 MJ/kg for renewable naphtha, Fuel 6 (aviation fuel) and Fuel 8 (renewable diesel).

3.1.5 Sulphur content

Legislation has reduced the sulphur content in fuel. Sulphur Emission Control Areas limits apply near specified shores and harbors. (International Maritime Organization MARPOL Annex VI, Reg. 14). When a vessel enters a sulphur emission control area, its fuel's sulphur content shall not exceed 0.10 % m/m (1000 mg/kg). European standard SFS-EN 590 (2022) has a maximum sulphur limit of 10 mg/kg.

The sulphur content of all the studied fuels was 1000 mg/kg or lower. The highest values were measured for kerosene, with 1000 mg/kg, followed by Fuel 6: (aviation fuel) with 900 mg/kg. HVO had the lowest sulphur content, at <1 mg/kg, followed by rapeseed methyl ester, with <5 mg/kg. The manufacturer of the renewable naphtha states its maximum sulphur content is 10 mg/kg (UPM Biofuels, 2024).

A high sulphur content, together with high density and high boiling point, increases particle matter and smoke emissions (Sarvi et al., 2008). The process of reducing the

sulphur content also destroys some of the fuel's natural lubricants (Arkoudeas et al., 2008). This may necessitate a fuel lubricity additive to inhibit engine wear.

3.1.6 Lubricity

Fuel lubricity has a significant role in preventing damage caused by friction, especially when low and ultra-low sulphur fuels are used (Sajjad et al., 2014). Additives can be used to adjust fuel lubricity. Another way to increase the lubricity level is to add biodiesel to create a fuel blend (Sirviö, 2018; Lahane & Subramanian, 2015).

Lubricity of the studied fuels ranged from 228 µm/60 °C (HVO) to 491 µm/60 °C (MGO). In Papers 2 and 3, a very small proportion of lubricity additive (1:4000) was added to Fuel 6 and kerosene to avoid possible engine malfunctions. This small amount of additive should not affect the autoignition properties of the two fuels.

3.1.7 Flash point

Flash point is the lowest temperature at which fuel can vaporise and create ignitable fuel-air mixture. Flash point is used to quantify a fuel's flammability hazard. It does not affect engine performance but must be considered in relation to safety of fuel storage and distribution (Mueller et al., 2014).

Of all the studied fuels in Papers 1 and 3, neat renewable naphtha and kerosene had low flash points, of 20 °C and 38 °C respectively. Coupled with their low viscosity, this called for additional safety procedures during their handling and engine experiments. The present research ensured the compatibility of the engine, fuel system and auxiliaries. Additionally, the engine operators used respirator masks and gloves during the measurements.

Several other fuel properties may also limit the use of a certain fuel or require additional safety actions. These properties are, for example, the fuel's oxidation stability, combustibility and acid value. Each of the properties can affect equipment performance and/or reliability, personnel safety or the safe operation of the engine (International Association of Classification Societes, 2018). It is for these reasons that fuel suppliers have to specify the fuel properties and confirm compliance with industry standards.

3.2 Experimental devices

The research for this dissertation was performed by using a combustion research unit (CRU), two different ignition analysis methods, two different high-speed, non-road diesel engines and a medium-speed, marine engine in laboratory conditions. Table 2 lists the main specifications of the CRU; Table 3 gives details of the ignition analyser; and Table 4 provides the engine specifications.

3.2.1 Combustion research unit

The combustion research unit (CRU) used in Paper 1 and depicted in Figure 2 was a constant-volume combustion chamber (CVCC) instrument designed to resemble engine conditions. There are no moving parts in the CRU and the starting conditions of the fuel injections are controlled more precisely than in a real compression-ignition engine. Fuel is injected in a fixed period through a twin-nozzle injection system into a chamber with fixed dimensions. One nozzle is the main injector; the other is the pilot injector, which can be activated or de-activated. The pilot injector was de-activated in this study. Electronic control of the injector gave precise adjustment of injection timing, opening period and pressure. Piezoelectric pressure sensors were used to monitor the combustion and fuel pressures. The air in the combustion chamber was heated by heating the chamber walls.

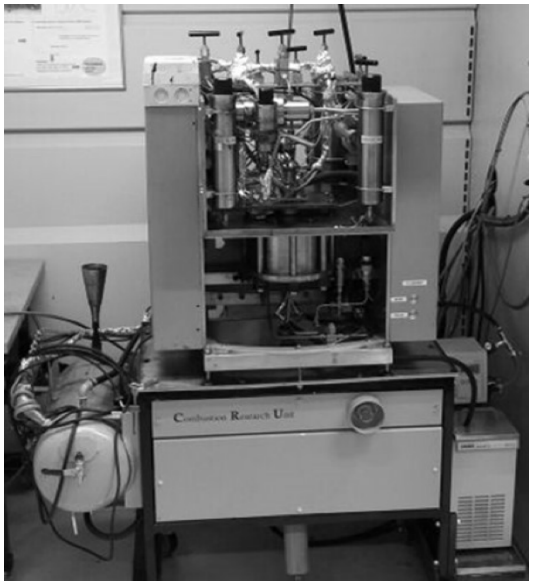

Figure 2. Combustion research unit (CRU)

All fuels were first centrifuged and then hot filtrated before the CRU measurements. The fuels were at room temperature when fed into the fuel injection system. The measurement results are averages of ten measurement rounds.

It should be noted that some conditions in the CRU differ from actual engine conditions. The main difference is cylinder pressure: this may exceed 200 bar in four-stroke engines, while the maximum pressure in the CRU was 81 bar. Other differences are related to fuel injection and injection timing.

A fixed period was used for this study in the CRU, and all fuel was injected before ignition. In engines, especially at high loads, fuel injection overlaps ignition and combustion (Steenberg & Forget, 2007). This means that a large amount of the fuel (80 %) in engines is injected into a space with a flame. Irrespective of the differences between the CRU and actual engine conditions, the CRU is a fast, easy and cost-effective device to investigate fuel feasibility in engine use.

Table 2. Specifications of the combustion research unit in Paper 1

Parameter	Value
Injection period	250–3000 µs
Injection system	Twin nozzle, pilot injector was de-activated
Chamber volume	500 ± 2 % cm^3
Injector	Bosch CR
Pressure sensors	Piezoelectric

3.2.2 Ignition analyser

The experiments in Paper 2 were carried out with a Herzog by PAC Cetane Ignition Delay 510 device (CID510). This commercial, fully automated CVCC instrument has an electronically controlled, high-pressure common-rail injection system and patented multipoint ID measurement. The CID510 fulfills the standards SFS-EN 16715 (2015), ASTM D7668 (2017) and IP 615 (2015). Figure 3 shows the measuring principle of the CID510, Table 3 lists its calibration settings based on the above-mentioned standards.

An ignition quality tester (IQT, SFS-EN 15195; 2023) was used to analyse the cetane number of fuels, for the verification of the measured derived cetane number (DCN) in the CID510.

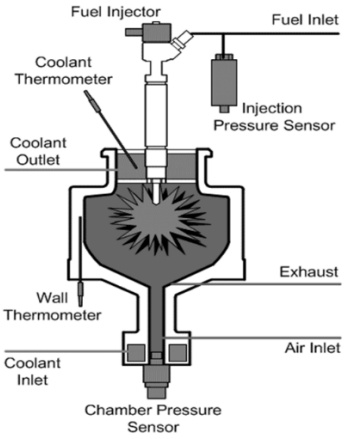

Figure 3. The measurement principle of the Herzog by PAC Cetane Ignition Delay 510 -analyzer (Herzog by PAC, 2017)

Table 3. CID510 device calibration settings in Paper 2

Parameter	Calibration setting
Injection pressure, pinj (bar)	1000
Injection period, tinj (µs)	2500
Initial chamber pressure, p0 (bar)	20
Initial chamber temperature, tch (°C)	596.5
Injector nozzle coolant jacket temperature, tc0 (°C)	50
Combustion chamber volume (ml)	473
Sample size (ml)	min. 60
Test duration (min)	approx. 30

3.2.3 Experimental engines

Table 4 lists the specifications of the three different research engines used in Papers 3–5. All the engines were used under laboratory conditions. Maximum torque values were measured with LFO in Paper 3 and with diesel fuel oil in Paper 4. In Paper 5, maximum shaft power output was based on the naphtha-LFO blend of 26 vol.-% naphtha and 74 vol.-% LFO.

The high-speed engines in Papers 3 and 4 were turbocharged, intercooled (air-to-water) non-road diesel engines with common-rail fuel injection system. They were loaded by means of a Horiba eddy-current dynamometer WT300. No exhaust gas aftertreatment was used.

Table 4. Specifications of the research engines in Papers 3–5

Paper	3	4	5
Cylinder number	4	4	4
Bore (mm)	108	108	200
Stroke (mm)	120	120	280
Swept volume (dm^3)	4.4	4.4	8.8
Rated power (kW)	81	92	
Rated speed (rpm)	2200	2200	1000
Maximum torque at rated speed (Nm)	351	400	
Shaft power output (kW)			640

Paper 5's medium-speed engine, designed for power plant and marine applications, was turbocharged, water-cooled and used common-rail fuel injection. The engine was driven at a constant speed of 1000 rpm and loaded by an alternator. The produced electricity was fed into the grid of the local energy company. Exhaust gas aftertreatment was not employed.

Paper 4 compared three solenoid-driven injector nozzles in a high-speed, non-road diesel engine. The nozzles had 6, 8 and 10 holes and a high mass flow rate (1.2 l/min at 100 bar). The spray angle (umbrella angle) was 149° for all nozzles. Table 5 lists the injector nozzle specifications.

Table 5. Specifications of the studied injector nozzles in Paper 4

Number of nozzle holes	6	8	10
Orifice diameter (mm)	0.2	0.162	0.148
Included spray angle	149°	149°	149°
Nozzle flow rate (dm^3/min)	1.2	1.2	1.2

Emissions of total hydrocarbons (HC), nitrogen oxides (NO_X), carbon monoxide (CO) and oxygen content were measured on a dry basis. Based on the measured HC, NO_X and CO concentrations, the brake-specific emissions of HC, NO_X and CO were calculated according to ISO 8178-4 (2017) standard. Table 10 in Chapter 3.3.4 lists the instruments used for emission measurements.

3.3 Experimental matrices and measurement procedures

The next sections introduce the experimental matrices and measurement procedures used for the CRU (Paper 1), the ignition analysers (Paper 2), the high-speed, non-road engines (Papers 3 and 4) and the medium-speed engine (Paper 5).

Measurement errors and uncertainty have been assessed by considering systematic and random errors (JCGM, 2008) and the effects of environmental conditions (Morris & Langari, 2015). The influence of systematic errors has been mitigated by regular calibration of instruments. The influence of random error effects has been mitigated by increasing the number of measurement repetitions. (Morris & Langari, 2015; Valkjärvi, 2022). Environmental conditions were followed carefully during every measurement. The text below deals with the measurement uncertainty separately for individual measurement procedures.

3.3.1 Combustion research unit

Table 6 shows the research set-up configuration of the CRU. The main injection period was fixed at 1000 µs for all fuels, despite differences in their kinematic viscosity. A fixed injection period was chosen to test broad fuel flexibility, with no or only minor changes to engine hardware. Two different pressure and temperature conditions were studied. The focus is on high pressure results since they are closer to real engine conditions. The results showed that the injection duration when using MGO was 1025 µs instead of 1000 µs. This slight difference means MGO is not completely comparable with the other studied fuels. Such a slight increase in the quantity of the injected fuel has no significant effect on delay period under normal operation conditions (Heywood, 2018). However, the delay increases during engine starting, due to the larger drop sizes which are associated with evaporating and heating the increased amount of fuel (Heywood, 2018).

The following phases are determined during the measurement:

- CRU measures the ignition delay (ID) from the start of the injection (t=0) until the pressure in the chamber increases by 0.1 bar.
- Pre-combustion period (PCP) starts at the point when the pressure is increased by 0.1 bar and ends when 10 % of the maximum pressure increase is reached.

- Main reaction delay (MRD) is considered from t=0 until the pressure increase is 10 % of the maximum pressure increase.
- Main combustion period (MCP) is measured from when the pressure is 10 % of the maximum pressure until 85 % of the maximum pressure increase is reached.
- After burning period (ABP) starts after MCP and continues until 95 % of the maximum pressure increase is achieved.
- End of combustion (EC) is at the point where 95 % of the maximum pressure increase is achieved.

Table 6. Research set-up configuration of CRU in Paper 1

		High pressure
Temperature at fuel injection (theoretical)	°C	590
Pressure at fuel injection	bar	70
Max. pressure	bar	81.2
Injection period, main (LFO, naphtha, kerosene)	µs	1000
Injection period, main (MGO)	µs	1025

Figure 4 shows the above-mentioned CRU parameters in a pressure diagram of LFO.

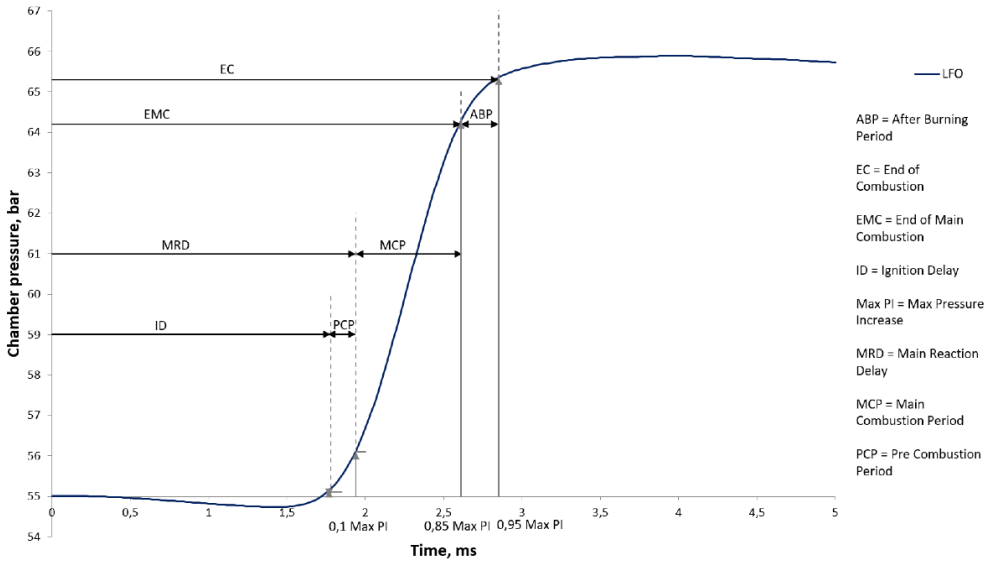

Figure 4. CRU parameters in pressure diagram of LFO

The used combustion research unit is commercially available but specially modified to provide an opportunity to study a wide range of different fuels under variable conditions. The measurements were performed at the fuel laboratory of Wärtsilä Finland Ltd in Vaasa, Finland. The detailed information of the device is not publicly accessible.

To achieve suitable repeatability for the measurements, the first ten measurements were done to set fuel sample and cylinder temperatures, cylinder pressure, injection pressure and duration at each studied measurement point. Then the ten saved measurements were done at each previously defined point. The presented results are the mean values of the ten saved measurements.

3.3.2 Ignition analyser

The CID510 was calibrated according to the standard SFS-EN 16715 (2015) before measuring the fuel samples. The calibration fuel was primary reference fuel, also used for calibration of the traditional cooperative fuel research engine (ASTM D613-24a, 2025).

The following values were recorded: ID period; combustion delay (CD) period; initial pressure in the combustion chamber; temperature of the combustion chamber walls; temperature of the injector coolant; and fuel injection pressure. The chamber was filled with synthetic air. The pressure in the combustion chamber was recorded with a sampling frequency of 25 kHz. The recording was considered to end after 220 ms. The fuel injection period was 2.5 ms.

The fuels were injected into the analyser at room temperature without any pre-preparation. A single measurement step was used for every fuel sample. The step included five preliminary combustion cycles, followed by 15 measurement cycles. One cycle included one fuel injection to the chamber. The preliminary cycles confirmed the calibration settings for the fuel. The average values of 15 measurement cycles formed the results of the ID, CD and DCN as explained below:

- The ID period is assumed to start at the moment when the impulse of injector solenoid control was triggered (t=0). The end of ID is when the pressure in the chamber is 0.2 bar greater than the initial pressure.

- The CD is considered to start at the fuel injection (t=0) and end when 50 % of the pressure increase is achieved in the combustion chamber.

- The DCN was determined by following the SFS-EN 16715 (2015) method, in which the cetane number is derived by using the averages of ID and CD across 15 injection cycles.

The device calculates the derived cetane number (DCN), based on SFS-EN 16715 (2015) from the averages of 15 measurement results of ID and CD values with Equation

$$\mathrm{DCN} = 13.028 + \frac{-5.3378}{\mathrm{ID}} + \frac{300.18}{\mathrm{CD}} + \frac{-1267.90}{\mathrm{CD}^2} + \frac{3415.32}{\mathrm{CD}^3} \quad (3)$$

For LFO, calculated DCN based on the averages of 15 measurement results of ID and CD values, was 56.86.

To estimate measurement uncertainty for calculated DCN(LFO) value, four steps were made based on method given in JCGM (2008). The steps are presented in Appendix 1.

Based on the steps in Appendix 1, the calculated derived cetane number for LFO is 56.86 ±0.68, k=2.

SFS-EN 16715 (2015) states that standard deviation for DCN determined with CID510 method is not different from that published repeatability, *r.* The difference between two test results obtained by the same operator with the same apparatus under constant operating conditions on identical test material in the normal and correct operation of the test method is expected to exceed with an approximate probability of 5 %.

In the standard, repeatability for DCN is given with Equation

$$r(DCN) = 0.01982 \times (DCN - 21) \quad (4)$$

where DCN is the measured DCN value. With mean value DCN of LFO, 56.86, Equation 4 gives *r*(DCN) = 0.71.

When compared to expanded standard uncertainty of LFO (0.68) with 95.5 % probability, we can notice that measured values fall under precision values given in the SFS-EN 16715 (2015).

The DCN results were verified with SFS-EN 15195 (2023) method (IQT, Ignition Quality Tester). The DCN measurements with IQT method were ordered outside the University of Vaasa. In SFS-EN 15195 (2023), the repeatability r for DCN with IQT method with a probability of 95 % is calculated with Equation

$$r(DCN, IQT) = 0.01380 \times DCN \quad (5)$$

For LFO's DCN value of 58, measured with the IQT method, the Equation 5 gives r(DCN, IQT) = 0.80. (The LFO sample patch was the same as in the DCN measurements with CID510.) This analysis, thus, proved that the measurement uncertainty was small enough and the results are reliable.

3.3.3 High-speed non-road diesel engines

All measurements in Paper 3 and 4 were performed under steady operation conditions, without engine modifications. The measurements were conducted based on ISO 8178-4 (2017) standard, known as the non-road steady cycle. Multistage injection was used throughout the studies (pilot, main and post injections).

In Paper 3, additionally, the 25 % load point was measured at an intermediate speed. The default engine control parameters were not suitable with low-viscosity kerosene and neat naphtha, and only intermediate speed and 75 and 50 % load points were achieved. The additional 25 % load point gave more information during the experiment, because engine parameter optimisation was not applied in the study.

The measurements in Paper 4 were conducted at three different engine loads and at two engine speeds. Table 7 gives the chosen operating conditions. Figure 5 depicts the experimental setup.

Table 7. The experimental matrices for high-speed engines in Papers 3–4

Paper	Engine speed (rpm)	2200			1500				Idle
	Load (%)	100	75	50	100	75	50	25	0
3	BMEP (bar)					9.7	6.4	3.2	
	Torque (Nm)					338	225	113	0
4	BMEP (bar)	11.4	8.6	5.7	17.4	13.1	8.7		
	Torque (Nm)	400	300	200	610	458	305		0

LabVIEW system design -software was used to collect sensor data from the engines in Papers 3 and 4. WinEEM diagnostic and service -software controlled fuel injection according to load-speed requests. The injected fuel mass was measured with a digital fuel scale and a clock at every load point once engine operation was stabilised. The average result of 5 minutes fuel consumption was used. A piezoelectric pressure sensor measured in-cylinder pressure: a charge amplifier filtered and amplified the signal, which was then transmitted to a Kistler KIBOX combustion analyser. The crankshaft position was recorded by a crank-angle encoder.

The maximum uncertainty of indirectly measured parameters was calculated using the partial divertive method following the original work by Kline & McClintock (1953). For directly measured quantities, either the device accuracy or standard deviation, which of them was higher, was used for measurement uncertainty. Measurement uncertainties are listed in Table 8.

Table 8. The directly and indirectly measured parameters for high-speed and medium-speed engines in Papers 3–5

Paper	Equipment	Model	Uncertainty	Range
Directly measured				
3, 4	Dynamometer	Horiba WT300	±5 rpm ±2 Nm	0–7500 rpm 1200 Nm
5	Generator	ABB M3LG 450LC	±5 rpm ±2 Nm	0–1007 rpm 10228 Nm
3, 4	Fuel consumption	Digital scale and hand watch	0.03 %	0–60 kg 0–300 s
5		AVL fuel balance	<±0.12 %	0–150 kg/h
3, 4	Crank angle encoder	Kistler 2614B1	±0.02 °CA	
5		Kistler 2614C11	<2 %	0.5 °CA
3, 4	In-cylinder pressure transducer	Kistler 6125C	±0.4 %	0–300 bar
5		Kistler 6613CG1	<±0.5 %	0–250 bar
3, 4	Intake air temperature	K-type thermocouple, Pietiko	-	-200–1100 °C
5		Resistance temperature detector, Nokeval P2T2	-	-50–250 °C
3–5	Air mass flow	ABB Sensyflow FMT700-P	≤ ±0.25 % of measured value	0–5000 kg/h
Calculated				
3–5	HRR, MFB	AVL Concerto Thermodynamics2-macro, uses AVL's own function iThermo2Avl	MFB: ± 5 %	
4, 5	BTE	shaft power output / fuel input power	±1%	

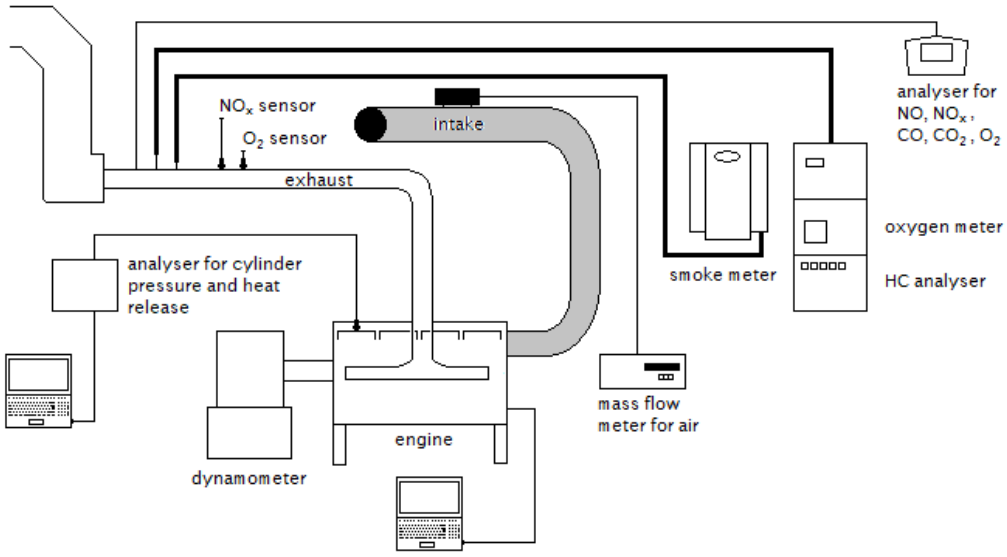

Figure 5. Engine measurement setup in Papers 3 and 4

3.3.4 Medium-speed marine engine

The engine in Paper 5 was driven at a constant speed of 1000 rpm and loaded by an ABB alternator. The maximum engine output was set at 640 kW for the full-load measurements. Four partial loads were also explored, as shown in Table 9. The studied load points followed the test cycle D2 of the ISO 8178-4 (2017) standard. Figure 6 is a diagram of the experimental setup of the medium-speed engine in Paper 5.

Table 9. The experimental matrix for medium-speed engine in Paper 5

Engine speed (rpm)	1000				
Load (%)	100	75	50	25	10
Shaft power output (kW)	640	480	320	160	64
BMEP (bar)	22	16	11	5	2

The measurement system used proper pressure and temperature sensors along the air and exhaust paths. Intake air flow was determined by means of an air nozzle, and fuel flow was measured with a scale and watch. Engine management software, supplied by the engine manufacturer, gathered the sensor data and followed the engine control parameters.

Table 10 lists the instruments used for emission measurements in Papers 3, 4 and 5. Emission instruments were calibrated before and after each measurement. The

engines were allowed to stabilise before taking the parameter recordings. The temperatures of cooling water, charge air in the manifold and the exhaust upstream of the turbine had to be stable. The emission measurement results are average results of 300 seconds after the engine was stabilized.

Table 10. Instruments for emission measurements in Papers 3–5

Paper	Parameter	Instrument	Technology	Uncertainty
4	CO	TSI CA-6203 CA-CALC	Electrochemical	0–100 ppm: ± 10 % 100–5000 ppm: ± 5 %
3, 5	CO	Siemens Ultramat 6	NDIR[a]	± 1 %
4, 5	O_2	Siemens Oxymat 61	Paramagnetic	± 0.25 %
4	NO, NO_X	TSI CA-6203 CA-CALC	Electrochemical	0–100 ppm: ± 10 % 100–4000 ppm: ± 5 %
3, 5	NO_X	Eco Physics CLD 822 M h	Chemilumi-nes-cence	-
3–5	HC	J.U.M. VE 7	HFID[b]	0–100 000 ppm: ± 1 %
3, 4	Smoke	AVL 415 S	Optical filter	± 5 %
5	Particle number	TSI EEPS 3090	Spectrometer	-

[a]NDIR=non-dispersive infra-red, [b]HFID=heated flame ionization detection.

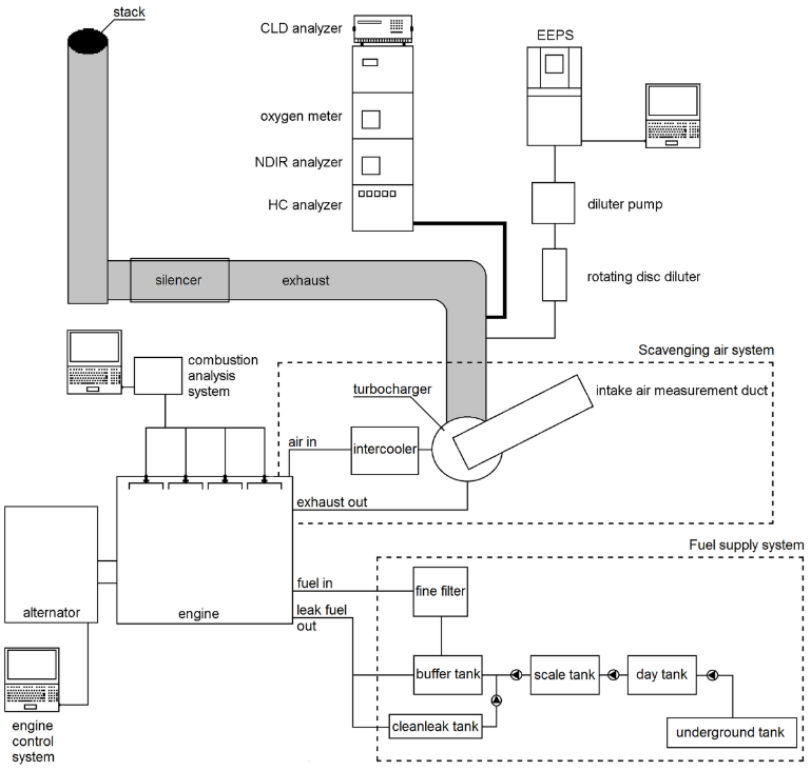

Figure 6. Experimental setup for medium-speed engine in Paper 5

Particle number recordings were split into three one-minute recordings. The uncertainty of PN measurement was approximated by calculating the standard deviation of PN averages, taken from each one-minute recording.

3.4 Processing the engine performance data

In Papers 3–5, a net heat release rate (HRR) and the mass fraction burned (MFB) were calculated via AVL Concerto's data-processing platform. Figure 7 shows the data post-processing routine. The used macro was Thermodynamics2: the smooth function was not used. The library functions have been used in the calculations.

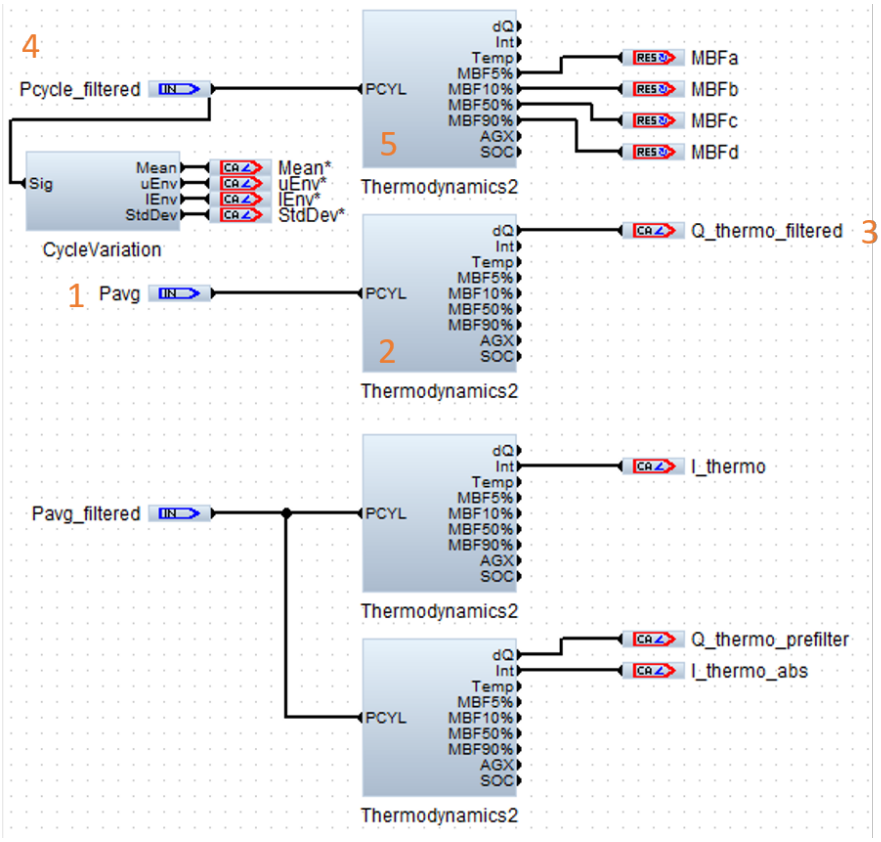

Figure 7. Data post-processing routine in AVL Concerto

The crank-angle encoder (Kistler 2614B1) used in Papers 3 and 4 (high-speed engine measurements) has a resolution of 0.1°CA. The encoder used for Paper 5's medium-speed engine measurements (Kistler 2614C11) has a resolution of 0.5°CA but this can be improved to 0.1°CA through the software. The calculation starting point was set to 30°CA before top dead centre and its end point to 90°CA after top dead centre.

Turning to the HRR results, the average values of in-cylinder pressure (100 consecutive cycles) were calculated first (1). Thereafter, the Thermodynamics2 -macro was used to calculate HRR values (2). The macro used a calculation resolution of 0.2°CA. Finally, the HRR curve was filtered with a digital low-pass filter (2500 Hz in Papers 3 and 5, 2000 Hz in Paper 4) (3).

In contrast, for the MFB results, pressure values were first filtered with a digital low-pass filter (4) and then the Thermodynamics2 -macro was used (5). The average values of 100 cycles were not used for MFB results, establishing the standard deviations.

4 RESULTS

This chapter presents the research results from Papers 1–5. The results are divided into three sections: Ignition studies (Papers 1 and 2), High-speed engine experiments (Papers 3 and 4) and Medium-speed engine experiments (Paper 5). This thesis primarily focuses on the results of renewable naphtha and recycled MGO. Although some results are also examined relative to those of renewable diesel (HVO). LFO works as the main baseline reference.

4.1 Ignition studies

This section presents the results of the ignition studies in the combustion research unit (CRU) and in two different ignition analysers. The CRU results are based on Paper 1 and the results of ignition analysers are based on Paper 2.

4.1.1 Combustion research unit

The CRU chamber pressure curve in Figure 8 presents the measured results under high chamber-pressure conditions for LFO, MGO, renewable naphtha and kerosene.

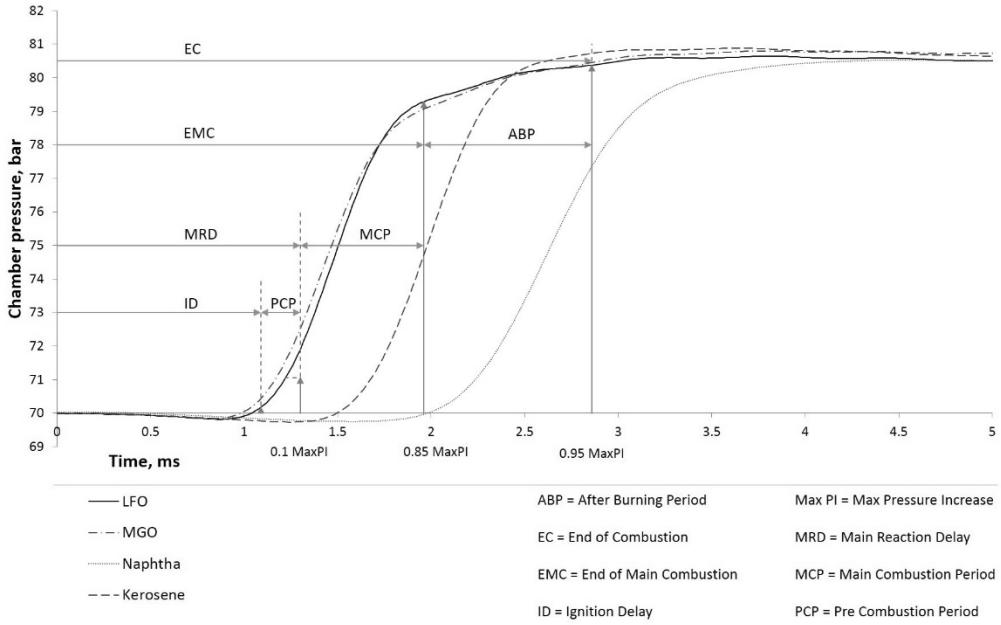

Figure 8. Chamber pressure diagrams of LFO, MGO, naphtha and kerosene at high chamber-pressure

The injection durations of the fuels were identical, except for MGO (+2.5 %), but the amount of the fuel during injection varied due to the different fuel viscosities.

MGO had the shortest ignition delay (1.04 ms) due to the significantly higher CN (68). LFO showed an ID of 1.08 ms (CN 52–58); naphtha's was 2.04 ms (CN 34). A longer ID in engine operation allows more fuel to be injected which, once ignited, usually gives a faster pressure rise and a higher peak pressure. These characteristics are associated with increased noise, malfunctions in engine operation and eventually engine damage (Kuszewski, 2019; Ogawa et al., 2017; CIMAC, 2011). The recorded IDs followed the fuels' CN values.

The main combustion period (MCP) lasted 0.98 ms for MGO, 0.78 ms for naphtha and 0.74 ms for LFO. The distillation curve of naphtha-LFO blend in Figure 9 shows that due to the light fractions of naphtha, the distillation started already at approximately 50 °C and ended at 350 °C. This curve reflects the measured results: lighter fractions of naphtha burn rapidly after ignition. However, renewable naphtha is a mix of lighter and heavier fractions of hydrocarbons. According to Bergeron & Hallett (1989), the higher mass components of a fuel also have longer ignition delay times. The heavier fractions distil later and might hinder the progress of total combustion. Additionally, fuel's heavier fractions might affect emissions by increasing hydrocarbon (HC) and carbon monoxide (CO) emissions. (Sirviö, 2018; Kalghatgi, 2014).

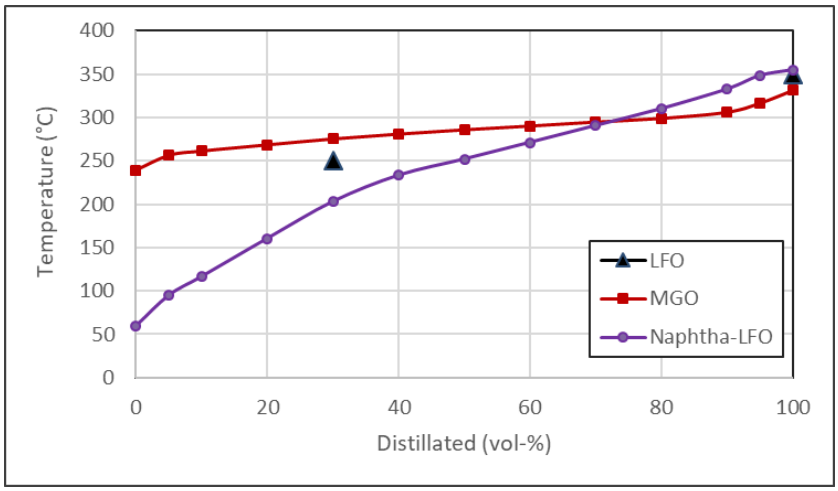

Figure 9. Distillation curve of LFO, MGO and renewable naphtha-LFO blend

Figure 10 shows the rate of heat release (ROHR) curves as converted to pressure rises versus time in the combustion chamber. MGO showed a maximum rate of heat release (MaxROHR) of 15.2 bar/ms; naphtha's was 11.7 bar/ms; and LFO's was 16.3 bar/ms. Although naphtha's main combustion period was fairly short, the shape of the MaxROHR curve shows that naphtha as a whole burned slower than the other fuels. The results depicted in Figures 8 and 10 are listed in Table 11, without kerosene's readings.

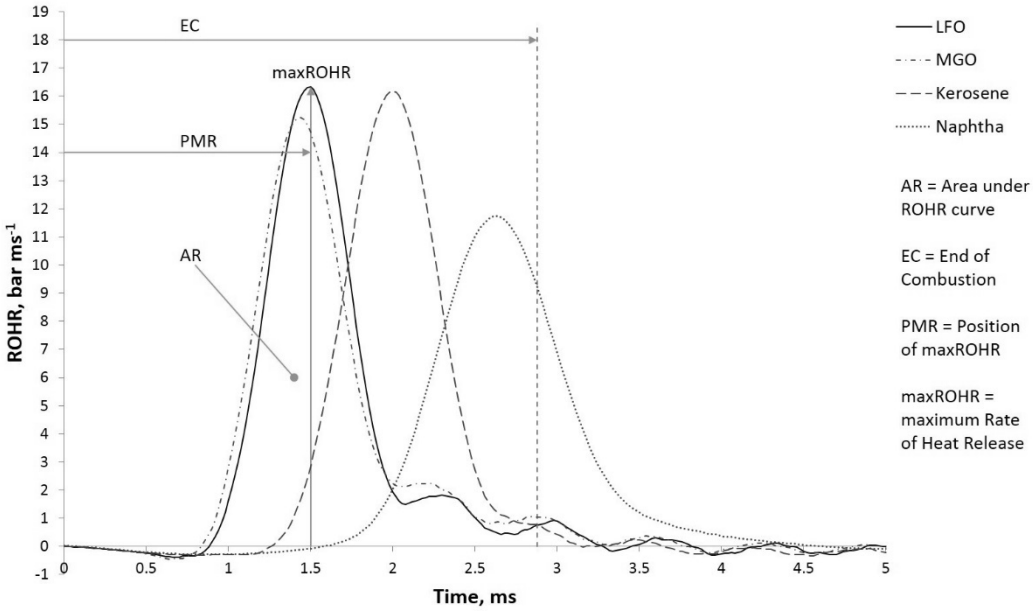

Figure 10. Rate of heat release curve of LFO, MGO, naphtha and kerosene at high pressure

Table 11. CRU measurement results

Chamber conditions 70 bar / 590 °C		LFO	MGO	naphtha
Ignition Delay (ID)	ms	1.08	1.04	2.04
Main Combustion Period (MCP)	ms	0.74	0.98	0.78
End of Combustion (EC)	ms	2.88	3.02	3.3
Max. Rate of Heat Release (MaxROHR)	bar/ms	16.3	15.2	11.7

Based on these CRU measurements, circular economy-based MGO produced very similar results to LFO and can be used like LFO in a compression-ignition engine without any modifications to the engine or injection system. Naphtha in a compression-ignition engine requires other fuel for starting and stopping the engine. Its low CN and low viscosity may limit naphtha's use as a drop-in fuel in compression-ignition engines because the retarded start of combustion and prolonged ignition delay may cause malfunctions in engine performance and increase noise and peak firing pressure (Mohammed et al., 2023; Subramanian et al., 2018). Fuel additives or blending may be needed to improve the ignition characteristics, i.e., to reduce ignition delay, leading to lower combustion temperature and thus less NO_X emissions (Mohammed et al., 2023; Subramanian et al., 2018).

In the studies of this dissertation, renewable naphtha was blended with low-sulphur LFO to enable its safe use in compression-ignition engines. Blending neat renewable naphtha with LFO (CN 52–58) produced a blend with a CN of 51 (Paper 3) or 52 (Paper 5). Both these values satisfy the SFS-EN 590 (2022) fuel standard relating to CN.

4.1.2 Ignition analysers

The auto-ignition properties of nine marine and power-plant fuels were determined with the Herzog by PAC Cetane Ignition Delay 510 instrument (CID510). The measured values were ignition and combustion delay periods (ID and CD respectively). The device calculates the derived cetane number (DCN), based on the ID and CD. The DCN results were verified with the IQT-method (SFS-EN 15195, 2023). The main goal was to determine if the CID510 generates sufficiently accurate information about the ignition properties of various marine and power-plant fuels.

Figure 11 illustrates the correlation between the DCN and ID, as determined by the CID510. It shows the DCN and ID correlated quite well for some fuels. The lowest DCN (Fuel 5) had the longest ID, while the shortest ID was for Fuel 3, which had the highest DCN. The highest DCN – 68, was measured for MGO. Renewable naphtha had the lowest DCN, of just 34, which is below SFS-EN 590's (2022) limit. LFO had a DCN value of 58 and HVO 62. The naphtha-LFO blend (20 vol.-% naphtha, 80 vol.-% LFO) had a DCN value of 52.

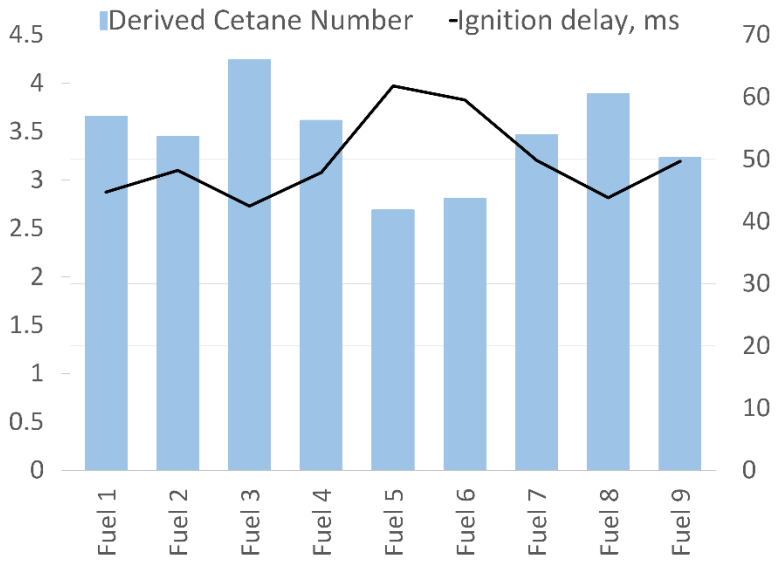

Figure 11. Measured ID and DCN values: ID on the left y-axis, DCN on the right

Furthermore, the CID510 results were fairly similar to those measured with other standardised methods. Figure 12 shows the correlation between the DCN values

determined by the CID510 and the IQT -methods. Both gave the same DCN for Fuels 6 and 7, despite the fuels having rather different properties. Fuel 6 had low viscosity and density, but a high sulphur content and LHV: renewable Fuel 7 had a high density and low LHV, but a low sulphur content.

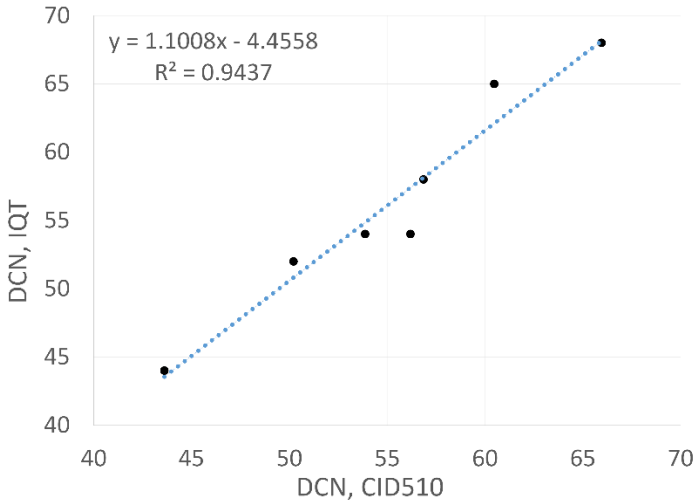

Figure 12. DCN correlation between CID510 and IQT -methods

The correlation seen in Figure 12 confirms that a wide range of fuels can be measured with both methods and the results are fairly satisfactory. The main difference between the methods is that CID510 uses a modern, high-pressure common-rail fuel injector, whereas IQT uses a lower pressure mechanical injector.

The calculated derived cetane number for LFO is 56.8 ±0.68, k=2, for MGO 65.96 ±1.53, k=2 and for naphtha-LFO 50.21 ±1.12, k=2.

MGO's DCN was 68 with IQT-method and 64.43–67.49 with CID510 method. European Standard for CID510-method (SFS-EN 16715, 2015) covers the DCN range from 67 DCN to 39 DCN. MGO's DCN at the upper limit of the standard's range might have caused higher measurement uncertainty to MGO's DCN results compared to LFO. Neat naphtha, instead, had a low DCN (34) that also might have affected the blend's higher measurement uncertainty of DCN compared to LFO. However, both fuels were in line with the IQT's DCN range from 76.8 DCN to 33.9 (SFS-EN 15195, 2023).

4.2 High-speed engine experiments

This section presents the results of two different sets of high-speed engine measurements. The first results are from combustion studies which examined the effects of several alternative liquid fuels on engine performance and gaseous exhaust

emissions. This study is based on Paper 3. The second results are from Paper 4's study, evaluating three different injector nozzles in a high-speed, non-road diesel engine.

4.2.1 Combustion studies with several alternative liquid fuels

The study focused on how the use of various alternative fuels affects combustion. It determined fuels' combustion characteristics in terms of an engine's in-cylinder pressure, the rate of heat release, mass fraction burned and combustion duration. The main results of gaseous exhaust emissions are also provided, based on the article of Ovaska et al. (2019). The studied fuels were LFO (baseline); recycled MGO from used lubricant oils; renewable wood-based naphtha and its blend with LFO; renewable diesel (HVO); rapeseed methyl ester (RME); and kerosene. The discussion of the results primarily concentrates on three of these fuels: MGO, naphtha and the naphtha-LFO blend, but few observations are also made about HVO.

A three-stage injection strategy was used for all fuels: pilot, main and post injections. The pilot started at 6.8 ± 0.1°CA before top dead center (BTDC) and ended at 4.1°CA BTDC. The main injection started at exactly 0.9°CA BTDC. Its duration varied, not only with the load, but also according to the fuel's heating value. The durations for all fuels, except RME, were very similar, at 4.8 to 7.7°CA according to engine load. The start of the post injection was linked to the end of the main injection. The duration of post injection varied only slightly in the range of 3.3°CA to 3.6°CA and was independent of the load.

Figures 13a and 13c depict the cylinder pressure traces; Figures 13b and 13d show the HRR curves. First of all, the maximum cylinder pressures were almost equal with all fuels, i.e. the relative standard deviation between the fuels was 1.2 %, both at the lowest load (3.2 bar BMEP) and the highest load (9.7 bar BMEP). The low load's HRR curve shows that the ID of naphtha was the longest, most probably due to the fuel's low CN. Thereafter, naphtha seemed to burn quickly, most likely due to its light, high-volatile compounds and the favourable effects of its low viscosity on fuel-air mixture formation. The distillation curve (Figure 9) shows naphtha-LFO blend's distillation starting point at approximately 50 °C, indicating that the blend included easily evaporated lighter compounds which burned rapidly after the longest ID. MGO showed a slightly earlier initial HRR than LFO and the naphtha-LFO blend. At high load (9.7 bar BMEP, Figures 13c and 13d), neat naphtha showed a higher initial HRR than other fuels.

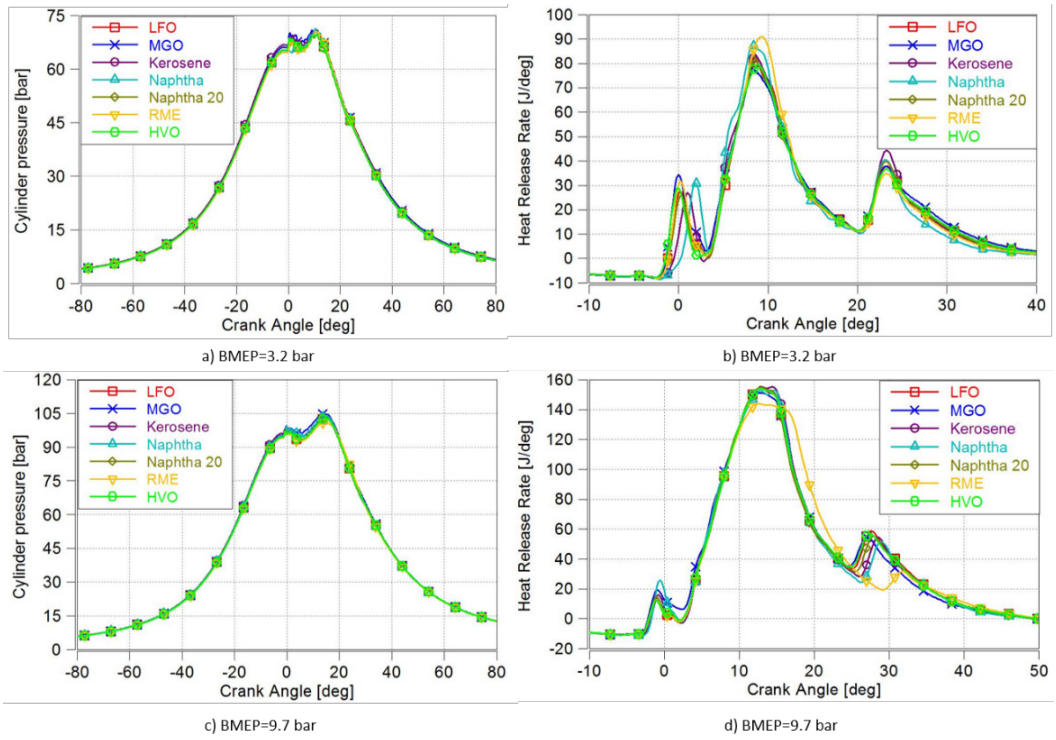

Figure 13. In-cylinder pressure and heat release rates at the lowest and highest engine loads

Combustion duration was characterised as the crank angle between the mass fraction burned at 5 % (MFB5 %) and MFB50 %. Figure 14 shows the results, linearly correlated for all fuels at constant engine speeds. MFB5 % occurred after the end of main injection for all fuels at all loads. MFB10 % and 50 % were reached before post injection. The relative standard uncertainty for MFB5 or MFB50 % for all fuels at all load engine load/speed points did not exceed 2 %.

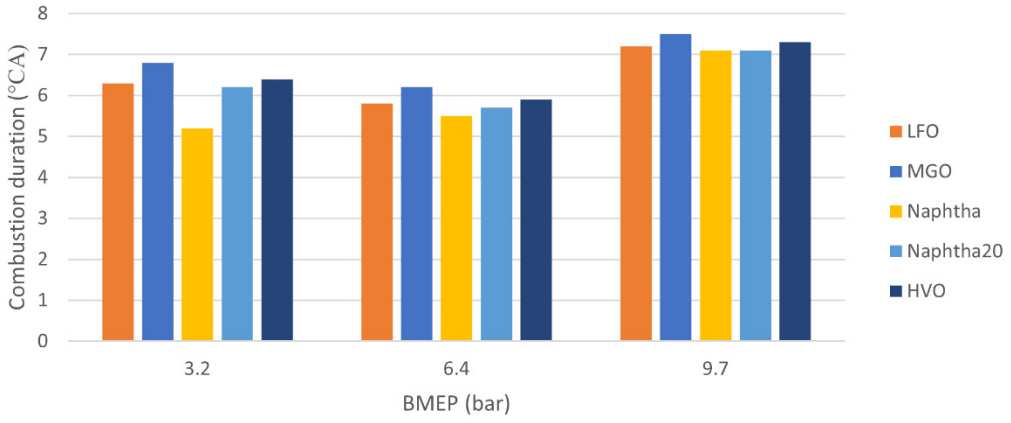

Figure 14. Combustion duration at different engine loads, determined as crank angles between MFB5 % and MFB50 %

At low load, the shortest combustion duration was for neat naphtha. Despite its lengthened ID due to low CN, naphtha's light fractions burned rapidly, resulting in a short combustion duration. The longest combustion durations were measured for MGO. One reason could be that its higher viscosity curbed fuel-air mixing. When the engine load was increased to medium load, combustion duration shortened. Again, neat naphtha had the shortest combustion duration while MGO had the longest.

At high load, combustion duration was prolonged due to an increase in fuel quantity (Prakash et al., 2015). The longest combustion duration was measured for MGO; the combustion duration of naphtha and naphtha20 (a blend of naphtha and LFO) was shorter. Although naphtha's low CN increased the ID, the blend burned rapidly due to improved premixed combustion (Vallinayagam et al., 2017) and the high fraction of light hydrocarbons. HVO, the drop-in fuel for compression-ignition engines (Spoof-Tuomi et al., 2021), showed a slightly longer combustion duration than the baseline LFO. Overall, HVO gave fairly similar combustion performance as LFO.

Ovaska et al. (2019) used the same engine measurements as in the current study to examine the effects of alternative diesel fuels on exhaust particle size distributions and on gaseous emissions. The smoke numbers were also recorded. The gaseous emission results (Figures 15 and 16) are cycle-weighted brake specific emissions of HC, CO and NO_X, calculated according to the non-road steady cycle.

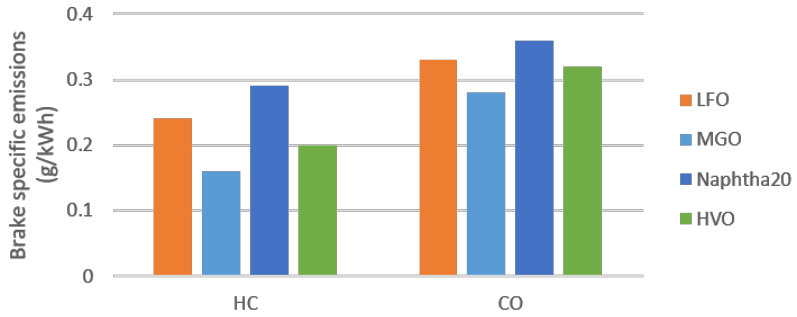

Figure 15. Cycle-weighted brake specific emissions of HC and CO

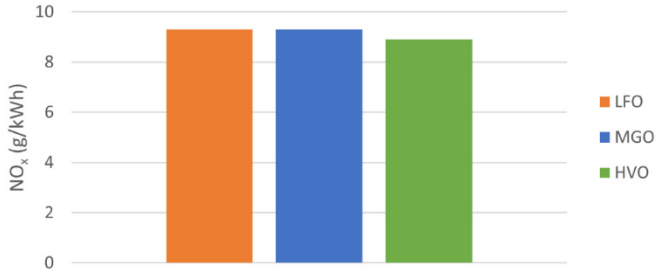

Figure 16. Cycle-weighted brake specific emissions of NO_X

MGO emitted less CO and HC than HVO, LFO and the naphtha-LFO blend. In general, NO_X emissions were lowest with HVO, while MGO's and LFO's NO_X results were both slightly higher and on a par with each other.

The smoke numbers were very low and varied, as follows:

- LFO, 0.014–0.038
- MGO, 0.014–0.033
- naphtha-LFO blend, 0.011–0.031
- HVO, 0.013–0.031

Ovaska et al. (2019) reported that for all fuels, the measured total particle number (TPN, from 5.6 to 560 nm) decreased when the engine load decreased from full load to 75 % load (Figure 17). Almost similar results were obtained for 50 % load point as at 75 % load. TPN increased clearly when load decreased further to 10 %. The naphtha-LFO blend was very competitive with neat LFO, while MGO generated the highest TPN at all loads.

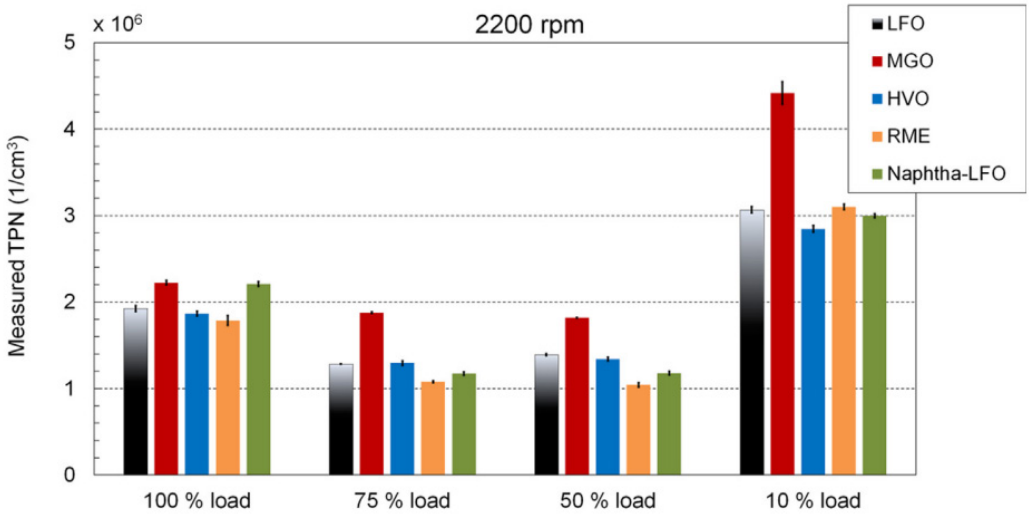

Figure 17. Measured TPN at rated speed (Ovaska et al., 2019)

4.2.2 Combustion studies with various injector nozzles

Paper 4's study compared and evaluated how three different injector nozzles affected the combustion and emissions of a high-speed, non-road diesel engine with common-rail injection. Commercial, low-sulphur LFO was used as fuel for this comparison.

The nozzles had 6, 8 and 10 holes with different orifice diameters, but the same mass flow rate (1.2 l/min at 100 bar) and the same spray angle (149°) Table 5 lists the nozzles' specifications. Measurements were made at three engine loads, each at two engine speeds. Table 12 sets out the injection strategy. The pilot injection was before top dead centre for all loads, while main injection occurred after top dead centre. Overall, the differences in the main injection durations of all three nozzles did not exceed 1°CA. Pilot injection durations increased when the engine load decreased.

Table 12. Injection strategy at different engine loads and speeds in Paper 4

	Engine speed (rpm) / load (bar BMEP)					
Injection phase	2200			1500		
	11.4	8.6	5.7	17.4	13.1	8.7
Pilot			x	x	x	x
Main	x	x	x	x	x	x
Post				only 8-hole nozzles	x	x

Figure 18 shows the HRR curves for the studied nozzles. At 2200 rpm, the ID seemed to be slightly longer for the 6-hole nozzles than the others at the medium and low loads. No difference in ID was noticed at high load. At 1500 rpm at all loads, the HRR of the 6-hole nozzle peaked later than the HRR of the other nozzles. There were discernible differences in the HRR between the 8- and 10-hole nozzles curves only at the highest load. At high loads at both speeds, the 6-hole nozzles led to the shortest combustion duration (MFB 5–50 %, Figure 19). Generally, the combustion duration of the 8-hole nozzle was placed in the middle of 6- and 10-hole nozzles, although the 8-hole nozzle gave the shortest combustion duration at low power, i.e., lowest load/speed. The relative standard uncertainty with MFB5 and MFB50 % did not exceed 5 % with any studied nozzles.

The maximum cylinder pressures were very similar for all three nozzles at all the measurement points. Differences in the brake thermal efficiency between the nozzles were minimal, the relative standard deviation did not exceed 2 % at any engine load/speed points.

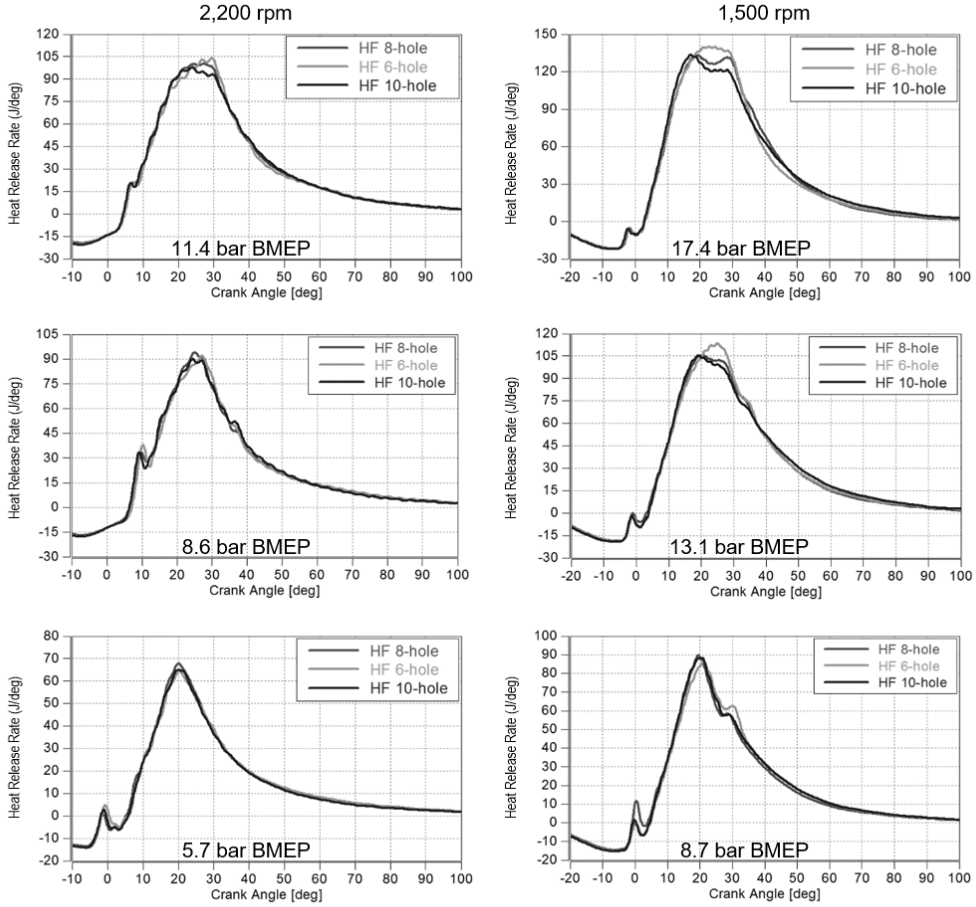

Figure 18. Heat release rates at the high (2200 rpm) and lower (1500 rpm) speeds

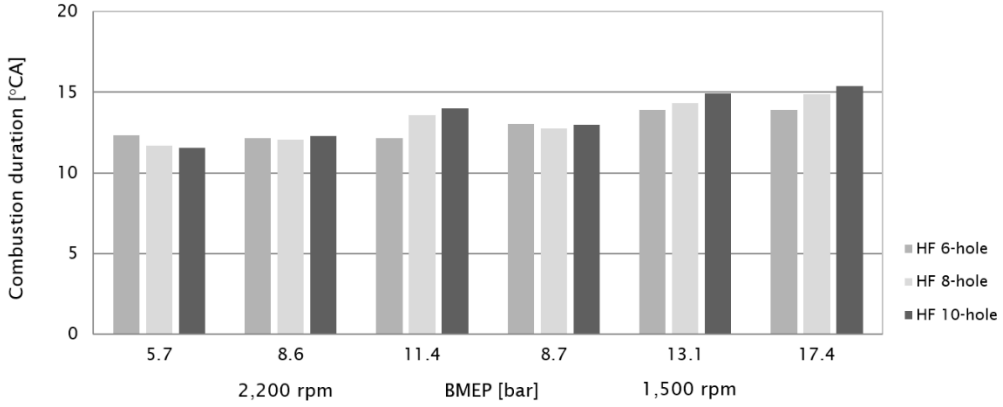

Figure 19. Combustion duration at all engine loads, determined as crank angles between MFB5 % and MFB50 %

4.3 Medium-speed engine experiments

This section discusses the results obtained from Paper 5's study of sustainable fuel options in a medium-speed engine. The fuels were marine gas oil (MGO) derived from the circular economy; and a blend of renewable naphtha and low-sulphur light fuel oil (LFO). Neat LFO served as the baseline fuel. The composition of the naphtha-LFO blend was slightly different from the 20 vol.-% naphtha blend used in the high-speed engine: the blend for the medium-speed engine contained 26 vol.-% of naphtha.

The medium-speed engine ran using similar engine settings with each fuel and without exhaust aftertreatment. The combustion characteristics were examined in terms of the rate of heat release (HRR); mass fraction burned (MFB); and brake thermal efficiency (BTE). The main results of gaseous exhaust emissions also are discussed including the exhaust particle size distributions and total particle number.

Figure 20 presents the HRR for all three fuels at 75 % load. The initial premixed peak of the naphtha-LFO blend was slightly higher than that of MGO and LFO. The initial combustion followed well the differences in CN: the lower the CN, the higher the premixed peak. In general, combustion progressed in a very similar manner with all the fuels.

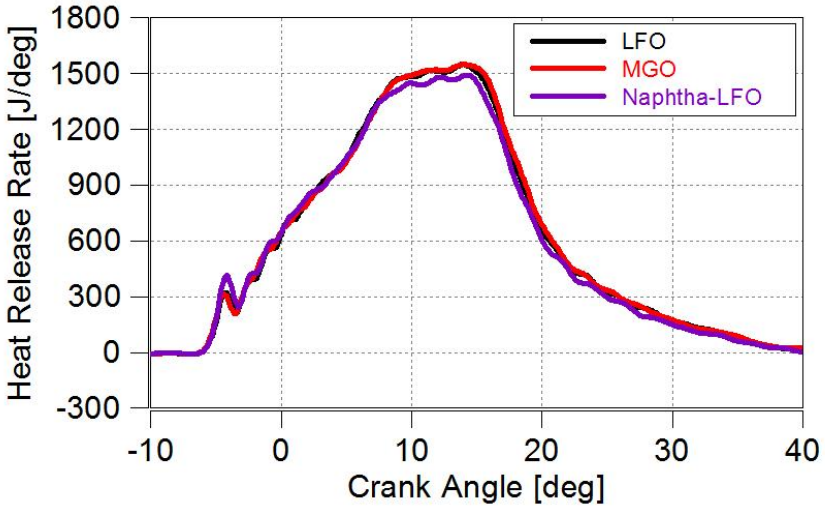

Figure 20. Heat release rate versus crank angle at 75 % load for studied fuels

The MFB values were calculated based on average values of 100 consecutive engine cycles. Figure 21 shows that the MFB50 % points were at very similar crank angles for all fuels at each of the five loads. At 16 bar BMEP, the relative standard deviation of MFB 50 % ranged from 1.8 % (LFO) to 2.5 % (blend). Injection timing varied at each load, which explains why the MFB50 % point also varied between the loads. The

injection timing was at 9°CA BTDC at half-load and lower but was advanced to 14°CA BTDC at higher loads.

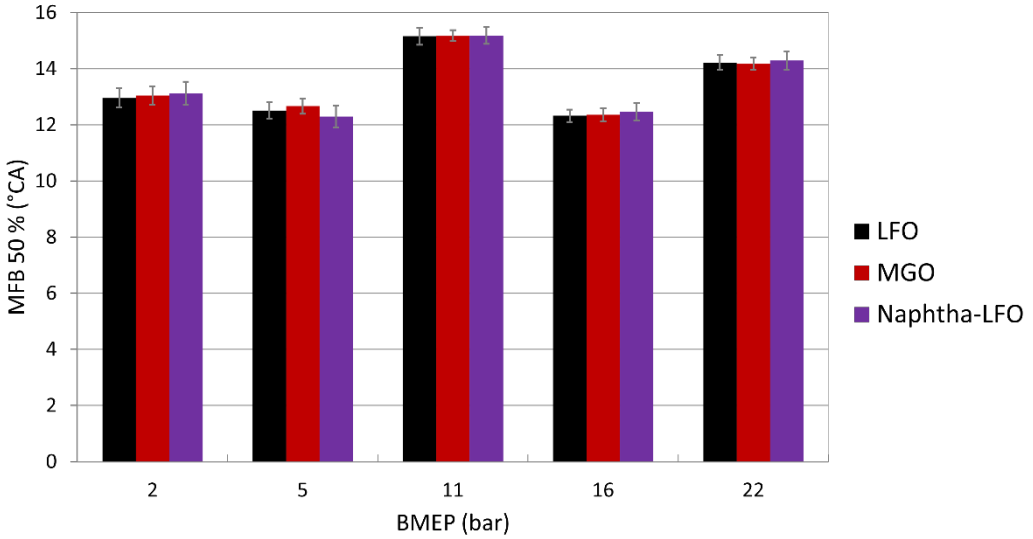

Figure 21. Crank angles for 50 % mass fractions of burned fuel at various engine loads

The engine's BTE also was very similar, irrespective of the fuel used. It was 40–41 % at full load and 36 % at half load. LFO and the blend showed a shade higher BTE than MGO at many loads, but the differences were within the measurement uncertainty.

Figure 22 illustrates the cycle-averaged emissions, calculated according to the D2 test cycle of the ISO 8178-4 (2017) standard. The NO_X emissions were almost the same for all the fuels. MGO's HC was the lowest; LFO showed the highest HC. The naphtha-LFO blend's CO was the lowest while MGO produced most CO. Overall, the HC and CO emissions also were quite similar for all the compared fuels.

The emissions of methane (CH_4) and nitrous oxide (N_2O) are important from the greenhouse gas emission perspective. Figure 23 presents the wet exhaust methane contents at various engine loads. It is immediately apparent that methane decreased with increasing engine load. The naphtha-LFO blend emitted less methane than LFO and MGO, especially at high loads. Methane contents were, however, very low, at below 5 ppm.

Wet exhaust contents of nitrous oxide also were negligible, at well below 1 ppm at all the loads. The highest recorded content was only slightly above 0.5 ppm, within the measurement accuracy of the FTIR analyser. No clear trend was detected between the fuels.

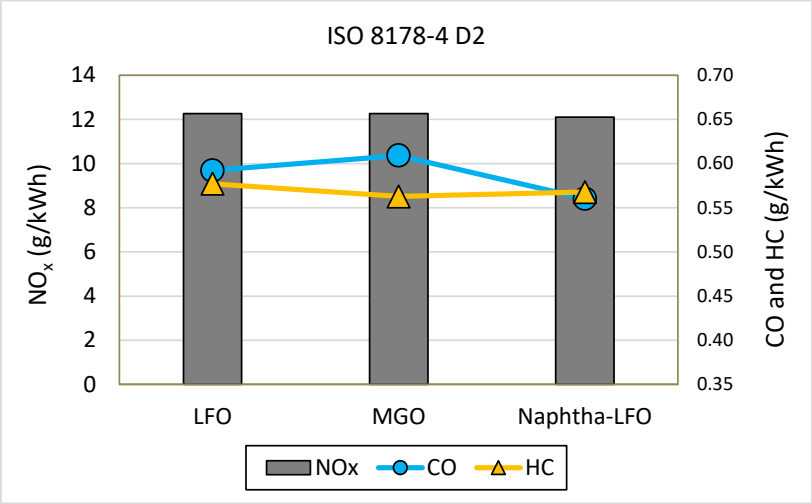

Figure 22. Calculated cycle-averaged brake specific emissions for the studied fuels

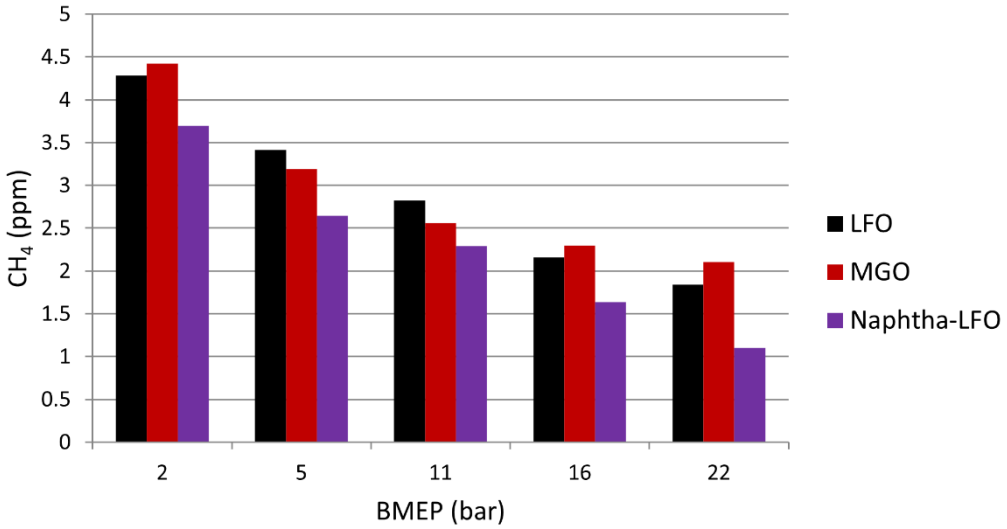

Figure 23. Wet exhaust methane contents versus engine load with different fuels

Figure 24 shows the exhaust particle size distributions for the studied fuels. The exhaust did not contain high numbers of nucleation mode particulates, but the peaks of the accumulation mode were usually higher by two orders of magnitude than those of the nucleation mode. The size distributions peaked within the size range of 30 to 50 nm at loads of up to 75 % load. However, the peak of every fuel moved towards larger particles of approximately 80 nm at full load.

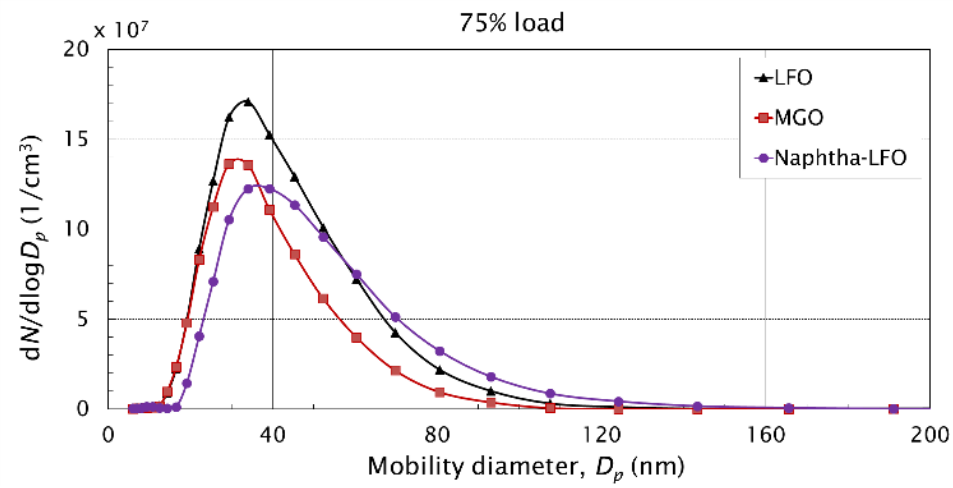

Figure 24. Exhaust particle size distributions for different fuels at 75 % load

Figure 25 presents total particulate number (TPN) within the size range of 5.6 to 560 nm for each of the three fuels. At low loads, TPN was the lowest with MGO and the highest with LFO. From 50 to 100 % load, MGO and naphtha-LFO blend generated almost similar TPNs, and clearly lower than LFO. It is apparent that blending LFO with naphtha resulted in a clear reduction in particulate number.

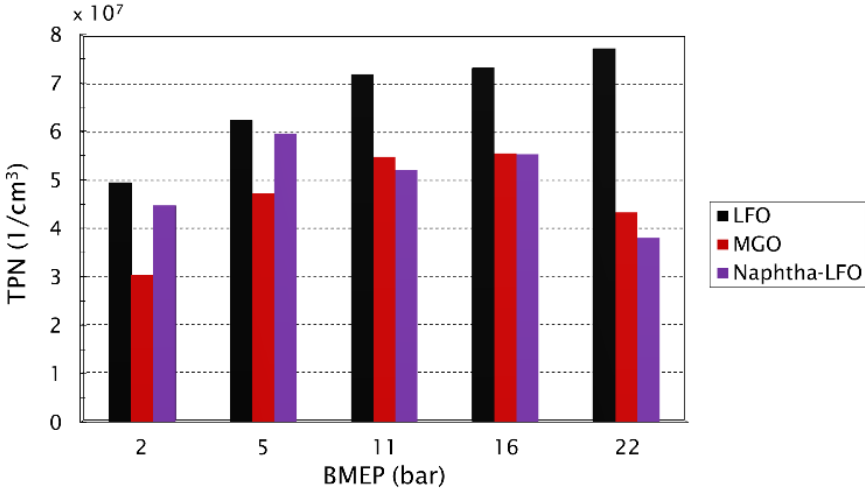

Figure 25. Total particulate number (TPN) of exhaust within the particle size range of 5.6 to 560 nm

5 DISCUSSION

In the ongoing energy transition, alternative fuels are an important part of internal combustion engine development work towards better combustion, more efficient exhaust aftertreatment and control systems (Reitz et al., 2019; Gabiña et al., 2019; Gilkes, 2019; Kalghatgi, 2018; Llamas & Eriksson, 2018). It is vital to analyse their various properties before using alternative fuels in compression ignition engines. Earlier studies of and experiences from conventional fuels of compression-ignition engine have shown that some fuel properties directly affect ignition delay and in-cylinder combustion, impacting engine performance, exhaust gas composition and safety (Heywood, 2018; Mueller et al., 2014; CIMAC, 2011). Therefore, appropriate use of recycled and renewable fuel alternatives requires continuous studies to understand their impact on combustion – especially on ignition delay and in-cylinder combustion. This dissertation focuses in particular on marine gas oil (MGO) derived from waste lubricating oils; and naphtha manufactured from crude tall oil (CTO). Naphtha was investigated both in its neat form and as blends with low-sulphur diesel fuel oil (LFO).

This research of alternative fuels' ignition and combustion performance in compression-ignition engines started with comprehensive fuel analyses. This was followed by ignition studies using a constant-volume combustion chamber (CVCC, Paper 1) and two different cetane analysers (Paper 2). These studies formed the basis for the selection of alternative fuels for further experiments in a high-speed engine (Paper 3) and a medium-speed engine (Paper 5). Fuel injection is one of the most critical elements when ascertaining if an engine needs to be modified and optimised for new fuels. Accordingly, three different injector nozzles were studied to provide wider knowledge of how the nozzle's hole number affects combustion and emission formation (Paper 4).

5.1 Effect of fuel properties on ignition and combustion in ignition analysers

The studies with a CVCC (Paper 1) showed that MGO had the shortest ignition delay, neat naphtha the longest, and LFO was between them. The results were a logical reflection of the cetane numbers. MGO derived from the circular economy proved to be a suitable neat drop-in alternative for compression-ignition engines in terms of its ignition delay and combustion duration. Naphtha, in turn, will serve as a renewable blending component for conventional fuels. The sections below discussing the engine experiments will consider the effects of ignition delay, combustion duration and other properties of these two alternative fuels in real engine use.

The ignition quality of a number of fuels was also measured with two different ignition analysers, a CID510 instrument and the IQT-method (Paper 2). The results from these two standardised ignition analysers confirmed that both methods can measure a wide range of fuels. The main difference between the methods is that CID510 uses modern, high-pressure, common-rail fuel injection instead of IQT's lower-pressure mechanical injector. The main advantage of CID510 and IQT -methods compared to a conventional cooperative fuel research engine is their fully automated, user-friendly interface. This makes measurements easy and cost-effective, thus enabling ignition studies of research fuels which may be only available in small quantities. The high R^2 -value of the correlation between the CID510 and the IQT-method verifies the suitability of CID510 for studying ignition quality of engine fuels.

The studies in Papers 1 and 2 provide no evidence to indicate that fuel viscosity directly affects the ignition delay (ID) or combustion delay (CD). For example, the aviation fuel in Paper 2 had the lowest viscosity but still had a long ID. One of the marine gas oils with a typical viscosity had an even longer ID. Renewable naphtha blend with LFO also had a low viscosity but a fairly average ID. The highest DCN and the shortest combustion delay was measured for one of the marine gas oils, although its kinematic viscosity was almost twice as high as another MGO which had the lowest DCN and the longest combustion delay.

The present study did not measure the possible, but improbable, content of CN improver. Such an improver may distort the results, so additional measurements are needed to enable a more precise device comparison.

5.2 Measurements with high-speed non-road engine

Paper 3 deals with combustion studies of a high-speed, non-road diesel engine with selected alternative fuels. Drawing on the results from Papers 1 and 2, naphtha was selected for blending with LFO to improve the ignition characteristics, i.e., to reduce ID. The blend comprised 20 vol.-% naphtha and 80 vol.-% LFO. Neat naphtha was also included in the engine experiments.

MGO derived from waste lubricating oils had the highest viscosity and also had a rapid start of combustion, due to its high CN. But its MFB50 % value was the latest at the low engine load, resulting in the lowest HRR peak. The maximum cylinder pressures were almost equal with the studied fuels. MGO's high viscosity with its high sulphur content may be a limiting factor in engine use. The high viscosity may have led to poorer fuel-air mixing, thus causing more inhomogeneity zones and leading to lower HRR and longer combustion duration compared to other studied fuels (Tira et al., 2012). MGO also had the longest combustion duration (MFB5–50 %) at the higher

in-cylinder temperature when the engine load was increased. However, as ignition studies in Papers 1 and 2 stated, viscosity does not directly affect the ID or combustion delay. The lower HRR of MGO may be caused by the short ID that shortened premixed combustion phase causing poorer fuel-air mixing and increased amount of inhomogeneity zones and longer combustion duration with lower HRR. Similarly, Gabiña et al. (2019) measured longer combustion duration for waste oil-based diesel-like fuel than for DFO in a marine scale diesel engine. The combustion period started slightly earlier and ended slightly later with the diesel-like fuel. The authors attributed this to diesel-like fuel's higher CN, which implied a shorter ID with a shorter premixed combustion phase, involving a lower pressure gradient, combustion pressure and HRR.

As a whole, differences in the IDs and combustion durations between the fuels diminished and became less clear when engine load increased. Overall, MGO can be considered as a drop-in fuel in a compression-ignition engine without any engine or injection system modifications: it offers very similar combustion performance to the LFO reference fuel. MGO also improved cycle-averaged HC, perhaps due to its high CN (Niemi et al., 2011). CO and smoke emission also improved relative to LFO. However, MGO's slightly higher sulphur content caused the highest total particle number at all loads at rated speed. The higher sulphur and lower lubricity can be limiting factors for its use in some applications, especially if low-load operation is particularly important.

Renewable neat naphtha benefits from the favourable effects of low viscosity on fuel-air mixture formation. Thus, after a long ID due to a low CN, naphtha burned fast due to smaller droplet sizes and faster vaporisation characteristics (Sonawane et al., 2023; Agarwal et al., 2013;Chen et al., 2013; Lee et al., 2012). Nevertheless, despite these advantages, naphtha's excessive ignition delay limited the achievable engine load.

The naphtha-LFO blend had a slightly shorter combustion duration than LFO, and it retained the efficient ignition of LFO. The blend ignites easily and the combustion is efficient by also lowering smoke emissions. The blend's hydrocarbon (HC) and carbon monoxide (CO) emissions were the highest of the tested fuels, remaining still low in an absolute scale, however. Sirviö (2018) and Kalghatgi (2014) mentioned that fuel's heavier fractions might affect emissions by increasing HC and CO emissions. Total particle number reduced with naphtha-LFO blend and was competitive with LFO. Ovaska et al., (2019) explained the lower TPN with clearly lower density of the blend than neat LFO. Naphtha-LFO blend is suitable for compression-ignition engine use if safety issues associated with naphtha's low flashpoint can be resolved.

5.3 Effect of injector nozzle hole number on ignition and combustion in high-speed non-road engine

Paper 4 set out to analyse three different injectors, where only the number of nozzle holes and orifice diameter varied, but the flow rate was constant. The used fuel was LFO. Reducing the nozzle hole number and their diameter has been shown to improve fuel atomisation, accelerating combustion and leading to increased HRR (Dong et al., 2018; Heywood, 2018; Sarvi et al., 2008; Jääskeläinen, 2017). Thus, ID and combustion duration depend closely on the nozzle characteristics. However, optimal injector parameters depend on the engine type and require modern simulations that must be still verified with engine testing to ensure optimal nozzle performance.

Paper 4's results indicated that reducing nozzle hole number did not affect heat release rate. Combustion durations were almost similar for all three nozzles. The differences in the maximum cylinder pressures and BTE were also minimal.

Overall, the selection of a suitable injector nozzle depends on the engine use and performance requirements. Selection criteria can be, for example, engine operating profile, exhaust gas system requirements or the fuel used. When gaseous and particulate matter (PM) emissions are reduced by using aftertreatment devices, such as a diesel oxidation catalyst, selective catalytic reduction or a diesel particulate filter, the exhaust gas through an aftertreatment system (e.g. selective catalytic reduction) needs to be maintained at a sufficiently high temperature to provide efficient conversion (Verschaeren & Verhelst, 2018). This highlights the criticality of engine BTE when selecting the injector nozzle. Attention also must be given to long-term smoke and hydrocarbon emission levels, in order to avoid ash accumulation on a catalyst causing degradation of its performance or clogging in diesel particulate filter (Yu et al., 2023).

Fuel properties also influence the injection nozzle selection. Fuel viscosity, for example, affects fuel atomisation and spray performance. Higher viscosity produces larger droplets during the injection, leading to a reduction in spray cone angle and increasing spray lengths (Heywood, 2018). This in turn causes cylinder wall impingement and poor combustion (Yadav et al., 2021). Similarly fuel surface tension, lower heating value and cetane number also set requirements when optimising injection nozzles. It is recommended to select the injector according to the characteristics of each individual fuel.

5.4 Measurements with medium-speed marine engine

Paper 5 measured the combustion performance of fuels in a medium-speed engine. The earlier results from Papers 1–3 are reflected in Paper 5's results. The premixed

HRR peak of naphtha-LFO blend was a shade higher than that of MGO and LFO. This is because the blend's ID was longer due to its lower CN (naphtha's share now 26 vol.-%.) The initial combustion followed well the differences in CN: the lower the CN, the higher the premixed HRR peak. Overall, combustion progressed in a very similar manner with all fuels.

The gaseous emission results from LFO, MGO and the naphtha-LFO blend also were generally very similar. The cycle-averaged HC emissions of the blend were between MGO's (the lowest) and LFO's (the highest). But the blend generated the highest HC emissions at the lowest load: naphtha's light fractions with low boiling points may have resulted in increased over-leaning and higher HC (Heywood, 2018). At high loads, the renewable naphtha-LFO blend's HC emissions were slightly lower than LFO's and MGO's. Reactivity conditions were beneficial at high load, even for lower-cetane fuels. A clear reduction in total particulate number (TPN) was observed for MGO and naphtha-LFO blend compared with LFO. The high-volatility fractions of naphtha most probably promoted fuel-air mixing and hence a reduction of particulates (Ovaska, 2020).

In summary, an almost equal combustion course, nearly similar cycle-weighted gaseous emissions and reduced particulate emissions support the use of both MGO and naphtha-LFO blend as alternative marine and power-plant fuels.

5.5 Engine suitability and safe use of the studied alternative fuels

The ignition and combustion studies in Papers 1 and 2 showed that MGO derived from the circular economy gave very similar results as LFO and can be used like LFO in a compression-ignition engine without any modifications to the engine or injection system. Engine measurements confirmed this conclusion: MGO can be considered as a drop-in fuel in a CI engine without modifications due to very similar combustion performance as the LFO reference fuel. Compared to LFO, MGO showed improved HC and CO and a similar low smoke number in a high-speed engine, and reduced HC and TPN emissions in a medium-speed engine. Nevertheless, MGO's high viscosity (and prolonged combustion duration), together with a slightly higher sulphur content and lower lubricity, can be limiting factors for MGO. However, the viscosity was lower in the second fuel patch (3.7 mm^2/s, Paper 5) of recycled MGO and inside SFS-EN 590 (2022) limits for kinematic viscosity. Lower lubricity may still manifest injection system failures in the long term (Bae & Kim, 2017). Thus, long-term engine measurements are required to evaluate the lubricity effect. Lubricating additives must be used, if necessary. Jiang et al. (2014) suggested that in the case of older ships, a fuel

change to MGO is more beneficial than a scrubber retrofit in order to gain access to sulphur-emission controlled areas or EU ports.

The neat form of renewable naphtha may be off-limited use as a drop-in fuel. Its low CN prolonged the ignition delay, and the start of combustion was retarded. Its low viscosity may also require some component modifications. In engine use, a longer ID allows more fuel to be injected: once ignited this usually gives a faster pressure rise and a higher peak pressure. The consequences are higher NO_X emissions, increased noise, malfunctions in engine operation and eventually, engine damage (Mohammed et al., 2023; Kuszewski, 2019; Subramanian et al., 2018; Heywood, 2018; Ogawa et al., 2017; CIMAC, 2011). Renewable naphtha needs fuel additives, or preferably blending, to improve ignition (Subramanian et al., 2018). Vallinayagam et al. (2017) suggest optimising the geometries of the combustion bowl and injector nozzle holes to adapt a compression-ignition engine for low-CN naphtha and support its auto-ignition. Adjustment of the fuel injection strategy and technology is also recommended to increase efficiency and reduce the emissions of naphtha (Vallinayagam et al., 2017). Naphtha's ignition delay was too long in the present study's high-speed engine measurements, and the engine load was limited, despite naphtha's compounds improving premixed combustion.

The blend of renewable naphtha and LFO gave better ignition quality than neat naphtha and reached the same engine loads as LFO and MGO. Additionally, improved gaseous emissions were measured both in the high-speed and medium-speed engines. The blend gave slight reductions of HC and CO compared to LFO in the medium-speed engine. A significant reduction of total particle number was measured with the blend in the medium-speed engine. The lubricity of naphtha-LFO blend was close to that of baseline LFO, so the blend should not harm lubrication of injector pumps lubricated by fuel.

A fuel's flash point is critical when discussing safety of fuel handling, usage and storage. Fuel suppliers need to specify the fuel properties and confirm compliance with industry standards. These properties include flash point, combustibility, stability, compatibility, viscosity, lubricity etc. Each of these properties, if not properly addressed, can affect equipment performance, reliability and, above all, safety of personnel or the safe operation of the engine. (International Association of Classification Societes, 2018). The low flash point and low viscosity of neat naphtha and its blend with LFO necessitated additional safety procedures when handling the fuels and making the engine measurements in the present studies. Compatibility with the engine, fuel system and auxiliaries was ensured for all the fuels. Additionally, the engine operators used respirator masks and gloves during the measurements.

The rules applied to methanol-fuelled ships can also be feasible for the safe use and storage of naphtha (Lloyd's Register, 2020), because methanol's flash point is approximately 12 °C, close to that of the current study's naphtha and its blend.

5.6 Availability of alternative fuels

The world's energy demand is still growing. Total primary energy consumption was 2 % higher in 2023 than in 2022, reaching 620 EJ (Energy Institute, 2024). Figure 26 summarises the figures from an International Maritime Organization report (2023) concerning fuel consumption of ships. Conventional fuels and liquefied natural gas in 2019 to 2021 are depicted in the left-hand plot; minority fuels in 2021 are in the right-hand plot. Biofuel consumption in ships in 2021 was slightly under 0.003 EJ, whereas conventional fuel consumption was slightly under 9 EJ. The report's business as usual -scenario suggests energy demand for seaborne transport will be between 11.1 and 15.8 EJ in 2050. The European Commission (2021) has stated that renewable and low-carbon fuels should represent between 6 % and 9 % of the international maritime transport fuel mix in 2030, and between 86 % and 88 % by 2050, to contribute to the EU economy-wide greenhouse gas emissions reduction targets. Factoring that into the International Maritime Organization's projected low-level energy demand scenario, means an energy requirement of at least 9.5 EJ for renewable and low-carbon fuels for maritime transport in 2050.

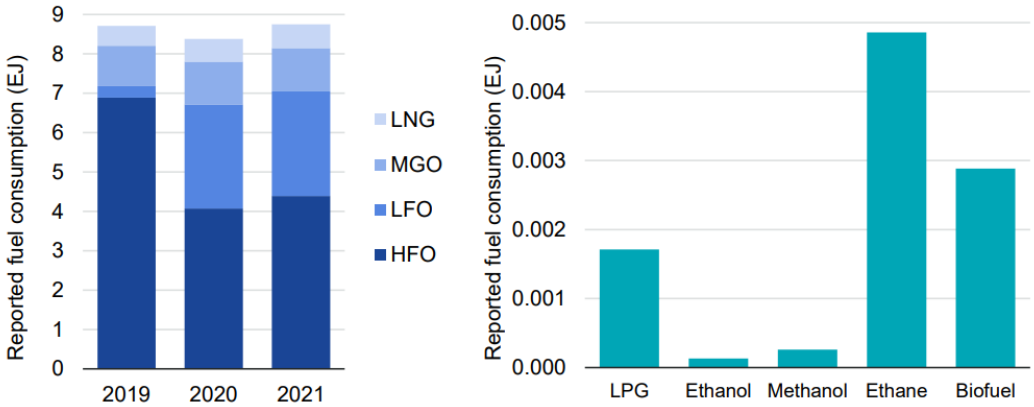

Figure 26. Reported fuel consumption of ships for conventional fuels and liquified natural gas (LNG) in 2019 to 2021 (left); and for minority fuels in 2021 (right) (International Maritime Organization, 2023)

Such a huge target for renewable fuels means that many alternatives must be researched and their commercial availability promoted. The renewable and circular economy-based fuels studied in the present project have shown their capability to provide reliable engine performance in neat or blended form and simultaneously

reduce engines' gaseous and particulate emissions. MGO derived from waste lubricating oil is part of a circular economy-based model and serves to minimise waste while producing products with added value for the economy and the environment. The naphtha, derived from crude tall oil, is an alternative choice for the renewable fuels market and answers the growing demand for greener fuel solutions for non-road, maritime and power sectors. Crude tall oil-based renewable diesel has already before proved to be a drop-in fuel and the current studies confirmed this. However, all these fuels are dependent on feedstock material. MGO production requires waste lubricating oils; HVO and naphtha need crude tall oil (CTO) which in turn is generated as a side product from crude sulphate soap during the softwood pulping process (Peters & Stojcheva, 2017). The feedstock limitations affect fuel availability and price.

Only relatively small volumes of CTO are globally available. CTO is produced during the pulp process at a rate of only 30–50 kg/tonne of pulp (Bajpai, 2018; Aro & Fatehi, 2017). Annual production of CTO was 1.85 million tonnes in 2019 and is expected to rise to 2.26 million tonnes per year in 2030 (Aryan & Kraft, 2021). But over half of globally produced CTO is used for biochemicals (Aryan & Kraft, 2021) and only 13 % (230,000 tonnes) was used for biofuel in 2017 (Peters & Stojcheva, 2017). This equates to around 10 PJ (0.01 EJ) of energy from CTO-derived biofuel. Even if all available CTO were converted to fuel in 2030, it would replace only 0.16 % of diesel/gas oil, 0.19 % of gasoline or 0.56 % of jet fuel/kerosene, based on the estimates of global fossil fuel demand (Churchill et al., 2024).

Nonetheless, CTO can be seen as a cost-effective and favourable feedstock for fuel production as it is a side product and it is produced simultaneously during the pulping process (Churchill et al., 2024; Peters & Stojcheva, 2017). However, this status as a side product also creates uncertainty about availability when demand grows for CTO-derived biofuel (Churchill et al., 2024; Peters & Stojcheva, 2017). Furthermore, CTO contains considerable impure content due to its crude nature, so needs refinement which increases costs for CTO-derived biofuel (Churchill et al., 2024). Measured against soy and canola-derived feedstock, CTO accounts for 70–95 % of the total production cost when biodiesel is produced (Churchill et al., 2024). However, the real cost is higher because the lower feedstock quality requires more pre-treatment (Churchill et al., 2024). According to Peters & Stojcheva (2017), CTO has a floor price equivalent to the cost of heavy oil or natural gas, as CTO can be used to substitute these fossil fuels as the process fuel in a pulp mill's lime kiln. On top of the floor price, additional value comes from the demand for distilled CTO products, such as tall oil rosin. This again competes with rosins from hydrocarbon origin and so is impacted by fossil fuel prices. Umenweke et al. (2023) and Tan et al. (2014) make some cost assumptions for CTO-derived biofuel, varying from approximately 0.39 €/l to 3.6 €/l or 40 to 370 €/MWh. However, the economics of industrial-scale production of CTO-

derived biofuels are confidential, with only minor public information. For comparison, the Rotterdam price for the intermediate fuel oil 380, a member of the group of residual fuels, was at a level of 40 €/MWh in January 2025 (Ship&Bunker, 2025).

The main drivers to increase CTO-derived renewable diesel production are good experimental engine results, improved production cost-effectiveness and non-edible feedstock. Legislation is already including tall oil fuels in the EU (Churchill et al., 2024;Aro & Fatehi, 2017; Peters & Stojcheva, 2017). The main barriers are again the uncertainty of feedstock availability, limited supply and lack of political commitment – at least in the US, where tall oil fuels are only partly included in the legislation (Churchill et al., 2024; Peters & Stojcheva, 2017).

Lubricants play a vital role in many industries, and the global lubricants market is expected to grow (Coherent Market Insights, 2024). Approximately 1.64 million tonnes of waste oil was collected in the EU in 2017 (European Commission, 2023). About 61 % was regenerated back to base oil, and 39 % was converted into fuel oils or used for energy recovery (Klenert et al., 2024). If the whole 39 % were converted to fuel oils, it would equate to around 27.5 PJ (0.0275 EJ) of energy. This figure must be set against the forecast demand for renewable and low-carbon maritime fuel of around 9.5 EJ in 2050. Waste lubricating oil has been designated as hazardous waste (European Comission, 2024), giving strong motivation to find re-use and regeneration opportunities to convert waste lubricating oil into valuable and cleaner products (Moses et al., 2023). The European Commission suggests a target to increase the share of collected waste oil for conversion into base or fuel oils to at least 80 % or even to 95 %, depending on the country, by 2030 (European Comission, 2024). Based on the economic study of waste oil recycling in the EU (Klenert et al., 2024), implementing the policies would yield 124–330 M€ savings in 2024–2045 inside the EU (27 countries). However, subsidies to finance the waste lubricating oil regeneration exceed expected savings, and the cost increase will be passed to different economic actors, including lubricant consumers.

Waste lubricating oil is generated globally (Moses et al., 2023), which is one of the main factors favouring its use. It is an effective option for generating energy fuel and is a source of valuable chemicals. What is otherwise hazardous waste is cost-effective feedstock for fuel or for regeneration into base oil. However, conversion into liquid fuel is more expensive (Klenert et al., 2024). Legislation is already pushing collection and reusability of waste lubricating oil as high as possible but there are some barriers to its progress. These include a shrinking supply if electric vehicles become more common, collection challenges and higher costs for conversion into liquid fuel. (Klenert et al., 2024; Moses et al., 2023).

As stated, circular economy-based MGO and renewable naphtha can be used as drop-in (MGO) or blend fuels (naphtha) without modifications to existing engines. They can be considered as technologically ready among the various alternatives currently under consideration for deep-sea shipping (Sustainable Shipping Initiative, 2019). However, both alternatives are still controversial, with questions concerning sufficient availability to meet the needs of different sectors (Klenert et al., 2024; Moses et al., 2023; Sustainable Shipping Initiative, 2019). Furthermore, the fuels' pricing is unclear because their feedstock costs are affected by the competing feedstock demands of other sectors (Sustainable Shipping Initiative, 2019).

6 CONCLUSIONS

This dissertation concentrated on the determination of the ignition delay (ID) and combustion delay (CD) of several alternative and conventional fuels. The studies continued with rigorous engine experiments focused on a few specific fuels, selected on the basis of the ID and combustion duration results. Particular attention was paid to circular economy-based marine gas oil (MGO), manufactured from waste lubricants; and to renewable naphtha, produced from crude tall oil. High-quality, low-sulphur diesel fuel oil (LFO) formed the reference.

The results obtained in the dissertation's experimental work allow the following conclusions to be drawn:

1. Based on the studies with constant-volume combustion chamber and ignition analysers, circular economy -based MGO proved to be a suitable neat drop-in alternative for compression-ignition engines, as far as ID and combustion delay are concerned. Naphtha in turn will serve as a renewable blending component for conventional fuels.

2. Two different ignition quality analysers were compared: CID510 and IQT. The high R^2-value of the compared cetane numbers of several fuels shows that a wide range of fuels can be measured with both methods and the results are very similar.

3. Naphtha's low viscosity and CN affected ignition delay (ID). The long ID prolonged the start of combustion, which in turn resulted in a high initial HRR in the high-speed engine.

4. The effect of different fuels' properties on the ID and combustion duration diminished significantly at high loads in the high-speed engine.

5. Neat naphtha can be used in CI engines. However, its long ID limited the loading of the high-speed engine. Ignition quality needs to be increased by blending or using another fuel for starting and stopping the engine. Naphtha's low flash point – similar to methanol's – dictates that additional safety procedures are required during its storage, handling and use.

6. Naphtha's ignition quality and engine suitability was increased by blending it with low-sulphur LFO. The blend ignited easily and combustion was efficient, showing lower smoke emissions and total particle number than neat LFO. However, increased HC and CO emissions were recorded for the naphtha-LFO blend in the high-speed engine.

7. MGO showed a short ID due to its high CN. However, in the high-speed engine, combustion duration was prolonged. The likely cause was a slight deterioration in fuel-air mixing due to MGO's somewhat higher viscosity and a shorter ID with a shorter premixed phase.

8. Despite the small drawback, MGO can be considered as a drop-in fuel in compression-ignition engines without any modifications to the engine or injection system. Additionally, MGO improved the cycle-averaged HC, CO and smoke emissions in the high-speed engine. Limiting factors for MGO's use can be its slightly higher sulphur content, plus lower lubricity.

9. MGO showed a shade lower BTE, and slightly higher CO emissions than LFO in the medium-speed engine. A short ID may have reduced the homogeneous mixing of air and fuel, thus slightly lowering MGO's combustion efficiency. In this second fuel patch of MGO, viscosity was inside SFS-EN 590 (2022) limits.

10. Naphtha's lower CN, combined with its low viscosity, meant the naphtha-LFO blend's HC and CO emissions were lower than neat LFO's in the medium-speed engine.

11. Both MGO and naphtha showed a significant reduction in the total particle number emissions within measured size range of 5.6 – 560 nm compared to LFO in the medium-speed engine at medium and high loads. MGO also was superior at low loads.

12. Both circular economy-based MGO and renewable naphtha can be considered as technologically ready alternative compression-ignition engine fuels: MGO as a drop-in option and naphtha as a blending component. However, their commercial progress will depend on several factors, like feedstock availability and pricing.

The next steps for implementing the use of neat MGO and blends containing naphtha in commercial engines would be optimisation of the injection strategy and equipment for each of the fuels. Endurance tests would also be necessary. Additional studies of the fuels' molecular structure, including chemical and physical bonds, would deepen the knowledge of their properties and their effects on the ignition and combustion phenomena.

7 SUMMARY

The main objective of this thesis was to investigate how different alternative fuels from renewable and circular economy feedstocks affect ignition delay and combustion phenomena in compression ignition engines. Various fuels were analysed during the first studies, leading to the selection of renewable naphtha produced from crude tall oil (CTO), and marine gas oil (MGO) derived from waste lubricating oils. They became the subject of further studies in the thesis to evaluate them as suitable novel alternatives for non-road and marine applications. Their performance was measured against baseline fuel of fossil LFO.

Five experimental studies (Papers 1-5) were performed in order to achieve the objective. Ignition studies in Papers 1 and 2 focused on ignition quality of the alternative fuels in a constant-volume combustion chamber and two ignition quality analysers. Combustion studies in Papers 3–5 focused on ignition and combustion in laboratory conditions. The studied engine in Papers 3 and 4 was a high-speed, non-road engine: the engine used for Paper 5 was a medium-speed, marine engine. The engines were not equipped with exhaust gas aftertreatment systems and the engine settings were not changed. Several laboratory instruments and standardised methods were used to obtain ignition delay and combustion data of the fuels, and to analyse engine performance and exhaust emissions.

The ignition studies showed that waste lubricating oil-derived MGO is a suitable neat drop-in alternative for compression-ignition engines, as far as ignition delay and combustion duration are concerned. Neat renewable naphtha had a long ignition delay, affecting its combustion. Naphtha will serve as a renewable blending component for conventional fuels. The high R^2-value of compared cetane numbers of several fuels shows that a wide range of fuels can be measured with very satisfactory results in both the studied ignition analysers.

The high-speed engine measurements included two stages. The first studied ignition and combustion of the selected fuels. Neat renewable naphtha derived from CTO could be used in the engine, but a long ID limited engine loading, and ignition quality needs to be improved by blending or using other fuel for starting and stopping the engine. Naphtha's low flash point is similar to methanol's and so requires additional safety actions during storage, handling and use. Renewable naphtha's ignition quality and engine suitability was increased by blending it with low-sulphur LFO. The blend ignited easily and combustion was efficient, showing lower smoke and total particle number emissions compared with neat LFO. However, increased HC and CO emissions were recorded for the blend in the high-speed engine.

Turning to MGO, the fuel's slightly higher viscosity caused slight deterioration of fuel-air mixing at low loads, leading to a longer combustion duration and lower heat release rate. This negative impact of viscosity was reduced at increased loads with higher in-cylinder temperatures. MGO derived from waste lubricating oils can be considered as a drop-in fuel in a compression-ignition engine without any engine or injection system modifications. Furthermore, improved cycle-averaged HC, CO and smoke emissions were observed for MGO in the high-speed engine. However, an increased total particle number was reported for MGO compared to LFO. Its higher viscosity, together with a slightly high sulphur content and lower lubricity, might be limiting factors for MGO's use.

The second stage of the high-speed engine measurements investigated the effects of three different injector nozzles on ignition and combustion with LFO. The results showed that either increasing or reducing the nozzle hole number improved CO, HC and NO_X emissions. Changing the number of nozzle holes led to an increase in smoke emissions.

The study of the medium-speed engine showed a shade lower BTE at many loads for the recycled MGO than for LFO. In turn, the cycle-weighted HC decreased, and the total number of exhaust particulates was considerably lower at all loads. Naphtha-LFO blend also reduced particulate emissions substantially at medium and high loads. Cycle-weighted CO also decreased, BTE with the blend was very similar and HC was slightly lower than with LFO.

Both circular economy-based MGO and renewable naphtha could be considered as technologically ready. They can be used as drop-in or blend fuels in CI engine applications. The primary concerns are most likely to be the limited availability of their feedstocks and the consequential uncertainty of the fuels' pricing.

This dissertation presents new scientific conclusions about the effects of renewable and recycled fuels on ignition delay and in-cylinder combustion, verified by different analysers and in different engines. The thesis provides scientifically measured data for various interested parties, from fuel producers and engine manufacturers to policy- and decision-makers. It enhances knowledge and understanding of alternative fuels and their benefits and constraints.

References

Aakko-Saksa, P. T., Lehtoranta, K., Kuittinen, N., Järvinen, A., Jalkanen, J. P., Johnson, K., Jung, H., Ntziachristos, L., Gagné, S., Takahashi, C., Karjalainen, P., Rönkkö, T., & Timonen, H. (2023). Reduction in greenhouse gas and other emissions from ship engines: Current trends and future options. *Progress in Energy and Combustion Science*, *94*, 101055. https://doi.org/10.1016/J.PECS.2022.101055

Agarwal, A. K., Srivastava, D. K., Dhar, A., Maurya, R. K., Shukla, P. C., & Singh, A. P. (2013). Effect of fuel injection timing and pressure on combustion, emissions and performance characteristics of a single cylinder diesel engine. *Fuel*, *111*, 374–383. https://doi.org/https://doi.org/10.1016/j.fuel.2013.03.016

Ahmad, Z., Kaario, O., Qiang, C., & Larmi, M. (2021). Effect of pilot fuel properties on lean dual-fuel combustion and emission characteristics in a heavy-duty engine. *Applied Energy*, *282*, 116134. https://doi.org/10.1016/j.apenergy.2020.116134

Arkoudeas, P., Zannikos, F., & Lois, E. (2008). The tribological behavior of essential oils in low sulphur automotive diesel. *Fuel*, *87*(17–18), 3648–3654. https://doi.org/10.1016/J.FUEL.2008.06.008

Aro, T., & Fatehi, P. (2017). Tall oil production from black liquor: Challenges and opportunities. *Separation and Purification Technology*, *175*, 469–480. https://doi.org/10.1016/J.SEPPUR.2016.10.027

Aryan, V., & Kraft, A. (2021). The crude tall oil value chain: Global availability and the influence of regional energy policies. *Journal of Cleaner Production*, *280*, 124616. https://doi.org/10.1016/J.JCLEPRO.2020.124616

ASTM D613-24a. Standard Test Method for Cetane Number of Diesel Fuel Oil. (2025).

ASTM D7668-14a. Standard Test Method for Determination of Derived Cetane Number (DCN) of Diesel Fuel Oils—Ignition Delay and Combustion Delay Using a Constant Volume Combustion Chamber Method. (2017).

Bae, C., & Kim, J. (2017). Alternative fuels for internal combustion engines. *Proceedings of the Combustion Institute*, *36*(3), 3389–3413. https://doi.org/10.1016/J.PROCI.2016.09.009

Bajpai, P. (2018). Brief Description of the Pulp and Papermaking Process. In P. Bajpai (Ed.), *Biotechnology for Pulp and Paper Processing* (pp. 9–26). Springer Singapore. https://doi.org/10.1007/978-981-10-7853-8_2

Bakhchin, D., Ravi, R., Faqir, M., & Essadiqi, E. (2023). A technical review on low temperature combustion alternatives for ultra-low emission vehicles. *Journal of the Energy Institute*, *111*, 101410. https://doi.org/10.1016/J.JOEI.2023.101410

Bergeron, C. A., & Hallett, W. L. H. (1989). Ignition characteristics of liquid hydrocarbon fuels as single droplets. *The Canadian Journal of Chemical Engineering*, *67*(1), 142–149. https://doi.org/https://doi.org/10.1002/cjce.5450670120

Chen, P. C., Wang, W. C., Roberts, W. L., & Fang, T. (2013). Spray and atomization of diesel fuel and its alternatives from a single-hole injector using a common rail fuel injection system. *Fuel*, *103*, 850–861. https://doi.org/10.1016/J.FUEL.2012.08.013

Churchill, J. G. B., Borugadda, V. B., & Dalai, A. K. (2024). A review on the production and application of tall oil with a focus on sustainable fuels. *Renewable and Sustainable Energy Reviews*, *191*, 114098. https://doi.org/10.1016/J.RSER.2023.114098

CIMAC. (2011). *Fuel Quality Guide - Ignition and Combustion*. https://www.cimac.com/cms/upload/Publication_Press/WG_Publications/CIMAC_WG07_2011_Guideline_Fuel_Quality_Ignition_Combustion.pdf

Coherent Market Insights. (2024). *Lubricants Market Analysis*. https://www.coherentmarketinsights.com/market-insight/lubricants-market-5004

Dec, J. (1997). A Conceptual Model of DI Diesel Combustion Based on Laser-Sheet Imaging. *SAE Technical Paper 970873*. https://doi.org/https://doi.org/10.4271/970873

Dong, S., Wang, Z., Yang, C., Ou, B., Lu, H., Xu, H., & Cheng, X. (2018). Investigations on the effects of fuel stratification on auto-ignition and combustion process of an ethanol/diesel dual-fuel engine. *Applied Energy*, *230*, 19–30. https://doi.org/10.1016/J.APENERGY.2018.08.082

Energy Institute. (2024). *73rd Statistical Review of World Energy 2024*. https://www.energyinst.org/__data/assets/pdf_file/0006/1542714/684_EI_Stat_Review_V16_DIGITAL.pdf

European Agricultural Machinery Association. (2022). *The role of agricultural machinery in decarbonising agriculture*. https://www.cema-agri.org/images/publications/position-papers/CEMA_decarbonising_agriculture_27-04-22.pdf

European Comission. (2024). *Waste oil*. https://environment.ec.europa.eu/topics/waste-and-recycling/waste-oil_en

European Commission. (2021). *Proposal for a Regulation of the European Parliament and of the Council on the use of renewable and low-carbon fuels in maritime transport and amending Directive 2009/16/EC*. https://eur-lex.europa.eu/legal-content/EN/TXT/HTML/?uri=CELEX:52021PC0562

European Commission. (2023). *Report from the Commission to the European Parliament and the Council - Circularity of mineral and synthetic lubrication and industrial waste*

oil management in the EU. https://eur-lex.europa.eu/legal-content/EN/TXT/?uri=COM:2023:670:FIN

European Council. (2024). *Fit for 55*. https://www.consilium.europa.eu/en/policies/green-deal/fit-for-55/

European Parliament. (2023). *Directive 2018/2001. Promotion of the use of energy from renewable sources*. https://eur-lex.europa.eu/legal-content/EN/TXT/PDF/?uri=CELEX:02018L2001-20231120

Feng, J., & Khan, A. M. (2024). Accelerating urban road transportation electrification: planning, technology, economic and implementation factors in converting gas stations into fast charging stations. *Energy Systems*. https://doi.org/10.1007/s12667-023-00638-4

Flynn, P., Durrett, R., Hunter, G., zur Loye, A., Dec, J., & Westbrook, C. (1999). Diesel Combustion: An Integrated View Combining Laser Diagnostics, Chemical Kinetics, And Empirical Validation. *SAE Technical Paper 1999-01-0509*, 1–16. https://doi.org/https://doi.org/10.4271/1999-01-0509

Gabiña, G., Martin, L., Basurko, O. C., Clemente, M., Aldekoa, S., & Uriondo, Z. (2019). Performance of marine diesel engine in propulsion mode with a waste oil-based alternative fuel. *Fuel*, *235*, 259–268. https://doi.org/https://doi.org/10.1016/j.fuel.2018.07.113

Gilkes, D. (2019, July 11). *JCB prepared to meet EU stage V emissions*. https://www.sae.org/news/2019/07/jcb-stage-v-emissions-plans

Guibet, J.-C. (1999). *Fuels and engines : technology, energy, environment.* (Revised edition). Éditions Technip.

Hellström, M. (2023, March 8). Towards a roadmap for clean propulsion. *The 3rd Clean Propulsion Technologies Review Meeting*.

Herzog by PAC. (2017). *Cetane ID510 - Cetane number analyzer*.

Heywood, J. B. (2018). *Internal combustion engine fundamentals* (Second edition). McGraw-Hill Education.

Higgins, B., Siebers, D., & Aradi, A. (2000). Diesel-Spray Ignition and Premixed-Burn Behavior. *SAE Technical Paper 2000-01-0940*, 1–26. https://doi.org/https://doi.org/10.4271/2000-01-0940

Hunicz J., Beidl C., Knost F., Münz M., Runkel J., & Mikulski M. (2020). Injection Strategy and EGR Optimization on a Viscosity-Improved Vegetable Oil Blend Suitable for Modern Compression Ignition Engines. *SAE International Journal of Advances and Current Practices in Mobility*, *3*(1), 419–427. https://doi.org/https://doi.org/10.4271/2020-01-2141

International Association of Classification Societes. (2018). *Fuel oil safety considerations associated with the January 2020 0.50% sulphur cap requirement*. www.iacs.org.uk

International Maritime Organization. (2020a). *Sulphur oxides (SOx) and Particulate Matter (PM) – Regulation 14*. https://www.imo.org/en/OurWork/Environment/Pages/Sulphur-oxides-(SOx)-%E2%80%93-Regulation-14.aspx

International Maritime Organization. (2020b, March 2). *IMO 2020 sulphur limit implementation - carriage ban enterss into force*. https://www.imo.org/en/MediaCentre/PressBriefings/pages/03-1-March-carriage-ban-.aspx

International Maritime Organization. (2023). *Reduction of GHG emissions from ships – Report on the study on the readiness and availability of low- and zero-carbon ship technology and marine fuels*. https://wwwcdn.imo.org/localresources/en/MediaCentre/WhatsNew/Documents/MEPC80.INF10.pdf

IP 615: Determination of ignition delay and derived cetane number (DCN) of middle distillate fuels – Ignition delay and combustion delay determination using a constant volume combustion chamber with direct fuel injection. (2015).

ISO 8178-4. Reciprocating internal combustion engines — Exhaust emission measurement. Part 4: Steady-state and transient test cycles for different engine applications. (2017).

ISO 8217/ISO-F-DMB, Petroleum products – Fuels (class F) – Specifications of marine fuels. (2017).

Jaarinen, S., & Niiranen, J. (2005). *Laboratorion analyysitekniikka* (5. uud. p.). Edita.

Jääskeläinen, H. (2017, August). *DieselNet Technology Guide - Diesel Fuel Injector Nozzles*. https://dieselnet.com/tech/engine_fi_nozzle.php

JCGM. (2008). *Evaluation of measurement data-Guide to the expression of uncertainty in measurement Évaluation des données de mesure-Guide pour l'expression de l'incertitude de mesure*. www.bipm.org

Jiang, L., Kronbak, J., & Christensen, L. P. (2014). The costs and benefits of sulphur reduction measures: Sulphur scrubbers versus marine gas oil. *Transportation Research Part D: Transport and Environment*, *28*, 19–27. https://doi.org/https://doi.org/10.1016/j.trd.2013.12.005

Kalghatgi, G. (2018). Is it really the end of internal combustion engines and petroleum in transport? *Applied Energy*, *225*, 965–974. https://doi.org/https://doi.org/10.1016/j.apenergy.2018.05.076

Kalghatgi, G. T. (2014). *Fuel/engine interactions*. SAE International.

Kiijärvi, J. (2022). The injection system of a diesel engine. In *Notes of the lecture No. 7 of the course Fluid mechanics*. University of Vaasa.

Klenert, D., García-Gutiérrez, P., Tonini, D., Saveyn, H., & Marschinski, R. (2024). The economics of waste oil recycling in the EU. *Journal of Environmental Economics and Policy*, 1–22. https://doi.org/10.1080/21606544.2024.2318385

Kline, S., & McClintock, F. (1953). Describing Uncertainties in Single Sample Experiments. *Mechanical Engineering*, *75*, 3–8.

Kuszewski, H. (2019). Experimental investigation of the autoignition properties of ethanol–biodiesel fuel blends. *Fuel*, *235*, 1301–1308. https://doi.org/https://doi.org/10.1016/j.fuel.2018.08.146

Lahane, S., & Subramanian, K. A. (2015). Effect of different percentages of biodiesel–diesel blends on injection, spray, combustion, performance, and emission characteristics of a diesel engine. *Fuel*, *139*, 537–545. https://doi.org/https://doi.org/10.1016/j.fuel.2014.09.036

Lee, J., Oh, H., & Bae, C. (2012). Combustion process of JP-8 and fossil Diesel fuel in a heavy duty diesel engine using two-color thermometry. *Fuel*, *102*, 264–273. https://doi.org/https://doi.org/10.1016/j.fuel.2012.07.029

Llamas, X., & Eriksson, L. (2018). Control-oriented modeling of two-stroke diesel engines with exhaust gas recirculation for marine applications. *Proceedings of the Institution of Mechanical Engineers, Part M: Journal of Engineering for the Maritime Environment*, *233*(2), 551–574. https://doi.org/10.1177/1475090218768992

Lloyd's Register. (2020). *Introduction to Methanol Bunkering - Technical Reference*. https://www.methanol.org/wp-content/uploads/2020/04/Introduction-to-Methanol-Bunkering-Technical-Reference-1.5.pdf

Merker, G. P., & Teichmann, R. (2019). *Grundlagen Verbrennungsmotoren: Funktionsweise und Alternative Antriebssysteme Verbrennung, Messtechnik und Simulation*. Wiesbaden: Springer Fachmedien Wiesbaden GmbH. https://doi.org/10.1007/978-3-658-23557-4

Mohammed, A. S., Atnaw, S. M., Ramaya, A. V., & Alemayehu, G. (2023). A comprehensive review on the effect of ethers, antioxidants, and cetane improver additives on biodiesel-diesel blend in CI engine performance and emission characteristics. *Journal of the Energy Institute*, *108*, 101227. https://doi.org/https://doi.org/10.1016/j.joei.2023.101227

Morris, A. S., & Langari, R. (2015). *Measurement and Instrumentation: Theory and Application*. San Diego: Elsevier Science & Technology.

Moses, K. K., Aliyu, A., Hamza, A., & Mohammed-Dabo, I. A. (2023). Recycling of waste lubricating oil: A review of the recycling technologies with a focus on catalytic cracking, techno-economic and life cycle assessments. *Journal of Environmental Chemical*

Engineering, *11*(6), 111273. https://doi.org/https://doi.org/10.1016/j.jece.2023.111273

Mueller, C. J., Cannella, W. J., & Kalghatgi, G. T. (2014). Fuels for Engines and the Impact of Fuel Composition on Engine Performance. In *Encyclopedia of Automotive Engineering* (pp. 1–27). https://doi.org/https://doi.org/10.1002/9781118354179.auto125

Musculus, M. (2004). On the Correlation between NOx Emissions and the Diesel Premixed Burn. *SAE Technical Paper 2004-01-1401*, 1–23. https://doi.org/https://doi.org/10.4271/2004-01-1401

Nabi, Md. N., Brown, R. J., Ristovski, Z., & Hustad, J. E. (2012). A comparative study of the number and mass of fine particles emitted with diesel fuel and marine gas oil (MGO). *Atmospheric Environment*, *57*, 22–28. https://doi.org/https://doi.org/10.1016/j.atmosenv.2012.04.039

Neste Ltd. (2024). *Neste Futura Diesel -40/-40*. https://www.neste.fi/tuote/neste-futura-diesel--40--40_en

Niemi, S. (2024). *Cetane number results from 45 diesel fuel analyses at the Turku University of Applied Sciences*.

Niemi, S. A., Murtonen, T. T., Laurén, M. J., & Laiho, V. O. K. (2002, March 4). Exhaust Particulate Emissions of a Mustard Seed Oil Driven Tractor Engine. *SAE 2002 World Congress & Exhibition*. https://doi.org/https://doi.org/10.4271/2002-01-0866

Niemi, S., Uuppo, M., Virtanen, S., Karhu, T., Ekman, K., Svahn, A., Vauhkonen, V., Agrawal, A., & Hiltunen, E. (2011). Animal Fat Based Raw Bio-Oils in a Non-Road Diesel Engine Equipped with a Diesel Particulate Filter. In W. J. Bartz (Ed.), *8th International Colloquium Fuels; Conventional and Future Energy for Automobiles* (pp. 517–528). Technische Akademie Esslingen.

Ogawa, H., Morita, A., Futagami, K., & Shibata, G. (2017). Ignition delays in diesel combustion and intake gas conditions. *International Journal of Engine Research*, *19*(8), 805–812. https://doi.org/10.1177/1468087417731410

Ovaska, T. (2020). *Exhaust Particle Numbers of High- and Medium-Speed Diesel Engines with Renewable and Recycled Fuels* [Ph.D Thesis, University of Vaasa]. https://urn.fi/URN:ISBN:978-952-476-929-7

Ovaska, T., Niemi, S., Sirviö, K., Nilsson, O., Portin, K., & Asplund, T. (2019). Effects of alternative marine diesel fuels on the exhaust particle size distributions of an off-road diesel engine. *Applied Thermal Engineering*, *150*, 1168–1176. https://doi.org/10.1016/j.applthermaleng.2019.01.090

Payri, F., Benajes, J., Pastor, J., & Molina, S. (2002). Influence of the Post-Injection Pattern on Performance, Soot and NOx Emissions in a HD Diesel Engine. *SAE Technical Paper 2002-01-0502*, 1–10. https://doi.org/https://doi.org/10.4271/2002-01-0502

Peters, D., & Stojcheva, V. (2017). *Crude tall oil low ILUC risk assessment - Comparing global supply and demand*. https://www.upmbiofuels.com/siteassets/documents/other-publications/ecofys-crude-tall-oil-low-iluc-risk-assessment-report.pdf

Pietikäinen, M., Väliheikki, A., Oravisjärvi, K., Kolli, T., Huuhtanen, M., Niemi, S., Virtanen, S., Karhu, T., & Keiski, R. L. (2015). Particle and NOx emissions of a non-road diesel engine with an SCR unit: The effect of fuel. *Renewable Energy*, *77*, 377–385. https://doi.org/https://doi.org/10.1016/j.renene.2014.12.031

Pischinger, F. (2009, July 9). *Sonderforschungsbereich 224 - Motorische Verbrennung*. http://www.sfb224.rwth-aachen.de/allgemeines.htm

Prakash, R., Singh, R. K., & Murugan, S. (2015). Experimental studies on combustion, performance and emission characteristics of diesel engine using different biodiesel bio oil emulsions. *Journal of the Energy Institute*, *88*(1), 64–75. https://doi.org/https://doi.org/10.1016/j.joei.2014.04.005

Pu, Y.-H., Dejaegere, Q., Svensson, M., & Verhelst, S. (2024). Renewable Methanol as a Fuel for Heavy-Duty Engines: A Review of Technologies Enabling Single-Fuel Solutions. *Energies*, *17*(7). https://doi.org/10.3390/en17071719

Reitz, R. D., Ogawa, H., Payri, R., Fansler, T., Kokjohn, S., Moriyoshi, Y., Agarwal, A. K., Arcoumanis, D., Assanis, D., Bae, C., Boulouchos, K., Canakci, M., Curran, S., Denbratt, I., Gavaises, M., Guenthner, M., Hasse, C., Huang, Z., Ishiyama, T., … Zhao, H. (2019). IJER editorial: The future of the internal combustion engine. *International Journal of Engine Research*, *21*(1), 3–10. https://doi.org/10.1177/1468087419877990

Röj, A. (2014, November 6). Volvo: Fueling future vehicles – challenges and opportunities. *Proceedings of Neste Oil Product Seminar*.

Sajjad, H., Masjuki, H. H., Varman, M., Kalam, M. A., Arbab, M. I., Imtenan, S., & Rahman, S. M. A. (2014). Engine combustion, performance and emission characteristics of gas to liquid (GTL) fuels and its blends with diesel and bio-diesel. *Renewable and Sustainable Energy Reviews*, *30*, 961–986. https://doi.org/https://doi.org/10.1016/j.rser.2013.11.039

Sarvi, A., Fogelholm, C.-J., & Zevenhoven, R. (2008). Emissions from large-scale medium-speed diesel engines: 1. Influence of engine operation mode and turbocharger. *Fuel Processing Technology*, *89*(5), 510–519. https://doi.org/https://doi.org/10.1016/j.fuproc.2007.10.006

SFS-EN 590. Automotive fuels. Diesel. Requirements and test methods. (2022).

SFS-EN 15195. Liquid petroleum products. Determination of ignition delay and derived cetane number (DCN) of middle distillate fuels by combustion in a constant volume chamber. (2023).

SFS-EN 16715. Liquid petroleum products. Determination of ignition delay and derived cetane number (DCN) of middle distillate fuels. Ignition delay and combustion delay determination using a constant volume combustion chamber with direct fuel injection. (2015).

Ship&Bunker. (2025). *World Bunker Prices*. https://shipandbunker.com/prices#IFO380

Sirviö, K. (2018). *Issues of various alternative fuel blends for off-road, marine and power plant diesel engines ACTA WASAENSIA 400* (Acta Wasaensia, Ed.) [Ph.D., University of Vaasa]. https://urn.fi/URN:ISBN:978-952-476-805-4

Sonawane, U., Jena, A., & Agarwal, A. K. (2023, April 11). Influence of Fuel Injection Pressure on Spray Characteristics of Diesel-Diethyl Ether Blends for Diesel Engine Applications: An Experimental Study. *WCX SAE World Congress Experience*. https://doi.org/https://doi.org/10.4271/2023-01-0309

Steenberg, K., & Forget, S. (2007, May 21). The effects of changing oil industry on marine fuel quality and how new and old analytical techniques can be used to ensure predictable performance in marine diesel engines. *25th CIMAC Congress*.

Su, C.-H., Nguyen, H. C., Pham, U. K., Nguyen, M. L., & Juan, H.-Y. (2018). Biodiesel Production from a Novel Nonedible Feedstock, Soursop (Annona muricata L.) Seed Oil. *Energies*, *11*(10). https://doi.org/10.3390/en11102562

Subramanian, T., Varuvel, E. G., Ganapathy, S., Vedharaj, S., & Vallinayagam, R. (2018). Role of fuel additives on reduction of NOX emission from a diesel engine powered by camphor oil biofuel. *Environmental Science and Pollution Research*, *25*(16), 15368–15377. https://doi.org/10.1007/s11356-018-1745-4

Sustainable Shipping Initiative. (2019). *The Role of Sustainable Biofuels in the Decarbonisation of Shipping - The findings of an inquiry into the Sustainability and Availability of Biofuels for Shipping*. https://sustainableworldports.org/wp-content/uploads/SSI_2019_The-role-of-sust.biofuels-in-decarb.-of-shipping-report.pdf

Tan, E. C. D., Marker, T. L., & Roberts, M. J. (2014). Direct production of gasoline and diesel fuels from biomass via integrated hydropyrolysis and hydroconversion process—A techno-economic analysis. *Environmental Progress & Sustainable Energy*, *33*(2), 609–617. https://doi.org/https://doi.org/10.1002/ep.11791

Tira, H. S., Herreros, J. M., Tsolakis, A., & Wyszynski, M. L. (2012). Characteristics of LPG-diesel dual fuelled engine operated with rapeseed methyl ester and gas-to-liquid diesel fuels. *Energy*, *47*(1), 620–629. https://doi.org/https://doi.org/10.1016/j.energy.2012.09.046

Umenweke, G. C., Pace, R. B., Santillan-Jimenez, E., & Okolie, J. A. (2023). Techno-economic and life-cycle analyses of sustainable aviation fuel production via integrated catalytic deoxygenation and hydrothermal gasification. *Chemical Engineering Journal*, *452*, 139215. https://doi.org/https://doi.org/10.1016/j.cej.2022.139215

Unglert, M., Bockey, D., Bofinger, C., Buchholz, B., Fisch, G., Luther, R., Müller, M., Schaper, K., Schmitt, J., Schröder, O., Schümann, U., Tschöke, H., Remmele, E., Wicht, R., Winkler, M., & Krahl, J. (2020). Action areas and the need for research in biofuels. *Fuel*, *268*, 117227. https://doi.org/https://doi.org/10.1016/j.fuel.2020.117227

United Nations. (2015, December 12). *The Paris Agreement*. https://unfccc.int/process-and-meetings/the-paris-agreement UPM Biofuels. (2024). *UPM BioVerno naphtha for traffic fuels*. https://www.upmbiofuels.com/traffic-fuels/upm-bioverno-naphtha-for-fuels/

Valkjärvi, P. (2022). *Integrated Data Acquisition for State-of-the-Art Large-Bore Engine Test Cell* [University of Vaasa]. https://urn.fi/URN:NBN:fi-fe2022110264145

Vallinayagam, R., Vedharaj, S., An, Y., Dawood, A., Izadi, N. M., Somers, B., & Johansson, B. (2017, March 28). Combustion Stratification for Naphtha from CI Combustion to PPC. *WCX™ 17: SAE World Congress Experience*. https://doi.org/https://doi.org/10.4271/2017-01-0745

Verschaeren, R., & Verhelst, S. (2018). Increasing exhaust temperature to enable aftertreatment operation on a two-stage turbo-charged medium speed marine diesel engine. *Energy*, *147*, 681–687. https://doi.org/https://doi.org/10.1016/j.energy.2018.01.081

Xue, J., Grift, T. E., & Hansen, A. C. (2011). Effect of biodiesel on engine performances and emissions. *Renewable and Sustainable Energy Reviews*, *15*(2), 1098–1116. https://doi.org/https://doi.org/10.1016/j.rser.2010.11.016

Yadav, P., Kumar, N., & Gautam, R. (2021). Improvement in performance of CI engine using various techniques with alternative fuel. *Energy Sources, Part A: Recovery, Utilization, and Environmental Effects*, 1–27. https://doi.org/10.1080/15567036.2020.1864517

Yu, T., Li, K., Wu, Q., Yao, P., Ke, J., Wang, B., & Wang, Y. (2023). Diesel Engine Emission Aftertreatment Device Aging Mechanism and Durability Assessment Methods: A Review. *Atmosphere*, *14*(2). https://doi.org/10.3390/atmos14020314

Zacharof, N., Bitsanis, E., Broekaert, S., & Fontaras, G. (2024). Reducing CO2 Emissions of Hybrid Heavy-Duty Trucks and Buses: Paving the Transition to Low-Carbon Transport. *Energies*, *17*(2). https://doi.org/10.3390/en17020286

Appendices

Appendix 1. Estimation of measurement uncertainty

To estimate measurement uncertainty for calculated DCN(LFO) value, four steps were made based on method given in *Guide to the expression of uncertainty in measurement*, (JCGM, 2008).

1. Calculate standard deviation *s(x)* for ID and CD values of 15 measurements for LFO with coverage factor k=1.

The standard deviation for ID and CD is calculated with Equation

$$s(x) = \sqrt{\sum_{i=1}^{n} \frac{(x_i - \bar{x})^2}{n-1}} \quad (1)$$

where $s(x)$ is standard deviation of calculated variable x, x_i is result of i^{th} measurement, $\bar{x}$ arithmetic mean of the n results considered, n is number of measurements.

2. Calculate the estimated standard uncertainties, $u(\mathrm{ID_m})$ of the mean ID and $u(\mathrm{CD_m})$ of the mean CD with Equation

$$u(x) = \frac{s(x)}{\sqrt{n}} \quad (2)$$

where $u(x)$ is estimated standard uncertainty, $s(x)$ is the standard deviation and n is the number of measurements.

3. Estimate measurement uncertainty for indirect results using partial derivative method originally proposed by Kline & McClintock (1953) with Equation

$$\Delta Y = \left[\sum_{i=1}^{n} \left(\frac{\partial Y}{\partial x_i} \times \Delta x_i\right)^2\right]^{\frac{1}{2}} \quad (3)$$

where Y is the calculated variable, x_i is the measured variable, Δx_i represents the error of measured variable and n is the number of independent measurements to calculate Y.

4. Calculate expanded standard uncertainty U for $\mathrm{DCN_{LFO}}$ with 95.5 % probability with Equation

$$U(\Delta Y) = \Delta Y \times k \quad (4)$$

where $U(\Delta Y)$ is the expanded standard uncertainty and k is the coverage factor. For 95.5 % probability, k=2.

Agronomy Research **16**(S1), 1032–1045, 2018
https://doi.org/10.15159/AR.18.089

Combustion property analyses with variable liquid marine fuels in combustion research unit

M. Hissa*, S. Niemi and K. Sirviö

University of Vaasa, School of Technology and Innovations, Department of Energy Technology, P.O. Box 700, FI-65101 Vaasa, Finland
*Correspondence: Michaela.Hissa@uva.fi

Abstract. The quality of ignition and combustion of four marine and power plant fuels were studied in a Combustion Research Unit, CRU. The fuels were low-sulphur Light Fuel Oil (LFO, baseline), Marine Gas Oil (MGO), kerosene and renewable wood-based naphtha. To meet climate change requirements and sustainability goals, combustion systems needs to be able to operate with a variety of renewable and 'net-zero-carbon' fuels. Due to the variations in the chemical and physical properties of the fuels, they generally cannot simply be dropped into existing systems. The aim of this research project was to understand how changes in fuel composition affect engine operation. The focus was on how various properties of the fuels impact on the combustion process – especially ignition delay and in-cylinder combustion. The goal of the research project was to allow broad fuel flexibility without any or only minor changes to engine hardware. Before the engine tests, the CRU forms an easy and cost-effective device to find out the engine suitability of the fuel. The results showed that the ignition delay decreased expectedly with all fuels when the in-cylinder pressure and temperature increased. The differences in the maximum heat release rates between fuels decreased in high-pressure conditions. MGO had the shortest ignition delay under both pressure and temperature conditions. Based on the CRU results MGO and kerosene are suitable to use in compression-ignited engines like the reference fuel LFO. In contrast renewable naphtha had a long ignition delay. If naphtha is used in a CI engine, the engine must be started and stopped with, e.g. LFO or MGO.

Key words: Diesel engines, alternative fuels, ignition delay, heat release rate.

INTRODUCTION

In compression ignition (CI) engines the combustion process starts when liquid fuel is injected as one or more jets into the cylinder fulfilled with hot high-pressured air near the top dead centre (TDC) position of the piston. The ignition delay (ID) is a period when injected fuel entrains to cylinder, atomizes and mixes with existing air. Chemical reactions start slowly and ignition occurs after the ID. Good atomization provides rapid air-fuel mixing decreasing the ID. The ignition of air-fuel mixture prepared during the ID causes a rapid pressure rise that is called as rapid uncontrolled or premixed combustion. Controlled combustion follows and is the part where preparation of fresh air-fuel mixture determines the rate of combustion. Combustion continues until all the fuel or air is utilized. This last phase is called as final combustion.

Due to variations in the chemical and physical properties of the fuels, they generally can not simply be dropped into existing systems. The aim of this research project was to understand how changes in fuel composition affect engine operation. The fuel properties have a significant effect on the ignition and combustion as well as pressure, temperature and mechanical issues (e.g. nozzles and their hole diameters). The viscosity, density, heating value and cetane number have a major effect on good atomization and ignition delay especially under low pressure conditions (Heywood, 1988; Bae & Kim, 2016). Too rapid a chamber pressure increase may cause engine damage and also increase NO_x emissions (Steenberg & Forget, 2007). Buchholz (2013) and Chang et al. (2013) even states that current diesel fuel ignites too easily causing poor mixing with oxygen, which leads to increasing levels of soot and NOx emissions. As a solution they suggest that one way to cut down number of aftertreatment devices and high injection pressure, is to use less processed fuel.

Currently most of the energy sources rely on fossil fuels which have limited resources. That is why alternative energies are necessary. Based on Bae & Kim (2016) significance of using alternative fuels can be defined as followes:

'(1) pursuing energy sustainability through the extended usage of those alternative fuels derived from renewable energy sources and mitigating the concerns of limited fossil fuel energy

(2) improving engine efficiency and engine-out emissions with the aid of superior physical or chemical properties of alternative fuels compared to those of conventional fuels

(3) relieving the unbalanced usage of conventional petroleum-based fossil fuels'.

In this study, the ignition characteristics of four marine and power plant fuels were studied in a Combustion Research Unit, CRU. The fuels were low-sulphur Light Fuel Oil (LFO, baseline), Marine Gas Oil (MGO), kerosene and renewable wood-based naphtha. MGO represents recycled fuels cause it is produced from used lubricant oils. LFO and kerosene may be called as heavier fuels and naphtha represents lighter fractions, which is generally the product of the initial distillation of crude oil. In this study, used naphtha was renewable wood-based naphtha.

Studies (Chang et al., 2013; Wang et al., 2013; Bae & Kim, 2016) have shown that crude oil-based naphtha, run in compression ignition engines, had a high efficiency with good transient operation and acceptable noise levels, while achieving NOx emissions below the EURO6 levels, lower particulate matter (PM) emissions and lower smoke levels than with diesel fuel. However, the low CN and viscosity of naphtha may cause increased NOx emissions due to the retarded start of combustion and prolonged ignition delay (Subramanian et al., 2018).

Kerosene is primarily used in the aviator sector particularly in gas turbine engines. Behind the kerosene usage in diesel engines is North Atlantic Treaty Organization (NATO) military's intending to use JP-8 fuel for all their automobiles and equipments, based on their Single Fuel Concept (SFC), due to logistical benefits. Another reason to study kerosene in diesel engine is adulteration of diesel by mixing it with kerosene, which is big problem in some parts of world. JP-8 has very similar chemical composition compared to the present Jet-A fuel despite some additives (Yadav et al., 2005; Lee et al., 2012). Based on the research of Vasu et al. (2007), JP-8 and Jet-A have very similar ignition delay times. Although, low lubrication may cause problems in the fuel pump system (Anastopoulos et al., 2002; Bae & Kim, 2016).

MGO is commonly known as shipping fuel. The ship owners have been driven to examine how to comply the forthcoming sulphur emission regulations (IMO, 2008), and MGO is promising alternative besides sulphur scrubbers and alternative fuels. MGO is required in a vessel by existing and upcoming regulations depending on time and location. For example a vessel uses MGO when it is inside Emission Controlled Area (ECA) or within EU ports. Outside the ECA, HFO is used. However, by 2020 low-sulphur heavy fuel oil (LSFO) is required outside of the ECA (Germanischer Lloyd and MAN, 2012). Jiang et al. (2014) calculated that it is more beneficial to use MGO in a old ships compared to use scrubber retrofits.

However, MGO has a higher viscosity and density compared to diesel fuel which may lead to poor atomization resulting in incomplete combustion with higher soot emissions (Nabi et al., 2012). However, the studied MGO had a significantly higher CN (68), compared to other studied fuels, which may count as a compensatory property to higher viscosity and density. In literature (i.e. Karavalakis et al., 2008; Nabi et al., 2012; Ushakov et al., 2013) the CN of MGO is generally around 47−55.

Due to the variations in the chemical and physical properties of the fuels, they generally cannot simply be dropped into existing systems. Proper fuel analysis is necessary before engine use to observe suitability of the fuel. Ensured fuel flexibility of IC engine is needed to manage with fuel availability and fuel price fluctuation, and to meet emission regulations set for industrial engines and end-users. The goal of the research project was to allow broad fuel flexibility without any or only minor changes to engine hardware. Before the engine tests, the CRU forms an easy and cost-effective device to find out engine suitability of the fuel.

MATERIALS AND METHODS

Fuels

The studied fuels were selected to enlarge the choice of fuel alternatives of marine engines. The fuels were Light Fuel Oil (LFO), Jet A-1 -type aviation fuel (100% kerosene), Marine Gas Oil (MGO) produced from used lubricant oils and wood-based naphtha that was a side-product of wood-based biodiesel production. Chemically, all the fuels contained several hydrocarbon compounds; that is why no simple chemical formulas could not be given.

The research started by analysing the basic fuel properties (Table 1). The kinematic viscosity has an important role in fuel injection and droplet formation. Too high or too low viscosity causes poor fuel injection and increases fuel consumption. Too high viscosity leads to poor atomization resulting in incomplete combustion. However, too low fuel viscosity may cause mechanical problems in engine use as leaking from the nozzle sealing and the fuel pump system. All selected fuels had a relatively low viscosity. At a temperature of 40 °C wood based-naphtha had the lowest viscosity (0.50 $mm^2 s^{-1}$) and MGO (8 $mm^2 s^{-1}$) the highest. Kerosene (0.94 $mm^2 s^{-1}$) and the reference fuel LFO (3.0 $mm^2 s^{-1}$) were between the values of naphtha and MGO. The lower viscosity of naphtha and kerosene, compared to diesel, could improve the fuel atomization, evaporation and air/fuel mixing process (Subramanian et al., 2018).

A high fuel density may indicate higher energy content and minimize fuel losses. Too high a density correlates with higher viscosity and it has a negative effect on the formation of the fuel spray incurring poor burning process and high emissions. Among the studied fuels, the correlation between kinematic viscosity and fuel density was correct. Wood-based naphtha had the lowest viscosity and the lowest density (722 kg m^{-3} at 15 °C). MGO had the highest viscosity and the highest density (843 kg m^{-3}). Kerosene (787 kg m^{-3}) and LFO (836 kg m^{-3}) were between the values of naphtha and MGO.

The cetane number (CN) indicates how quickly fuel auto-ignites under compression. A low CN increases ignition delay causing problems for engine starting and running, e.g. unstable engine running leads to noise and smoke. MGO had a relatively high CN, 68, probably caused by used lubricants that formed the feedstock. The calculated cetane index of LFO (EN ISO 4264) was 54. The CN of kerosene (41) and wood-based naphtha (34) were lower, most likely resulting in a longer ignition delay.

A high lower heating value (LHV) implicates good heat release rate during the burning process improving the engine performance. The level of LHV of alternative fuels must meet the level of that of conventional fuels, other way there will be problems in volumetric fuel consumption (Bae & Kim, 2016). Unexpectedly the highest LHV was with wood-based naphtha (44 MJ kg^{-1}). However, the LHV of wood-based naphtha equated to earlier studied values of crude oil-based naphtha (Chang et al., 2013; Bae & Kim, 2016). All the other studied fuels had the same LHV, 43 MJ kg^{-1}.

Table 1. Studied fuel properties

		LFO	MGO	naphtha	kerosene
C	wt.%	87	83	81	89
H	wt.%	14	14	15	15
N	wt.%	< 0.1	0	0	0
S	wt.%	0	0	0	0
Pour point	°C	-42	Max. -6	< -50	
Flash point	°C	64	110	10	Min. 38
Boiling point	°C			20–220	170–300
Density at 15 °C	kg m^3	836	843	722	787
Kinematic viscosity at 40 °C	mm^2 s^{-1}	3.0	8.0	0.5	0.94
Surface tension at 20 °C	mN m^{-1}		29	20	25
HHV	MJ kg^{-1}		46	47	46
LHV	MJ kg^{-1}	43	43	44	43
Cetane number		54*	68	34	41
Sulphur	wt.%	< 0.01	Max. 0.1		0.1
Ash cotent	wt.%	< 0.01	< 0.001	0.005	0.001
Water content	mg kg^{-1}	< 100	22		35
Lubricity	µm	345	491		

*calculated cetane index (EN ISO 4264).

Combustion Research Unit

The Combustion Research Unit, CRU, is a constant volume combustion chamber based instrument designed to resemble engine conditions. In the CRU there are no moving parts and the starting conditions of the fuel injections are controlled more precisely than in a real compression ignition (CI) engine. Fuel is injected in a fixed injection period (250–3000 µs) through a twin nozzle injection system into a chamber with fixed dimensions (500 cm^3 ± 2%). In the injection system the first nozzle is the main injector and the second is a pilot injector, which can be activated or de-activated. In this study the pilot injector was de-activated. The used injector was a BOSCH CR injector which has electronic control of timing, opening period and pressure. The combustion and fuel pressures were observed with piezoelectric pressure sensors. Air was heated by heating the chamber wall. Fig. 1 illustrates the CRU used in this study.

To meet broad fuel flexibility without any or only minor changes to engine hardware, the fuel injection duration was assigned to be 1,000 µs with all fuels despite the differences in kinematic viscosity between the fuels. The pilot injector was de-activated and research was conducted under two different pressure and temperature conditions, 50 bar; 550°C and 70 bar; 590 °C. The results showed, however, that with MGO the injection duration had been 1,025 µs instead of 1,000 µs. Due to this slight difference, MGO is not completely comparable with other studied fuels. Based on Heywood (1988), under normal operation conditions, increasing the quantity of injected fuel has no significant effect on delay period. However, under engine starting conditions, the delay increases due to the larger drop sizes which are associated with evaporating and heating the increased amount of fuel.

All fuels were first centrifuged and then hot filtrated through a 10 µm filter before the CRU measurements. The fuels were at room temperature when injected into the fuel injection system. Measurements were performed two to three times under the both measurement conditions. Information about the set-up configurations of the CRU can be found in Table 2.

Table 2. Research set-up configurations of the CRU

		High pressure	Low pressure
Temperature at fuel injection (theoretical)	°C	590	550
Pressure at fuel injection	bar	70	55
Max. chamber pressure	bar	70	55
Max, pressure	bar	81.2	65.9
Injector period, main (LFO, naphtha, kerosene)	µs	1,000	1,000
Injector period, main (MGO)	µs	1,025	1,025

It should be noted that the actual engine conditions differ from conditions in the CRU. The major difference is the cylinder pressure that in 4-stroke engines reaches even more than 200 bar while the pressure in the CRU was max. 81 bar. Other differences are the fuel injection process and injection timing. In the CRU fuel is injected in a fixed period (1,000 µs), in this study, all fuel was injected before ignition, since all fuels had

an ignition delay of longer than 1 ms. In engines, especially at high loads, the fuel injection overlaps ignition and combustion (Steernberg & Forget, 2007). This means that in an engine large amount of the fuel (max. 80%) is injected into a space with a flame. Despite the differences between the CRU and actual engine conditions, the CRU is fast, easy and cost-effective device to find out the engine suitability of the fuel.

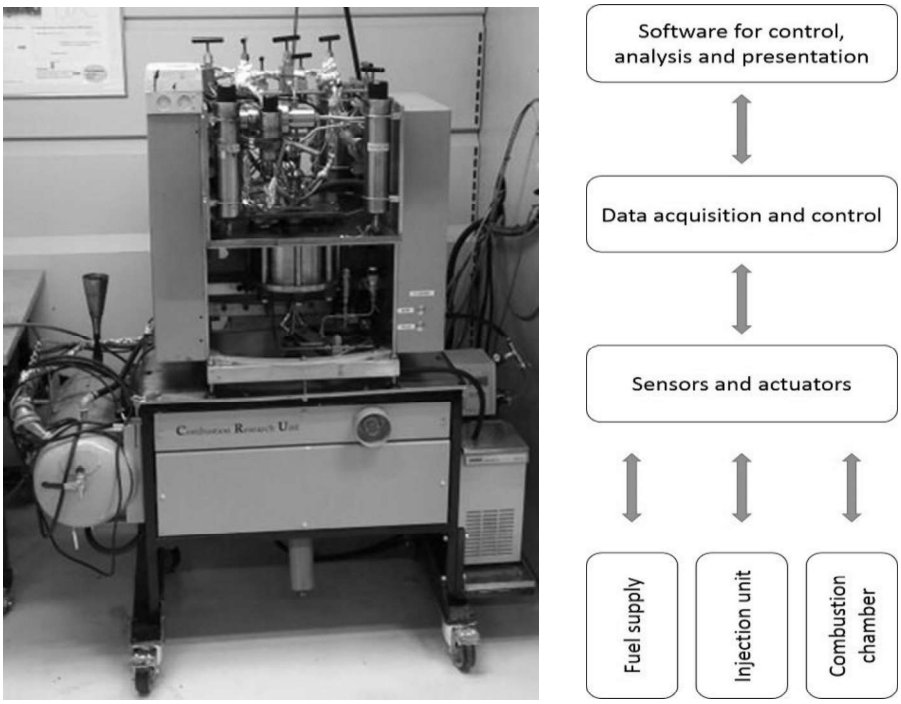

Figure 1. Combustion Research Unit and its modules. (Modules based on Fueltech AS, 2005).

CRU measures the Ignition Delay (ID) from the start of injection (t = 0) until the pressure in the chamber increases 0.1 bar. The following phases are determined:

- Pre Combustion Period (PCP) starts at the point where pressure is increased by 0.1 bar and ends when pressure is 1% of maximum pressure increase.
- Main Reaction Delay (MRD) is considered when pressure is increased 10% of the maximum pressure increase.
- The time between fuel ignition until 10% of the maximum pressure increase is achieved is called as Pre Combustion Period (PRP).
- Main Combustion Period (MCP) is measured from the MRD until 85% of the maximum pressure increase is reached.
- After the main combustion period, After Burning Period (ABP) starts, which continues until 95% of the maximum pressure increase is reached. At the end point of ABP, the combustion is considered end (EC).

In the next chapter, Fig. 2 shows these above-mentioned parameters in a pressure diagram with LFO.

RESULTS AND DISCUSSION

Based on the obtained results in the CRU, the ignition delays, complete combustion periods, maximum chamber pressure increases, and maximum rate of heat release rates of the fuels are examined in this chapter. The CRU chamber pressure results are presented as a function of time at high and low initial chamber pressures. The heat release curves are converted to pressure rises versus time in the combustion chamber. The effects of the measured fuel properties on the above-mentioned combustion parameters are considered.

High pressure

Fig. 2 presents the CRU chamber pressure results as a function of time for the studied fuels at high initial chamber pressure. All the variables were calculated from the raw data of one measurement and the results of LFO are marked in Fig. 2. The injection duration of the fuels was identical, despite the MGO (+2.5%), but the amount of the fuel during injection varied due to the different densities of the fuels. The results of MGO are only directional due to the slightly longer main injector period. The results determined from Fig. 2 are listed in Table 3.

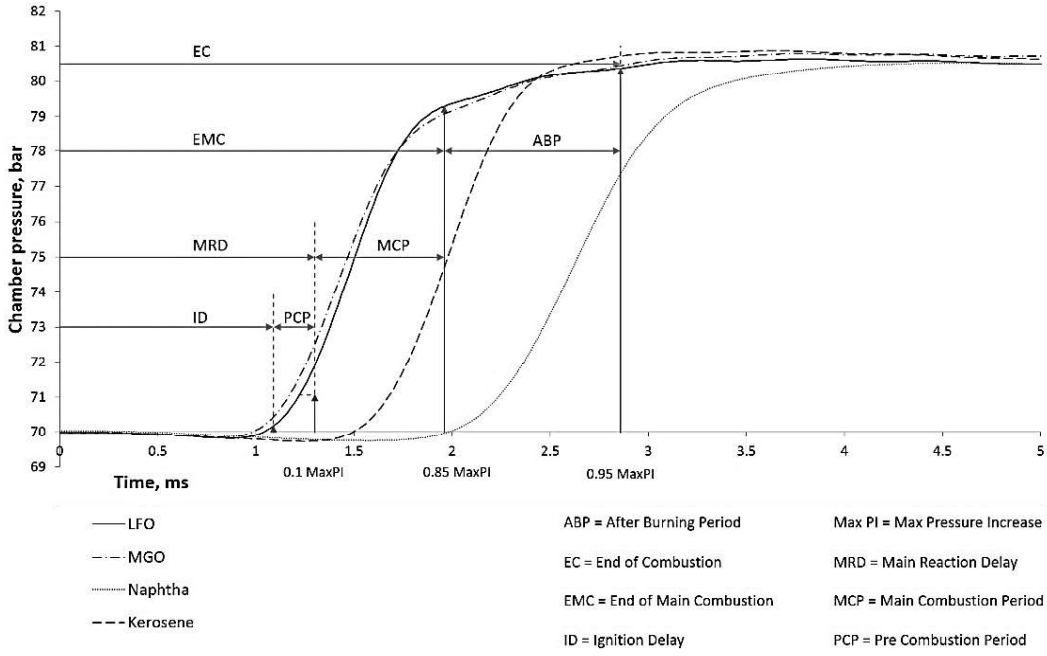

Figure 2. Chamber pressure diagram of LFO, MGO, naphtha and kerosene at high pressure.

Fig. 2 and Table 3 show that MGO had the shortest ignition delay (1.04 ms), perhaps partly due to slightly longer main injector period (MGO 1.025 ms versus other fuels' 1 ms) and significantly higher CN, as Grab-Rogalinski & Szwaja (2016) also noticed. Among other studied fuels, LFO had the shortest ID (1.08 ms), kerosene was the second (1.54 ms) and the longest ID was detected with naphtha (2.04 ms). The difference between ID of MGO and naphtha was 1.0 ms. In engine use the longer ignition

delay allows more fuel to be injected which once ignited gives a stronger pressure peak. Steenberg & Forget (2007) suggests that too strong a pressure peak may lead not only to engine damage but also to increased NOx emissions. The ignition delay period can be shortened by increasing the fuel injection pressure (Chen et al., 2013). On the other hand, Agrawal et al. (2013) noticed that too high a fuel injection pressure may lead even into too short an ignition delay. In that case, homogenous mixing may decrease and combustion efficiency reduce. Gnanasekaran et al. (2016) even noticed that the prolonged ignition delay may also be exhibited as lower smoke levels because the better mixture formation.

Table 3. CRU measurement results at high pressure

High pressure conditions		LFO	MGO	naphtha	kerosene
Ignition Delay (ID)	ms	1.08	1.04	2.04	1.54
Pre Combustion Period (PCP)	ms	0.16	0.14	0.22	0.16
Main Reaction Delay (MRD)	ms	1.24	1.18	2.26	1.7
Main Combustion Period (MCP)	ms	0.74	0.98	0.78	0.6
End of Main Combustion (EMC)	ms	1.98	2.16	3.04	2.3
After Burning Period (ABP)	ms	0.9	0.86	0.26	0.26
End of Combustion (EC)	ms	2.88	3.02	3.3	2.56
Max. Pressure Increase	bar	80.9 at 10.5 ms	81.2 at 10.3 ms	80.2 at 47.7 ms	80.9 at 10.9 ms
Max. Rate of Heat Release (MaxROHR)	bar ms^{-1}	16.3	15.2	11.7	16.2
Position of MaxROHR (PMR)	ms	1.5	1.44	2.62	2

Naphtha had a slightly higher LHV but it required more time to ignite than other fuels. Kerosene, MGO and LFO had a very similar LHV, but MGO had the shortest ID.

Despite the longer ID of kerosene, the complete combustion period (EC) of kerosene (2.56 ms) was shorter than that of LFO (2.88 ms), MGO (3.02 ms) or naphtha (3.3 ms). This can be assumed to relate to light components of kerosene that burns more rapidly than the heavier compounds of other fuels. Kerosene's lower viscosity and surface tension, compared to LFO and MGO, leads to a more rapid EC due to better fuel-air-mixing caused by smaller droplet sizes and faster vaporization characteristics (Lee et al., 2012; Agarwal et al., 2013; Chen et al., 2013). Based on Steenberg & Forget (2007) the EC may give information on the formation of combustion products and unburned or burned fuel components that affect emission, and may also relate to the formation of engine deposits and wear. The studies of Gnanasekaran et al. (2016) and Nabi et al. (2012) concerning a DI diesel engine showed that a shorter ignition delay and combustion duration results in lower heat release rate, peak pressure and rate of pressure rise.

The maximum pressure increase (Max.PI) of MGO (81.2 bar at 10.3 ms) was a slightly higher than Max.PI of kerosene (80.9 bar at 10.7 ms) and LFO (80.9 bar at 10.5 ms) but the peaks were almost equal. Naphtha had a long ID and that caused delay in the position of the peak of Max.PI (80.2 bar at 47.7 ms). Naphtha also included more heavier compounds that take time to burn and evaporate. Grab-Rogalinski & Szwaja (2016) also noticed a correlation between an ID and pressure increase.

Fig. 3 shows the heat release curves as converted to pressure rises versus time in the combustion chamber. The heat release (bar msec^{-1}) was the fastest with LFO (16.3 bar msec^{-1}) and kerosene (16.2 bar msec^{-1}). The placement of the curve against time depends on the fuel ID. The MaxROHR of naphtha was the lowest (11.7 bar msec^{-1}) and the position was delayed due to its long ID. The shape of MaxROHR curve shows that naphtha burned more slowly and the curve was not as spiky as with other fuels.

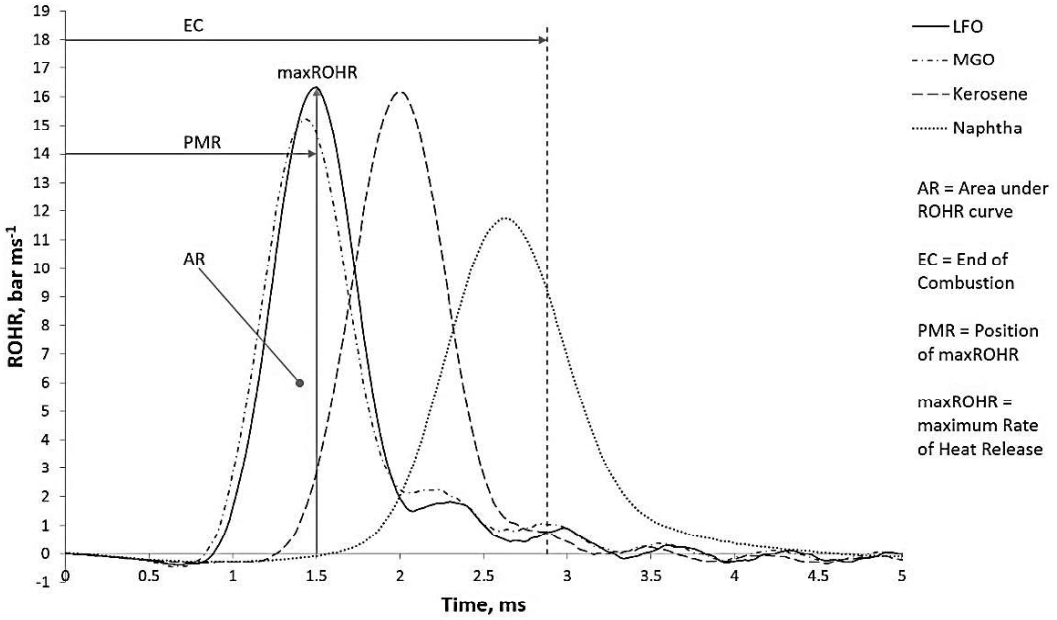

Figure 3. Rate of heat release curve of LFO, MGO, naphtha and kerosene at high pressure.

Low pressure

Fig. 4 presents the CRU chamber pressure results as a function of time for the studied fuels at low chamber pressure that was adjust at 55 bar. All the variables were calculated from the raw data of one measurement, and the results of LFO are marked in Fig. 4. The injection duration of the fuels were identical, despite the MGO (+2.5%), but the amount of the fuel during injection varied due to the different densities of the fuels.

The lower pressure conditions set higher demands for the used fuels and the differences between the research fuels were clearer. The injection temperature of the fuels was also dropped from 590 °C to 550 °C. Based on the CRU results, the fuels can roughly be divided into two groups; LFO and MGO, kerosene and naphtha.

Wood-based naphtha had almost twice as long an ID (3.20 ms) as LFO (1.76 ms) and MGO (1.74 ms). Figs 4−5 and Table 4 show that a long ID also reflected to the position of MaxROHR and the position of Max.PI. The Max.PI of naphtha (64.6 bar) was near the values of other studied fuels (LFO 65.9 bar, MGO 66.0 bar and kerosene 65.0 bar), but the slow ignition is shown in the position of Max.PI of naphtha (35.8 ms). The position of Max.PI of naphtha occurred 9.1 times later than that of LFO (3.92 ms) or MGO (3.94 ms). The study of Grab-Rogalinski & Szwaja (2016) also showed that a lower initial chamber temperature and pressure lead to worse atomization and evaporation and delayed ignition. With constant volume vessel, Bae & Kim (2016)

observed that the ID of the kerosene type JP-8 fuel (CN 38) was 25% to 50% higher compared to diesel fuel (CN 48). It was also noticed that when the CNs of the fuels meet, the difference in the ID's is no longer detected.

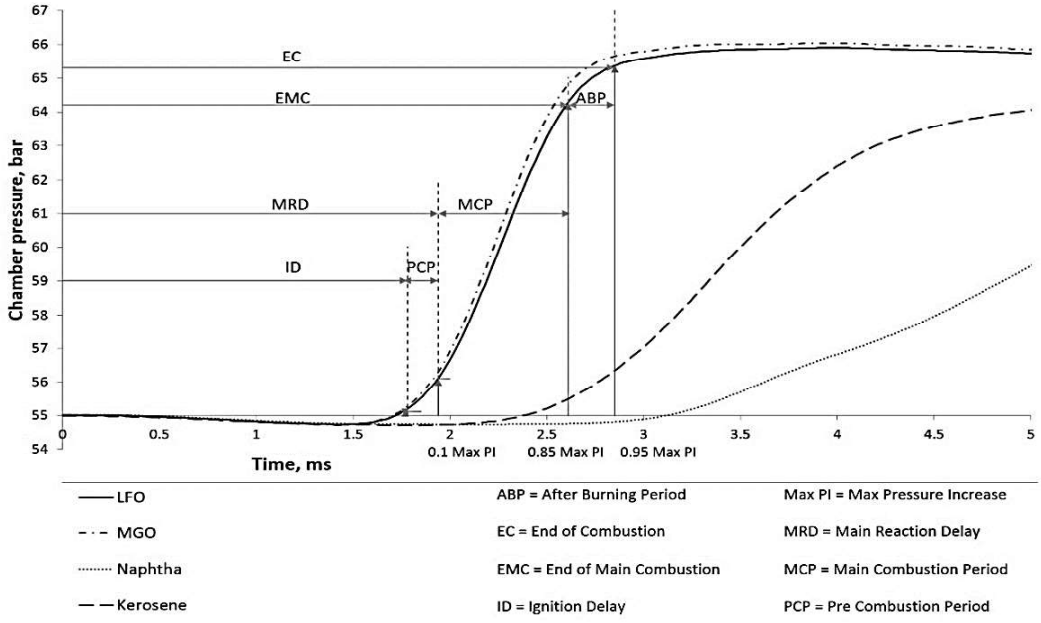

Figure 4. Chamber pressure diagram of LFO, MGO, naphtha and kerosene at low pressure.

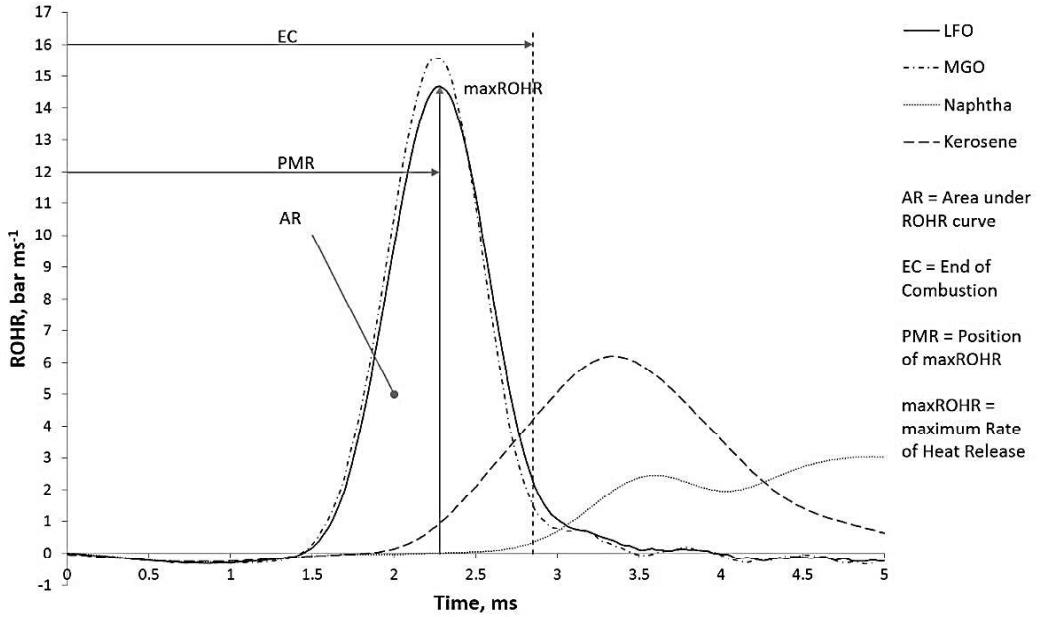

Figure 5. Rate of heat release curve of LFO, MGO, naphtha and kerosene at low pressure.

The whole combustion period (EC) was the fastest with MGO. The fast ignition and good combustion of MGO under low pressure conditions may be related to the high CN (68). In high pressure conditions, kerosene had the fastest combustion (EC), maybe due to the major amount of the light compounds in the fuel. Now, it can be assumed that the chamber pressure and the injection temperature were too low to burn the light compounds of kerosene well enough.

The MaxROHR varied more under the low than the high pressure conditions, Fig. 5. LFO and MGO burned almost similarly in both pressure conditions. MGO released heat even faster at the low (15.6 bar ms^{-1}) than high pressure (15.2 bar ms^{-1}). The MaxROHR curves of kerosene and naphtha differed considerably. The combustion was slow and the peak of the MaxROHR curve was low. The MaxROHR curve of naphtha also had a little drop at time of 4 ms. The reason might be that the light components of naphtha burned first and heavier compounds needed more time to ignite. Once the heavier compounds were also ignited, the MaxROHR reached its highest peak at 4.92 ms (3.03 bar ms^{-1}). According to Bergeron & Hallett (1989) higher mass components of a fuel have also higher ignition delay times.

Table 4. CRU measurement results at low pressure

Low pressure conditions		LFO	MGO	naphtha	kerosene
Ignition Delay (ID)	ms	1.76	1.74	3.20	2.46
Pre Combustion Period (PCP)	ms	0.18	0.18	0.42	0.32
Main Reaction Delay (MRD)	ms	1.94	1.92	3.62	2.78
Main Combustion Period (MCP)	ms	0.68	0.64	4.26	1.72
End of Main Combustion (EMC)	ms	2.62	2.56	7.88	4.50
After Burning Period (ABP)	ms	0.24	0.22	3.92	3.84
End of Combustion (EC)	ms	2.86	2.78	11.8	8.34
Max. Pressure	bar	65.9 at 3.92 ms	66.0 at 3.94 ms	64.6 at 35.8 ms	65.0 at 12.5 ms
Max. Rate of Heat Release (MaxROHR)	bar ms^{-1}	14.7	15.6	3.03	6.19
Position of MaxROHR (PMR)	ms	2.28	2.26	4.92	3.34

Based on the received results of the CRU measurements, kerosene can be used in CI engines without or with only minor changes. The possible modifications could be starting and stopping an engine with other fuel (e.g. LFO) or the change of the nozzles to have smaller diameter holes. Based on Heywood (1988) the nozzles with smaller diameter holes improves droplet formation and may promote better combustion with a shorter ID. The low lubricity of kerosene may result in malfunction of the injection system. Lubricity improvers and additives may be required in engine use (Bae & Kim, 2016).

Naphtha in CI engine use needs other fuel for starting and stopping engine. The lower CN and lower viscosity may limit the use of naphtha as a drop-in fuel to a diesel in CI engines because the retarded start of combustion and prolonged ignition delay may cause increased NOx emissions. Fuel additives may be needed to improve the ignition i characteristics and decrease NOx emissions. (Subramanian et al., 2018).

Due to the very similar results of MGO and LFO, MGO can be used in a CI engine like LFO without any modifications to engine or injection system.

Continue of the research

The research continues with engine measurements to validate the engine operation with each fuel. At the same time, the correlation between combustion parameters from the CRU (e.g. EC, EMC, ID) and engine parameters are studied. Only few similar studies have been performed. One is the study of Steenberg & Forget (2007) where the correspondence of the Fuel Ignition Analyzer (FIA) parameters and engine parameters was examined. Good results of the correlation between the FIA and the engine combustion parameters were achieved at high loads. At low loads, poor correlation between the FIA and the engine combustion parameters was detected. It might be partly due to the differences in the test conditions between the FIA and the engine. The fuel injection in the engine was also very different and strongly affected the combustion process.

CONCLUSIONS

The quality of ignition and combustion of four marine and power plant fuels were studied in a Combustion Research Unit, CRU. The fuels were low-sulphur Light Fuel Oil (LFO, baseline), Marine Gas Oil (MGO), kerosene and renewable wood-based naphtha. The research fuels were selected to broaden the choice of alternatives of marine and power plant engine fuels.

Based on the results obtained in the study, the following conclusions could be drawn:

Under the high pressure conditions:

- MGO had the shortest ID that indicated good atomization and high CN. A good atomization provides rapid fuel-air mixing decreasing ID.
- Naphtha had the longest ID, maybe due to the high amount of heavy components of naphtha. Heavy components also affects atomization and the whole combustion process.
- Kerosene burned quickly due to its light components, lower viscosity and surface tension, and showed a short EC period. Naphtha had the longest EC which may in engine use lead to higher emissions and engine damages.
- Under the higher pressure conditions, the combustion parameters of the fuels were closer to each other than under the lower pressure conditions.

Under the low pressure conditions:

- The lower chamber pressure and the lower fuel injection temperature affected clearly the combustion performance of the fuels.
- Fuels could be roughly divided into two groups:

1) Straightly usable in engine without any modifications: LFO & MGO

2) Fuels that require some minor modifications (e.g. starting and stopping the engine with another fuel): kerosene and naphtha.

- The long ID of naphtha and kerosene affected the positions of Max.PI curve and MaxROHR curve.
- Kerosene was competitive under high pressure conditions but fell behind when the chamber pressure and injection temperature were lowered.

ACKNOWLEDGEMENTS. This project has received funding from the European Union's Horizon 2020 research and innovation programme under grant agreement No 634135. The authors wish also thank the staff of Wärtsilä Fuel Laboratory for the possibility to perform the CRU measurements and for kind assistance.

REFERENCES

Agarwal, A., Srivastava, D., Dhar, A., Maurya, R., Shukla, P. & Singh, A. 2013. Effect of fuel injection timing and pressure on combustion, emissions and performance characteristics of a single cylinder diesel engine. *Fuel*, Volume 111, pp. 374−383.

Anastopoulos, G., Lois, E., Zannikos, F., Kalligeros S. & Teas, C. 2002. HFRR lubricity response of an additized aviation kerosene for use in CI engines. *Tribology International* **35**, 599−604.

Bae, C. & Kim, J., 2016. Alternative fuels for internal combustion engines, *Proceedings of the Combustion Institute 0000*, pp. 1−25.

Bergeron, C.A. & Hallett, W.L.H., 1989. Ignition characteristics of liquid hydrocarbon fuels as single droplets, *Can J Chem Eng.* **67**, 142−149.

Buchholz, K. 2013. Naphtha-fueled research car meets emissions, other targets. *AEI* **121**(4), 6–8. ISSN: 1543-849X.

Chang, J., Kalghatgi, G., Amer, A., Adomeit, P., Rohs, H. & Heuser, B., 2013. Vehicle Demonstration of Naphtha Fuel Achieving Both High Efficiency and Drivability with EURO6 Engine-Out NOx Emission. *SAE Int. J. Engines,* Volume **6**(1), 101−119.

Chen, P-C, Wang, W-C., Roberts, W. & Fang, T., 2013. Spray and atomization of diesel fuel and its alternatives from a single-hole injector using a common rail fuel injection system. *Fuel* **103**, 850−861.

EN ISO 4264:2007 standard, *International Organization for Standarsdization (ISO)*. 2007.

Fueltech AS, Combustion Research Unit - CRU, specification. 2005.

Germanischer Lloyd & MAN, Costs and Benefits of LNG as Ship Fuel for Container Vessels, Key results from a GL and MAN joint study, Germanischer Lloyd, Hamburg. 2012.

Gnanasekaran, S., Saravanan, N. & Ilangkumaran, M., 2016. Influence of injection timing on performance, emission and combustion characteristics of a DI diesel engine running on fish oil biodiesel. *Energy* **116**(1), 1218−1229.

Grab-Rogalinski, K & Szwaja, S., 2016. The combustion properties analysis of various liquid fuels based on crude oil and renewables. In *IOP Conference Series: Materials Science and Engineering*, Volume **148**(1) DOI: 10.1088/1757-899X/148/1/012066.

Heywood, J. 1988. *Internal Combustion Engine Fundamentals*, pp. 541−562. ISBN: 0-07-100499-8.

IMO 2008. MARPOL Annex VI: Regulations for the prevention of air pollution from ships and NOx. *IMO Marine Environmental Protection Committee (MEPC)*.

Jiang, L., Kronbak, J. & Christensen, L., 2014. The costs and benefits of sulphur reduction measures: Sulphur scrubbers versus marine gas oil. *Transportation Research Part D: Transport and Environment*, Vol. **28**, pp. 19–24.

Karavalakis, G., Tzirakis, E., Mattheou, L., Stournas, S., Zannikos, F. & Karonis, D., 2008. The impact of using biodiesel/marine gas oil blends on exhaust emissions from a stationary diesel engine. *Journal of Environmental Science and Health, Part A,* **43:14**, 1663–1672.

Lee, J., Oh, H. & Bae, C. 2012. Combustion process of JP-8 and fossil Diesel fuel in a heavy duty diesel engine using two-color thermometry. *Fuel* **102**, 264−273.

Nabi, Md.N., Brown, R., Ristovski, Z. & Hustad, J. 2012. A comparative study of the number and mass of fine particles emitted with diesel fuel and marine gas oil (MGO). *Atmospheric Environment* **57**, 22–28.

Steernberg, K. & Forget, S. 2007. The effects of a changing oil industry on marine fuel quality and how new and old analytical techniques can be used to ensure predictable performance in marine diesel engines. In *25th CIMAC Congress*, Vienna. Paper no. 198.

Subramanian, T., Varuvel, E., Ganapathy, S., Vedharaj, S. & Vallinayagam, R. 2018. Role of fuel additives on reduction of NOx emission from a diesel engine powered by camphor oil biofuel. In *Environmental Science and Pollution Research*, pp. 1−10.

Ushakov, S., Halvorsen, N., Valland, H., Williksen, D. & Æsøy, V. 2013. Emission characteristics of GTL fuel as an alternative to conventional marine gas oil. *Transportation Research Part D: Transport and Environment* **18**, 31–38.

Vasu, S., Davidson, D. & Hanson, R. 2007. Jet fuel ignition times: Shock tube experiments over wide conditions and surrogate model predictions. *Combustion and Flame* **152**, 125−143.

Wang, B., Yang, H., Shuai, S., Wang, Z., He, X. & Xu, H. 2013. Numerical Resolution of Multiple Premixed Compression Ignition (MPCI) Mode and Partially Premixed Compression Ignition (PPCI) Mode for Low Octane Gasoline, *SAE Technical Paper*, No. 2013-01-2631.

Yadav, S., Murthy, K., Mishra, D. & Baral, B. 2005. Estimation of petrol and diesel adulteration with kerosene and assessment of usefulness of selected automobile fuel quality test parameters. *International Journal of Environmental Science & Technology* **1**(4), 253−255.

CIMAC CONGRESS 19
VANCOUVER, JUNE 10–14, 2019

2019 | 121

Ignition Studies of Liquid Marine Fuels with Different Ignition Analyzers

5 - Low Carbon Combustion - What Are the Alternative Fuels for the Future

Michaela Hissa, University of Vaasa

Seppo Niemi, University of Vaasa
Katriina Sirviö, University of Vaasa

ABSTRACT

To dampen climate change and meet sustainability goals, combustion systems needs to be able to operate with a variety of renewable and alternative fuels. When emission legislations are straighten, the role of the fuel quality is increased. Due to the variations in the chemical and physical properties of the fuels, they generally cannot simply be dropped into existing systems. The fuel quality affects the choice of engine materials and dictate limits for engine calibration and optimization, which has an effect on e.g. emissions, engine power output and drivability. The current study was a part of a larger project, the goal of which was to improve engine fuel flexibility without any or only minor changes to engine hardware. The present study focused on clarifying how various properties of the fuels affect the combustion process – especially the ignition delay and in-cylinder combustion. The ignition quality of nine marine and power plant fuels was studied in Herzog by PAC Cetane Ignition Delay (CID) 510 analyzer. The derived cetane numbers were also verified with the EN 15195 (IQT) method. The studied fuels were categorized into four groups: Group 1 – Low sulphur light fuel oils, baseline, Group 2 – Commercial alternative fuels, Group 3 – Renewable alternative fuels and Group 4 – Fuel blend with renewable share. The CID510 analyzer results showed that some renewable alternative fuels had better ignition qualities than some already commercial alternative fuels. Some alternative fuels, also renewables, are suitable to use in compression-ignited engines like baseline fuels. In contrast, some of the fuels had a long ignition delay and in a CI engine use, the engine must be started and stopped with a fuel of better ignition quality.

INTRODUCTION

There is a growing demand to increase renewable and alternative energy resources. The population of the world increases rapidly which is expected to increase global demand for commercial transport energy by 50% by the year 2040 [1, 2]. Although the evolution of transport and shipping energy will vary in different parts of the world, there is a complex interplay between many drivers e.g. the energy demand and supply, energy policy, climate change, population and economic growth and technology trends [3]. Today, there are many different scenarios how transport energy evolves. In Finland, Ministry of Transport and Communications has set a national goal to increase the share of liquid and gaseous biofuels in heavy transport at least to 70% by the year 2050 [4]. Some of the projections [5, 6] suggest that even by 2040 around 90 % of transport energy will come from combustion engines powered by petroleum. Fuel efficiency, strength and durability make marine diesel engines prime offshore energy producers. Maritime sector has developed different environmentally friendly strategies [7], e.g. hybrid propulsion, energy auditing, energy waste heat recovery, speed and voyage optimization and development of alternative fuels.

Traditional petroleum-based fuels, like gasoline, diesel and jet fuel, are still expected to dominate despite the strong growth of renewable and alternative energy [1]. However, to meet climate change requirements and sustainability goals, combustion systems need to be able to operate with a variety of renewable and alternative fuels. At this point, the role of the fuel quality is increased. When emission legislations are tightened, the sensitivity of the fuel quality is increased. Due to the variations in the chemical and physical properties of the fuels, they generally cannot simply be dropped into existing systems. The fuel quality affects the choice of engine materials and dictate limits for engine calibration and optimization, which has effect on, e.g., emissions, engine power output and drivability. The fuel is also integrated to the quality assurance system of engine manufacturers, through the technical functionality and performance, emissions and warranty issues [8].

Current specifications of commercial residual fuels of marine transport cannot reliably predict the ignition and combustion characteristics of a fuel due to the lack of a suitable test parameter [9, 10]. A proper fuel analysis is necessary before engine use to observe suitability of the fuel. For example, the energy density of the fuel is a significant factor, since many industrial applications involve long daily operating hours and additional tank volumes are not feasible [11]. Additionally, fuel handling has to be easy and safe even in extremely conditions, e.g., at very low or very high temperatures.

After the properties of an alternative fuel are confirmed, one must be sure that the existing fuel infrastructure is suitable and operation can be secured without high-cost establishments [11]. Ensured fuel flexibility of a CI engine is required to manage with fuel availability and fuel price fluctuation, and to meet emission regulations set for marine and industrial engines and end-users.

The combustion properties, chemical and physical (e.g. cetane number, CN and lower heating value, LHV) directly determine if the given alternative fuel is suitable for engine operation. The lower heating value defines the effectiveness of the fuel as energy carrier and it must meet the LHV level of conventional fuels to avoid problems in fuel consumption [12]. The CN, in turn, is one of the most important properties of ignition quality. The CN indicates how quickly fuel auto-ignites under compression.

Ignition characteristics of the fuel determine, e.g., the smoothness of engine operation, misfire, smoke emissions, noise and ease of starting [13]. A low CN and low viscosity of the fuel may cause increased NOx, smoke and noise emissions due to the prolonged ignition delay and retarded start of combustion [14, 15]. In CI engines, the combustion process starts when liquid fuel is injected as one or more jets into the cylinder filled with hot high-pressured air near the top dead centre (TDC) position of the piston. The ignition delay (ID) is a period when injected fuel entrains to cylinder, atomizes and mixes with existing air but does not yet ignite. Chemical reactions start slowly and ignition occurs after the ID. ID has a direct effect on the heat release rate and an indirect impact on engine noise and exhaust gas emission formation [15, 16]. A long ID results in a rapid pressure increase in the combustion chamber when unburned fuel finally ignites. The rapid pressure increase leads to diesel knock, higher soot emissions, malfunctions in engine operation and engine damages [9, 15, 17].

Consequently, a high enough CN is required for proper engine operation. The CN is determined from the ignition delay of the fuel. The traditional CN test method is the Cooperative Fuel Research (CFR) engine based on the ASTM D613 standard. The CFR method is time consuming, requires skilled personnel and a large amount of expensive chemicals. The method is not either suitable for heavy fuels. The high expense of acquiring and maintaining a CFR engine and its limitations have driven to develop alternative ways to measure the CN [13, 18, 19]. The Constant Volume Combus-

tion Chamber (CVCC) based methods, EN 15195 for the Ignition Quality Tester or IQT, EN 16144 for the Fuel Ignition Tester (FIT), IP 617 for the Advanced Fuel Ignition Delay Analyser (AFIDA), and EN 16715 for the Cetane Ignition Delay (CID510) have become replacing procedures to determine the cetane number of a fuel. The target of the CID510 and all CVCC methods is to simulate conditions inside a CI engine cylinder right before fuel injection. The measurements are made automatically using temperature and pressure sensors.

The CID510 analyzer, the subject of the present study, is said to provide more repeatable conditions and results than an engine [20]. It is used in a different kind of autoignition research [20−24]. Kuszewski et al. [25] concluded that the use of the CID510 analyzer provides an alternative method for ignition delay testing and requires much less effort compared to the engine research.

The current study was a part of a larger research project, the final goal of which was to allow broad engine fuel flexibility without any or only minor changes to engine hardware. Before the engine tests, the autoignition properties of the fuel options had to be determined. The CID510 measurements were used for this task to find out the engine suitability of the fuels. The CN determination was based on the ID and combustion delay (CD) periods resulting in a CN value, called in this instrument as the derived cetane number (DCN) value. The results enlarge knowledge of ignition characteristics of alternative marine fuels and help to optimize engines to run with new fuel choices.

MATERIALS AND METHODS

Fuels

To analyze autoignition properties of nine (9) fuels, they were categorized into four groups: Group 1 – Low sulphur light fuel oils, baseline; Group 2 – Commercial alternative fuels; Group 3 – Renewable alternative fuels; and Group 4 – Fuel blend with renewable share. Before the measurements in a CID510 analyzer, the kinematic viscosity, density, lower heating value (LHV) and sulphur content of the fuels were determined (Table 1). For verification of the measured DCN in the CID510, the cetane number of the fuels were also analyzed with another method, IQT (EN 15195).

Two commercial low sulphur light fuel oils were selected for baseline fuels forming the Group 1 (Fuel1 and Fuel 2). These fuels fulfill the EN 590 [26] standard for diesel fuel.

The Fuels 3−6 were selected in the Group 2: commercial alternative fuels. Fuels 3−5 were marine gas oils and Fuel 6 was aviation fuel. The Fuel 3 had the highest kinematic viscosity (8.0 mm^2/s), whereas the Fuel 5 had the highest density (886 kg/m^3). The high viscosity leads to poor atomization and decreases the flow performance of the injector which results [12] in longer total injection duration and leads to incomplete combustion resulting in higher soot emissions [27]. Fuel 6 had a low viscosity and density, which may cause mechanical problems in engine use as leakage through the injector or fuel pumping system, as well as problems with ignition and engine starting. The lower density may also decrease maximum engine power and affect fuel consumption [12]. However, the lower viscosity could improve the fuel atomization, evaporation and air/fuel mixing process [14]. A minor portion of lubrication additive (1:4000) was added to Fuel 6 to avoid possible malfunctions in engine use. This amount of lubrication additive should not have any effect on the autoignition properties of the fuel.

The Group 3 consists of two already commercial renewable fuels (Fuel 7 and Fuel 8). Fuel 7 was biodiesel and Fuel 8 hydrotreated vegetable oil (HVO). The LHV of HVO was at the same level as that of the conventional fuels (42−44 MJ/kg). This fuel also had a suitable viscosity and density. The lower LHV of the biodiesel (38 MJ/kg) may limit engine performance and increase volumetric fuel consumption.

Finally, a non-commercial renewable fuel, wood produced naphtha, with a low viscosity and density was blended with baseline Fuel 1. The blend ratio was 74 vol-% for Fuel 1 and 26 vol-% for the renewable share. This blend was called as Fuel 9 and it formed the Group 4.

Method

The experiments were carried out in a Herzog by PAC Cetane Ignition Delay 510 (CID510) device. It is a commercial, fully automated CVCC instrument with an electronically controlled high-pressure common-rail injection system and patented Multi Point ID measurement. The CID510 fulfills the standards EN 16715, ASTM D7668 and IP 615. The design of the CID510 combustion chamber mimics a diesel engine combustion chamber and its light-duty diesel injector is very similar to an automotive common-rail injection system. The CID510 is equipped with a dynamic pressure sensor to measure the chamber pressure, a static pressure sensor to correct the temperature offset of the dynamic sensor, an injection pressure sensor, an inlet air pressure sensor and two thermocouples type K for the chamber inner wall and the cooling jacket. [28, 29] The same type of device was used, e.g., in the studies [15, 20−25, 30−32]. The measuring principle of the CID510 is given in Fig. 1.

Table 1. Fuel properties.

		Kinematic viscosity at 40 °C	LHV	Density at 15 °C	Sulphur content	Lubricity
		mm^2/s	MJ/kg	kg/m^3	mg/kg	mm/60 °C
		EN ISO 3104	ASTM D240	EN 12185	EN 20846	EN ISO 12156-1
Group 1	Fuel 1	3.1	43	836	6	350
	Fuel 2	2.9	43	833		
Group 2	Fuel 3	7.7	43	843	<100	491
	Fuel 4	3.7	43	838	30	484
	Fuel 5	3.9	42	886		
	Fuel 6	1.0	44	787	900	447*
Group 3	Fuel 7	4.5	38	883	<5	196
	Fuel 8	3.5	44	813	<5	
Group 4	Fuel 9	1.8	43	810	<5	335

* value incl. additive

Before measuring the fuel samples, the device was calibrated according to the procedure specified in the standard EN 16715. The used calibration fuel was the same Primary Reference Fuel (PRF) as also used for calibration of the CFR engine (ASTM D613). The calibration parameters are summarized in Table 2.

The following values were recorded in the study: ID period, CD period, initial pressure in the combustion chamber (p_0), temperature of the combustion chamber walls (t_{ch}), temperature of the injector coolant (t_{co}) and fuel injection pressure (p_{inj}). The chamber was fulfilled with synthetic air that met the requirements given by the device manufacturer (19.5 to 20.5% O_2 with the balance N_2, where contaminants: <0.003 vol-% hydrocarbons and <0.025 vol-% water) [33].

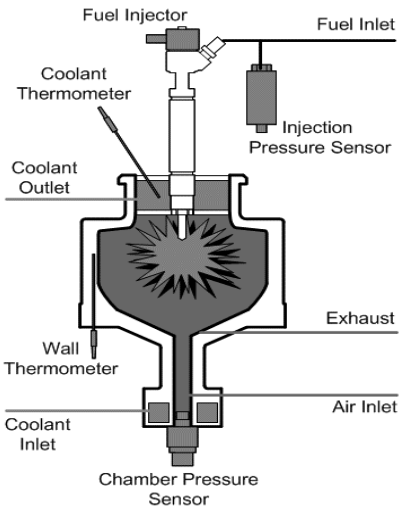

Figure 1. The measuring principle of the Herzog by PAC Cetane Ignition Delay 510. [28]

The pressure in the combustion chamber was recorded with a sampling frequency of 25 kHz. The recording was considered to end after 220 ms.

Table 2. Testing device calibration settings.

Parameter	Calibration setting
Injection pressure, p_{inj} (bar)	1000
Injection period, t_{inj} (µs)	2500
Initial chamber pressure, p_0 (bar)	20
Initial chamber temperature, t_{ch} (°C)	596.5
Injector nozzle coolant jacket temperature, t_{co} (°C)	50
Combustion chamber volume (ml)	473
Sample size (ml)	Min. 60
Test duration (min)	30 (approx.)

The CID510 can determine the DCN of the fuel for the range of 15 to 100 [33]. However, the manufacturer does not provide specific limits for e.g. kinematic viscosity of a fuel that can be analyzed with the device.

Measurements

Fuels were injected to the analyser at room temperature without any pre-preparations. The fuel sample was set into the analyser, which took a required fuel quantity to the measurement. There was a single measurement step for every sample, which included 5 preliminary combustion cycles and 15 measurement cycles. One cycle included one fuel injection to the chamber. The 5 preliminary cycles confirmed the calibration settings for the studied fuel. The average values of 15 measurement cycles formed the results of the ID, CD and DCN.

The ID was measured based on Standard EN 16715. The beginning of the ID period was assumed to be the moment when the impulse of

injector solenoid control was triggered (t=0). The ID ended when the pressure in the chamber was 0.2 bar greater than the initial pressure. A diagram of ID is shown in Fig. 2.

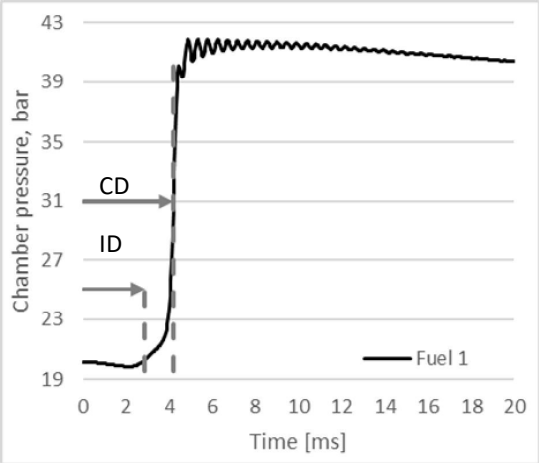

Figure 2. The average chamber pressure of Fuel 1 against time; ID and CD periods also illustrated.

The parameters related to CD according the standard EN 16715 are also shown in Fig. 2. The CD was considered to start at the fuel injection (t=0) and end when half of the pressure increase was achieved in the combustion chamber. The DCN was determined following the EN method 16715. The standard derives the cetane number by using the average ID and CD across 15 injection cycles in a temperature-controlled chamber.

The injection period was 2.5 ms, Table 2. In this study, all fuel samples were managed to inject before ignition, since all fuels had an ignition delay of longer than 2.5 ms.

RESULTS AND DISCUSSION

The autoignition properties of nine marine and power plant fuels were determined with the Herzog by PAC Cetane Ignition Delay 510 instrument. The measured quantities were the ignition delay (ID) period and combustion delay (CD) period. The derived cetane number DCN was calculated based on the ID and CD.

It should be noted that the actual engine conditions differ from those of CID510. The major difference is the cylinder pressure that in 4-stroke engines reaches even more than 200 bar while the cylinder pressure in the CID510 was max. 42 bar. In the CVCC device, fuel is also injected in a fixed period before ignition. In engines, especially at high loads, the fuel injection overlaps ignition and combustion [14]. This means that in an engine, a large amount of fuel is injected into a space with a flame [34]. Despite the differences between the CVCC device and actual engine conditions, the CID510 analyser produced comparable results as far as the engine suitability of the fuel is considered.

Ignition delay

Fig. 3 shows that the longest ID was measured for Fuel 5 (3.97 ms). Fuel 6 also had a relatively long ID, 3.83 ms. The IDs of Fuels 7, 9, 2 and 4 also were over 3 ms, 3.20 ms, 3.19 ms, 3.10 ms and 3.08 ms, respectively. The IDs of Fuels 1 and 8 were 2.88 ms and 2.82 ms, respectively. Fuel 3 had the shortest ID, 2.73 ms. With every fuel sample, the ignition delay was, thus, longer than the injection period (2.5 ms).

The ID depends on the CN. A low CN and low viscosity of the fuel may cause a prolonged ID and retard the start of combustion [14, 15]. In this study, the viscosity did not seem to clearly explain the IDs. Fuel 6 had the lowest viscosity, 1.0 mm^2/s, and a long ID. Still longer ID was, however, measured for Fuel 5 that had a usual viscosity of 3.9 mm^2/s. Another low-viscosity Fuel 9 (1.8 mm^2/s) had a fairly average ID. Fuel 3 had the shortest ID and the highest viscosity (7.7 mm^2/s). Fuel 8, though, also showed a short ID while the viscosity was a common one of 3.5 mm^2/s. A long ID can be shortened by increasing combustion chamber temperature or injection pressure. [10].

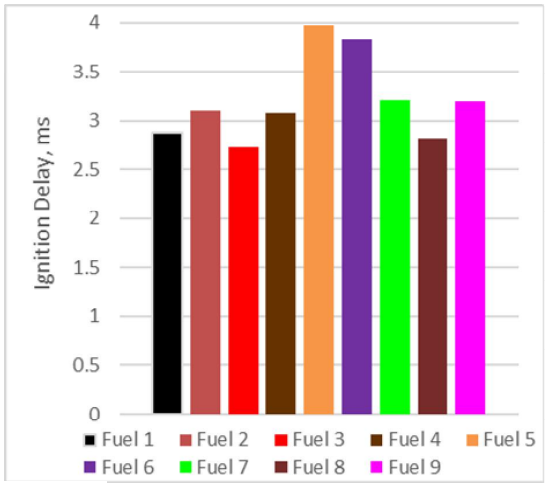

Figure 3. Ignition delay, average values of 15 cycles.

The ID is a very important parameter in terms of engine and emissions performance. In an optimization study of Köten and Parlakyiğit [35], it was found that the engine speed, load and fuel temperature significantly affect ignition delay. Generally, a short ID is desirable. However, Agrawal et

al. [33] noticed that a too short ID may decrease homogenous mixing of a fuel and air and reduce combustion efficiency. A longer ID allows more fuel to be injected which once ignited gives a stronger pressure peak. This may, however, lead to higher NOx, smoke and noise emissions [14, 15].

Combustion delay

The combustion delay period can be considered as a complementary assessment factor of the autoignition properties of the fuel. The CD and ID periods are used to calculate the DCN of the fuel.

Fig. 4 shows the combustion delay periods as the average values of 15 cycles. Fuel 5 had the longest CD period (6.12 ms) as well as the longest ID. The CD periods decreased in the same fuel order than the observed ID: Fuel 6, 9, 2, 7, 4 and Fuel 1. The CD period values were, respectively, 5.72, 4.75, 4.44, 4.42, 4.25 and 4.20 ms. Shorter than 4 ms showed Fuel 8 (3.99) and Fuel 3 (3.74). Fuel 3 had 39% shorter combustion delay than Fuel 5. A high viscosity, for example, increases total injection duration due to decreased flow of the injector [12].

Figure 5 illustrates combustion speed (ms), that is the difference of combustion delay (CD) and ignition delay (ID). The difference was calculated from the average values of 15 measurement cycles. Combustion speed determines the time from ignition of a fuel to the point where a half of the pressure increase was achieved in the combustion chamber (CD-ID). Fuel 5 had the slowest combustion speed (and the longest ID). The most rapid combustion was observed with Fuel 3, also showing the shortest ID.

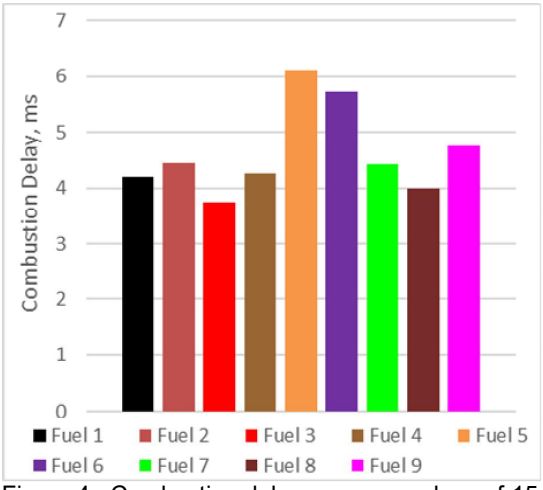

Figure 4. Combustion delay, average values of 15 cycles.

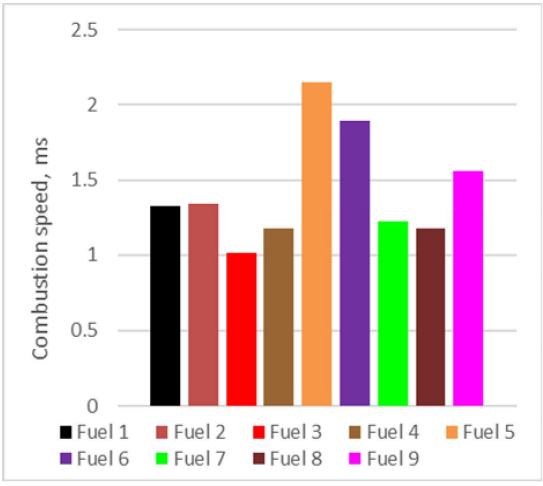

Figure 5. Combustion speed, average values of 15 cycles.

Derived Cetane Number

The CN is a primary decisive factor when the suitability of an alternative fuel for CI engine applications is considered. The results for the DCN using the CID510 analyser are given in Fig. 6. The DCN results were also verified with the EN 15195 (IQT) method (Table 3).

Fuel 5 (DCN 42) and Fuel 6 (DCN 44) had the lowest CN values as well as the longest IDs (Fig. 3). Fuel 3 had the highest DCN (66) and the shortest ID.

Table 3. Cetane Number results with standardized methods.

	Cetane number IQT / EN 15195 CFR /* ISO 5165 CI /** ISO 4264	Derived cetane number CID510/ EN 16715
Fuel 1	58	57
Fuel 2	55**	54
Fuel 3	68	66
Fuel 4	54	56
Fuel 5	38*	42
Fuel 6	44	44
Fuel 7	54	54
Fuel 8	65	60
Fuel 9	52	50

Generally, the CID results were fairly similar to those, measured with other methods. Fig. 7 shows the correlation between the DCN from CID510 and CN from the IQT method. The main difference between the methods is that the CID510 uses a modern, high-pressure common-rail diesel injector, whereas the IQT uses a lower-pressure mechanical injector.

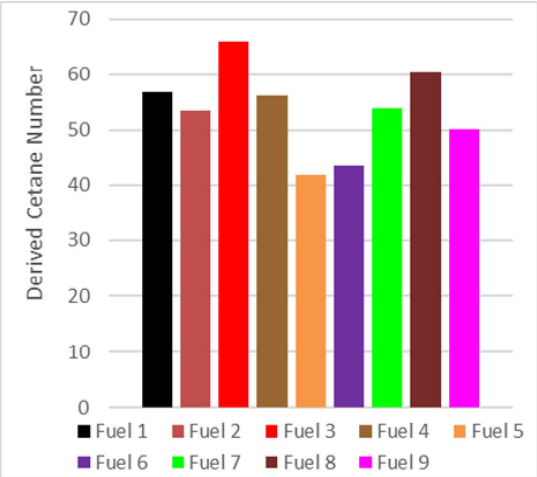

Figure 6. Derived Cetane Number results using the CID510.

The DCN of the reference fuel, Fuel 1, was 57 or 1 unit lower than the value determined using the IQT. The IQT value for the derived cetane number of Fuel 3 was 68 against 66 with the CID. The lowest values were recorded with Fuel 5 (42 with CID510 and 38 with ISO 5165, CFR method). Fuel 8 had the biggest difference between the measuring methods: the CID510 gave a DCN result of 60 and IQT 65. For Fuel 2, the Cetane Index was determined and for Fuel 5, CN was measured based on the CFR method, ISO 5165. Therefore, Fuel 2 and 5 are not compared in Figs. 7 and 8. Based on the low DCN results, Fuels 5 and 6 may require modifications to the engine parameters.

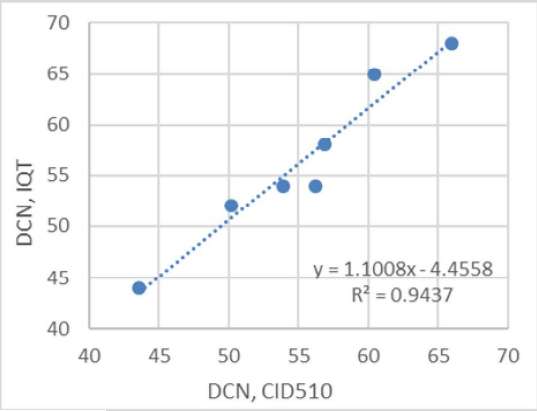

Figure 7. The DCN correlation between the CID510 and the IQT methods.

Fuels 6 and 7 had quite different fuel properties. Commercial alternative Fuel 6 had a low viscosity and low density as well as high sulphur content and LHV. Renewable Fuel 7 had a high density and low LHV with low sulphur content. For Fuels 6 and 7, both methods, CID510 and IQT gave, however, the same cetane result. This confirms that a wide range of fuels can be measured with both methods.

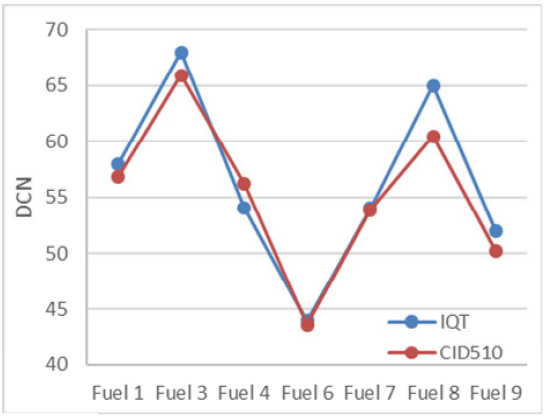

Figure 8. The DCN results of seven fuel samples.

The difference in the results of the renewable, commercial HVO, Fuel 8, requires repetition of the measurement. To verify the error, more samples should be analysed, and the repeatability should be measured. In the present study, the possible, but improbable CN improver content was not measured. The possible improver may distort the results. As a whole, Fuel 8 fulfilled EN 590 standard for diesel fuel.

CONCLUSIONS

The growing demand to increase renewable and alternative energy resources creates the need for maritime sector to develop environmentally friendly strategies. In marine applications, diesel and gas engines will be prime energy producers for a long time due to their high power density, excellent thermal efficiency, strength and durability, and overall profitability.

Renewable and alternative fuels must, however, be developed for marine engines. Due to the variations in the properties of the fuels, they generally cannot simply be dropped into existing systems without verification. A proper fuel analysis is necessary before engine use to ensure the suitability of the fuel.

The cetane number (CN) is one of the most important properties when assessing the feasibility of a fuel. The CN indicates how quickly fuel autoignites under compression. A high enough CN is required for proper engine operation. The traditional CN measurement method is the Cooperative Fuel Research (CFR) engine. This engine-based method is time consuming, requires skilled personnel and a large amount of expensive chemicals. The method is not either suitable for heavy fuels.

Therefore, alternative ways have been developed to measure the CN. This study focused on the determination of the CN of nine alternative marine fuels using the Cetane Ignition Delay (CID510) method. The Herzog by PAC CID510 analyzer (EN 16715) was used to determine the derived cetane numbers (DCN) of the fuels. For comparison, the DCN results were verified with the IQT method (EN 15195).

For the analyses, the fuels were divided into four groups: Group 1 – Low sulphur light fuel oils, baseline; Group 2 – Commercial alternative fuels, three different marine gas oils (MGO) and an aviation fuel; Group 3 – Renewable alternative fuels; and Group 4 – Fuel blend with renewable share.

Based on the performed measurements, the following conclusions could be drawn:

- With every fuel sample, the ignition delay was longer than the injection period. It means that the total amount of the fuel was injected into the combustion chamber before ignition.
- In Group 2, one of the MGOs had the highest DCN (66) while the other MGO showed the lowest DCN (42). The aviation fuel also had a low DCN (44).
- In Group 3, HVO had the second highest DCN (60). Biodiesel showed a relatively high DCN (54). Both fuels can be considered as alternative choices in a CI engine.
- In Group 4, the fuel blend with a renewable share of naphtha had a moderate DCN (50). This fuel had an ID period as long as biodiesel, but the CD period was longer. The blend can also be considered as an alternative choice for marine engines.
- For most fuels, the CID510 method seemed to produce cetane numbers very similar to those measured by the IQT instrument. In one, the worst case, the difference was five units or approx. 10%. To verify the error, more samples should be analysed, and the repeatability should be measured. In the present study, the possible, but improbable CN improver content was not measured.
- Despite the observed few differences in DCN values between the CID510 analyser and IQT method, the former was, as a whole, considered as a suitable method for studying the engine suitability of the fuel.

ACKNOWLEDGEMENTS

This project has received funding from the European Union's Horizon 2020 research and innovation programme under grant agreement No 634135.

This study was also granted by Henry Ford Foundation. The authors would like to thank the Foundation for the support of this research. The authors would also like to appreciate Berner Ltd. and Mr. Heikki Suortti and Mr. Michael Murer for the assistance in the measurements.

REFERENCES

[1] Alabbad, M., Issayev, G., Badra, J., Voice, A.K., Giri, B.R., Djeppi, K. Ahmed, A., Sarathy, S.M. and Farooq, A. 2018. Autoignition of straight-run naphtha: A promising fuel for advanced compression ignition engines, *Combustion and Flame* 189, 337-346.

[2] Sirviö, K. 2018. Issues of various alternative fuel blends for off-road, marine and power plant diesel engines. Dissertation. Acta Wasaensia 400, University of Vaasa, Finland.

[3] Kalghatgi, G. 2018. Is it really the end of internal combustion engines and petroleum in transport?*Applied Energy* 225, 965-974.

[4] Ministry of Transport and Communications. 2013. *Tulevaisuuden käyttövoimat liikenteessä. Työryhmän loppuraportti*. Working group Final Report, Finland. In Finnish.

[5] U.S. Energy Information Administration (EIA). 2016. *International energy outlook 2016*.

[6] World Energy Council. 2011. *Global transport scenarios 2050*. WEC London, UK.

[7] Gabiña, G., Martin, L., Basurko, O.C., Clemente, M., Aldekoa, S. and Uriondo, Z. 2019. Performance of marine diesel engine in propulsion mode with a waste-oil based alternative fuel, *Fuel* 235, 259-268.

[8] Röj, A. 2014. Volvo: Fuelling future vehicles – challenges and opportunities. Proceedings of *Neste Oil Product seminar*, 6.11.2014, Porvoo, Finland. Ppt-show.

[9] The International Council on Combustion Engines, CIMAC. 2011. *Fuel quality guide – Ignition and combustion*.

[10] Plank, M., Wachtmeister, G., Remmele, E., Thuneke, K. and Emberger, P. 2017. Ignition characteristics of straight vegetable oils in relation

to combustion and injection parameters, as well as their fatty acid composition, *Fuel Processing Technology* 167, 271-280.

[11] Omari, A., Heuser, B., Wiartalla, A. and Bergmann, D. 2018. Electricity-generated Fuels for Mobile Machinery, *ATZ offhighway worldwide* 11, 40-45.

[12] Bae, C. and Kim, J. 2016. Alternative fuels for internal combustion engines, *Proceedings of the Combustion Institute* 0000, 1-25.

[13] Heywood, J.B. 2018. *Internal Combustion Engine Fundamentals*, 2nd Edition, McGraw-Hill Education, USA.

[14] Subramanian, T., Varuvel, E., Ganapathy, S., Vedharaj, S. and Vallinayagam, R. 2018. Role of fuel additives on reduction of NOx emission from a diesel engine powered by camphor oil biofuel, *Environmental Science and Pollution Research* 25(16), 15368–15377.

[15] Kuszewski, H. 2019. Experimental investigation of the autoignition properties of ethanol-biodiesel fuel blends, *Fuel* 235, 1301-1308.

[16] Aldhaidhawi, M., Chiriac, R. and Badescu, V. 2017. Ignition delay, combustion and emission characteristics of Diesel engine fueled with rapeseed biodiesel -A literature review, *Renewable and Sustainable Energy Review* 73, 178-186.

[17] Ogawa, H., Morita, A., Futagami, K. and Shibata, G. 2018. Ignition delay in diesel combustion and intake gas conditions, *International Journal of Engine Research* 19(8), 805-812.

[18] Karonis, D., Zahos-Siagos, I., Filimon, D. and Vasileiou, F. 2017. A multivariate statistical analysis to evaluate and predict ignition quality of marine diesel fuel distillates from their physical properties, *Fuel Processing Technology* 166, 299-311.

[19] Yanowitz, J., Ratcliff, M.A., McCormick, R.L., Taylor, J.D. and Murphy, M.J. 2017. Compendium of Experimental Cetane Numbers. Technical Report. *The National Renewable Energy Laboratory* (NREL).

[20] Fisher, B.T., Allen, J.C., Hancock, R.L. and Bittle, J.A. 2017. Evaluating the Potential of a Direct-Injection Constant-Volume Combustion Chamber as a Tool to Validate Chemical-Kinetic Models for Liquid Fuels, *Combustion Science and Technology* 189:1, 1-23.

[21] Lapuerta, M., Sanz-Argent, J. and Raine, R. 2014. Ignition Characteristics of Diesel Fuel in a Constant Volume Bomb under Diesel-Like Conditions. Effect of the Operation Parameters, *Energy & Fuels* 28, 5445-5454.

[22] Lapuerta, M., Sanz-Argent, J. and Raine, R. 2014. Heat release determination in a constant volume combustion chamber from the instantaneous cylinder pressure, *Applied Thermal Engineering* 63, 520-527.

[23] Mayo, M.P. and Boehman, A.L. 2015. Ignition Behavior of Biodiesel and Diesel under Reduced Oxygen Atmospheres, *Energy & Fuels* 29, 6793-6803.

[24] Kang, D., Kalaskar, V., Kim, D., Martz, J., Violi, A. and Boehman, A. 2016. Experimental study of autoignition characteristics of Jet-A surrogates and their validation in a motored engine and a constant-volume combustion chamber, *Fuel* 184, 565-580.

[25] Kuszewski, H., Jaworski, A., Ustrzycki, A., Lejda, K., Balawender, K. and Woś, P. 2017. Use of the constant volume combustion chamber to examine the properties of autoignition and derived cetane number of mixtures of diesel fuel and ethanol, *Fuel* 200, 564-575.

[26] SFS-EN 590:2013. Automotive fuels. Diesel. Requirements and test methods. 2013. *Finnish Petroleum and Biofuels Association*.

[27] Nabi, Md.N., Brown, R., Ristovski Z. and Hustad, J. 2012. A comparative study of the number and mass of fine particles emitted with diesel fuel and marine gas oil (MGO), *Atmospheric Environment* 57, 22-28.

[28] Herzog by PAC, Cetane ID510 – Cetane number analyzer, 2017. Ppt-show.

[29] Herzog by PAC Cetane Ignition Delay 510, 2017. Brochure.

[30] Lapuerta, M., Hernández, J.J. and Sarathy, S.M. 2016. Effects of methyl substitution on the auto-ignition of C16 alkanes, *Combustion and Flame* 164, 259-269.

[31] Lapuerta, M., Hernández, J.J., Frenández-Rodríguez, D. and Cova-Bonillo, A. 2017. Autoignition of blends of n-butanol and ethanol with diesel or biodiesel in a constant volume combustion chamber, *Energy* 118, 613-621.

[32] Kuszewski, H. 2018. Experimental investigation of the effect of ambient gas temperature on the autoignition properties of ethanol-diesel fuel blends, *Fuel* 214, 26-38.

[33] Herzog by PAC, Cetane Ignition Delay 510, Technical Specification, 2017. Brochure.

[34] Steernberg, K. and Forget, S. 2007. The effects of a changing oil industry on marine fuel quality and how new and old analytical techniques can be used to ensure predictable performance in marine diesel engines. Proceedings of *25th CIMAC Congress*, Vienna. Paper no. 198.

[35] Köten, H. and Parlakyiğit, A.S. 2018. Effects of the diesel engine parameters on the ignition delay, *Fuel* 216, 23-28.

CONTACT

Michaela Hissa
Project researcher
Ph.D. student
School of Technology and Innovations
University of Vaasa, Finland
E-mail: Michaela.hissa@univaasa.fi

energies

MDPI

Article

Combustion Studies of a Non-Road Diesel Engine with Several Alternative Liquid Fuels

Michaela Hissa *, Seppo Niemi, Katriina Sirviö, Antti Niemi and Teemu Ovaska

School of Technology and Innovations, University of Vaasa, P.O. Box 700, FI-65101 Vaasa, Finland; Seppo.Niemi@univaasa.fi (S.N.); Katriina.Sirvio@univaasa.fi (K.S.); Antti.Niemi@univaasa.fi (A.N.); Teemu.Ovaska@univaasa.fi (T.O.)

* Correspondence: Michaela.Hissa@univaasa.fi

Received: 20 May 2019; Accepted: 23 June 2019; Published: 25 June 2019

check for updates

Abstract: Sustainable liquid fuels will be needed for decades to fulfil the world's growing energy demands. Combustion systems must be able to operate with a variety of renewable and sustainable fuels. This study focused on how the use of various alternative fuels affects combustion, especially in-cylinder combustion. The study investigated light fuel oil (LFO) and six alternative liquid fuels in a high-speed, compression-ignition (CI) engine to understand their combustion properties. The fuels were LFO (baseline), marine gas oil (MGO), kerosene, rapeseed methyl ester (RME), renewable diesel (HVO), renewable wood-based naphtha and its blend with LFO. The heat release rate (HRR), mass fraction burned (MFB) and combustion duration (CD) were determined at an intermediate speed at three loads. The combustion parameters seemed to be very similar with all studied fuels. The HRR curve was slightly delayed with RME at the highest load. The combustion duration of neat naphtha decreased compared to LFO as the engine load was reduced. The MFB values of 50% and 90% occurred earlier with neat renewable naphtha than with other fuels. It was concluded that with the exception of renewable naphtha, all investigated alternative fuels can be used in the non-road engine without modifications.

Keywords: CI engines; alternative fuels; in-cylinder combustion; heat release rate; combustion duration

1. Introduction

Limiting global warming requires rapid, far-reaching actions in land, energy, industry, buildings, transport and cities [1]. There is already strong growth of alternative energy sources. However, sustainable liquid fuels will be needed for decades to satisfy the world's growing energy demands [2]. Furthermore, internal combustion engines are set to continue as prime energy producers because there is an established worldwide infrastructure for liquid fuel distribution [3] and the engines offer fuel efficiency, strength and durability [4]. Combustion systems need to be able to operate with a variety of renewable and sustainable fuels and yet also meet increasingly stringent emission legislation. Expanding fuel choice calls for a clearer focus diversification, quality, and usability of any new fuel [5]. Alternative fuels can reduce diesel engine emissions and several beneficial results have already been obtained in practice [6]. However, availability of alternative fuels must evolve to ensure energy security and sustainability. Moreover, their higher price presents a challenge when making new fuel choices [6]. According to Sirviö [6], an alternative fuel must fulfil quality assurance and standard requirements to secure consumer acceptance. In addition, after-treatment applications support a conventional and alternative target for fuels to reduce exhaust emissions.

The distinguishing features of diesel combustion are spontaneous ignition (resulting from the high air temperature and pressure in the cylinder when injection commences) and the fact that fuel-air

mixing controls the burning rate [7]. Diesel exhaust emissions depend greatly on fuel and lubricating oil properties, engine parameters and exhaust after-treatment technology. Driving and environmental conditions also influence emissions [8]. Cylinder gases' temperature, pressure, density and composition as well as injection timing and injector type, have a direct effect on combustion and emission formation for a given fuel [9]. In-cylinder pressure has a fundamental role in combustion characteristic analyses and it is needed to control combustion-related parameters. Primarily, the peak cylinder pressure depends on the burned fuel fraction during the premixed combustion phase. A large amount of fuel burned in premixed combustion corresponds to a high peak cylinder pressure. [10]

The delay period between the start of injection and start of combustion must be kept short, because injection timing is used to control combustion timing. A short delay is also needed to hold the maximum cylinder gas pressure below the maximum the engine can tolerate. [7] Therefore, the main ignition characteristic of a diesel fuel—its cetane number (CN) must be above a certain value.

This study focused on how the use of various alternative fuels affects combustion, especially in-cylinder combustion. A baseline fuel and six alternative liquid fuels were investigated in a high-speed compression-ignition (CI) engine to understand their combustion properties. The fuels were light fuel oil (LFO, baseline), marine gas oil (MGO), kerosene, rapeseed methyl ester (RME), renewable diesel (HVO), renewable wood-based naphtha and its blend with LFO.

One potential substitute for conventional fuels is mineral origin alternative oils, such as recycled waste oils. Recycling waste lubricant oils (WLO) into diesel-like fuels is an environmentally friendly solution because waste oils are classified as a hazardous waste [11,12]. In this study, the first alternative was marine gas oil (MGO), produced from waste lubricating oils. MGO is commonly known as a shipping fuel, and currently it is largely used when a vessel is inside an emission control area (ECA) or within EU ports. Sulphur emission regulations are becoming increasingly stringent and, in the case of older ships, the use of MGO is suggested to be more beneficial than retrofitting scrubbers [13]. Recently, Wang and Ni [14] and Gabiña et al. [4] have also investigated diesel-like fuel (DLF) manufactured from WLO.

Kerosene is primarily used in the aviation sector. However, the U.S. Army and the North Atlantic Treaty Organization (NATO) have a single military fuel policy—mandating the use of kerosene-based jet fuels in ground vehicles equipped with CI engines, thereby simplifying supply chain logistics [15]. Kerosene has been studied for its pollutants reduction potential. Amara et al. [16] presents studies where kerosene's higher volatility lowered NO_X emissions compared to diesel in a CI engine. Hissa et al. [17] also investigated neat kerosene in a combustion research unit (CRU) and concluded that other fuel may be needed for starting and stopping the engine, or different injection nozzles used. Kerosene's low lubricity may also cause a malfunction in the injection system. Nevertheless, kerosene was considered an interesting alternative for future special CI engine applications.

First generation biodiesels, known as FAME or fatty acid methyl esters, have been studied for a long time. Despite some problems, they still arouse great interest [6]. In Europe, the maximum FAME content in conventional diesel fuel is 7 V-% according to EN590:2013. However, in the United States, the renewable share is in some cases above 20 V-%, and even their own standard EN 16709 for B20 and B30 fuels. [6] Biodiesel fuels' different types of properties have a strong relation with their fatty acid composition. Poor cold properties and poor storage stability are the main problems associated with the use of FAME fuels [6]. The review article of Shahabuddin et al. [18] reported that the combustion characteristics of a bio-fuelled engine are slightly different from the engine running with petroleum diesel. This was one of the main reasons also to include rapeseed methyl ester (RME) in the present study.

Hydrotreated vegetable oils (HVO) are one of the easiest ways to increase the bio-component in diesel fuel. Moreover, they are highly recommended by vehicle and engine manufacturers [19]. The production process of hydrotreated fuels differs from FAME and this neat renewable diesel can be used in diesel engines without blending. HVO is sulphur and aromatic-free fuel which can be produced from various wastes such as animal fats, residues of forest industry and wastes from the food industry.

HVO offers some advantages compared to FAME (e.g., RME), including a higher cetane number (CN), better storage stability and fewer problems with cold operability and deposits [8]. HVO's properties correspond to those of traditional fossil fuels but a significant reduction of up to 80% in greenhouse gaseous emissions is achieved [5]. Furthermore, crude tall oil-based (CTO) fuels do not compete with the food chain and there is no direct land-use change [5]. A Finnish forestry company manufactured the CTO renewable diesel used in the study.

Renewable, wood-based naphtha is another interesting and novel fuel. This study's naphtha was made from CTO extracted in the pulp production process. This colourless, sulphur-free, paraffinic product is chemically pure hydrocarbon and can be used as a bio-component in fossil gasoline [20]. Conventionally, naphtha is produced from crude oil and is suitable for use in compression-ignition (CI) engines [14,21,22]. However, raw naphtha has a low cetane number (CN) which may cause prolonged ignition delay (ID) and hence may retard the start of combustion [23]. Hissa et al. [17] observed that ignition of neat wood-based naphtha had a retarded start of combustion and prolonged ID when measured in a CRU. This may limit use of neat naphtha as fuel in diesel engines. Neat naphtha also needs other fuel (e.g., LFO) for starting and stopping the engine. However, there is very little research into wood-based naphtha, prompting the inclusion of this fuel in the current study as an interesting renewable option, especially for blending.

Various liquid fuel options are needed in the near future for flexible power generation, marine and heavy-duty applications. Consequently, this study was carried out to evaluate the effects of alternative fuels' properties in an engine use and to promote the development of fuel processes and standard to meet engine requirements. The focus was on how various properties of the alternative fuels affects combustion, especially in-cylinder combustion. The cylinder pressures, heat release rates (HRR), mass fractions burned (MFB) and combustion duration were determined at an intermediate speed at three loads. The experimental engine was a high-speed common-rail diesel engine intended for non-road applications. All measurements were performed under steady operation conditions without engine modifications. The study continued with the emission analysis in the article by Ovaska et al. [24].

2. Materials and Methods

The engine experiments were conducted by the University of Vaasa (UV) at the Internal Combustion Engine (ICE) laboratory of the Technobothnia Research Centre in Vaasa, Finland.

2.1. Fuels

The studied fuels were selected with the aim of increasing the choice of fuel alternatives for non-road compression-ignition engines. The baseline fuel was a commercial low-sulphur light fuel oil (LFO) from Teboil, Finland. Jet A-1 aviation fuel (100% kerosene) was produced by Neste, Finland. Marine gas oil (MGO) produced from waste lubricant oils, was a product of STR Tecoil, Finland. Hydrotreated vegetable oil (HVO), also known as CTO-based renewable diesel, was produced by UPM, Finland. Rapeseed methyl ester (RME) was a product of Analytik-Service Gesellschaft mbH, Germany. Wood-based naphtha was made from CTO, extracted in the pulp production process, and was produced by UPM, Finland. Renewable naphtha was also blended with LFO (20 V-% naphtha and 80 V-% LFO), also known as naphtha20. Chemically, all the fuels contained several hydrocarbon compounds, therefore simple chemical formulas could not be given. Table 1 summarises the specifications of the studied fuels.

Cetane number (CN) is an indicator of the ignition quality of diesel fuel [7]. A high CN indicates good ignitability in a diesel engine. As shown in Table 1, the CN of the fuels ranged from 34 (neat naphtha) to 68 (recycled MGO). The CN of kerosene, naphtha20, LFO, RME and HVO were 41, 51, 52, 53 and 65, respectively.

There is an indirect relationship between density and other fuel parameters such as CN, viscosity, volatility and distillation characteristics [25]. It has also been shown that fuel density can have a direct

effect on the progress of fuel pressure in the injection system and a consequent effect on the dynamic start of fuel injection [25]. Neat naphtha had the lowest density (722 kg m^{-3}), markedly lower than that of the baseline LFO (827 kg m^{-3}). Lower density may result in lower engine power and also affects volumetric fuel consumption. The highest density was measured for RME (883 kg m^{-3}).

A higher mass-basis lower heating value (LHV) may result in a higher heat input to the engine, i.e., higher cylinder pressures and increased power output. The LHV of most of the studied fuels was 43–44 MJ kg^{-1}. The one exception was RME, with a LHV of 37 to 38 MJ kg^{-1}.

Legislation has driven down fuel's sulphur content. A lower, new sulphur limit (5,000 mg kg^{-1}) will be implemented in the maritime sector on 1 January 2020 [26]. In Finland, non-road diesel engine fuels must comply with EN 590:2013 standard, setting a maximum limit for sulphur content of 10 mg kg^{-1} [27]. Regarding the studied fuels, kerosene (1000 mg kg^{-1}) and MGO (<100 mg kg^{-1}) had sulphur exceeding EN 590:2013's limit.

Diesel fuel injection systems are lubricated mainly by the fuel itself. However, when sulphur level of a fuel is reduced, the process also destroys some of the fuel's natural lubricants [28]. To avoid wear in the fuel injection system, a minor portion of lubrication additive (1:4000) was added to kerosene to avoid possible malfunctions in engine use. This amount of lubrication additive should not have any effect on the autoignition properties of the fuel. Also, MGO had lower lubricity than LFO. This might be shown as injection system failures over the time. In addition, longer engine measurements are required to examine the effect of the lubricity.

Table 1. Fuel specifications.

Parameter	Unit	LFO	MGO	Naphtha	Kerosene	RME	HVO	Naphtha20
Flash point	°C	63	110	20	38	179	78 [b]	
Density at 15 °C	kg m^{-3}	827	843	722	787	883	813	805
Kin. viscosity (40 °C)	mm^2 s^{-1}	1.84	7.69	0.50	0.94	4.49	3.5	1.37
LHV	MJ kg^{-1}	43	43	44	43	37–38 [b]		
Cetane number	-	52	68	34	41	53	65	51
Sulphur content	mg kg^{-1}	8.3	<100		1000	<5	<1[b]	6.8
Ash content (775 °C)	wt.%	<0.001	<0.001	0.005	0.001		<0.005 [c]	
Water content	mg kg^{-1}	61	22		35	<30	<30 [c]	
Lubricity	µm	345	491		447 [a]		228 [c]	

[a] Value includes added lubricity improver, [b] Hassaneen et al. [29], Tira et al. [30], [c] Niemi et al. [5]

Safety issues are also critical when introducing new fuels. Fuel suppliers have to specify the fuel properties and confirm compliance with industry standards. These properties include flashpoint, combustibility, stability, compatibility, viscosity, lubricity, etc. Every one of these properties, if not properly addressed, can affect equipment performance and/or reliability and above all, affect safety of personnel or the engine's safe operation [31]. In the present study, the low flash points of neat naphtha (20 °C) and kerosene (38 °C), and their low viscosity (naphtha 0.50 mm^2 s^{-1} and kerosene 0.94 mm^2 s^{-1}) necessitated additional safety procedures when handling the fuels and making measurements in the engine. For the studied fuels, the compatibility of the engine, fuel system and auxiliaries was ensured. Additionally, the engine operators used respirator masks and gloves during the measurements.

2.2. Engine

The test engine, an AGCO Power 44 AWI, was a high-speed four-cylinder diesel engine for non-road applications. It was turbocharged, intercooled and had Bosch common-rail fuel-injection. It was loaded by means of a Horiba eddy-current dynamometer WT300. The engine's specification is in Table 2.

Table 2. Test engine specification.

Engine	AGCO POWER 44 AWI
Cylinder number	4
Bore (mm)	108
Stroke (mm)	120
Swept volume (dm^3)	4.4
Rated speed (min^{-1})	2200
Rated power (kW)	101
Maximum torque at 1500 1 min^{-1} (Nm)	585

2.3. Analytical Instruments

LabVIEW system-design software was used to collect the sensor data from the engine. The recorded variables were engine speed and torque, cylinder pressure and injection timing, duration and quantity. A WinEEM4 program provided by the engine manufacturer, AGCO Power, controlled fuel injection according to load-speed requests. The basic settings of WinEEM4 were the same for all fuels. A schematic of the setup of the test bench is in Figure 1.

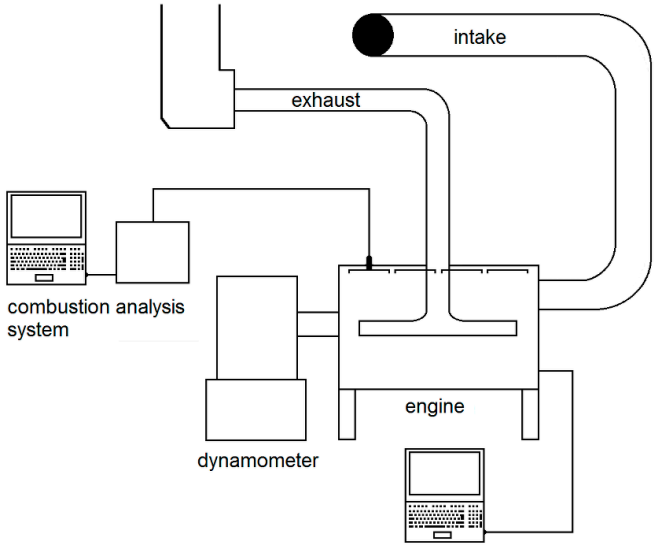

Figure 1. Schematics of the experimental system.

A piezoelectric Kistler 6125C pressure sensor was used to measure in-cylinder pressure. The sensor was mounted on the head of the fourth cylinder. A charge amplifier filtered and amplified the signal, which was then transmitted to a Kistler KIBOX combustion analyser. The crankshaft position was recorded by a crank-angle encoder (Kistler 2614B1), which can output a crank-angle signal with a resolution of 0.1 °CA by means of an optical sensor. The cylinder-pressure data was averaged over 100 consecutive cycles to smooth irregular combustion. The averaged data was used to calculate HRR.

The HRR and MFB were calculated via AVL Concerto's data-processing platform, using the Thermodynamics2 macro. The macro used a calculation resolution of 0.2 °CA. The start of the calculation was set at −30 °CA. The data were filtered with the DigitalFilter macro and a frequency of 2500 Hz. For the HRR results, the average values of in-cylinder pressure were calculated first. Thereafter, the macro was used to calculate HRR values. Finally, the HRR curve was filtered. In contrast, for the MFB results, pressure values were first filtered and then the macro was used. The average values of 100 cycles were not used for MFB results, establishing the standard deviations.

2.4. Experimental Matrix and Measurement Procedure

All measurements were performed under steady operation conditions without engine modifications. The measurements were conducted based on ISO 8178-4 standard, known as non-road steady cycle (NRSC). Additionally, the 25% (3.2 bar) load point was measured at an intermediate speed. With low-viscosity kerosene and neat naphtha, the default engine control parameters made running the engine possible only at an intermediate speed. The added 25% load point gave more information during the experiment, because no engine parameter optimization was applied. Multistage injection (pilot, main and post injections) was used throughout the study. The operating conditions chosen were an engine speed of 1500 min^{-1} and three different loads—Brake-mean effective pressures (BMEP) of 3.2 bar, 6.4 bar and 9.7 bar. The loads are in Table 3.

Table 3. Engine operating conditions with light fuel oil (LFO).

Engine Speed (min^{-1})	**1500**		
BMEP (bar)	3.2	6.4	9.7
Load (%)	25	50	75
Torque (Nm)	113	225	338

2.5. Injection Strategy

Pilot injection shortens the ID of a fuel by increasing in-cylinder temperatures for main injections. Post injections, in turn, are used to reduce particulate and soot emissions, primarily at lighter loads and lower engine speeds [7].

For all the fuels at all loads, the pilot injection was constant. It started at 6.8 ± 0.1 °CA BTDC and ended at 4.1 °CA BTDC. The main injection started at exactly 0.9 °CA BTDC. The duration of the main injection varied not only with the load, but also according to the fuel's heating value. The main injection was always longest with RME (5.2 to 8.2 °CA depending on the load), due to its lower LHV. The main injection durations for the other fuels were very similar (4.8–7.7 °CA according to engine load). The start of post injection was linked to the end of main injection, and was thus delayed according to the fuel's LHV. The duration of post injection varied only slightly in the range of 3.3 °CA and 3.6 °CA and was independent of the load. The pilot and main injections are the most important factors when considering ignition delay, that is, HRR and MFB values.

The engine was started with LFO in all fuel tests. Then, fuel was changed to test fuel and the engine was warmed-up and the load was applied. The intake-air temperature was adjusted to 100 °C downstream of the charge-air cooler to support auto-ignition of the fuels at each load. The temperature was controlled manually by regulating the flow of cooling water to the heat exchanger. The valve setting was kept constant. Therefore, the charge temperature changed with the load. All measurements were taken only after the engine had stabilized, as determined by stability of the temperature of coolant water, intake air and exhaust.

3. Results and Discussion

This section presents and discusses the results of the studied fuel's combustion characteristics in terms of engine in-cylinder pressure, the rate of heat release and mass fraction burned. The main results of the emission analysis are provided, based on the article of Ovaska et al. [24].

3.1. Heat Release Rate (HRR)

The combustion process includes three stages. In the first stage, the rate of burning is rapid, lasts for only few CA degrees and produces the first spike in the HRR. The second stage is the main heat-release period and it has more rounded profile with longer duration. The third stage, the tail, is the remainder of the fuel's chemical energy released when burned gases mix with excess air that was not involved in the main combustion. [7] Figure 2a–c depicts the cylinder pressure traces and

Figure 2d–f the HRR curves. A slight loss in HRR curves was observed at the beginning due to the heat transfer into the liquid fuel, vaporizing and heating it [7].

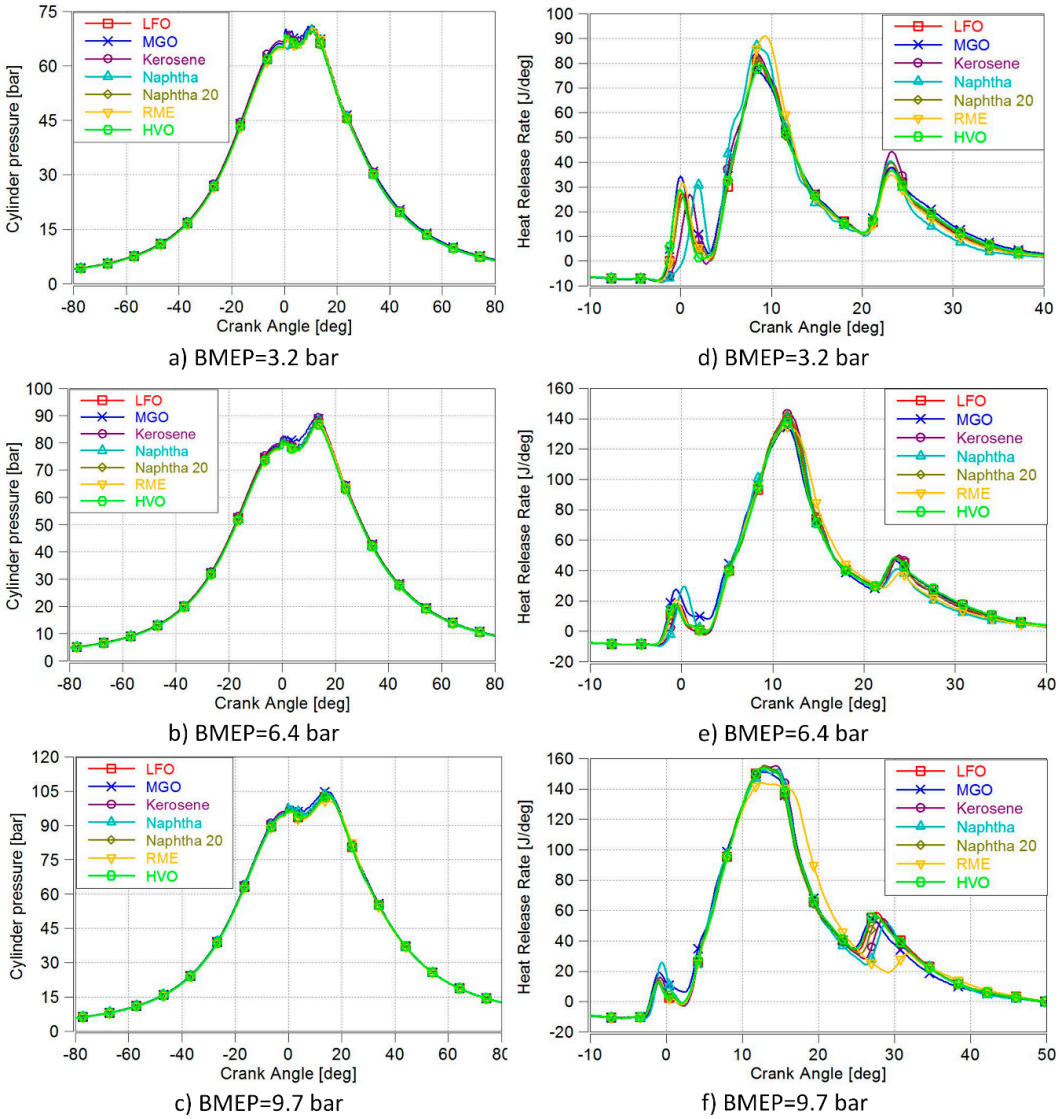

Figure 2. In-cylinder pressure and heat release rates at different engine loads.

At the lowest load (3.2 bar BMEP), the longer ID of naphtha and kerosene are apparent. Other fuels burned in a quite similar way, although MGO showed a slightly higher initial HRR. The highest maximum HRR peak was recorded with RME, maybe due to its high oxygen content triggering rapid initial combustion. Aldhaidhawi et al. [32] also mentioned that an increase in the fuel's oxygen fraction provided an increase in the premixed combustion stage. More rapid combustion of oxygen-containing bio-fuel has previously been noted, for example by Niemi et al. [33]. After a longer ID due to low CN, naphtha seemed to also burn fast, most probably due to light high-volatile compounds and the favourable effects of the low viscosity on fuel/air mixture formation. The HRR peaks of other fuels were rather similar.

At the medium load (6.4 bar BMEP), no clear differences in the ID were detected. The initial HRR of kerosene was low, but kerosene showed the highest HRR peak. Kerosene's low CN delayed start of

combustion but rapid burning may be a result of higher volatility of its lighter fractions. (Amara et al. 2016) MGO once again showed the highest initial but the lowest peak for HRR. Naphtha had a high initial HRR, but lower post injection HRRs peak than other fuels, except RME, which also showed low HRR after post-injection.

At high load (9.7 bar BMEP), the highest HRR values were rather similar for all fuels except RME. Its HRR curve was slightly delayed due to its lower LHV and lengthened main injection. Consequently, there was also a delay in RME's post-injection HRR peak. Neat naphtha showed a higher initial HRR than other fuels at high load, and its post-injection HRR peak was moderate, unlike its low peak at medium load.

3.2. Mass Fraction Burned (MFB)

At all loads, MGO had the earliest MFB 5% and 10% positions due to the high CN and short ID (Table 4). Neat naphtha had the earliest MFB 50% and MFB 90% at low and medium loads. Although naphtha's low CN increased the ID, it burned rapidly due to improved premixed combustion [34].

Table 4. Mass fraction burned and combustion durations (MFB 5−50% and MFB 5−90%).

BMEP	Fuel	MFB 5%	MFB 10%	MFB 50%	MFB 90%	CD 5−50%	CD 5−90%
bar		°CA	°CA	°CA	°CA	°CA	°CA
3.2	LFO	7.5	8.1	14	29	6.3	22
	MGO	7.0	7.7	14	30	6.8	23
	Kerosene	7.5	8.1	14	28	6.2	21
	Naphtha	7.2	7.7	12	27	5.2	20
	Naphtha20	7.5	8.1	14	29	6.2	21
	RME	7.3	7.9	13	28	5.2	21
	HVO	7.3	8.0	14	29	6.4	22
6.4	LFO	8.1	8.9	14	28	5.8	20
	MGO	7.2	8.1	13	28	6.2	21
	Kerosene	8.0	8.8	14	27	5.6	19
	Naphtha	7.7	8.5	13	26	5.5	19
	Naphtha20	8.0	8.8	14	28	5.7	20
	RME	7.9	8.7	14	27	5.7	19
	HVO	8.0	8.8	14	28	5.9	20
9.7	LFO	8.4	9.4	16	31	7.2	23
	MGO	7.7	8.9	15	30	7.5	22
	Kerosene	8.4	9.4	16	31	7.1	22
	Naphtha	8.1	9.2	15	31	7.1	23
	Naphtha20	8.3	9.3	15	31	7.1	23
	RME	8.4	9.4	16	31	7.5	23
	HVO	8.3	9.4	16	31	7.3	23

At low load (3.2 bar BMEP), the latest MFB 5% was measured for naphtha20 (7.5 °CA ATDC); the latest MFB 10% was for kerosene (8.1 °CA ATDC). The earliest positions for MFB 5% and MFB 10% were observed for MGO (7.0 and 7.6 °CA ATDC, respectively). However, MFB 50% and 90% were latest with MGO (14 and 30 °CA ATDC). MGO's high CN facilitated the early start of combustion. However, MGO had the highest viscosity (7.69 mm^2 s^{-1}) and this may have led to poorer mixing, giving more inhomogeneity zones than with neat naphtha. Poor mixture formation lead to a longer combustion duration and a lower rate of heat release [30]. The earliest MFB 50% and 90% were with neat naphtha (12 and 27 °CA ATDC), which had a low CN but higher volatility and considerably lower density than MGO.

At medium load (6.4 bar BMEP), LFO gave the latest MFB 5%, 10% and 50% (8.1, 8.9 and 14 °CA ATDC, respectively). MFB 90% was the latest for HVO (28 °CA ATDC). Neat naphtha and MGO showed rapid combustion at the medium load.

At the high load (9.7 bar BMEP) with higher in-cylinder pressure and temperature, MGO also had the earliest MFB 50% (15 °CA ATDC, Table 5) and MFB 90% (30 °CA ATDC). The latest MFB 90% was measured for RME (31 °CA ATDC). In fact, at this highest load, RME was the latest fuel at all MFB positions. This was also evident in the cylinder pressures: RME was slightly lower than with other fuels. The HRR curve of RME was also delayed compared with other fuels. It was assumed that RME's high oxygen content accelerated combustion at lower loads. At high load, however, RME's lengthened injection period, stemming from its low LHV, outweighed the advantage of high oxygen content. It is possible that higher in-cylinder pressures and temperatures also improved the HRR of other fuels relative to RME.

Table 5. Average values and standard deviations of mass fractions burned (MFB) 50%.

Fuels	BMEP 3.2 bar		BMEP 6.4 bar		BMEP 9.7 bar	
	MFB 50%	Stdev	MFB 50%	Stdev	MFB 50%	Stdev
Unit	°CA	°CA	°CA	°CA	°CA	°CA
LFO	14	0.16	14	0.083	16	0.095
MGO	14	0.22	13	0.11	15	0.11
Kerosene	14	0.19	14	0.095	16	0.10
Naphtha	12	0.17	13	0.081	15	0.088
Naphtha20	14	0.19	14	0.095	15	0.088
RME	13	0.12	14	0.091	16	0.10
HVO	14	0.15	14	0.084	16	0.093

3.3. Combustion Duration

Combustion duration (CD) can be expressed as the time interval between MFB 5% and MFB 50% (Figure 3 and Table 4) and the interval between MFB 5% and MFB 90% (Figure 4 and Table 4) which are linearly correlated at constant engine-speeds. For all the fuels at all loads, even MFB 5% occurred after the end of the main injection (Table 4). MFB 10% and 50% were achieved before post injection. MFB 90% occurred after the end of post injection.

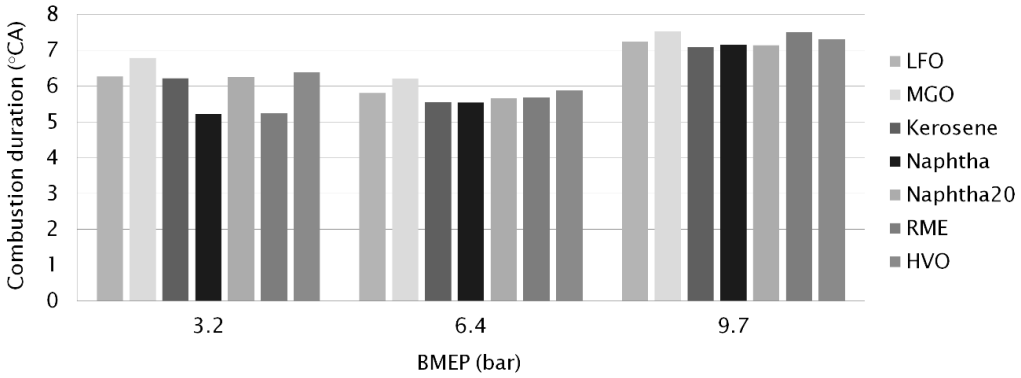

Figure 3. Combustion duration (°CA) at different engine-loads, determined as crank angles between MFB 5% and MFB 50%.

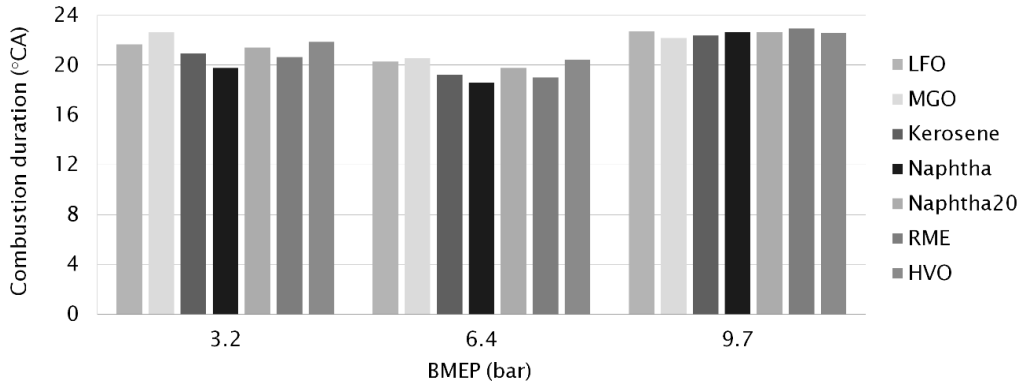

Figure 4. Combustion duration (°CA) at different engine-loads, determined as crank angles between MFB 5% and MFB 90%.

Both CD values (MFB 5−50% and MFB 5−90%) were the shortest for neat naphtha (5.2 and 20 °CA respectively) at the low load of 3.2 bar BMEP. Naphtha's low CN increased its ID but light fractions of neat naphtha burned rapidly, giving a short CD, especially MFB 5−50%. RME's high oxygen content showed as rapid early burning—its MFB 5−50% CD of 5.2 °CA was the same as naphtha's. The longest CD values at low load were measured for MGO (6.8 and 23 °CA) due to its high viscosity that led to poor fuel/air mixing and hence longer combustion duration.

When engine-load was increased, the CD was first shortened (at 6.4 bar BMEP) and then prolonged (at 9.7 bar BMEP). Longer combustion duration is associated with an increase in fuel quantity for the higher engine-load [35]. At the medium load (6.4 bar BMEP), neat naphtha had the shortest CD figures (5.5 and 19 °CA) while MGO again had the longest CD (6.2 and 21 °CA). HVO showed almost as long as the total CD as MGO. Gabiña et al. [4] also measured longer (10−17%) combustion durations for waste oil-based DLF than for diesel fuel oil (DFO) in a marine scale diesel engine. The combustion period started slightly earlier and ended slightly later with the DLF. The authors attributed this to DLF's higher CN, which implied a shorter ID with a shorter premixed combustion phase, involving a lower pressure gradient, maximum combustion pressure and HRR.

At the high load (9.7 bar BMEP), the longest CD between MFB 5−50% was measured for MGO and RME (7.5 °CA) and the shortest for kerosene, naphtha and naphtha20 (7.1 °CA). Unlike at lower loads, the shortest total CD was, however, observed for MGO (22 °CA). A higher in-cylinder temperature may have reduced the impact of MGO's higher viscosity. The longest total CD was measured for RME (23 °CA). Figure 4 clearly shows that the differences between the fuels' CD values decreased when the load increased. RME had relatively short CD values at the low engine-loads, but was left behind when the load increased. Aldhaidhawi et al. [32] concluded in their review article that one of the disadvantages of using biodiesel is the longer combustion duration. RME's higher viscosity and density hinder mixture formation, leading to longer combustion duration and a lower rate of heat release.

3.4. Cylinder Pressure

At all loads, there were no major differences in maximum cylinder pressures between the studied fuels, as shown in Figure 5. The highest maximum cylinder pressure (105 bar at 14 °CA ATDC) was measured with MGO at the highest load. For comparison, the lowest maximum cylinder pressure at high engine-load was recorded with RME (101 bar at 15 °CA ATDC), despite RME having the largest amount of injected fuel. Figure 2a–c illustrate the cylinder-pressure traces.

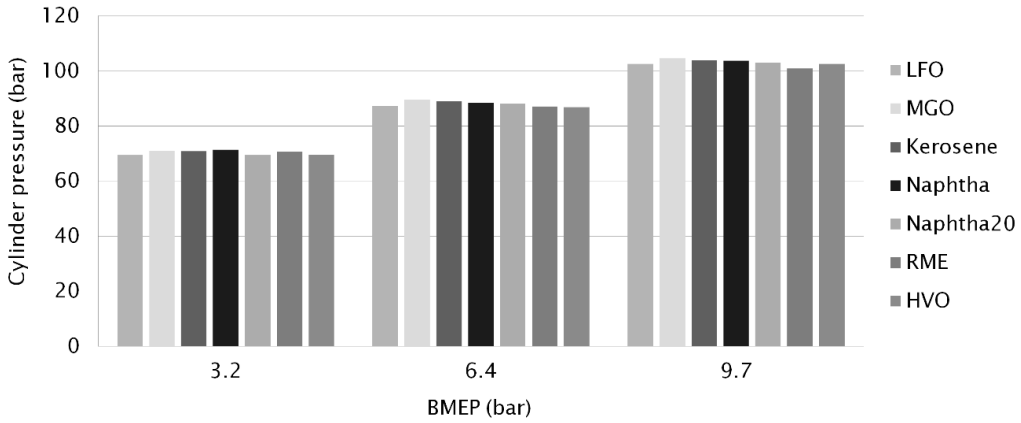

Figure 5. Maximum cylinder pressure versus engine load for different fuels.

At the low load (3.2 bar BMEP), rapid burning of neat naphtha produced the highest cylinder pressure. At the medium and high loads, the highest peaks of cylinder pressure were measured for MGO. Hissa et al. [17], showed a shorter ID and a higher maximum pressure increase for MGO than for LFO, naphtha or kerosene. Studies by Gabiña et al. [4] found that diesel-like fuel from WLO had almost the same combustion performance as pure diesel, and that the differences between the two fuels' performance decreased when engine size was increased.

CTO-based diesel (HVO) gave a very similar combustion performance as diesel. Even differences in combustion durations were minimal, at no more than 0.1 °CA. Similar results were found by Heuser et al. [36] and Niemi et al. [5], where HVO from CTO was studied in passenger-car diesel engines and in a non-road diesel engine respectively.

3.5. Gaseous Emissions and Smoke

In the study by Ovaska et al. [24], the effects of alternative marine diesel fuels on the exhaust particle size distributions and gaseous emissions were observed. The results were provided from the same engine measurements as the current study. However, the research by Ovaska et al. (2019) does not include the results of neat naphtha and kerosene. In addition, the gaseous emission results are cycle-weighted brake specific emissions of HC, NO_X, CO according to the NRSC cycle (Table 6). The smoke number was also recorded.

Table 6. Cycle-weighted brake specific emissions of HC, NO_X, CO and smoke number ranges from lowest to highest within the non-road steady cycle (NRSC) with different fuels (Ovaska et al. [24]).

	HC	NO_X	CO	Smoke
	(g/kWh)	(g/kWh)	(g/kWh)	(FSN)
LFO	0.24	9.3	0.33	0.014–0.038
MGO	0.16	9.3	0.28	0.014–0.033
HVO	0.20	8.9	0.32	0.013–0.031
RME	0.12	10.8	0.30	0.005–0.015
Naphtha20	0.29	-	0.36	0.011–0.031

In general, NO_X emissions were the lowest with HVO, while MGO and RME were favorable in terms of CO and HC emissions. The smoke numbers were minor with all fuels. More detailed results are provided in the article by Ovaska et al. [24].

4. Conclusions

The present study was carried out to evaluate the effects of the properties of alternative fuels in engine use, especially in-cylinder combustion, and to promote the development of fuel processes and standards to meet engine requirements. The results are useful to understand current trends in the fuel market and the impact that alternative fuels have in CI engine combustion.

Baseline fuel and six alternative liquid fuels were investigated in a high-speed diesel engine for non-road applications. The fuels were light fuel oil (LFO, baseline), recycled, waste lubricating oil (WLO), origin marine gas oil (MGO), kerosene, rapeseed methyl ester (RME), renewable diesel from crude tall oil (HVO), renewable wood-based naphtha and its blend with LFO (naphtha20). All measurements were performed under steady operation conditions without engine modifications. Multistage injections (pilot, main and post injections) were used throughout and the engine-speed of 1500 min^{-1} was maintained while conducting studies at three different engine-loads with brake mean effective pressures (BMEP) of 3.2 bar, 6.4 bar and 9.7 bar.

The investigated combustion parameters were very similar with all studied fuels. WLO-based MGO showed good combustion performance due to its high CN and short ID. The highest peak of cylinder pressure was measured for MGO, but the overall differences in cylinder pressures between fuels were minor. MGO's high CN and short ID meant the combustion started slightly earlier, but it also ended slightly later, giving a longer CD at the low and medium-load points. MGO's high viscosity may increase the combustion duration by hindering mixture formation. However, at the highest load, MGO's CD decreased relative to the other studied fuels. Similarly, MGO's combustion performance relative to the other fuels improved when the engine load was increased. However, high viscosity and its high sulphur-content are limiting factors for the use of MGO.

Naphtha's low CN increased the ID, but neat naphtha burned rapidly due to its low viscosity and density and the high volatility of its lighter compounds, which improved early combustion. Compared to LFO, naphtha's CD shortened as engine load decreased. Naphtha was level with MGO and kerosene in showing the highest cylinder pressures at all loads. Naphtha's HRR curve was slightly ahead of the other fuels, maybe because its low flash point and low viscosity promoted good air/fuel mixing. Neat naphtha's prolonged ID detracts from its combustion performance and limits its use as a drop-in fuel in a diesel engine. Moreover, neat naphtha needs other fuel (e.g. LFO) for starting and stopping the engine.

Naphtha20 was a blend of LFO and CTO-based naphtha—it showed overall combustion performance comparable to LFO's. That was also the case for CTO-based diesel, HVO. Both naphtha20 and HVO may be used in a diesel engine without any modifications.

Kerosene's light fractions not only increased its HRRs and cylinder pressures, but also decreased combustion duration compared to LFO. Nevertheless, kerosene's high sulphur-content limits its use in CI engines.

MGO with RME were favourable in terms of CO and HC emissions while the lowest NO_X emissions were recorded with HVO. Smoke emission was negligible for all fuels. However, the emission results of neat naphtha or kerosene were not included.

All investigated alternative fuels can be used in a non-road engine without any modifications, except neat renewable naphtha. Despite the improved premixed combustion due to low viscosity and high-volatile, light compounds of naphtha, the ignition delay was prolonged and the engine load was limited. Moreover, naphtha had poor auto-ignition properties and required LFO for starting and stopping the engine. However, as a blend with LFO, renewable naphtha is suitable for CI engines if safety issues associated with its low flash point are solved.

Author Contributions: M.H., K.S. and T.O., investigation; M.H. and A.N., formal analysis; M.H. and T.O., writing—original draft preparation; S.N. and K.S., writing—review and editing; S.N., supervision

Funding: This project has received funding from the European Union's Horizon 2020 research and innovation program under grant agreement No 634135 (Hercules 2).

Acknowledgments: The authors offer their appreciation toe Mrs. Sonja Heikkilä, Mr. Olav Nilsson and Ms. Nelli Vanhala for the assistance in the measurements.

Conflicts of Interest: The authors declare no conflicts of interest. The funders had no role in the design of the study; in the collection, analyses, or interpretation of data; in the writing of the manuscript, or in the decision to publish the results.

Nomenclature

ATDC	after top dead center
BMEP	brake mean effective pressure
BTDC	before top dead center
CA	crank angle
CD	combustion delay
CI	compression ignition
CN	cetane number
CRU	combustion research unit
CTO	crude tall oil
DLF	diesel-like fuel
ECA	Emission Control Area
EN	European Standard
EU	European Union
FAME	fatty acid methyl ester
HRR	heat release rate
HVO	hydrotreated vegetable oil
ICE	internal combustion engine
ID	ignition delay
LFO	light fuel oil
LHV	lower heating value
MFB	mass fraction burned
MGO	marine gas oil
NATO	North Atlantic Treaty Organization
RME	rapeseed methyl ester
UV	University of Vaasa
WLO	waste lubricant oils

References

1. Intergovernmental Panel on Climate Change (IPCC). IPCC Press Release, 8 October 2018. Available online: https://www.ipcc.ch (accessed on 9 October 2018).
2. Alabbad, M.; Issayev, G.; Badra, J.; Voice, A.K.; Giri, B.R.; Djebbi, K.; Ahmed, A.; Sarathy, S.M.; Farooq, A. Autoignition of straight-run naphtha: A promising fuel for advanced compression ignition engines. *Combust. Flame* **2018**, *189*, 337–346. [CrossRef]
3. Hoppe, F.; Benedikt, H.; Thewes, M.; Kremer, F.; Pischinger, S.; Dahmen, M.; Hechinger, M.; Marquardt, W. Tailor-made fuels for future engine concepts. *Int. J. Engine Res.* **2016**, *17*, 16–27. [CrossRef]
4. Gabiña, G.; Martin, L.; Basurko, O.C.; Clemente, M.; Aldekoa, S.; Uriondo, Z. Performance of marine diesel engine in propulsion mode with a waste oil-based alternative fuel. *Fuel* **2019**, *235*, 259–268. [CrossRef]
5. Niemi, S.; Vauhkonen, V.; Mannonen, S.; Ovaska, T.; Nilsson, O.; Sirviö, K.; Heikkilä, S.; Kiijärvi, J. Effects of wood-based renewable diesel fuel blends on the performance and emissions of a non-road diesel engine. *Fuel* **2016**, *186*, 1–10. [CrossRef]
6. Sirviö, K. Issues of Various Alternative Fuel Blends for Off-Road, Marine and Power Plant Diesel Engines. Ph.D. Thesis, University of Vaasa, Vaasa, Finland, June 2018.
7. Heywood, J.B. *Internal Combustion Engine Fundamentals*, 2nd ed.; McGraw-Hill Education: New York, NY, USA, 2018; p. 1028.

8. Pirjola, L.; Rönkkö, T.; Saukko, E.; Parviainen, H.; Malinen, A.; Alanen, J.; Saveljeff, H. Exhaust emissions of non-road mobile machine: Real-world and laboratory studies with diesel and HVO fuels. *Fuel* **2017**, *202*, 154–164. [CrossRef]
9. Sarvi, A.; Fogelholm, C.-J.; Zevenhoven, R. Emissions from large scale medium-speed diesel engines: 1. Influence of engine operation mode and turbocharger. *Fuel Prosess. Technol.* **2008**, *89*, 510–519. [CrossRef]
10. Bayindir, H.; Işik, M.Z.; Argunhan, Z.; Yücel, H.L.; Aydin, H. Combustion, performance and emissions of a diesel power generator fueled with biodiesel-kerosene and biodiesel-kerosene-diesel blends. *Energy* **2017**, *123*, 241–251. [CrossRef]
11. Naima, K.; Liazid, A. Waste oils alternative fuel for diesel engine: A review. *J. Pet. Technol. Altern. Fuels* **2013**, *4*, 30–43. [CrossRef]
12. Aramkitphotha, S.; Tanatavikorn, H.; Yenyuak, C.; Vitidsant, T. Low sulfur fuel oil from blends of microalgae pyrolysis oil and used lubricating oil: Properties and economic evaluation. *Sustain. Energy Technol. Assess.* **2019**, *31*, 339–346. [CrossRef]
13. Jiang, L.; Kronbak, J.; Christensen, L. The costs and benefits of sulphur reduction measures: Sulphur scrubbers versus marine gas oil. *Transp. Res. Part D Transp. Environ.* **2014**, *28*, 19–24. [CrossRef]
14. Wang, X.; Ni, P. Combustion and emission characteristics of diesel engine fueled with diesel-like fuel from waste lubrication oil. *Energy Convers. Manag.* **2017**, *133*, 275–283. [CrossRef]
15. Kang, D.; Kim, D.; Kalaskar, V.; Violi, A.; Boehman, A.L. Experimental characterization of jet fuels under engine relevant conditions—Part 1: Effect of chemical composition on autoignition of conventional and alternative jet fuels. *Fuel* **2019**, *239*, 1388–1404. [CrossRef]
16. Amara, A.B.; Dauphin, R.; Babiker, H.; Viollet, Y.; Chang, J.; Jeuland, N.; Amer, A. Revisiting diesel fuel formulation from Petroleum light and middle refinery streams based on optimized engine behaviour. *Fuel* **2016**, *174*, 63–75. [CrossRef]
17. Hissa, M.; Niemi, S.; Sirviö, K. Combustion property analyses with variable liquid marine fuels in combustion research unit. *Agron. Res.* **2018**, *16*, 1032–1045. [CrossRef]
18. Shahabuddin, M.; Liaquat, A.M.; Masjuki, H.H.; Kalam, M.A.; Mofijur, M. Ignition delay, combustion and emission characteristics of diesel engine fueled with biodiesel. *Renew. Sustain. Energy Rev.* **2013**, *21*, 623–632. [CrossRef]
19. World Wide Fuel Charter (WWFC5). Available online: http://www.oica.net/wp-content/uploads//WWFC5-2013-Final-single-page-correction2.pdf (accessed on 11 January 2019).
20. Brochure of BioVerno Naphtha, UPM. Available online: https://www.upmbiofuels.com/products/upm-bioverno-naphtha/ (accessed on 9 January 2019).
21. Chang, J.; Kalghatgi, G.; Amer, A.; Adomeit, P.; Rohs, H.; Heuser, B. Vehicle Demonstration of Naphtha Fuel Achieving Both High Efficiency and Drivability with EURO6 Engine-Out NO_X Emission. *SAE Int. J. Engines* **2013**, *6*, 101–119. [CrossRef]
22. Bae, C.; Kim, J. Alternative fuels for internal combustion engines. *Proc. Combust. Inst.* **2017**, *36*, 3389–3413. [CrossRef]
23. Subramanian, T.; Varuvel, E.; Ganapathy, S.; Vedharaj, S.; Vallinayagam, R. Role of fuel additives on reduction of NO_X emission from a diesel engine powered by camphor oil biofuel. *Environ. Sci. Pollut. Res.* **2018**, *25*, 15368–15377. [CrossRef]
24. Ovaska, T.; Niemi, S.; Sirviö, K.; Nilsson, O.; Portin, K.; Asplund, T. Effects of alternative marine diesel fuels on the exhaust particle size distributions of an off-road diesel engine. *Appl. Therm. Eng.* **2019**, *150*, 1168–1176. [CrossRef]
25. Fernandes, G.; Fuschetto, J.; Filipi, Z.; Assanis, A.; McKee, H. Impact of military JP-8 fuel on heavy-duty diesel engine performance and emissions. *J. Automob. Eng.* **2007**, *221*, 957–970. [CrossRef]
26. International Maritime Organization (IMO). *Assessment of Fuel Oil Availability—Final Report*; CE Delft: Delft, The Netherland, 2016; p. 183.
27. Finnish Standards Association (SFS). *Automotive Fuels—Diesel—Requirements and Test Methods*; SFS-EN 590:2013; Finnish Petroleum and Biofuels Association: Helsinki, Finland, 2013.
28. Arkoudeas, P.; Zannikos, F.; Lois, E. The tribological behavior of essential oils in low sulphur automotive diesel. *Fuel* **2008**, *87*, 3648–3654. [CrossRef]

29. Hassaneen, A.; Munack, A.; Ruschel, Y.; Schroeder, O.; Krahl, J. Fuel economy and emission characteristics of Gas-to-Liqui (GTL) and Rapeseed Methyl Ester (RME) as alternative fuels for diesel engines. *Fuel* **2012**, *97*, 125–130. [CrossRef]
30. Tira, H.S.; Herreros, J.M.; Tsolakis, A.; Wyszynski, M.L. Characteristics of LPG-diesel dual fueled engine operated with rapeseed methyl ester and gas-to-liquid diesel fuels. *Energy* **2012**, *47*, 620–629. [CrossRef]
31. International Association of Classification Societies (IACS). *Fuel Oil Safety Considerations Associated with the January 2020 0.50% Sulphur Cap Requirement*; Position Paper: London, UK, 2018; p. 2.
32. Aldhaidhawi, M.; Chiriac, R.; Badescu, V. Ignition delay, combustion and emission characteristics of Diesel engine fuelled with rapeseed biodiesel—A literature review. *Renew. Sustain. Energy Rev.* **2017**, *73*, 178–186. [CrossRef]
33. Niemi, S.A.; Murtonen, T.T.; Laurén, M.J.; Laiho, V.O.K. Exhaust Particulate Emissions of a Mustard Seed Oil Driven Tractor Engine. *SAE Trans. J. Fuels Lubr.* **2002**, *111*, 335–346. [CrossRef]
34. Vallinayagam, R.; An, Y.; Vedharaj, S.; Sim, J.; Chang, J.; Johansson, B. Naphtha vs. dieseline—The effect of fuel properties on combustion homogeneity in transition from CI combustion towards HCCI. *Fuel* **2018**, *224*, 451–460. [CrossRef]
35. Prakash, R.; Singh, R.K.; Murugan, S. Experimental studies on combustion, performance and emission characteristics of diesel engine using different biodiesel bio oil emulsions. *J. Energy Inst.* **2015**, *88*, 64–75. [CrossRef]
36. Heuser, B.; Vauhkonen, V.; Mannonen, S.; Rohs, H.; Kolbeck, A. Crude tall oil-based renewable diesel as a blending component in passenger car diesel engines. *SAE Int. J. Fuels Lubr.* **2013**, *6*, 817–825. [CrossRef]

Agronomy Research **18**(3), 2033–2048, 2020
https://doi.org/10.15159/AR.20.165

Combustion and emission studies of a common-rail direct injection diesel engine with various injector nozzles

M. Hissa*, S. Niemi and A. Niemi

University of Vaasa, School of Technology and Innovations, P.O. Box 700, FI-65101 Vaasa Finland
*Correspondence: Michaela.Hissa@univaasa.fi

Abstract. Fuel injection has a critical role in an internal combustion engine and a significant effect on the quality of the fuel spray. In turn, fuel spray directly affects an engine´s combustion, efficiency, power and emissions. This study evaluated three different injector nozzles in a high-speed, non-road diesel engine. It was run on diesel fuel oil (DFO) and testing was conducted at three different engine loads (100%, 75% and 50%) and at two engine speeds (2,200 rpm and 1,500 rpm). The nozzles had 6, 8 and 10 holes and a relatively high mass flow rate (HF). The study investigated and compared injection and combustion characteristics, together with gaseous emissions. The combustion parameters seemed to be very similar with all studied injector nozzles. The emission measurements indicated general reductions in hydrocarbons (HC), carbon monoxide (CO) and nitrogen oxides (NOx) at most load/speed points when using the 6- and 10-hole nozzles instead of the reference 8-hole nozzles. However, smoke number increased when the alternative nozzles were used.

Key words: diesel engine, fuel injection, injector nozzle, combustion performance, emissions.

INTRODUCTION

The European Parliament has set three key targets for more efficient energy use: improve energy efficiency by 35%; increase the share of renewables in energy consumption to at least 35%; and ensure that at least 12% of energy in transport comes from renewable sources (European Parliament, 2018). The deadline to achieve all three targets is 2030, so, coupled with changing fuel prices and fuel availability issues, significant shifts in the fuel market can be expect during the next decade. Diesel engines and their injection systems in the future must be capable of handling various alternative fuels as efficiently as possible.

When modifying a diesel engine to suit new fuels, one of the most critical elements is fuel injection. It has a key role in the optimisation of the trade-off between thermal efficiency and exhaust emissions (Jääskeläinen, 2017; Heywood, 2018; Salvador et al., 2018). The injection system has a significant impact on the duration of both fuel injection and combustion, as well as combustion noise (Salvador et al., 2018). Moreover, the injector nozzle´s design - the number of nozzle holes, the hole diameter and the spray angle - affects spray atomisation and fuel-air mixing (Sarvi et al., 2008; Jääskeläinen, 2017; Dong et al., 2018a). Fuel atomisation and fuel-air mixing must improve to meet

the EU's energy efficiency target and more stringent emission regulations, including those for nitrogen oxides (NOx) (Salvador et al., 2018).

The injector nozzle is responsible for delivering the fuel spray. The injected spray consists of fuel droplets smaller than the nozzle hole diameter (Sarvi et al., 2008). Reducing nozzle hole diameter has been shown to improve atomisation efficiency, leading to increased heat release rate (HRR) and less soot formation (Sarvi et al., 2008; Jääskeläinen, 2017; Dong et al., 2018a). However, those studies found that there are limits to the reduction of nozzle diameter. These are related to total injection time and combustion durations (especially at high loads) or the potential for nozzle coking. Additionally, the accelerated combustion leads to rising combustion temperature that increases NOx emissions (Satyanarayana & Muraleedharan, 2012). NOx formation in the combustion chamber is related to the flame area, which depends on the number and size of the fuel nozzle holes (Sarvi et al., 2008; Dong et al., 2018a). Decreasing the number of holes gives a smaller cone angle of fuel spray, changing the fuel/air mixing and reducing NOx production.

If nozzle hole diameter is reduced it is necessary to increase injection pressure or raise nozzle hole count to maintain the same fuel injection rate and nozzle flow area for maximum engine torque, power objectives and engine efficiency (Jääskeläinen, 2017). Jääskeläinen (2017) states that coupling hole size reduction to several other factors may improve combustion characteristics, like reducing the potential for overlapping of the burning zones of individual fuel sprays. These factors are: injection pressure increase, changes in combustion chamber design, improvements in nozzle flow performance and increase in the number of nozzle holes.

Increasing the number of nozzle holes, however, affects the fuel penetration length. Sayin et al. (2013), reported that raising the hole count could lead to poor combustion efficiency, mainly because the shorter penetration weakens the fuel/air mixing. Lee et al. (2010) noticed a decrease in penetration length when the hole count was raised. That led to a reduction in cylinder pressure and HRR, despite the improved evaporation and atomisation.

Overall, the optimal injector nozzle parameters depend on the engine type and have to be found by testing, since there is no theory that properly describes nozzle performance (Sarvi et al., 2008). Furthermore, the suitability for each fuel has to be studied individually (Niemi et al., 2011).

The present study compares three different injector nozzles in a high-speed, non-road diesel engine powered by DFO fuel. Tests were carried out at three different engine loads (100%, 75%, 50%) and at engine speeds of 2,200 rpm and 1,500 rpm. The nozzles had 6, 8 and 10 holes and a relatively high mass flow rate (HF). No other modifications were made to the engine components or control settings. Engine performance was kept constant. Detailed injection and combustion characteristics and gaseous emissions were measured. The injection map was optimized for the reference 8-hole nozzles and the map was kept constant with the other nozzles.

The study´s main aim was to evaluate how the selected fuel nozzles affect the combustion and emission characteristics of a modern high-speed, common-rail diesel engine using commercial low-sulphur DFO. The measurements generated new information relating to nozzle choice, supporting the aim to increase efficiency of high-speed non-road engines.

MATERIALS AND METHODS

Experimental setup

The experiments were conducted by the University of Vaasa (UV) at the Internal Combustion Engine (ICE) laboratory of the Technobothnia Research Centre in Vaasa, Finland. The laboratory is managed by Novia University of Applied Sciences.

Engine setup and nozzles

The experimental engine, an AGCO Power 44 CWA, was a turbocharged, high-speed four-cylinder diesel engine for non-road applications. It was intercooled (air-to-water) and had a Bosch common-rail fuel-injection system. The engine had no exhaust after treatment devices. It was loaded by means of a Horiba eddy-current dynamometer WT300. Table 1 lists the engine´s main specification.

Testing was conducted at three different engine loads (100%, 75%, 50%) and at two engine speeds of (2,200 rpm and 1,500 rpm). Three solenoid-driven injector nozzles were compared. The nozzles had 6, 8 and 10 holes and a high mass flow rate (1.2 L min^{-1} at 100 bar). The spray angle (umbrella angle) was 149° for all nozzles. Most diesel combustion systems include spray angles in the range of 145−158° (Salvador et al., 2018). The injection map was optimised for the 8-hole nozzles by the engine manufacturer. The map was kept constant with the other nozzles. Fig. 1 and Table 2 provide detailed information about the nozzles.

The fuel used was a commercial low-sulphur diesel fuel oil (DFO). It had a cetane number (CN) of 54, lower heating value of 43 MJ kg^{-1}, its was density 835 kg m^{-3} and kinematic viscosity 3 mm^2 s^{-2}.

Table 1. Main engine specifications

Engine	AGCO POWER 44 CWA
Cylinder number	4
Bore (mm)	108
Stroke (mm)	120
Swept volume (dm^{-3})	4.4
Rated speed (min^{-1})	2,200
Rated power (kW)	96
Intermediate speed (min^{-1})	1,500

Figure 1. Spray angle schematics of the injector nozzles.

Table 2. Specifications of different injector nozzles

Number of nozzle holes	6	8	10
Orifice diameter (mm)	0.2	0.162	0.139
Total orifice areas (mm^2)	0.188	0.165	0.152
Included spray angle	149°	149°	149°
Nozzle flow rate (L min^{-1}) at 100 bar	1.2	1.2	1.2
Needle lift (mm)	0.4	0.4	0.4

Analytical instruments

LabVIEW system-design software was used to collect sensor data from the engine. The recorded variables were engine speed and torque, cylinder pressure and injection timing, duration and quantity. WinEEM3 diagnostic and service software provided by the engine manufacturer, AGCO Power, controlled fuel injection according to load-speed requests. The basic settings of WinEEM3 were the same for all nozzles and fuels. Fig. 2 depicts a schematic of the test bench setup.

Injected fuel mass flow rate was measured with a Kern digital fuel scale for 300 seconds at every load point once engine operation was stabilised. The average result was saved via LabVIEW software. The relative uncertainty for fuel mass flow measurement was 0.03%.

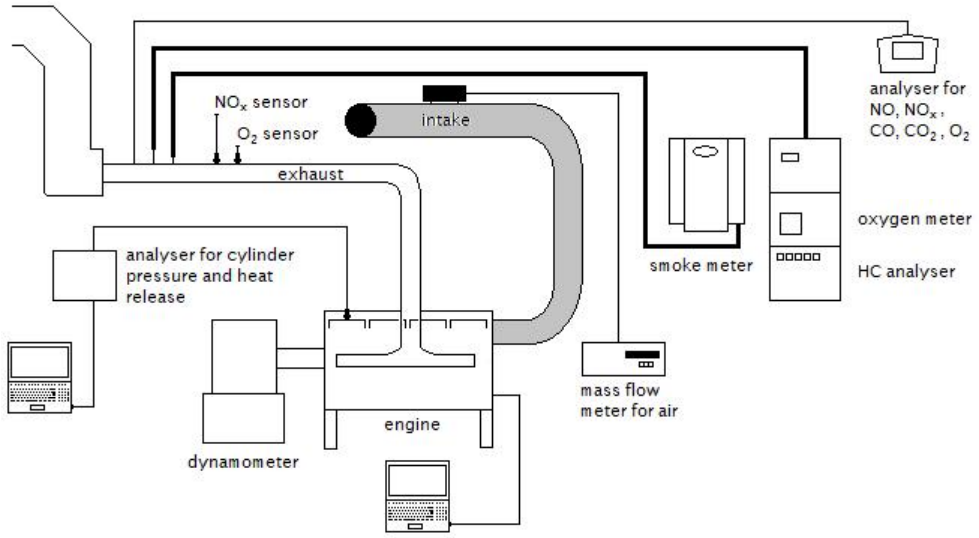

Figure 2. Engine measurement setup.

A piezoelectric Kistler 6125C pressure sensor was used to measure in-cylinder pressure. The sensor was mounted into the head of the fourth cylinder. A charge amplifier filtered and amplified the signal, which was then transmitted to a Kistler KIBOX combustion analyser. The crankshaft position was recorded by a crank-angle encoder (Kistler 2614B1), which can output a crank-angle signal with a resolution of 0.1° CA by means of an optical sensor. Cylinder pressure data were averaged over 100 consecutive cycles to smooth irregular combustion. The averaged data were used to calculate HRR. The raw data over 100 cycles were used to calculate the standard deviations for the maximum cylinder pressures.

HRR and MFB were calculated via AVL Concerto's data-processing platform, using the Thermodynamics2 macro. The macro used a calculation resolution of 0.2 °CA. The start of the calculation was set at -30 °CA. Data were filtered with the DigitalFilter macro and a frequency of 2,000 Hz. For HRR results, the average values of in-cylinder pressure were calculated first. Thereafter, the macro calculated HRR values. Finally, the HRR curve was filtered. In contrast, for MFB results, pressure values were first filtered

and then the macro was used. Average values of 100 cycles were not used for MFB results, thus establishing the standard deviations.

Exhaust temperatures were recorded by K type thermocouples (NiCu-NiAl). Air and exhaust pressures were determined by industrial transmitters. Engine air-flow was measured by an ABB Sensyflow FMT700-P air mass flow rate meter. Exhaust emissions were determined by means of the instruments listed in Table 3.

Table 3. Instruments for emission measurements

Parameter	Analyser	Technology	Accuracy*
CO	TSI CA-6203 CA-CALC	Electrochemical	0–100 ppm: ± 10% 100–5,000 ppm: ± 5%
O2	Siemens Oxymat 61	Paramagnetic	± 0.25%
NO, NOx	TSI CA-6203 CA-CALC	Electrochemical	0–100 ppm: ± 10% 100–4,000 ppm: ± 5%
HC	J.U.M. VE 7	HFID	0–100,000 ppm: ± 1%
Smoke	AVL 415 S	Optical filter	± 5%

* Accuracy provided by manufacturer.

Experimental matrix and measurement procedure

All measurements were performed under steady operation conditions without engine modifications. The comparison of injector nozzles used six load/speed points from the ISO 8178-4 standard: 100%, 75%, 50% loads at engine speeds of 2,200 rpm and 1,500 rpm. Brake mean effective pressure (BMEP) values ranged from 17.4 to 5.7 bar. The load/speed points are listed in Table 4.

Table 4. Engine operating conditions

Engine speed (rpm)	2,200			1,500		
BMEP (bar)	11.4	8.6	5.7	17.4	13.1	8.7
Load (%)	100	75	50	100	75	50

At the beginning of every measurement, the engine was warmed-up and the load was applied. The intake-air temperature was adjusted to 85 ± 1 °C downstream of the charge-air cooler to support auto-ignition of the fuels at each load. The temperature was controlled manually by regulating the flow of cooling water to the heat exchanger. The valve setting was kept constant. Therefore, the charge temperature changed with the load. All measurements were taken after the engine had stabilised, as determined by the stability of the temperatures of coolant water, intake air and exhaust upstream the turbine.

RESULTS AND DISCUSSION

Injector nozzles

The measurement results from the three injector nozzles were compared. The nozzles had 6, 8 and 10 holes but each had the same mass flow rate of 1.2 L min^{-1} at 100 bar. The rail pressure values of 8-hole nozzles were 83, 74, 66 MPa at measurement points of 11.4, 8.6 and 5.7 bar 2,200 rpm. Respectively, 61, 46 and 40 MPa at 17.4, 13.1 and 8.7 bar BMEP 1,500 rpm. The 6- and 10-hole nozzles had a minor increase in rail pressures. The maximum rail pressure increase was 4% with 6-hole nozzles at medium load (8.6 bar BMEP) at 2,200 rpm compared to rail pressure with 8-hole nozzles. The

following sections provide results and discussion from the measurements of injection timing, specific fuel consumption, heat release rate and cylinder pressure, brake thermal efficiency, mass fraction burned and combustion duration as well gaseous emissions and smoke.

Injection timing and brake specific fuel consumption

For all test conditions, pilot injections were set before top dead centre (BTDC) while main injections occurred after top dead centre (ATDC). The exact timings and durations are shown in Table 5. Fig. 3 depicts brake specific fuel consumption (BSFC).

Only main injections occurred at load points of 11.4 bar and 8.6 bar BMEP (engine speed 2,200 rpm). At this engine speed, pilot injections occurred only with the lowest BMEP of 5.7 bar (50% load). The timing and duration of these pilot injections were similar for all the nozzles. The main injection duration was slightly shorter (by just one crank angle degree) with the 8-hole nozzles. There was no post injection for any of the three loads at 2,200 rpm.

Pilot injection was used for all the nozzles at all loads (17.4, 13.1 and 8.7 bar) at the lower engine speed of 1,500 rpm. Minor variations of starting times and durations were noticed. At full load (17.4 bar) at this engine speed, post injection occurred only with the 8-hole nozzles. Post injection occurred with all the nozzles at the two smaller loads at 1,500 rpm.

Table 5. Injection timing

Nozzle	BMEP	Pilot Injection (BTDC)		Main injection (ATDC)		Post injection (ATDC)	
		Start	Duration	Start	Duration	Start	Duration
	bar	°CA	°CA	°CA	°CA	°CA	°CA
6	11.4	8.6	0	4	21	31	0
8		8.6	0	4	20	30	0
10		8.6	0	4	21	31	0
6	8.6	7.6	0	3	17	28	0
8		7.6	0	3	16	27	0
10		7.6	0	3	17	28	0
6	5.7	13	4	3.5	12	22	0
8		13	4	3.5	12	22	0
10		13	4	3.5	12	22	0
6	17.4	8.3	2.8	2.4	25	31	0
8		8	2.8	2	24	31	2.2
10		8.3	2.8	2.4	24	31	0
6	13.1	8.6	3.2	2.3	20	28	3.1
8		8.5	3.3	2.1	20	27	3.1
10		8.6	3.2	2.3	21	28	3.1
6	8.7	8.7	3.5	2.1	13	21	4.5
8		8.7	3.7	1.9	12	20	4.7
10		8.7	3.5	2.1	13	21	4.6

The amount of injected fuel was assumed to correlate to injection durations because fuel injection was controlled according to load/speed requests. Overall, the differences in main injection durations of all the nozzles did not exceed 1 °CA.

As expected, pilot injection duration increased when the engine load was reduced and main injection duration increased when the engine load was raised. At 1,500 rpm, post injection duration increased when the engine load was reduced. A longer pilot is used to shorten the ignition delay (ID) of a fuel by increasing in-cylinder temperatures for main injections. Post injections, in turn, are used to reduce particulate and soot emissions, primarily at lighter loads and lower engine speeds (Heywood, 2018).

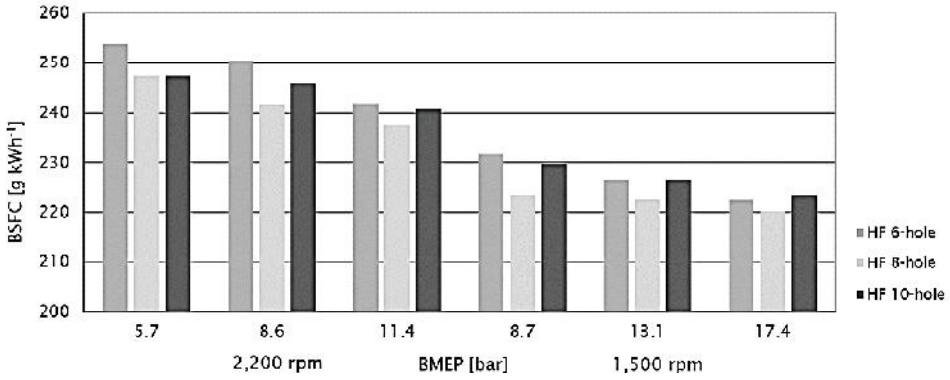

Figure 3. Brake specific fuel consumption at rated and intermediate speeds.

Brake specific fuel consumption (BSFC) is the fuel flow rate per hour (g h^{-1}) divided by engine brake power (kW). Generally, BSFC decreased when brake mean effective pressure (BMEP) or load of the engine increased. The 8-hole nozzles produced the lowest BSFC at five out of the six load/speed points. In other words, either raising the hole count to 10 or reducing it to 6 increased BSFC. The highest BSFC values were measured for the 6-hole nozzles at all load/speed points, except at full load at 1,500 rpm, where BMEP was at its maximum value of 17.4 bar. At this point, however, the difference between the 10-hole and 8-hole nozzles was minor (3.1 g kWh^{-1}, 1.4%). The maximum difference was 8.7 g kWh^{-1} or 3.6% at 8.6 bar BMEP, between the 6-hole and 8-hole nozzles.

Sayin et al. (2013) investigated 2-, 4-, 6- and 8-hole nozzles in a single-cylinder diesel engine using DFO. They also observed that increasing or decreasing the number of nozzle holes increased BSFC compared to the original nozzle. They assumed that a reduction in hole count led to enlarged fuel droplets and lengthened the ignition delay period, increasing BSFC. Conversely, raising the hole count shortened the ID period, reducing homogeneous mixture, and so once again BSFC increased. Mekonen et al. (2020) studied 3-, 4- and 5-hole nozzles in a single-cylinder diesel engine using preheated palm oil methyl ester. They observed decrease in BSFC when nozzle hole number increased from 3 to 4, due to increased fine droplets of injected fuel and improved fuel atomisation. However, BSFC increased when the nozzle hole count was raised further, from 4 to 5. They assumed that was caused by the higher number of fine droplets leading to a shorter ID and hence increasing the chance of non-homogeneous mixing.

Heat release rate (HRR)

The compression pressure was at its maximum at 2°CA before top dead centre at an engine speed of 1,000 rpm. This had no effect on measurement results, but must be considered when the results are examined.

Combustion starts with a rapid burning phase that lasts only a few CA degrees and produces the first spike in the heat release rate curve. It is followed by the main heat release period, which has a longer duration and more rounded profile. The HRR curve´s tail is the remainder of the fuel's chemical energy released when burnt gases mix with excess air that was not involved in the main combustion (Heywood, 2018). Fig. 4 shows HRR curves for the studied injector nozzles. The small dip near the beginning of each curve is the loss due to the heat transfer into the liquid fuel for vaporising and heating (Heywood, 2018).

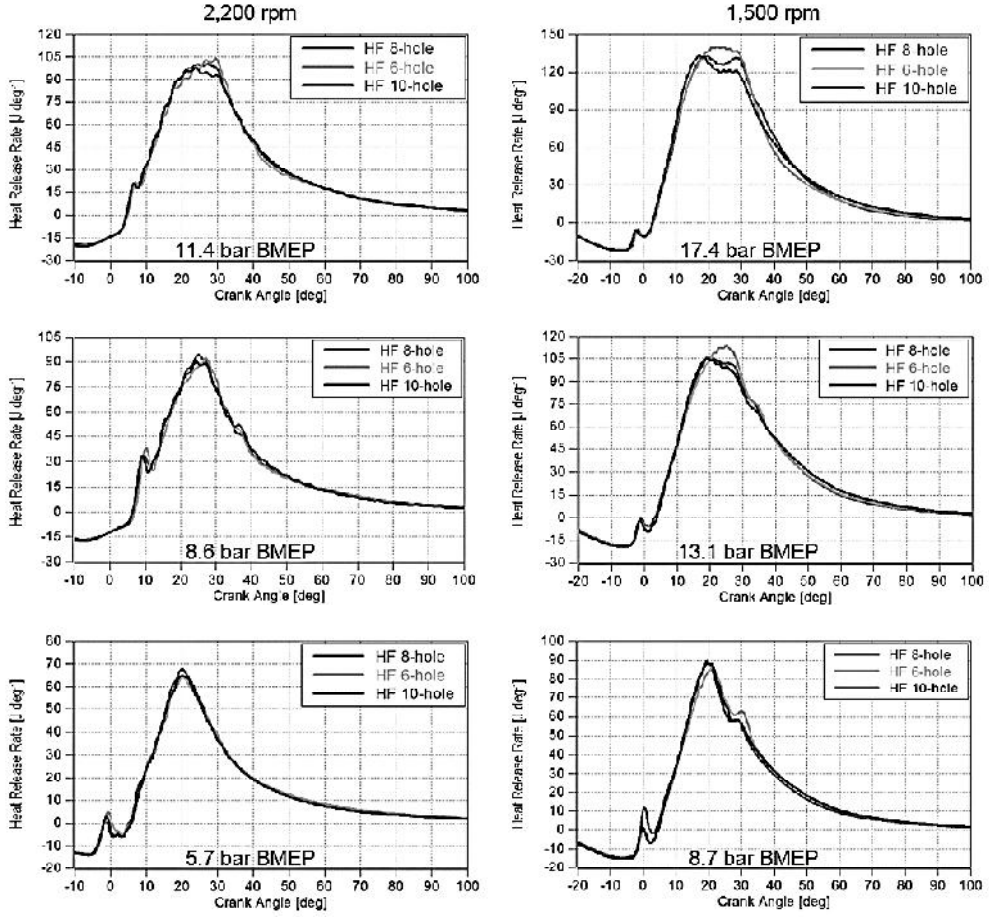

Figure 4. Heat release rates at rated and intermediate speeds.

At rated speed (2,200 rpm) and full load (11.4 bar BMEP), the maximum HRR for the 6-hole nozzles was 104 J °CA^{-1}, just before the start of post injection (27 °CA). The 10-hole nozzles´ maximum HRR peak (98 J °CA^{-1}) came earlier, at the end of main injection (24 °CA). This difference in the arrival of the HRR peak may be due to the

larger droplet sizes created by the 6-hole nozzles evaporating more slowly than the smaller droplet sizes from the 10-hole nozzles. The start of all injections, as well as injection durations, were similar for the 6- and 10-hole nozzles.

A slightly longer ignition delay observed for the 6-hole nozzles at medium (8.6 bar BMEP) and low (5.7 bar BMEP) loads is due to larger droplet size generated by larger nozzle hole diameter. Otherwise, the HRR curves are similar. The 8-hole nozzles achieved a higher HRR than the other two nozzles at medium and low loads (94 J °CA^{-1} and 68 J °CA^{-1} respectively).

At intermediate speed and full load (17.4 bar BMEP), only the 8-hole nozzles had a post injection, although this is not evident on the HRR curve. The curve of the 6-hole nozzles differs from those of the other two nozzles at peak HRR.

At high loads, the maximum HRR decreased as the nozzle-hole count rose. Maximum HRR occurred later at intermediate speed with the 6-hole nozzles due to the larger droplet size generated by the greater hole diameter. Additionally, this delayed HRR peak with the 6-hole nozzles also may be due to increased spray penetration length, decreased cone angle and the slower mixing that is the consequence of the larger fuel droplets´ longer evaporation time (Hoang, 2019), combined with slightly increased BSFC or fuel amount. Lee et al. (2010) studied 6-, 8- and 10-hole nozzles in a diesel engine and noticed that the strongest penetration of liquid spray from 6-hole nozzles impinged against the piston bowl, lowering in-cylinder temperature. Without the impingement, the HRR of the 6-hole nozzles should be the highest due to less uniform fuel/air distribution that enhanced combustion. They also observed the lowest HRR values for the 10-hole nozzles due to incomplete combustion caused by the poorly distributed fuel/air mixture and the highest concentration of unburned fuel during combustion process.

Cylinder pressure

Maximum cylinder pressures (MCP) were very similar with all injector nozzles at all studied load/speed points (Fig. 5 and Table 6). MCP at rated speed and full load with all nozzles were 106 to 108 bar. At 1,500 rpm, MCP at full load was 116 to 117 bar. Table 6 shows the standard deviations of MCP of 100 consecutive cycles.

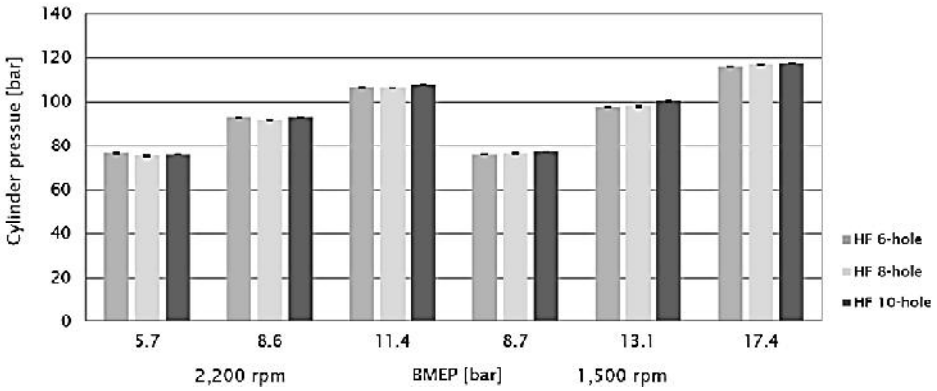

Figure 5. Maximum cylinder pressures at rated and intermediate speed with standard deviations.

Maximum cylinder pressure depends on the burned fuel fraction during the premixed combustion phase. A larger amount of fuel burned in premixed phase shows a higher MCP (Hissa et al., 2019). The fuel/air mixing rate mainly controls the combustion process of diesel engines. Slowing the rate results in retarded ignition and lower MCP. Dong et al. (2018b) noticed a lower pressure peak with a reduced number of nozzle holes, mainly due to the slower fuel/air mixing rate. In turn, Lee et al. (2010) noticed shorter penetration length when the number of nozzle holes was increased. This led to lower cylinder pressure and HRR, despite the improved evaporation and atomisation.

Table 6. Maximum cylinder pressure and standard deviations

Nozzle	BMEP bar	Max. cylinder pressure (avg) °CA	StDev	Nozzle	BMEP bar	Max. cylinder pressure (avg) °CA	StDev
6	11.4	107	0.135	6	17.4	116	0.165
8		106	0.150	8		117	0.147
10		108	0.173	10		117	0.189
6	8.6	93.0	0.114	6	13.1	97.7	0.179
8		91.9	0.140	8		97.9	0.209
10		93.1	0.133	10		100	0.264
6	5.7	76.6	0.251	6	8.7	75.9	0.154
8		75.4	0.192	8		76.4	0.237
10		76.0	0.187	10		77.2	0.158

Brake thermal efficiency (BTE)

BTE indicates how efficiently the energy in the fuel was converted into mechanical output. BTE increased with load for all nozzles due to relative reductions in heat and mechanical losses at higher load (e.g., Perumal et al., 2017). Fig. 6 shows BTE was very similar with different nozzles. At full load at 2,200 rpm, BTE was 34 to 35% and at half load 33 to 34%. At full load at 1,500 rpm, BTE was 37 to 38% and at half load 36 to 37%. Differences between nozzles were minimal and within the measurement accuracy.

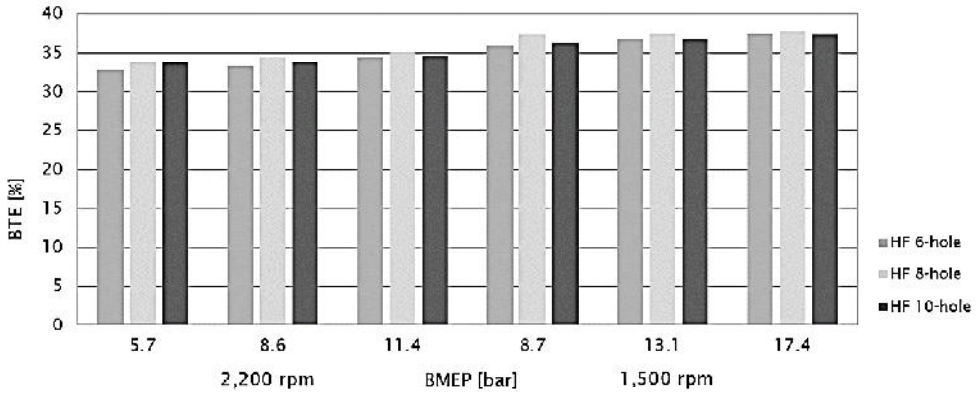

Figure 6. Brake thermal efficiency at rated and intermediate speeds.

Sayin et al. (2013) noticed an increase in BTE with higher number of nozzle holes and assumed it was because of finer atomisation of fuel. However, they also noticed an

increase in the nozzle-hole count could lead to poor combustion efficiency, mainly stemming from the shorter penetration weakening the fuel/air mixing. Mekonen et al. (2020) also measured an increased BTE when nozzle-hole number was increased from 3 to 4. This was attributed to a better fuel spray and turbulence. BTE fell when the number of nozzle holes was increased from 4 to 5. It is assumed that when the nozzle-hole count exceeds a certain range, combustion and emissions are adversely affected due to lack of the air entrainment required for the achievement of a stoichiometric mixture (Lee et al., 2010; Mekonen et al., 2020).

Mass fraction burned (MFB)

Table 7 presents MFB values with their standard deviations. It shows that the nozzles had the same MFB 5% values, except at full load at 2,200 rpm (11.4 bar BMEP) and 75% load at 1,500 rpm (13.1 bar BMEP). At these two load/speed points, the 6-hole nozzles achieved MFB 5% slightly later than the other nozzles. This may be due to increased droplet size leading to increased ID. At 50% load at 1,500 rpm (8.7 bar BMEP), the 8-hole nozzles had the earliest MFB 5%.

Table 7. Mass fraction burned and standard deviations

Nozzle	BMEP bar	MFB 5% °CA	StDev	MFB 50% °CA	StDev	MFB 90% °CA	StDev
6	11.4	19	0.14	32	0.21	65	1.0
8		18	0.15	32	0.22	63	1.1
10		18	0.13	32	0.26	64	1.3
6	8.6	20	0.14	32	0.22	67	1.1
8		19	0.15	32	0.24	65	1.2
10		20	0.11	32	0.28	64	1.1
6	5.7	17	0.17	30	0.30	67	1.6
8		17	0.16	29	0.32	65	1.6
10		17	0.16	29	0.27	64	1.3
6	17.4	14	0.13	28	0.22	55	1.2
8		14	0.11	29	0.21	53	1.0
10		14	0.14	29	0.31	58	1.5
6	13.1	16	0.15	29	0.23	58	1.3
8		15	0.13	29	0.23	56	0.94
10		15	0.15	30	0.33	61	1.1
6	8.7	16	0.17	29	0.26	58	1.2
8		15	0.13	28	0.26	56	1.1
10		16	0.12	29	0.26	58	0.97

MFB 50% values were similar with all nozzles at high loads. However, some difference between the nozzles was observed at lower cylinder pressures. At rated speed and 50% load (5.7 bar BMEP), MFB 50% of the 6-hole nozzles occurred one CA degree later than with the other nozzles. At 1,500 rpm and 75% and 50% loads (13.1 and 8.7 bar BMEP respectively), MFB 50% for the 8-hole nozzles was one CA degree ahead of the other nozzles. As a whole, differences in MFB 5% and 50% values were very small.

MFB 90% was achieved first with the 8-hole nozzles in the majority of cases. However, the 10-hole nozzles had the earliest MFB 90% values at rated speed with 75% and 50% loads (8.6 and 5.7 bar BMEP respectively). Conversely, the 10-hole nozzles

showed the latest values of MFB 90% at all loads with an engine speed of 1,500 rpm. At rated speed, the cylinder pressure and in-cylinder temperature were, perhaps, more favourable for formation, evaporation and burning of the smaller droplets from 10-hole nozzles (Chauhan et al., 2010; Hoang, 2019).

Combustion duration

Combustion duration (CD) can be defined either as the time interval between MFB 5% and MBF 50% or the time interval between MFB 5% and MFB 90%. Measurements using both definitions of CD are depicted in Fig. 7 and 8 respectively, using the data from Table 7. MFB 5% always occurred during the main injection, irrespective of nozzle or load. MFB 50% was achieved at 30 ± 2° CA. MFB 90% was observed after the end of any post injections.

CD values of MFB 5−50% were fairly similar for all the nozzles at all load/speed points, with two exceptions (Fig. 7). In the first of these, the 6-hole nozzles had a shorter CD at rated speed and full load (11.4 BMEP) because increased fuel supply at higher loads with the 6-hole nozzles enhance combustion. However, at lower loads mixing with the six-hole nozzles is poorer, ID may be delayed and combustion is more prolonged relative to the other nozzles. The second exception relates to the 10-hole nozzles; these showed longer CD values at 1,500 rpm with 75% and 100% loads (13.1 and 17.4 bar respectively). Effective fuel/air mixing with the 10-hole nozzles gave a shorter CD at low loads but at higher load CD increased, due to smaller orifice diameters that led to lengthened combustion duration. Studies of Sarvi et al. (2008), Jääskeläinen (2017) and Dong et al. (2018) stated that there is a limit to the reduction of nozzle diameter that related to e.g. total injection time and combustion durations especially at high loads.

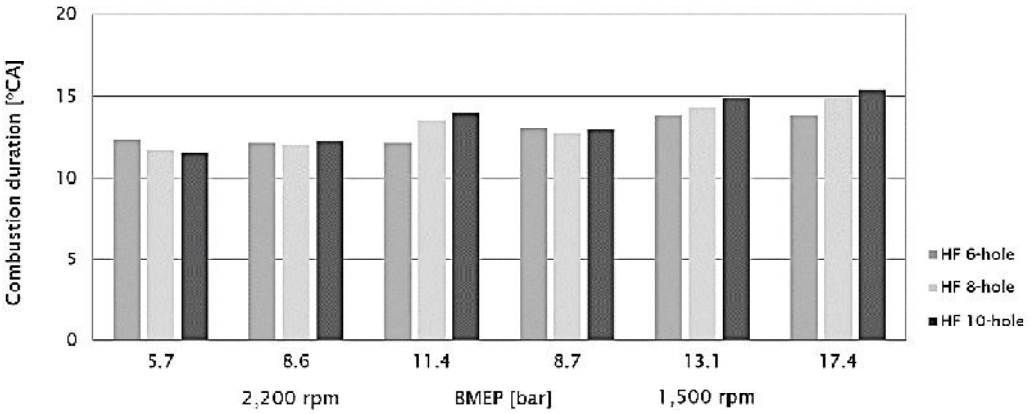

Figure 7. Combustion duration (°CA) at all engine loads, determined as crank angles between MFB 5% and MFB 50%.

Fig. 8 shows MFB 5−90% values at all load/speed points. At 2,200 rpm, the 6-hole nozzles always had the longest CD. Their larger hole diameters created larger droplets than the other nozzles; larger droplet sizes require more time to evaporate and burn (Heywood, 2018). At 1,500 rpm engine speed, the 10-hole nozzles had the longest CD and the difference compared to the other nozzles increased as engine load grew.

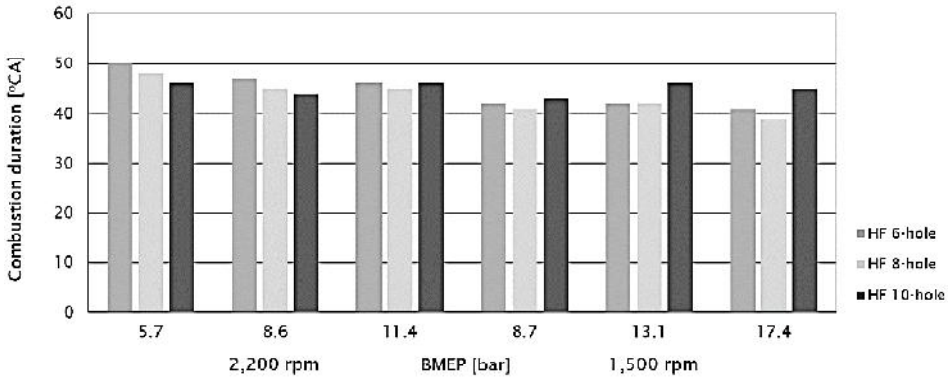

Figure 8. Combustion duration (°CA) at all engine loads, determined as crank angles between MFB 5% and MFB 90%.

Gaseous emissions and smoke

Fig. 9 illustrates the brake specific emissions of NOx, CO and HC. The smoke numbers are also depicted.

Using 6- and 10-hole nozzles instead of 8-hole nozzles generated less NOx. The 6-hole nozzles gave the lowest NOx at low loads at both speeds: 14% lower at rated speed and 18% lower at intermediate speed compared with the 8-hole nozzles. At full loads, the lowest NOx values were measured with the 10-hole nozzles. They cut NOx emissions by 11% at 2,200 rpm and by 13% at 1,500 rpm compared with 8-hole nozzles. Low smoke and high BTE indicate that combustion was efficient with 8-hole injectors, although that often is accompanied by the trade-off involving greater NOx formation. Mekonen et al. (2020) observed more NOx when they increased nozzle hole number from 3 to 4, attributing it to smaller particles that increased the combustion rate and in-cylinder gas temperature. They also measured a reduction in NOx when the nozzle number was raised from 4 to 5. The reason given was greater fuel supply to the cylinder, reducing in-cylinder gas temperature and NOx emissions. The results are consistent with the experimental observations of Lee et al. (2010) where the highest NOx emission was measured for the 8-hole nozzles. The lowest NOx values with the 10-hole nozzles were due to presence of fuel-rich zones developed from the poor mixture formation.

Carbon monoxide (CO) is mainly formed due to lack of oxygen in locally rich mixtures in the cylinder, although dissociation of CO_2 may also increase CO. The 6-hole nozzles improved CO performance at rated speed, cutting CO emissions by 20% at low load and by 39% at full load compared with the 8-hole nozzles. The 10-hole nozzles reduced CO by 15% at low load and by 19% at medium load, respectively. The 8-hole and the 10-hole nozzles produced the same amount of CO at full load. At intermediate speed, the 10-hole nozzles now produced the highest CO emissions at all load points. The increases compared with the 8-hole nozzles were considerable: 36% at low load, 26% at medium load and 83% at high load. Conversely, the 6-hole nozzles performed better than the 8-hole nozzles, reducing CO by 2%, 39% and 54% at low, medium and high loads respectively. At full load at 1,500 rpm, CO formation with 10-hole nozzles was four times higher than with the 6-hole nozzles, maybe due to the prolonged combustion. The effects of CO_2 dissociation on CO were assumed to be quite similar for all nozzles because the high temperatures prevailed in the cylinder for quite similar periods with them all.

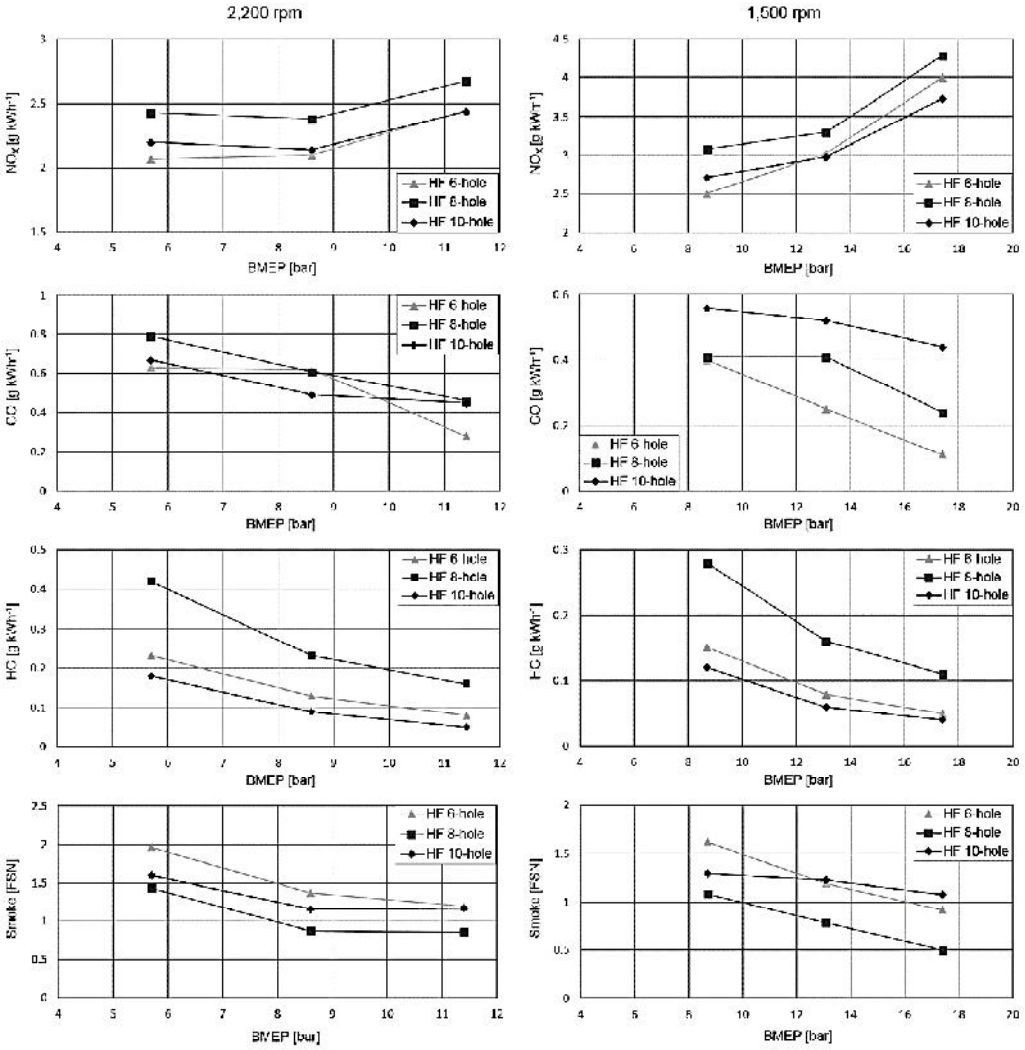

Figure 9. Brake specific emissions of NOx, CO and HC and smoke numbers versus engine load at two speeds.

Total hydrocarbon emissions (HC) are considered to reflect the presence of unburnt or partially burnt fuel in the exhaust gas (Hoang, 2019). Most exhaust HC originate from the fuel but some are formed by unknown chemical reactions within the cylinders (Satyanarayana & Muraleedharan, 2012). An increase in HC emissions is indicative of reduced thermal efficiency and a raised level of pollutants (Hoang, 2019). In our study, both the alternative nozzles gave better HC performance than the reference nozzles at all loads and speeds, with the 10-hole nozzles being slightly the most beneficial. At rated speed, the 10-hole nozzles reduced HC emissions by 57% at low load, 60% at medium load and 68% at high load compared with 8-hole nozzles. At intermediate speed, 10-hole nozzles achieved HC reductions of 57%, 62% and 63% respectively.

Exhaust smoke increased when engine load reduced. Smoke number at the engine´s rated speed was always highest with 6-hole nozzles. The smoke result was less clear-cut

at intermediate speed: the 6-hole nozzles generated the highest smoke at low load but the 10-hole nozzles produced the most smoke at the highest load. The 8-hole nozzles gave the lowest smoke at both speeds and all loads, ranging from 0.9 to 1.5 FSN at rated speed and from 0.5 to 1.1 at intermediate speed.

Sarvi et al. (2008) reported that NOx decreased when the number of nozzle holes was reduced for a given fuel consumption in a medium-speed diesel engine driven with light fuel oil (LFO). However, that was accompanied by the penalty of greater smoke (FSN), HC and CO concentrations. Dong et al. (2018a), say that combustion efficiency improves with smaller fuel droplets. Heat release is accelerated and combustion temperature rises, giving higher NOx. On the other hand, NOx formation in the combustion chamber is related to the flame area. A lower number of nozzle holes gives a smaller fuel jet area, resulting in different fuel/air mixing which reduces NOx production (Dong et al., 2018a; Sarvi et al., 2008).

Generally, NOx formation increased with engine load. Higher combustion temperature promoted NOx formation. Fig. 8 shows that higher engine load improved fuel/air mixing and fuel oxidation processes. The improved mixing rate led to reductions of CO, HC and smoke when engine load was increased.

CONCLUSIONS

The present study compared three different injector nozzles in a high-speed non-road diesel engine at different engine loads and speeds. The main aim was to find out how the selected nozzles affect combustion and emission characteristics of the common-rail experimental engine, fuelled by commercial low-sulphur DFO. The nozzles had 6, 8 and 10 holes. The injection map was kept constant and the engine control module set the injection for each nozzle automatically. The measurements generated new information of fuel injection nozzles supporting the development of more efficient high-speed non-road engines.

Based on the performed measurements and analyses, the following conclusions could be drawn:

- The BSFC for the 6- and 10-hole nozzles were higher than that of the 8-hole nozzles.
- The HRRs were fairly similar for all nozzles at all loads. However, the HRR remained slightly longer at a high level with 6-hole nozzles.
- Differences in maximum cylinder pressures and BTE were minimal between the nozzles.
- Combustion durations were almost similar for all the nozzles.
- The 6- and 10-hole nozzles improved CO and HC formation.
- The 8-hole tips generated the highest NOx but lowest smoke at all loads.

ACKNOWLEDGEMENTS. This project was one part of the national Future Combustion Engine Power Plant research program. The authors wish to thank Business Finland for the financial support of the program.
The authors offer their appreciation to Dr. Katriina Sirviö, Mr. Olav Nilsson, Mr. Markus Uuppo and Mr. Teemu Ovaska for the assistance in the measurements. The authors also express their gratitude to Mr. Henri Huusko and Mr. Marko Vallinmäki at AGCO Power Inc. for their kind assistance in providing test nozzles and their specifications for the study.

REFERENCES

Chauhan, B.S., Kumar, N., Du Jun, Y. & Lee, K.B. 2010. Performance and emission study of preheated Jatropha oil on medium capacity diesel engine. *Energy* **35**, 2484–2492.

Dong, S., Wang, Z., Yang, C., Ou, B., Lu, H., Xu, H. & Cheng, X. 2018a. Investigations on the effects of fuel startification on auto-ignition and combustion process of an ethanol/diesel dual-fuel engine. *Applied Energy* **230**, 19–30.

Dong, S., Yang, C., Ou, B., Lu, H. & Cheng, X. 2018b. Experimental investigation on the effects of nozzle-hole number on combustion and emission characteristics of ethanol/diesel dual-fuel engine. *Fuel* **217**, 1–10.

European Parliament. 2018. MEPs set ambitious targets for cleaner, more efficient energy use. https://www.europarl.europa.eu/news/en/press-room/20180112IPR91629/meps-set-ambitious-targets-for-cleaner-more-efficient-energy-use. Accessed 15.1.2020.

Heywood, J.B. 2018. *Internal Combustion Engine Fundamentals*, 2nd Edition, McGraw-Hill Education, USA, 1028 pp.

Hissa, M., Niemi, S., Sirviö, K., Niemi, A. & Ovaska, T. 2019b. Combustion Studies of a Non-Road Diesel Engine with Several Alternative Liquid Fuels. *Energies* **12**, 2447.

Hoang, A.T. 2019. Experimental study on spray and emission characteristics of a diesel engine fueled with preheated bio-oils and diesel fuel. *Energy* **171**, 795–808.

Jääskeläinen, H. 2017. *DieselNet Technology Guide – Diesel Fuel Injection Nozzles.* https://dieselnet.com/tg. Accessed 20.9.2019.

Lee, B.H., Song, J.H., Chang, Y.J. & Jeon, C.H. 2010. Effect of the number of fuel injector holes on characteristics of combustion and emissions in a diesel engine. *International Journal of Automotive Technology* **11**(6), 783–791.

Mekonen, M. W. & Sahoo, N. 2020. Combined effects of fuel injection pressure and nozzle holes on the performance of preheated palm oil methyl ester used in a diesel engine. *Biofuels* **11**(1), 19–35.

Niemi, S., Uuppo, M., Virtanen, S., Karhu, T., Ekman, K., Svahn, A., Vauhkonen, V., Agrawal, A. & Hiltunen, E. 2011. Animal Fat Based Raw Bio-Oils in a Non-Road Diesel Engine Equipped with a Diesel Particulate Filter. In Bartz, W.J. (ed) (2011): *8th International Colloquium Fuels; Conventional and Future Energy for Automobiles*. Ostfildern, Germany: Technische Akademie Esslingen. pp. 517–528.

Perumal, V. & Ilangkumaran, M. 2017. Experimental analysis of engine performance, combustion and emission using pongamia biodiesel as fuel in CI engine. *Energy* **129**, 228–236.

Salvador, F.J., Lopez, J.J., De la Morena, J. & Crialesi-Esposito, M. 2018. Experimental investigation of the effect of orifices inclination angle in multihole diesel injector nozzles. Part 1 – Hydraulic performance. *Fuel* **213**, 207–214.

Sarvi, A., Fogelholm, C-J. & Zevenhoven, R. 2008. Emissions from large-scale medium-speed diesel engines: 1. Influence of engine operation mode and turbocharger. *Fuel Processing Technology* **89**, 510–519.

Satyanarayana, M. & Muraleedharan, C. 2012. Experimental Studies on Performance and Emission Characteristics of Neat Preheated Vegetable Oils in a DI Diesel Engine. *Energy Sources, Part A: Recovery, Utilization, and Environmental Effects* **34**, 1710–1722.

Sayin, C., Gumus, M. & Canakci, M. 2013. Influence of injector hole number on the performance and emissions of a DI diesel engine fueled with biodiesel-diesel fuel blends. *Applied Thermal Engineering* **61**, 121–128.

2020-01-2126 Published 15 Sep 2020

Performance and Emissions of a Medium-Speed Engine Driven with Sustainable Options of Liquid Fuels

Seppo Niemi, Michaela Hissa, Teemu Ovaska, Katriina Sirviö, Sonja Heikkilä, Olav Nilsson, Saana Hautala, Kirsi Spoof-Tuomi, Janne Suomela, Antti Niemi, and Antti Kiikeri University of Vaasa

Kaj Portin and Tomas Asplund Wartsila Corp.

Citation: Niemi, S., Hissa, M., Ovaska, T., Sirviö, K. et al., "Performance and Emissions of a Medium-Speed Engine Driven with Sustainable Options of Liquid Fuels," SAE Technical Paper 2020-01-2126, 2020, doi:10.4271/2020-01-2126.

Abstract

Energy production and transport are major global contributors of greenhouse gas emissions. Both sectors should reduce their use of fossil energy sources. Pollutant emissions must also be reduced without jeopardizing energy efficiency, reliability, and profitability. The internal combustion engine will dominate in marine and power plant applications for a long time because it offers high energy density, efficiency, durability, and the ability to respond rapidly to load changes. Ever-tightening emissions legislation encourages development of new solutions for engine-driven power. One example is exploring the use of alternative fuels in large engines. Low-carbon liquid fuels with high energy density are ideal for applications working far from any infrastructure. This study evaluated how three liquid fuel alternatives perform in a medium-speed engine. One new fuel was a circular economy-based marine gas oil (MGO). The second novelty was a blend of renewable naphtha and low-sulfur light fuel oil (LFO). Neat LFO served as the baseline fuel. The study started with thorough fuel analyses, including the fuels' ignition properties. Then, a medium-speed engine was driven with each fuel by using similar engine settings and without exhaust aftertreatment. The results indicate that the thermal efficiencies were almost equal for all fuels at all studied loads. No notable differences were observed in the heat release curves. The naphtha/LFO blend produced slightly increased HC emissions at low loads but showed the lowest HC at full load. NO_x emissions were very similar with all fuels. MGO and naphtha/LFO blend usually emitted fewer ultrafine exhaust particles than LFO. Methane and nitrous oxide emissions were always very low. Overall, both novel fuels could be adopted for medium-speed engines.

Introduction

Energy production and transport are major contributors to global greenhouse gas (GHG) emissions. Both sectors should make drastic reductions in their use of fossil energy sources. At the same time, their pollutant emissions must be reduced without jeopardizing high energy efficiency, reliability and profitability.

In road transport, particularly in urban areas, electric and hybrid propulsion is likely to expand [1]. However, the internal combustion engine (ICE) will most probably dominate in marine, hybrid power plant and non-road applications for a long time because it has so many attributes. It provides high energy density and thermal efficiency, strength, durability, the ability to burn various fuels, rapid response to load changes, and affordability. The ICE also continues to improve as a result of better combustion, exhaust aftertreatment, and control systems [1, 2, 3, 4, 5, 6, 7, 8].

Nevertheless, increasingly stringent emissions legislation encourages development of new solutions for engine-driven power. One example of this is exploring the use of alternative fuels to mitigate emissions from large engines. Low-carbon liquid fuels must become part of the energy agenda because sustainable liquid fuels will be needed for a long time to satisfy global growth in energy demands. The superior energy density of liquid fuels is ideal for applications working for long periods, far from any infrastructure. In addition, biofuels gradually are becoming economically attractive [8, 9, 10, 11, 12, 13, 14, 15]. Local and cost-effective fuels also increase the self-sufficiency of energy generation. Thus, various liquid fuel alternatives potentially play an important role in flexible power generation and in marine and heavy-duty non-road applications.

Engine business, universities and research institutes have investigated many fuel alternatives in different engines over recent decades. The feedstock palette is enormous. Fuels originating from waste or residue are preferred since their GHG emissions are low [15, 16, 17, 18, 19, 20, 21, 22, 23]. In addition to renewable alternatives, power and engine companies are interested in condensates or side streams of oil and gas production. The aim is to use side streams for on-site power in oil and gas fields and stop flaring: the World Bank has set a global target to eliminate routine gas flaring by 2030 [24]. The

adoption of surplus fuels with low octane numbers may also become an important topic [8].

Synthetic residue-derived fuels are already very high-quality drop-in fuels [8, 25]. The worldwide share of renewables in transport is, however, still very limited [26]. Rohbogner et al. (2019) assume that the distillate fuel pool is not large enough to serve road transport, aviation and marine [27]. Therefore, there is interest in generation of new, low-sulfur liquid fuels for medium-speed engines. The most tempting of these new fuel options are those that are less processed and more cost-effective [15, 27, 28, 29] However, fuel flexibility is also an important issue because in future applications, engines must be able to switch between fuels [30].

Meeting the ambitious CO_2 reduction targets in shipping appears to be possible only using CO_2-neutral fuels, assuming such fuels could be produced in a cost-effective and energy-efficient manner. Synthetic paraffinic hydrocarbon fuels are one such option. They would be easy to use in existing ship engines: an important issue, given that the typical life cycle of a ship is 25-30 years [1].

Renewable naphtha offers a route towards decarbonizing. In general, naphtha is one of the fuels that would make it easier for engine manufacturers to fulfil the regulatory requirements of reducing both greenhouse gas and criteria pollutants from diesel engines. Naphtha is suitable for mixing-controlled combustion. It is also less energy-intensive at refinery level than conventional diesel fuel if the naphtha is refined from crude oil, which is still the main production method [31, 32, 33, 34]. Naphtha has also produced promising results in new combustion concepts such as partially premixed compression ignition (PPCI) and low-temperature combustion (LTC). It has enabled recalibration of the engine for lower NO_x because soot formation has decreased considerably [31]. Consequently, use of naphtha in CI engines has aroused interest in recent years.

Naphtha is particularly advantageous when it has been manufactured from renewable sources. In this study, naphtha was derived from crude tall oil (CTO) extracted during wood pulp production [35]. Neat naphtha has a low cetane number (CN) and viscosity [36]. Therefore, and because of its so far limited market availability, renewable naphtha worked as a blending bio-component in low-sulfur light fuel oil (LFO) in the current study. A previous study with a high-speed engine had also shown that the engine does not need any modification when fueled with a naphtha-LFO blend [37].

The other test fuel of the present study, marine gas oil (MGO), seems to be an increasingly common shipping fuel, especially inside emission control areas (ECAs) and within EU ports. MGO is a feasible alternative in those special regions because heavy fuel oil engines need an exhaust scrubber to meet their sulfur emission regulations.

Circular-economy based MGO is an environmentally friendly MGO option because its present feedstock, waste lubricating oils (WLOs) are considered to be a hazardous waste [38, 39]. Recycling potential energy feedstock is a step towards more sustainable solutions. EU countries are encouraged to recycle WLOs. As a result, recycling of WLOs is said to have increased to 75-85% and there is an EU-wide target of 100% collection of waste oils [39, 40].

Promoting the adoption of new and more sustainable alternative fuels requires a large amount of research about those fuels, their blends with conventional fuels, and engine experiments, as shown for instance in [28, 29]. Responding to this demand, the present study evaluated the performance of two liquid fuel alternatives in a medium-speed engine, intended for marine applications and on-shore power generation. One fuel was a blend of renewable naphtha and low-sulfur LFO and the other a circular economy-based MGO. Neat low-sulfur LFO served as the baseline fuel. In the experiments, a medium-speed engine was driven with each of the three fuels. At this first stage of the project, all fuels were studied using similar engine settings and without adopting any exhaust aftertreatment.

Experimental Setup

Fuels

The renewable naphtha was a product of a manufacturing process of hydrotreated vegetable oil (HVO). Both products are based on CTO extracted during wood pulp production. Sulfur-free paraffinic naphtha is chemically pure hydrocarbon [35]. The manufacturing process has several phases, as illustrated in Figure 1. The hydrotreated raw fuel consists of mid-distillate diesel components in addition to lighter naphtha components that are separated by fractionation [37]. UPM of Finland delivered the naphtha for this study. The fuel is produced in Lappeenranta, Finland.

Naphtha's low CN and viscosity may lead to a lengthened ignition delay (ID) and retarded start of combustion [36]. The investigated naphtha did indeed show a prolonged ID and late combustion start in a combustion research unit [41]. Consequently, and because of its expected limited availability, renewable naphtha was used as a blending bio-component in low-sulfur LFO. The blend contained 26 vol.-% of naphtha. This mixing ratio was chosen on the basis of the observed

FIGURE 1 Manufacturing process of renewable naphtha [after 37].

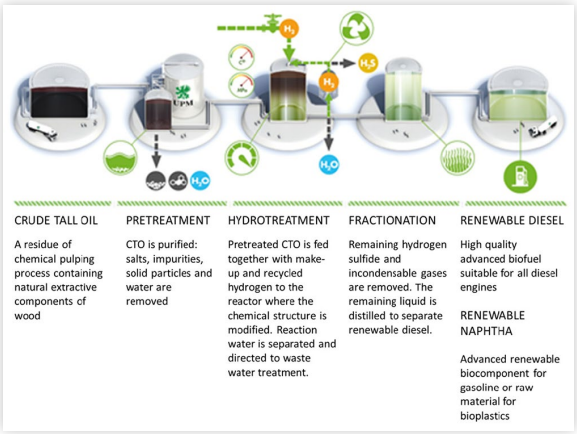

TABLE 1 Fuel specifications

	LFO	MGO	Naphtha-LFO	Unit
Kin. viscosity at 40 °C	3.1	3.7	1.8	mm^2/s
Density at 15 °C	836	838	809	kg/m^3
Cetane number	58	54	52	-
Sulfur	6	30	4.5	mg/kg
Carbon	84.5	84.8	85.0	wt.-%
Hydrogen	13.4	13.7	13.8	wt.-%
Total aromatics	16.8	15	18	wt.-%
Polyaromatics	1.4	1.3	1.6	wt.-%
Ash	< 10	< 10		mg/kg
LHV	43.2	43.3	43.5	MJ/kg
Lubricity	350	484	335	µm

FIGURE 2 Distillation data for the experimental fuels

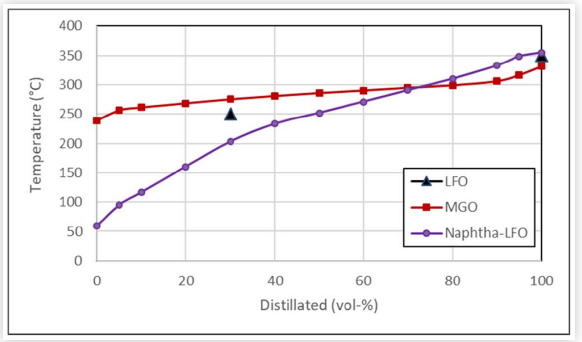

favorable combustion results of a 20/80 vol.-% blend in a pre-study with a high-speed engine [42].

The second studied alternative fuel, MGO, was a circular-economy based pilot product. It was the light fraction of the hydrotreaters of the regeneration process of used lubricating oils. With its low sulfur content of less than 100 mg/kg, MGO seems to be a feasible option for marine and on-shore power applications. The company STR Tecoil delivered MGO to our university [43, 44].

Table 1 lists the fuels' main characteristics. As shown, the properties of MGO and LFO were very similar. MGO, however, had a slightly higher sulfur content but a shade lower contents of aromatic compounds, less favorable lubricity and slightly lower CN than LFO. Naphtha-LFO blend showed lower viscosity, density and CN than pure LFO but a shade higher contents of aromatics. However, its sulfur content was low and lubricity beneficial.

The methods, used for fuel analyses were the following:

- kinematic viscosity, EN ISO 3104/ASTM D7042
- density, EN ISO 12185/ASTM D7042
- cetane number, EN 15195
- sulfur content, EN ISO 20884/EN ISO 20846
- carbon content, ASTM D5291
- hydrogen content, ASTM D5291
- aromatics, EN 12916
- lubricity, EN ISO 12156-1

Ash contents are based on the information provided by the fuel suppliers. Lower heating values were calculated based on the fuel elementary analyses.

Figure 2 depicts the distillation curves for the studied fuels. Due to the light fractions of naphtha, the distillation of the naphtha-LFO blend started already at approx. 50 °C and ended at 350 °C. MGO distilled at quite high temperatures, ranging from approx. 240 °C to 330 °C. For LFO, only two points were available. They indicated that LFO distillation was similar to MGO's, but the temperature range was probably larger, but only by a slight amount.

Engine and Loading

The experimental engine was a medium-speed Wärtsilä engine, intended for power plants and marine applications. The engine is turbocharged and the charge air is cooled by water before entering the cylinders. No exhaust gas aftertreatment was adopted.

The engine was driven at a constant speed of 1000 rpm and loaded by an ABB alternator. The produced electricity was fed into the grid of the local energy company. The engine specification is given in Table 2. The maximum engine output was set at 640 kW for the full-load measurements in the current study. Experimental measurements were also performed at four partial loads, corresponding to 75, 50, 25 and 10% of the full load. The load points followed those of the test cycle D2 of the ISO 8178-4 standard.

Analytical Procedures

The experimental setup's measurement system comprised proper pressure and temperature sensors along the air and exhaust paths. Intake air flow was determined by means of an air nozzle and fuel flow with a scale and watch. Engine management software, supplied by the engine manufacturer, gathered the sensor data and followed the engine control parameters. Additionally, several analyzers were included for combustion and emissions analyses. Table 3 lists those instruments.

The emissions instruments were calibrated before and after the measurements. The engine was allowed to stabilize before taking the parameter recordings. The temperatures of

TABLE 2 Specification of the experimental engine

Swept volume/cylinder	8.8 dm^3
Cylinder number	4
Bore	200 mm
Stroke	280 mm
Compression ratio	16
Number of valves	4
Speed	1000 rpm
Shaft power output	640 kW

TABLE 3 Measuring equipment

Parameter	Instrument	Technology
Cylinder pressure	Kistler KiBox®	
Exhaust HC	J.U.M. VE7	HFID
Exhaust NO_x	Eco Physics CLD 822 M h	Chemiluminescence
Exhaust CO, CO_2	Siemens Ultramat	NDIR
Exhaust O_2	Siemens Oxymat 61	Paramagnetic
Exhaust particle number	TSI EEPS 3090	Spectrometer

FIGURE 3 Experimental setup [45]

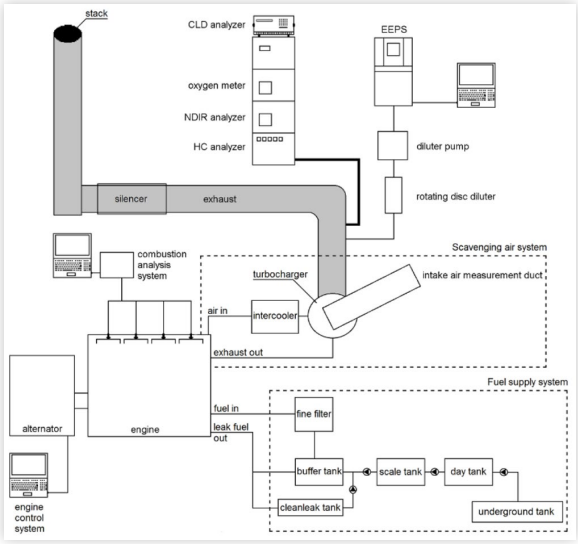

cooling water, charge air in the manifold, and the exhaust upstream of the turbine had to be stable. - Figure 3 shows a diagram of the experimental setup [45].

Results

Combustion

Figure 4 depicts the heat release rate (HRR) versus the degrees of crank angle (deg) for all fuels at 75% load. The premixed peak of the naphtha-LFO blend was a shade higher than that of MGO and LFO. The initial combustion followed well the differences in CN: the lower the CN, the higher the premixed peak. In general, however, combustion progressed in a very similar manner with all fuels.

Figure 5 illustrates that 50% of all fuels had burned at very similar crank angles (CA) at each load. The CA values were different at various loads since the injection timing was different, as shown in Figure 6. At half and lower loads, the timing was 9° CA before top dead center (bTDC) while at higher loads, the timing was advanced.

FIGURE 4 Heat release rate versus crank angle at 75% load for the studied fuels

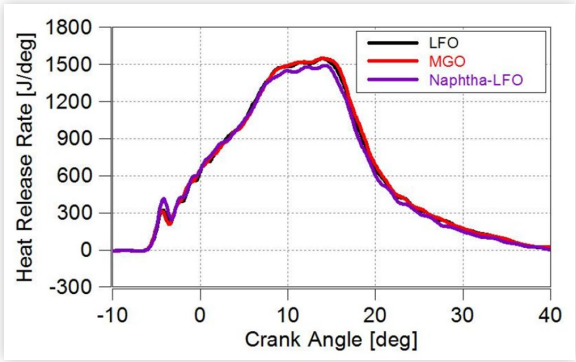

FIGURE 5 Crank angles for 50% mass fractions of burned fuel (MFB) at various engine loads

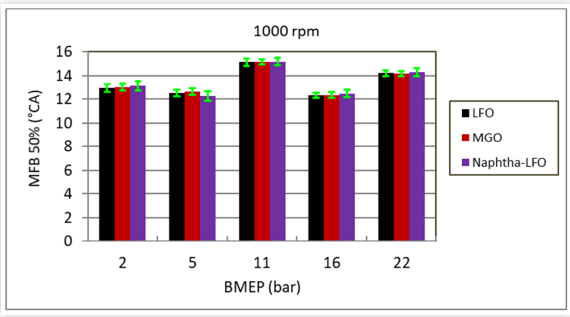

FIGURE 6 Injection timing at different loads

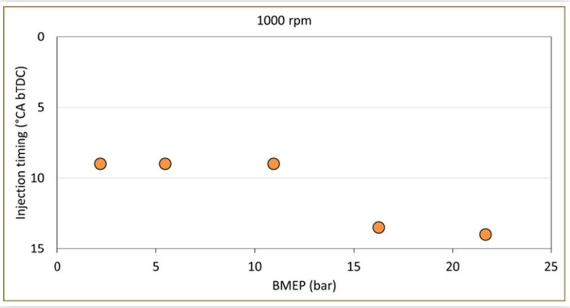

Finally, Table 4 lists the crank angles at which 50% of each fuel had burned at 75% load. As shown, the average values of 100 consecutive engine cycles are very close to each other for all fuels and the standard deviations vary from 1.8% (LFO) to 2.5% (blend).

Efficiency

Figure 7 shows that the brake thermal efficiency (BTE) of the engine was very similar when fueled with different fuels. At

TABLE 4 Crank angles for 50% mass fractions of burned fuel at 75% load. Avg, average for 100 consecutive cycles; Stdev, standard deviation.

	Avg	Stdev	Unit
LFO	12.3	0.22	° CA
MGO	12.4	0.24	° CA
Naphtha-LFO	12.5	0.31	° CA

FIGURE 7 Brake thermal efficiency of the engine at different loads for various fuels

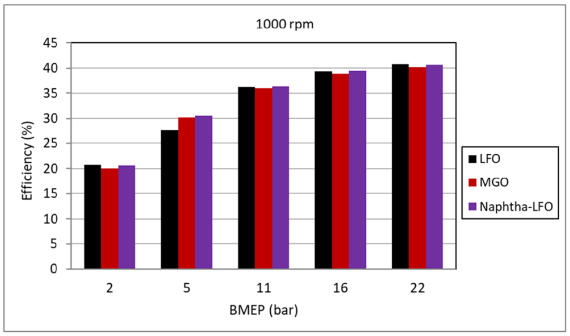

full load, the BTE was 40 to 41% and at half load 36%. At many loads, the BTE seemed to be a shade higher with LFO and the blend than with MGO. The differences were, however, within the measurement accuracy. The LFO result at 25% load was, quite evidently, wrong.

Emissions

Gaseous Emissions Figure 8 shows brake specific NO_x emissions were high with the engine settings that were used, reaching slightly more than 14 g/kWh at full load. Every fuel emitted very similar NO_x emissions, although MGO was slightly higher at high loads and slightly lower at low loads than LFO and naphtha-LFO blend. Again, one can see that some problems had occurred with LFO measurements at 25% load.

FIGURE 8 Brake specific NO_x emissions against engine load with the studied fuels

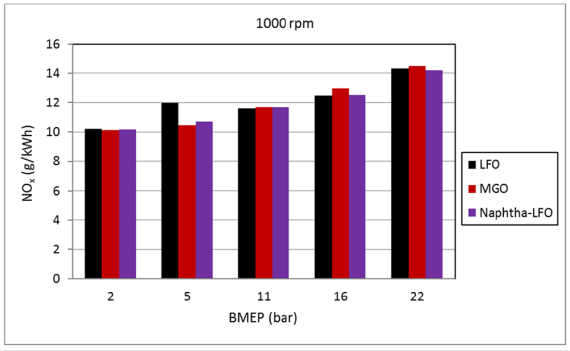

FIGURE 9 Brake specific emissions of total hydrocarbons as a function of engine load for different fuels

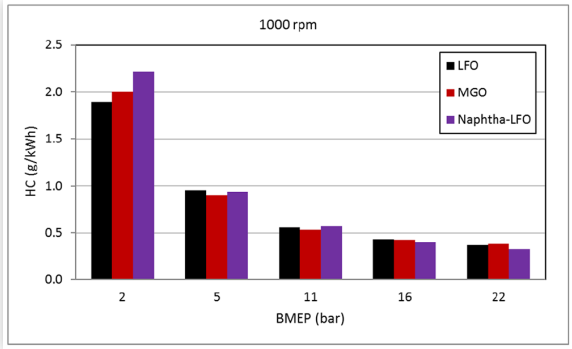

Figure 9 illustrates total hydrocarbons (HC), showing all fuels produced very similar HC emissions, except at the lowest load. At this point, HC emissions with the blend were highest, approximately 17% above the baseline LFO. Light fractions of naphtha with low boiling points may have resulted in increased over-leaning and higher HC at this very low load [28]. The opposite result was seen at high loads, where naphtha-LFO produced the lowest HC emissions. Reactivity conditions are beneficial at high load, even for lower-cetane fuels.

Carbon monoxide (CO) emissions were very similar for all fuels within the load range of 50 to 100%, Figure 10. At lower loads, the results varied slightly but the differences were not significant. At 10% load, MGO emitted slightly more CO than LFO (+10%) and the blend (+14%). At 25% load, the blend also resulted in the lowest CO, MGO showing the highest, 24% higher than the blend.

Figure 11 depicts the calculated cycle-averaged emissions. NO_x emissions were almost equal for MGO and LFO (12.3 g/kWh) while the blend resulted in slightly lower NO_x of 12.1 g/kWh. In terms of HC, MGO's 0.56 g/kWh was the lowest whereas LFO showed the highest or 0.58 g/kWh. The blend's CO was the lowest, 0.56 g/kWh, while MGO produced the highest, 0.61 g/kWh.

FIGURE 10 Brake specific CO emissions versus engine load for the studied fuels

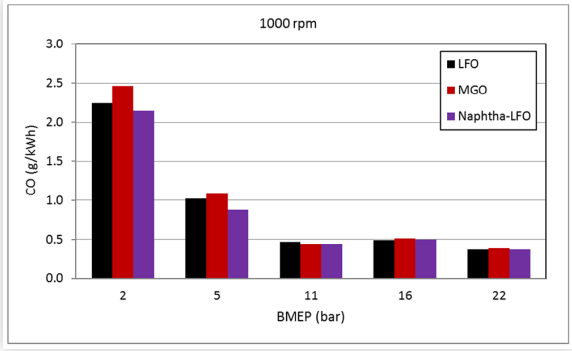

FIGURE 11 Calculated cycle-averaged brake specific emissions for the studied fuels

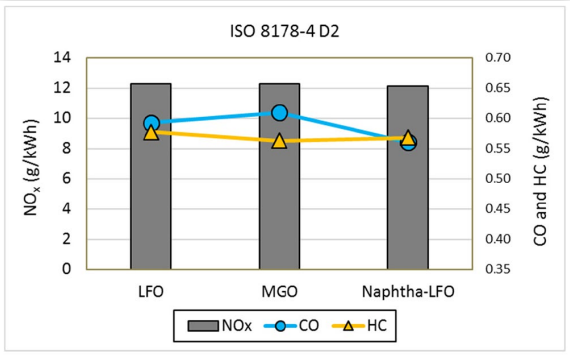

FIGURE 12 Wet exhaust methane contents versus engine load with different fuels

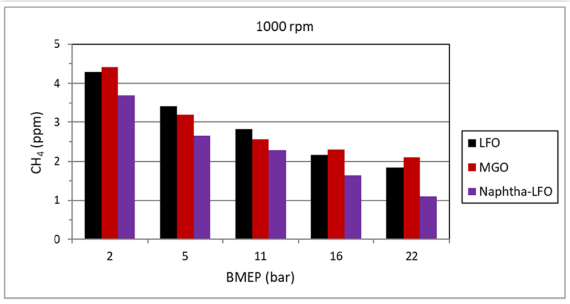

From the GHG viewpoint, emissions of methane and nitrous oxide are also important. Figure 12 illustrates the wet exhaust methane contents at various engine loads. Methane decreased with increasing engine load. Naphtha-LFO blend emitted lower CH_4 content than LFO and MGO, especially at high loads. However, CH_4 contents were generally very low, at below 5 ppm.

Figure 13 shows that the wet exhaust contents of nitrous oxide were also very low, well below 1 ppm at all loads. The highest recorded content was slightly higher than 0.5 ppm, within the measuring accuracy of the FTIR analyzer. No clear trend was detected between the fuels.

Particulates The exhaust did not contain high numbers of nucleation mode particulates but the accumulation mode peaks were usually higher by two orders of magnitude than those of nucleation mode tops [45]. Up to 75% load, the size distributions peaked within the size range of 30 to 50 nm, as illustrated for 75% load in Figure 14. At full load, the peak of every fuel moved towards larger particles, up to approximately 80 nm.

Figure 15 depicts the total particulate number (TPN) within the size range of 5.6 to 560 nm. At low loads, TPN was the lowest with MGO and highest with LFO. From 50 to 100% load, MGO and naphtha-LFO blend generated almost similar TPNs, both clearly lower than LFO. It is apparent that blending

FIGURE 13 Wet exhaust contents of nitrous oxide against engine load with various fuels

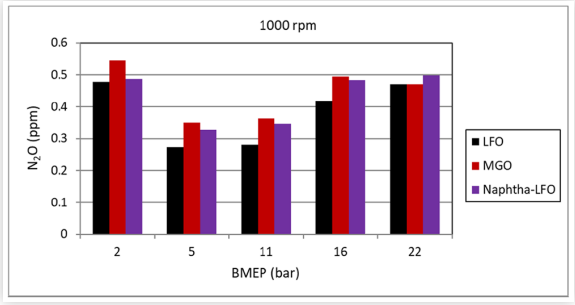

FIGURE 14 Exhaust particle size distributions for different fuels at 75% load (after [45])

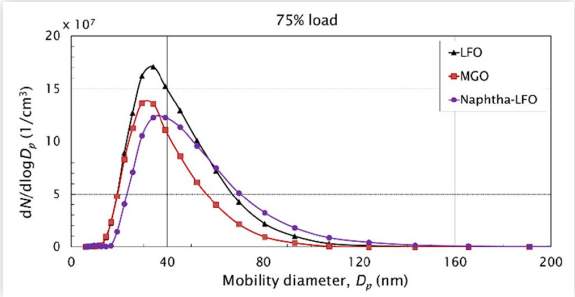

FIGURE 15 Total particulate number (TPN) of exhaust within the particle size range of 5.6 to 560 nm (after [45])

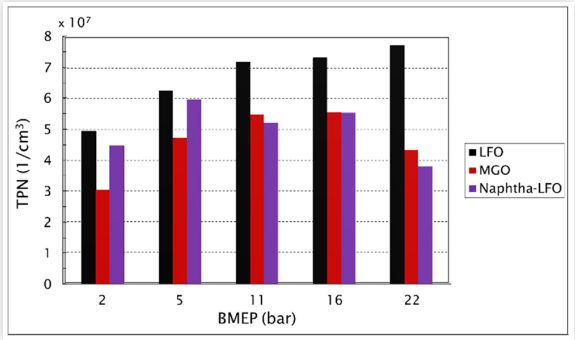

naphtha with LFO resulted in a clear reduction in particulate number.

Discussion

The use of the studied blend of renewable naphtha and LFO was pioneering. There are few publications available on the use of this type of blend in medium- or high-speed engines. Some results, however, do exist. Hissa et al. (2019) detected

that a slightly weaker naphtha-LFO blend (20/80 vol.-%) burned as favorably as LFO in a high-speed diesel engine [42]. That result supports the observations of the present study.

Niemi et al. (2019) reported that the same 20/80 vol.-% blend in the same engine resulted in almost similar BTE and NO_x but somewhat higher CO (+9%) and HC (+26%) emissions than neat LFO [37]. In some respects, the results of the present study were in line with that of [37]. With the current slightly stronger blend (26/74%), the engine efficiency and NO_x emissions were again almost equal for naphtha-LFO and neat LFO. Unlike in [37], however, the blend's cycle-weighted CO was now lower than LFO's by 5% and HC was almost similar.

Ovaska et al. (2019) detected that the weaker naphtha-LFO blend (20/80%) reduced the number of exhaust particle above 50 nm at rated and intermediate speeds [46]. In the present study, the blend also reduced particulates. Together with its competitive CO and HC performance, the blend's improved particulate results may be explained by favorable mixture formation. The boiling point has an important role in the fuel evaporation rate [47] and high volatility plus low viscosity improve mixture formation. Most likely, naphtha's higher volatility promoted fuel-air mixing. Combined with naphtha's low aromatic content, this probably led to the reduction in the number of particulates with the blend [31]. Chang et al. (2013) also detected that naphtha improved the particulate/NO_x trade off when operating the engine in the relevant drive cycle [32].

It must be noted that naphtha has some special properties that affect its usability. Sirviö et al. (2019) detected that the naphtha-LFO blend (20/80%) had improved cold properties relative to neat LFO, so no specific measures are needed for fuel pumping and filtering. On the other hand, the blend had a very low flash point that calls for particular consideration of safety aspects during both storage and use [44]. Rules applied to methanol-fueled ships can also be feasible for the safe use of naphtha [48], since the flash point of methanol is approx. 12 °C, close to that of current naphtha and its blend (approx. 10 °C).

Additionally, the low boiling temperature of some naphtha compounds may necessitate sufficient backpressure in the fuel return line of the injection system [32]. The lubricity of the naphtha-LFO blend in the current study was close to that of the baseline LFO so the blend should not harm lubrication of injection pumps lubricated by fuel.

As a whole, the results of the present study showed that the blend worked beneficially at all loads. So, the blends of naphtha and conventional fuels offer a realistic way to improve the sustainability of maritime and power generation applications.

Viollet et al. (2014) also examined the role of naphtha and considered that future compression ignition engines will use, for example, low-quality gasoline such as naphtha fuels. The authors speak about fossil naphtha and suggest that using it in the gasoline compression ignition (GCI) concept has several advantages. It would mitigate anticipated demand imbalance between heavy and light fuels and offer diesel-like efficiency at lower cost [49]. Our university will, however, continue to focus primarily on renewable naphtha. It will be studied in the planned combustion concept project investigating Reaction Controlled Compression Ignition (RCCI), a field in which our staff already has experience [50].

As with renewable naphtha, there are also only few engine results available for circular-economy MGO. Gabiña et al. (2019) evaluated the suitability of an alternative fuel produced from waste oils for an actual marine diesel engine. However, the fuel had considerably higher kinematic viscosity than our MGO (21 mm^2/s vs. 3.7 mm^2/s) and slightly higher density (+15%) and CN (57 vs. 54). Accordingly, the fuel was preheated to reduce its viscosity before injection into the cylinders. The tested fuel proved to suit the engine well as regards combustion and emissions. Combustion differences were insignificant when compared with diesel fuel oil (DFO) and efficiencies were almost equal for both fuels. The MGO produced from waste oils emitted less NO_x than DFO, whereas CO was slightly higher but still low. As a whole, this alternative fuel derived from waste lube oil was suitable for use in medium-speed marine diesel engines [2].

Ovaska et al. (2019) observed that circular-economy MGO generated high TPN at all loads at rated speed in high-speed engine tests, most probably due to its higher sulfur content. MGO was, though, favorable in terms of HC and CO emissions. Cycle-weighted HC was only two thirds of that with LFO. CO was 15% lower with MGO, while NO_x emissions were similar. Smoke as filter smoke number (FSN) was negligible for both fuels [46]. Hissa et al. (2019) also reported on a beneficial emissions performance of the same MGO [42]. Unfortunately, the viscosity and CN of the MGO in the batch used in the studies [46] and [42] were clearly higher than those of the present study's MGO. The density was also slightly higher. Therefore, the results of [46] and [42] are not completely comparable with the results at hand.

In the present study, the MGO results of engine combustion, efficiency and most of the emissions were quite similar to those recorded with baseline LFO. The TPN was even lower. Regarding performance, the studied MGO proved, thus, to be a suitable fuel for the investigated medium-speed engine. For long-term use, the only issue may be MGO's lubricity since it was slightly above the maximum, allowed for automotive diesels (484 vs. 460 µm) [51].

Conclusions

The current work studied how two liquid fuel alternatives operate in a medium-speed diesel engine, intended for marine applications and on-shore power generation. One fuel was a blend of renewable naphtha and low-sulfur LFO (26/74 vol.-%) and the other a circular economy-based MGO. Neat low-sulfur LFO formed the baseline fuel. All three fuels fueled the engine in the experiments, one after another. The engine speed was constant and the investigated parameters were recorded at five loads. In this preliminary project, the engine settings were similar for all fuels and the experimental setup did not include any exhaust aftertreatment.

Based on the conducted measurements, the following conclusions could be drawn:

- All fuels burned in a very similar, efficient way. The ignition delay followed coherently the differences in the

CN, with the naphtha-LFO blend showing a slightly longer ID than the other fuels. However, the 50% burned fraction of each fuel occurred at almost equal crank angles at all loads.

- All fuels resulted in very similar brake thermal efficiencies of the engine at any given load. The variation was within one percentage point at each load.
- The brake specific NO_x emissions were also quite similar at each load with all fuels. The cycle-weighted emissions, calculated according to the ISO 8178-4 D2 cycle, were a shade lower for the blend (12.1 g/kWh) than for MGO and LFO (12.3 g/kWh).
- There was also little difference in CO emissions: the cycle-averaged brake specific CO ranged from 0.56 to 0.61 g/kWh for all fuels. MGO led to slightly higher CO than the other fuels because it emitted slightly more CO at low loads. The blend showed the lowest CO.
- The cycle-weighted brake specific HC emissions ranged from 0.56 to 0.58 g/kWh. MGO's result was the lowest and LFO's the highest. At an engine load of only 10%, the blend emitted 17% higher HC than the baseline LFO.
- The wet exhaust contents of the heavy GHG emissions, methane and nitrous oxide, were very low at all engine loads for all fuels. Methane was always below 5 ppm and nitrous oxide below 0.6 ppm.
- The number of nucleation mode particulates was drastically lower than the number of accumulation mode particles with all fuels at all loads. Up to 75% load, the size distributions peaked within the size range of 30 to 50 nm while at full load, the peak moved towards larger particles. At low loads, the TPN within the size range of 5.6 to 560 nm was the lowest with MGO. From 50 to 100% load, MGO and naphtha-LFO blend generated broadly similar TPNs, clearly lower than with LFO. Blending naphtha with LFO gave a clear reduction in particulate number.
- All in all, the studied circular-economy MGO proved to be very suitable for the medium-speed engine. Combustion, performance and emissions were quite close to those obtained with low-sulfur LFO. The lubricity should be slightly improved, however. - A share of 26 vol.-% renewable naphtha in the naphtha-LFO blend resulted in very similar engine combustion, performance and emissions to LFO. The blend's very low flash point will require specific protocols during storage and use.

References

1. Conference Report: 17th FAD Conference, https://dieselnet.com/newsletter/2019/11.php, accessed Dec. 3, 2019.
2. Gabiña, G., Martin, L., Basurko, O.C., Clemente, M. et al., "Performance of Marine Diesel Engine in Propulsion Mode with a Waste-Oil Based alternative Fuel," *Fuel* 235:259-268, 2019, doi:10.1016/j.fuel.2018.07.113.
3. Kalghatgi, G., "Is It Really the End of Internal Combustion Engines and Petroleum in Transport?" *Applied Energy* 225:965-974, 2018, doi:10.1016/j.apenergy.2018.05.076.
4. Llamas, X., and Eriksson, L., "Control-Oriented Modeling of Two-Stroke Diesel Engines with Exhaust Gas Recirculation for Marine Applications," *Journal of Engineering for the Maritime Environment (Part M)*, 2018, doi:10.1177/1475090218768992.
5. Gilkes, D., "JCB Prepared to Meet EU Stage V emissions," published Nov. 7, 2019, https://www.sae.org/news/2019/07/jcb-stage-v-emissions-plans, 2019.
6. Ribó-Pérez, D., Bastida-Molina, P., Gómez-Navarro, T., and Hurtado, E. "Choosing the Best Configuration for a Hybrid Microgrid of Renewable Energy Sources by Means of the Analytic Network Process," in *Proceedings of the 14th SDEWES Conference*, Paper No. 0565, Dubrovnik, Croatia, Oct.16, 2019, 8pp.
7. Rinaldi, F., Moghaddampoor, F., Najafi, B., and Marchesi, R., "Economic Feasibility Analysis and Optimization of Hybrid Renewable Energy Systems for Rural Electrification in Different Climatic Zones of Peru," in *Proceedings of the 14th SDEWES Conference*, Paper No. 0854, Dubrovnik, Croatia, Oct. 1-6, 2019, 27pp.
8. IJER Editorial: The Future of the Internal Combustion Engine," *International Journal of Engine Research* 21(1):3-10, 2020, doi:10.1177/1468087419877990.
9. Küchen, C., "Perspectives for Liquid Fuels in the Energy Transition," in: Schubert, N. (ed.), *Fuels, Conventional and Future Energy for Automobiles* (Ostfildern, Germany: Technische Akademie Esslingen, 2019), 19-21, ISBN: 978-3-943563-09-2.
10. Alabbad, M., Issayev, G., Badra, J., Voice, A.K. et al., "Autoignition of Straight-Run Naphtha: A Promising Fuel for Advanced Compression Ignition Engines," *Combustion and Flame* 189:337-346, 2018, doi:10.1016/j.combustflame.2017.10.038.
11. Hoppe, F., Benedikt, H., Thewes, M., Kremer, F. et al., "Tailor-Made Fuels for Future Engine Concepts," *Int. J. Engine Res.* 17(1):16-27, 2016, doi:10.1177/1468087415603005.
12. "CIMAC Is Joining the Getting to Zero Coalition," Press Release, Sept. 23, 2019, International Council on Combustion Engines, Frankfurt, Germany, https://www.cimac.com/press-media/press-releases/cimac-is-joining-the-getting-to-zero-coalition.html.
13. Chang, C.-C., Tu, J.-S. and Chen, Y.-C., "Life Cycle Assessment of Diesel and Alternative Fuels in a Public Vehicle," in *Proceedings of the 14th SDEWES Conference*, Paper No. 0468, Dubrovnik, Croatia, Oct. 1-6, 2019, 15pp.
14. Deniz, C., and Zincir, B., "Environmental and Economical Assessment of Alternative Marine Fuels," *Journal of Cleaner Production* 113(1):438-449, 2015, doi:10.1016/j.jclepro.2015.11.089.
15. Kołwzan, K., and Narewski, M., "Alternative Fuels for Marine Applications," *Latvian Journal of Chemistry* (4):398-406, 2012, doi:10.2478/v10161-012-0024-9.
16. Su, C.-H., Nguyen, H. C., Pham, U. K., Nguyen, M. L. et al., "Biodiesel Production from a Novel Nonedible Feedstock, Soursop (*Annona muricata* L.) Seed Oil," in: Chen, W.-H. et al. (ed), *Biofuel and Bioenergy Technology* (2019), https://

www.mdpi.com/journal/energies/special_issues/biofuel_bioenergy.

17. Niemi, S., Vauhkonen, V., Hiltunen, E., Virtanen, S. et al., "Results of an Off-Road Diesel Engine Driven with Different Animal Fat Based Biofuels," *ASME Paper ICEF2009-14010*, 2009, doi:10.1115/ICEF2009-14010.
18. Pietikäinen, M., Väliheikki, A., Oravisjärvi, K., Kolli, T. et al., "Particle and NO_x Emissions of a Non-Road Diesel Engine with an SCR Unit: The Effect of Fuel," *Renewable Energy* 77:377-385, 2015, doi:10.1016/j.renene.2014.12.031.
19. Niemi, S.A., Murtonen, T.T., Laurén, M.J., and Laiho, V.O.K., "Exhaust Particulate Emissions of a Mustard Seed Oil Driven Tractor Engine," SAE Technical Paper 2002-01-0866, 2002, https://doi.org/10.4271/2002-01-0866.
20. Niemi, S., Uuppo, M., Virtanen, S., Karhu, T. et al., "Animal Fat Based Raw Bio-Oils in a Non-Road Diesel Engine Equipped with a Diesel Particulate Filter," in Bartz, W. J. (ed), *8th International Colloquium Fuels; Conventional and Future Energy for Automobiles* (Ostfildern, Germany: Technische Akademie Esslingen, 2011), 517-528, ISBN: 3-924813-86-8.
21. Schlott, S., "Synthetische Kraftstoffe im Wartestand," *MTZ* 76(6):9-13.
22. Kim, Y.-M., Park, Y.-K., Watanabe, A., and Kim, S., "Supercritical Pyrolysis of Kraft Lignin using a High Pressure Tandem μ-Reactor-GC/MS," in *Proceedings of the 14th SDEWES Conference*, Paper No. 0272, Dubrovnik, Croatia, Oct. 1-6, 2019, 8pp.
23. Rajak, U., Nashine, P., Verma, T.N., and Pugazhendhi, A., "Performance, Combustion and Emission Analysis of Microalgae Spirulina in a Common Rail Direct Injection Diesel Engine," *Fuel* 255:115855, doi:10.1016/j.fuel.2019.115855.
24. Jay, D., Monnet, G., and Laine, M., "Design of a New Condensate Gas Fuel Injection System for Wärtsilä Engines," in *29th CIMAC World Congress 2019*, Paper No. 392, 12pp.
25. Niemi, S., Vauhkonen, V., Mannonen, S., Ovaska, T. et al., "Effects of Wood-Based Renewable Diesel Fuel Blends on the Performance and Emissions of a Non-road Diesel Engine," *Fuel* 186(1-10), 2016, doi:10.1016/j.fuel.2016.08.048.
26. REN21, "Renewables 2017 Global Status Report," 2017, http://www.ren21.net/wp-content/uploads/2017/06/17-8399_GSR_2017_Full_Report_0621_Opt.pdf, accessed on Feb. 18, 2019.
27. Rohbogner, C., Loibl, A., Staudacher, M., Bacu, D. et al., "0.5 % Sulphur Regulation for Marine-Fuels in 2020: An Approach for Fuel Development and Application Testing," in: Schubert, N. (ed.), *Fuels, Conventional and Future Energy for Automobiles* (Ostfildern, Germany: Technische Akademie Esslingen, 2019), 273-282, ISBN: 978-3-943563-09-2.
28. Juoperi, K., and Ollus, R., "Alternative Fuels for Medium-Speed diesel engines," *Wärtsilä Technical Journal* 01, 2008.
29. Juoperi, K., "Alternative Fuels from a Medium-Speed Engine Manufacturer's Perspective," in *CIMAC World Congress 2016*, Paper No. 238, 10pp.
30. "Hercules-2 Plan: Fuel Flexible, Near-Zero Emissions, Adaptive Performance Marine Engine—Hercules-2, Grant Agreement Number—634135," European Commission, *Innovation and Networks Executive Agency*, 2015.
31. Zhang, Y., Kumar, P., Traver, M., and Cleary, D., "Conventional and Low Temperature Combustion Using Naphtha Fuels in a Multi-Cylinder Heavy-Duty Diesel Engine," *SAE Int. J. Engines* 9(2):1021-1035, 2016, https://doi.org/10.4271/2016-01-0764.
32. Chang, J., Kalghatgi, G., Amer, A., Adomeit, P. et al., "Vehicle Demonstration of Naphtha Fuel Achieving Both High Efficiency and Drivability with EURO6 Engine-Out NOx Emission," *SAE Int. J. Engines* 6(1):101-119, 2013, https://doi.org/10.4271/2013-01-0267.
33. Wang, X., and Ni, P., "Combustion and Emission Characteristics of Diesel Engine Fueled with Diesel-Like Fuel from Waste Lubrication Oil," *Energy Conversion and Management* 133:275-283, 2017, doi:10.1016/j.enconman.2016.12.018.
34. Bae, C., and Kim, J., "Alternative Fuels for Internal Combustion Engines," *Proceedings of the Combustion Institute* 000:1-25, 2016, doi:10.1016/j.proci.2016.09.009.
35. UPM, "Brochure of BioVerno Naphtha," 2019, https://www.upmbiofuels.com/products/upm-bioverno-naphtha/, accessed Jan. 9, 2019.
36. Subramanian, T., Varuvel, E., Ganapathy, S., Vedharaj, S. et al., "Role of Fuel Additives on Reduction of NO_x Emission from a Diesel Engine Powered by Camphor Oil Bio-Fuel," *Environmental Science and Pollution Research* 25(16):15368-15377, 2018, doi:10.1007/s11356-018-1745-4.
37. Niemi, S., Hissa, M., Ovaska, T., Sirviö, K. et al., "Performance and Emissions of a Non-road Diesel Engine Driven with a Blend of Renewable Naphtha and Diesel Fuel Oil," in Schubert, N. (ed), *12th International Colloquium Fuels, Conventional and Future Energy for* (Automobiles, Ostfildern, Germany: Technische Akademie Esslingen, 2019), 241-251, ISBN: 978-3-943563-09-2.
38. Naima, K., and Liazid, A., "Waste Oils Alternative Fuel for Diesel Engine: A Review," *J. Pet. Technol. Altern. Fuels* 4:30-43, 2013, doi:10.5897/JPTAF12.026.
39. Aramkitphotha, S., Tanatavikorn, H., Yenyuak, C., and Vitidsant, T., "Low Sulfur Fuel Oil from Blends of Microalgae Pyrolysis Oil and Used Lubricating Oil: Properties and Economic Evaluation," *Sustain. Energy Technol. Assess.* 31:339-346, 2019, doi:10.1016/j.seta.2018.12.019.
40. "Waste Framework Directive Revision: European Waste Oil Re-Refining Industry Position," https://www.geir-rerefining.org/wp-content/uploads/GEIRpositionpaperWFD_2016_FINAL.pdf, accessed Jan. 24, 2020.
41. Hissa, M., Niemi, S., and Sirviö, K., "Combustion Property Analyses with Variable Liquid Marine Fuels in Combustion Research Unit," *Agronomy Research* 16(S1):1032-1045, 2018, doi:10.15159/AR.18.089.
42. Hissa, M., Niemi, S., Sirviö, K., Niemi, A. et al., "Combustion Studies of a Non-Road Diesel Engine with Several Alternative Liquid Fuels," *Energies* 12:2447, 2019, doi:10.3390/en12142799.
43. Sirviö, K., Niemi, S., Heikkilä, S., Help, R. et al., "Fuel Blends Behavior in Freezing-Melting Phase Transition," in Schubert, N. (ed), *12th International Colloquium; Fuels, Conventional and Future Energy for Automobiles* (Ostfildern, Germany: Technische Akademie Esslingen), 89-94, ISBN: 978-3-943563-09-2.

44. Sirviö, K., Niemi, S., Heikkilä, S., Kiijärvi, J. et al., "Feasibility of New Liquid Fuel Blends for Medium-Speed Engines," *Energies* 12:2799, 2019, doi:10.3390/en12142799.
45. Ovaska, T., Niemi, S., Sirviö, K., Heikkilä, S.et al., "Effect of Alternative Liquid Fuels on the Exhaust Particle Size Distributions of a Medium-Speed Diesel Engine," *Energies*, 12: 2050, 14p., 2019, doi:10.3390/en12112050.
46. Ovaska, T., Niemi, S., Sirviö, K., Nilsson, O. et al., "Effects of Alternative Marine Diesel Fuels on the Exhaust Particle Size Distributions of an Off-Road Diesel Engine," *Appl. Therm. Eng.* 150:1168-1176, 2019, doi:10.1016/j.applthermaleng.2019.01.090.
47. Kaario, O.T., Vuorinen, V., Kahila, H., Im, H.G. et al., "The Effect of Fuel on High Velocity Evaporating Fuel Sprays: Large-Eddy Simulation of Spray A with Various Fuels," *Int J Engine Res* 21(1):26-42, 2020, doi:10.1177/1468087419854235.
48. Lloyd's Register Group Limited, "Rules for the Classification of Methanol Fuelled Ships," 32pp., 2019, https://www.lr.org/en/rules-for-the-classification-of-methanol-fuelled-ships/, accessed on Jan. 31, 2020.
49. Viollet, Y., Chang, J., and Kalghatgi, G., "Compression Ratio and Derived Cetane Number Effects on Gasoline Compression Ignition Engine Running with Naphtha Fuels," *SAE Int. J. Fuels Lubr.* 7(2):412-426, 2014, https://doi.org/10.4271/2014-01-1301.
50. Mikulski, M., Ramesh, S., and Bekdemir, C., "Reactivity Controlled Compression Ignition for Clean and Efficient Ship Propulsion," *Energy* 182:1173-1192, 2019, doi:10.1016/j.energy.2019.06.091.
51. EU, "Fuels: Automotive Diesel Fuel," https://dieselnet.com/standards/eu/fuel_automotive.php#y2004, accessed June 11, 2020.

Contact Information

Kindly contact **Professor Seppo Niemi**, the University of Vaasa, PO Box 700, FI-65101 Vaasa, Finland. seniemi@uva.fi. +358 50 430 8519.

Acknowledgments

This project was conducted as part of the EU Hercules-2 program under the Grant Agreement No. 634135. In addition to the authorities of the EU, the authors wish to thank the company UPM for delivering renewable naphtha and the company STR Tecoil for supplying circular-economy MGO for the research.

Abbreviations

BTE - brake thermal efficiency
bTDC - before top dead center
CH_4 - methane
CLD - chemiluminescence detector
CA - crank angle
CN - cetane number
CO - carbon monoxide
CTO - crude tall oil
deg - degrees crank angle
DFO - diesel fuel oil
ECA - emission control area
EEPS - engine exhaust particle sizer
EU - European Union
FTIR - Fourier-transform infra-red
GHG - greenhouse gas
HC - total hydrocarbons
HFID - heated flame ionization detector
HRR - heat release rate
ID - ignition delay
ICE - internal combustion engine
ISO - International Standard Organization
LFO - light fuel oil
LHV - lower heating value
LTC - low-temperature combustion
MFB - mass fraction burned
MGO - marine gas oil
N_2O - nitrous oxide
NDIR - non-dispersive infra-red
NO_x - oxides of nitrogen
PPCI - partially premixed compression ignition
Stdev - standard deviation
TPN - total particle number
WLO - waste lubricating oil

ISSN 0148-7191